

PHYSICO-CHEMICAL STUDIES OF POLYMERS CONTAINING CYCLOALKYL
AND AZA-CROWN-ETHER UNITS

A thesis submitted to the University of Stirling
for the degree of
Doctor of Philosophy

Hak Hung Wu

Department of Chemistry
February 1987

10/87

PREFACE

This thesis is submitted for the degree of Doctor of Philosophy at the University of Stirling, having been submitted for no other degree. It is a record of research undertaken in the Department of Chemistry. This work is wholly original except where due reference is made.

ACKNOWLEDGEMENTS

I wish to express my thanks to my supervisor, Professor J.M.G. Cowie for his immense patience, continuous encouragement and inspiring discussion throughout the period of my studies.

I wish to thank Dr. I.J. McEwen for his help in instrumentation. I am also indebted to Mr G. Castle for providing the most needed chemicals, glassware and particularly his willingness in filling the solvent bottles on the rainy days. I also wish to thank 'Shuggy' for taking some of the photographs contained in this work.

An 'apple' a day, you need the 'Doctor' rightaway; I wish to thank Dr. R. Ferguson for helping me to tackle the Apple II word processor and in obtaining the calorimetric data.

Had my beloved sister not looked after my parents, I would not have be able to concentrate on my studies, and so I must once again express my gratitude to her at this point.

Finally, to all of my struggling fellow researchers, my thoughts are always with you.

ABSTRACT

Part One of this thesis covers the synthesis and characterisation of new thermotropic mainchain liquid crystalline polymers containing cyclooctyl units and aza-18-crown-ether units. The effects upon the structure-property relationships of these polymers in terms of the following parameters were studied, and the results are reported here: spacer length, different substituents, copolymerisation, mesogenic group length, different mesogens and variable ring size. The liquid crystalline transitions and textures of these polymers are identified by using optical polarising microscopy and differential scanning calorimetry (DSC).

Part Two includes study of the mechanical properties of polymers containing cycloalkyl units and aza-crown-ethers. The effect of catalysts and solvents in polyurethane preparation has also been looked at. Secondary relaxations ($T < T_g$) were identified by using torsional braid analysis (TBA).

CONTENTS **PART ONE**

	<u>Page</u>
1. <u>CHAPTER ONE</u>	
Introduction	1
1.1 States of matter	
1.2 The fourth state of matter	
1.3 Liquid crystal mesophases	
1.3.1 Nematic mesophase	
1.3.2 Cholesteric mesophase	
1.3.3 Smectic mesophase	
1.3.3.1 Smectic A	
1.3.3.2 Smectic B	
1.3.3.3 Smectic C	
1.3.4 Discotic mesophase	
2. <u>CHAPTER TWO</u>	
Polymer liquid crystals	7
2.1 Chemical constitution of liquid crystals	
2.2 Applications of liquid crystals	
2.3 Polymer liquid crystals	
2.4 Classification of polymer liquid crystals	
2.5 Chemical constitution of thermotropic polymer liquid crystals	

CONTENTS PART ONE (contd.)

	<u>Page</u>
3. <u>CHAPTER THREE</u>	
Identification of mesophases	14
3.1 Identification of mesophase exhibited by thermotropic liquid crystalline polymers	
3.2 Microscopy	
3.2.1 Nematic modifications	
3.2.2 Smectic modifications	
3.2.3 Cholesteric modifications	
3.3 Thermal analysis	
3.4 X-ray diffraction	
3.5 Miscibility studies	
3.6 Nomenclature and notation	
4. <u>CHAPTER FOUR</u>	
Instrumentation	26
4.1 Thermal analysis	
4.2 Microscopy	
4.2.1 Examination between crossed polarisers	
5. <u>CHAPTER FIVE</u>	
Experimental	30
5.1 Synthesis of 4,4'-azodibenzoic acid	
5.2 Synthesis of 4,4'-azoxydibenzoic acid	
5.3 Synthesis of 4,4'-stilbenedicarboxylic acid	
5.4 Synthesis of 4,4'-terphenyldicarboxylic acid	
5.5 Synthesis of 4,4'-terphenyldicarbonyl chloride	
5.6.1 Synthesis of 4,4'-dihydroxyazoxybenzene	
5.6.1.1 Synthesis of 4-nitrosophenol	

CONTENTS**PART ONE****(contd.)****Page**

- 5.6.1.2 Synthesis of 4,4'-dihydroxyazoxybenzene
- 5.6.2 Synthesis of 4,4'-azoxydiphenylene diacrylate
- 5.7.1 Synthesis of 4-carbonyloxy phenol
- 5.7.2 Synthesis of 4,4'-dibenzyl-terephthalate
- 5.7.3 Synthesis of 4-carbobenzoxyl benzoic acid
- 5.7.4 Synthesis of 4-carbobenzoxyl benzoyl chloride
- 5.7.5 Synthesis of benzyl 4-(carbobenzoxy) phenyl terephthalate
- 5.7.6 Synthesis of 4-carboxyphenyl hydrogen terephthalate
- 5.8 Synthesis of cis-1,5-cyclooctane bis(p-hydroxybenzoate)
- 5.8.1 Synthesis of p-ethoxycarbonyloxybenzoic acid
- 5.8.2 Synthesis of p-ethoxycarbonyloxybenzoyl chloride
- 5.8.3 Synthesis of cis-1,5-cyclooctane bis(p-ethoxycarbonyloxybenzoate)
- 5.8.4 Synthesis of cis-1,5-cyclooctane bis(p-hydroxybenzoate)
- 5.9 Synthesis of diaza-18-crown-6-ether bis(p-hydroxybenzoate)
- 5.10 Synthesis of polymers
 - 5.10.1 Polyesters
 - 5.10.2 Polyamides
 - 5.10.3 Polyurethanes and polyureas
- 5.11 Notation of monomers and nomenclature of polymers

CONTENTS PART ONE (contd.)

	<u>Page</u>
RESULTS AND DISCUSSION	
6. <u>CHAPTER SIX</u>	
Flexible spacer in mainchain liquid crystalline polymers	41
6.1 Introduction	
6.2 Smectic polymers	
6.2.1 Polymer COHB-4	
6.2.2 Polymer COHB-10	
6.2.3 Polymer COHB-3	
6.2.4 Discussion	
6.3 Nematic polymers	
6.3.1 Polymer COHB-5	
6.3.2 Polymer COHB-6	
6.3.3 Polymer COHB-7	
6.3.4 Polymer COHB-8	
6.3.5 Polymer COHB-9	
6.4 The odd-even effect	
7. <u>CHAPTER SEVEN</u>	
Effect of substituents	72
7.1 Polymer TA-III	
7.2 Polymer BTA	
7.3 Polymer NTA	
7.4 Comparison of polymers with different substituents	

CONTENTS PART ONE (contd.)

	<u>Page</u>
8. <u>CHAPTER EIGHT</u>	
Chiral liquid crystalline polymers	78
8.1 Copolymer TA-MAAs	
8.2 Copolymer BTA-MAAs	
8.3 Copolymer NTA-MAAs	
8.4 Comparison of cholesteric polymers with different substituents	
9. <u>CHAPTER NINE</u>	
Effect of mesogenic length	88
9.1 Polymer TA-III	
9.2 Polymer TA-II	
9.3 Polymer TA-I	
9.4 Comparison of polymers of different mesogenic length	
10. <u>CHAPTER TEN</u>	
Effect of mesogens	95
10.1 Azo-link	
10.2 Azozy-link	
10.3 Stilbene-link	
10.4 Comparison of polymers containing different mesogens	

CONTENTS PART ONE (contd.)

11.	<u>CHAPTER ELEVEN</u>	<u>Page</u>
	Effect of ring size	102
	11.1 Polymer AZO-AZA18C	
	11.2 Polymer AZOXY-AZA18C	
	11.3 Polymer STIL-AZA18C	
	11.4 Polymer TA-AZA18CHB	
	11.5 Polymer TER-AZA18C	
	11.6 Polymer APDA-AZA18C	
12.	<u>CHAPTER TWELVE</u>	
	Conclusion	108
13.	REFERENCES - PART ONE	112

<u>CONTENTS</u>	<u>PART TWO</u>	<u>Page</u>
14.	<u>CHAPTER ONE</u>	
	Mechanical properties of polymers	123
	1.1 Introduction	
	1.2 Mechanical properties	
	1.2.1 Description of mechanical properties	
	1.2.2 Linear viscoelastic solids	
	1.2.3 Step function experiments	
	1.2.4 Dynamic experiments	
	1.3 Transitions and relaxations in amorphous polymers	
	1.3.1 The glass transition	
	1.3.2 Secondary transition	
15.	<u>CHAPTER TWO</u>	
	Instrumentation	132
	2.1 Torsional braid analysis(TBA)	
	2.1.1 Introduction	
	2.1.2 Sample preparation	
	2.1.3 Theory and interpretation of results	
	2.2 Osmometry	
	2.2.1 Membrane osmometer	
	2.2.2 Vapour phase osmometer	
	2.3 Nuclear magnetic resonance(nmr)	
	2.4 Mass spectrometry	
	2.5 Gas liquid chromatography	
	2.6 Elemental analysis	

CONTENTS PART TWO (contd.)

16.	<u>CHAPTER THREE</u>	<u>Page</u>
	Ring systems	139
	3.1 Introduction	
	3.2 Polymers containing ring units	
	3.2.1 Polymers containing rings in the sidechains	
	3.2.2 Polymers containing saturated rings in the mainchains	
	3.2.2.1 Polymers containing cycloalkyl units	
	3.2.2.2 Polymers containing crown ether units	
	3.3 Synthetic routes to polymers containing rings in the mainchain	
	3.3.1 Step growth polymerisation	
	3.3.2 Ring open polymerisation	
	3.3.3 Ring forming polymerisation	
17.	<u>CHAPTER FOUR</u>	
	Experimental	145
	4.1 Synthesis of medium and large rings	
	4.1.1 Synthesis of 10 membered ring	
	4.1.2 Synthesis of 12 membered ring	
	4.1.3 Synthesis of 16 membered ring	
	4.1.4 Synthesis of 18 membered ring	
	4.1.5 Synthesis of 22 membered ring	
	4.2 Synthesis of diazacrown ethers	
	4.2.1 Synthesis of diaza-12-crown-4-ether	
	4.2.1.1 Synthesis of 1,5-diamino-3-oxapentane	
	4.2.1.2 Synthesis of diglycolic acid dichloride	

CONTENTS PART TWO (contd.)

Page

- 4.2.1.3 Synthesis of 5,9-dioxo-1,7-dioxo-
-4,10-diazacyclododecane
- 4.2.1.4 Synthesis of 1,7-dioxo-4,10-diazacyclododecane
- 4.2.2 Synthesis of diaza-24-crown-8-ether
 - 4.2.2.1 Synthesis of 1,11-diamino-3,6,9-trioxaundecane
 - 4.2.2.2 Synthesis of tetraglycolyl acid chloride
 - 4.2.2.3 Synthesis of 5,15-dioxo-1,7,10,13,19,22-
-hexaoxa-4,16-diazacyclotetracosane
- 4.3 Synthesis of polymers

RESULTS AND DISCUSSION

18. CHAPTER FIVE

- Polymers containing cycloalkane
and aza-crown-ethers in the backbone** 164
- 5.0 Introduction
 - 5.1 Polyurethanes and polyureas
 - 5.1.1 General chemistry
 - 5.1.2 Reactivity of intermediates
 - 5.2 Effect of catalysts and solvents
 - 5.3 Polymers containing aza-crown-ethers
 - 5.3.1 Polyamides
 - 5.3.2 Polyureas
 - 5.3.2.1 Aza-18-crown-6-ether
 - 5.3.2.2 Aza-12-crown-4-ether
 - 5.3.2.3 Aza-24-crown-8-ether
 - 5.3.3 Conclusion

CONTENTS PART TWO (contd.)

Page

5.4	Cycloalkanes	
5.4.1	Cyclooctyl unit	
5.4.1.1	Effect of linking units	
5.4.1.2	Effect of copolymerisation	
5.4.2	Cyclodecyl unit	
5.4.3	Polymers containing larger rings	
5.4.4	Conclusion	
19.	REFERENCES - PART TWO	188

PART ONE

THERMOTROPIC MAINCHAIN LIQUID CRYSTALLINE POLYMERS

CONTAINING CYCLOALKYL AND AZA-CROWN-ETHER RINGS

'I am at a loss to give a distinct idea of the nature of this liquid, and cannot do so without many words.'

The narrative of Arthur Gordon Pym of Nantucket,
Edgar Allan Poe.

CHAPTER ONE

INTRODUCTION

INTRODUCTION

1.1 States of Matter

Conventionally, matter exists in one of three distinct states of aggregation: the solid state, where constituent molecules or atoms execute small vibrations about firmly fixed lattice positions but cannot rotate; the liquid state, characterized by relatively unhindered rotation but no long range order, and the gaseous state, where particles move freely through the entire volume of the container, under almost no constraint. The melting of normal solids involves the abrupt collapse of the overall positional order of the lattice array and marks the onset of essentially free rotation of the particles, although short range correlations of the position and orientation of molecules occur in the liquid phase.

1.2 The Fourth State Of Matter

The botanist Reinitzer discovered in 1888 a new phenomenon exhibited by cholesteryl acetate and ^{in a} more pronounced ^{form} by cholesteryl benzoate^{<1>}. These substances exhibited irridescent colours in certain temperature ranges which are characteristic of a state that was to later become known as liquid-crystalline. Reinitzer's description, which was correct in all details included the melting point(146.6C) and clearing point(180.6C) for the benzoate. Similar colour phenomena which may have been based on observations of liquid crystal phases have been mentioned even earlier, but it is difficult to separate reality from fiction. For instance in chapter 19 of his fictional work 'The Narrative of Arthur Gordon Pym' (1838)

Edgar Allen Poe describes a miraculous water that could be a liquid crystal^{<2>}.

The historical development began with morphology. The honour of discovery and for the pioneering work goes principally to Lehmann^{<3>}, Reinitzer^{<1,4>}, Gattermann^{<5,6,7>}, Vorlander^{<8>}, and Schenck^{<9>}. There was a long and fruitless argument concerning the right of discovery, but both Lehmann and Reinitzer contributed considerable amounts of knowledge and deserve recognition. Thanks to the effort of these individuals, the concept of liquid crystals was, at least in outline form, clearly defined by the turn of the century.

Lehmann used the term 'liquid crystal' to describe this state of aggregation that exhibits a molecular order in a size range similar to that of a crystal but acts more or less as a viscous liquid. However, these states are neither truly crystalline nor truly liquid, Reinitzer proposed a term 'mesophase' for these materials. Nowadays, both terms are used synonymously.

1.3 Liquid Crystal Mesophases

In 1922, Friedel^{<10>} published the classic article in the *Annales de Physique* of detailed optical studies of these mesomorphic states, in which as a result of his studies, he was able to distinguish clearly three different types of mesophase. He designated them as nematic, cholesteric and smectic.

Liquid crystals are further classified as 'thermotropic' or 'lyotropic' depending upon whether the mesophase is induced by a change of temperature or variation of solvent content.

A thorough classification of liquid crystals is illustrated in Figure 1-1.

1.3.1 Nematic mesophase

The molecular order characteristic of nematic liquid crystals is shown in Figure 1-2, and two features are immediately apparent from the figure:

(i) There is no long range orientational order, ie the molecules tend to align parallel to each other.

(ii) The nematic phase is fluid, ie there is no long range correlation of the molecular centre of mass positions.

In the state of thermal equilibrium in the nematic phase symmetry ∞/∞ and is therefore uniaxial. The direction of the principal axis \hat{n} (the director) is arbitrary in space.

1.3.2 Cholesteric Mesophase

Figure 1-3 shows the equilibrium structure of the cholesteric phase. As in the nematic phase, lack of long range translational order imparts fluidity to the cholesteric phase. On a local scale, it is evident that cholesteric and nematic ordering are very similar. However on a layer scale, the cholesteric director \hat{n} follows in a helix of the form

$$n_x = \cos(q_0 z + \theta)$$

$$n_y = \sin(q_0 z + \theta)$$

$$n_z = 0$$

where both the direction of the helix z in space and the magnitude of the phase angle θ are arbitrary. Thus the structure of a cholesteric liquid crystal is periodic with a spatial period, L , given by

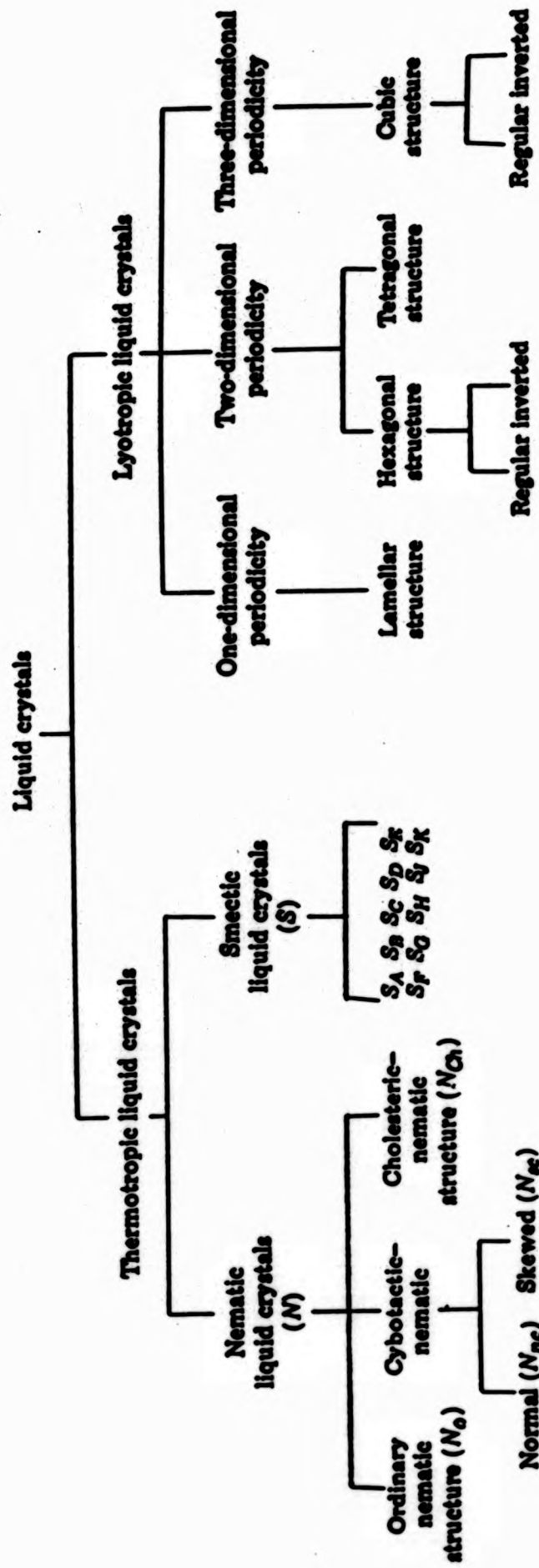


Fig. 1-1 Classification of liquid crystal structures. In addition to the normal smectic C, the cholesteric-smectic C or chiral-S_C has been identified.

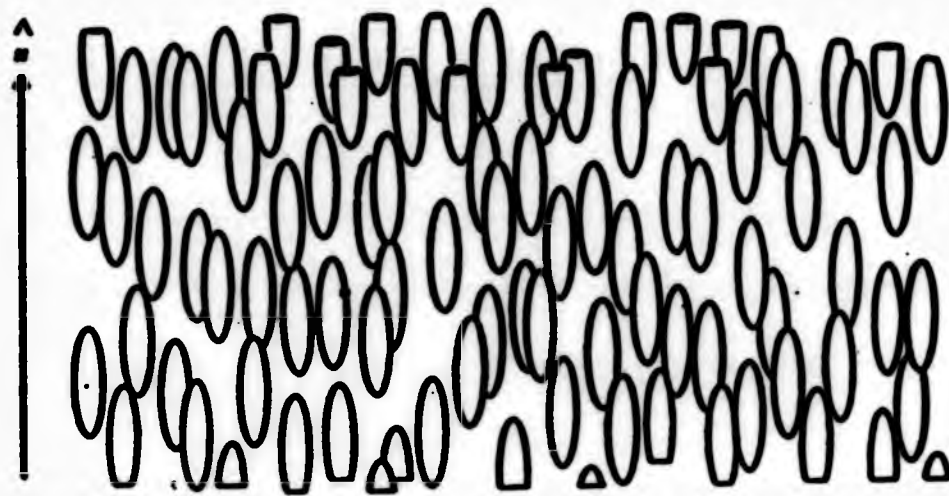


Fig. 1-2 Molecular alignment of nematic phase in low molecular weight liquid crystals.

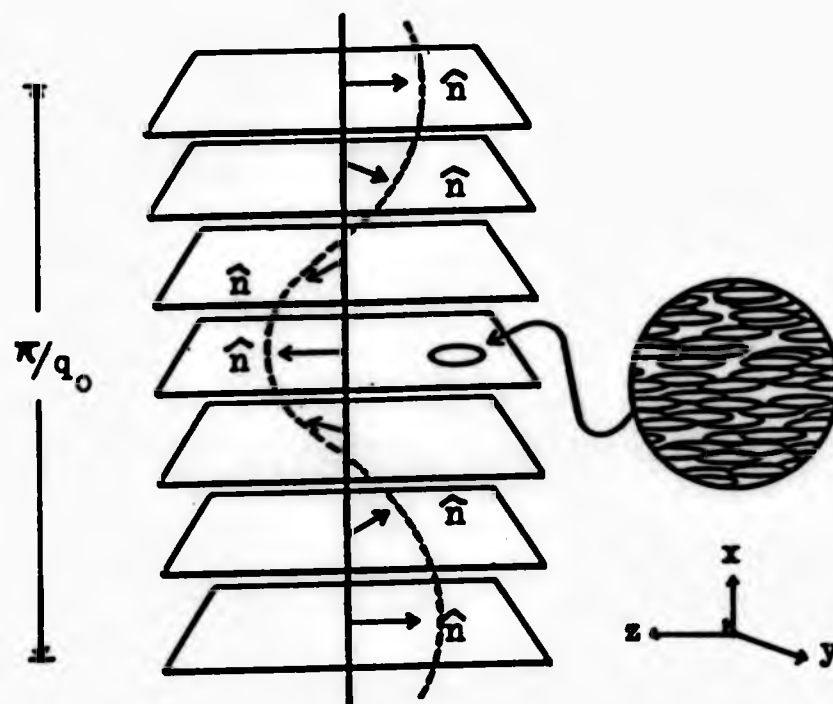


Fig. 1-3 Molecular alignment of cholesteric phase in low molecular weight liquid crystals.

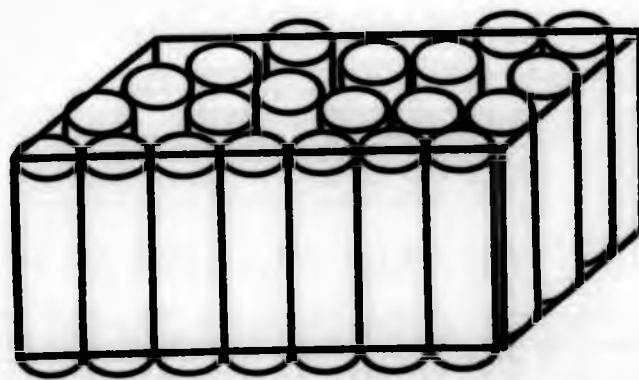


Fig. 1-4 Molecular alignment of smectic A phase in low molecular weight liquid crystals.

$$L = \pi / (q_0)$$

The sign of q_0 distinguishes between left and right helices and its magnitude determines the spatial period. When L is comparable to optical wavelengths, the periodicity results in strong Bragg scattering of light. If the wavelength of the scattered light happens to be in the visible region of the spectrum, the cholesteric phase will appear brightly coloured.

It is interesting to note that a nematic liquid crystal is really nothing more than cholesteric with $q_0 = 0$ (infinite pitch). In fact, the two are substances of the same family, the distinction being whether the equilibrium value of q_0 is zero or finite. If the constituent molecules are optically inactive, i.e. are superimposable on their mirror image, then the mesophase will be nematic. If on the other hand, the constituent molecules are optically active, i.e. are not superimposable on their mirror image, then the mesophase will be cholesteric. The term 'chiral nematic' is usually employed for these optically active, non-steroidal molecules.

1.3.3 Smectic Mesophase

As many as eight smectic phases have been tentatively identified; however, except for three that have been reasonably well characterized, considerable uncertainty still exists about the exact nature of the molecular ordering in these phases.

All smectic phases have one common feature, viz. one degree of translational ordering, resulting in a layered structure. As the consequence of this partial translational ordering, the smectic phases are much more viscous than either the nematic

or cholesteric phases.

1.3.3.1 Smectic A

Within the layers of a smectic A phase, the molecules are aligned parallel to the layer normal and are uncorrelated with respect to the centre of mass position, except over very short distances. Thus the layers are individually fluid, with a substantial probability for inter-layer diffusion as well. The layer thickness, determined from X-ray scattering data, is essentially identical to the full molecular length. At thermal equilibrium the smectic A phase is optically uniaxial due to the finite-fold rotational symmetry about an axis parallel to the layer normal. Schematic representation of smectic A order is shown in Figure 1-4.

1.3.3.2 Smectic C

The smectic C structure is similar to that of the smectic A except that the molecules in the layers are tilted at a uniform angle with respect to the normal and the structure is optically biaxial. The molecules within a smectic C layer are disorganised positionally and easily slide past one another. In some smectic C modifications, the tilt angle varies significantly with temperature, in others it remains fairly constant. A schematic diagram of the smectic C phase is depicted in Figure 1-5.

1.3.3.3 Smectic B

Smectic B differs from A and C phases, respectively in that an ordered arrangement of the molecules is obtained in the

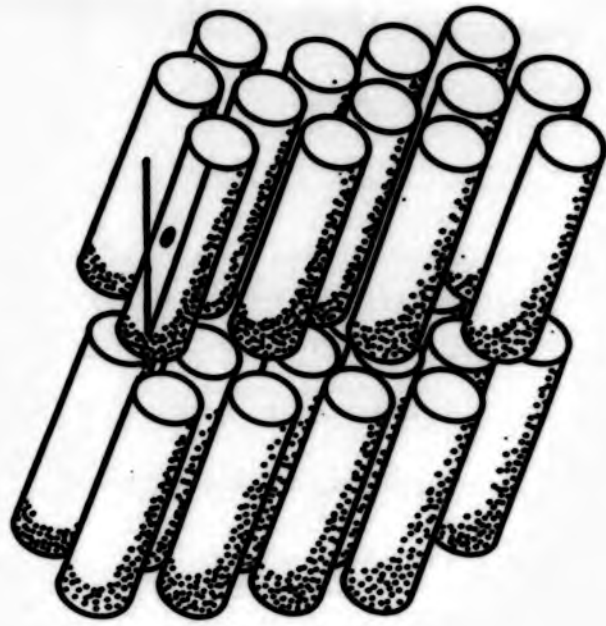


Fig. 1-5 Molecular alignment of smectic C phase in low molecular weight liquid crystals.

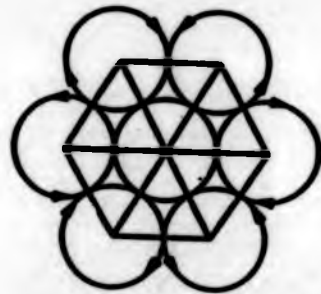
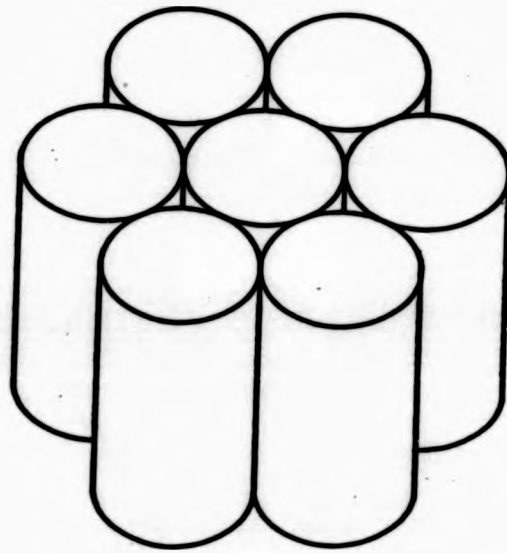


Fig. 1-6 Molecular alignment of smectic B phase in low molecular weight liquid crystals.

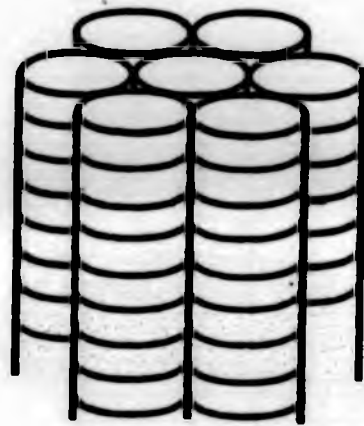


Fig. 1-7 Molecular alignment of discotic phase in low molecular weight liquid crystals.

layers rather than a disordered one. X-ray photographs of monodomains of smectic B liquid crystals indicate a hexagonal arrangement of molecules in planes that are perpendicular to the long axes (Figure 1-6). It seems that the smectic B phase is a soft solid with three dimensional ordering of finite range.

1.3.4 Discotic Mesophase

Liquid crystal states formed by disk-like molecules were first discovered by Chandrasekhar et al<11,12>. Nematic and cholesteric like low viscosity phases have been reported recently. In these, the director vector is perpendicular to the plane of alignment of the flat molecules<13>, in contrast to the normal nematics and cholesterics where it is parallel to the molecular axis. Most frequently, however, discotics form columnar arrangements as shown in Figure 1-7.

The order within the columns may change from liquid to quasi-crystalline. The columns are then packed in hexagonal or tetragonal coordination but are forced to slide in the direction parallel to their axes<14>. The viscosity of these more ordered discotics is considerably higher than the nematic discotics.

CHAPTER TWO
POLYMER LIQUID CRYSTALS

2.1 Chemical Constitution of Liquid Crystals

Our conception of the correlations between chemical constitution and liquid crystalline properties is largely based on the work of Vorlander<15>, Weygand<16>, and Gray<17>. These investigators discovered four general criteria that indicate a molecule's predisposition to form a liquid crystal:

- (a) Long, narrow, rod shaped molecules have the most suitable geometry, especially in cases where rigid groups are implied.
- (b) Permanent dipolar groups are present in almost all molecules that form mesophases.
- (c) Almost all mesomorphically arranging molecules have a high anisotropy of polarizability.
- (d) In addition, the melting point must not be too high, lest only supercooled metastable mesophases be formed monotropically.

2.2 Applications of Liquid Crystals

In his pioneering work more than 50 years ago, Vorlander<18> had already considered the idea of technical applications of liquid crystals without, however, finding a possibility. Only in the last two decades has a renewed and intensive study begun to make technological use of the unique properties of liquid crystals.

The orientational association of liquid crystals is only partial and as the nature of the intermolecular forces is delicate, they are extraordinarily sensitive to external perturbations, eg temperature, pressure, electric or magnetic field, or foreign vapours. It is this unique feature which allows them to be used as practical devices to monitor ambient changes or to transduce an environmental fluctuation into a

useful output. Liquid crystals are used widely in electric display devices, eg, digital watches and calculators; oscillographic and television displays use LC screens; radiation and pressure sensors; optical switches and shutters, and thermography<19>.

It is well known that the utilisation of low molecular weight thermotropic liquid crystals(MWLC) in most cases is restricted by the necessity for special hermetic protective shells(electrooptical cells, microcapsules etc.) which endow a constructional shape needed and protect LC compounds from outside influence. In the case of thermotropic LC polymers there is no need for such sandwich-like constructions because the properties of low MWLC and of the polymeric body are combined in a single individual material. This opens up new perspectives for their application.

2.3 Polymer Liquid Crystals

Even before Staudinger had finally recognised the true nature of macromolecular compounds, Vorlander<18> had postulated that 'infinitely long molecules' would be comparable with the supramolecular organisation constraints in liquid crystals. After Vorlander's early contributions, research on polymeric liquid crystals(PLC) in the second quarter of this century was, for all practical purposes, dormant.

Birefringent solutions of rod-like virus particles(lyotropic PLC) were reported in the late 1930s and early 1940s<20>. The α -helical, rod-like, synthetic polypeptide, poly(γ)-benzyl-L-glutamate(PBLG), was shown to

form a lyotropic PLC in a variety of common organic solvents in the early 1950s<21>. It was during the preparation of oriented specimens for I.R.-dichromism studies of the α -helix that the unusual properties of the concentrated solutions of PBLG were first noticed.<22> Robinson and coworkers then characterized the PBLG liquid crystal, demonstrating that the chiral rods(right-handed α -helices) assumed a twisted nematic(cholesteric) supramolecular arrangement in the lyotropic mesophase<23-27>.

In the mid 1960s monomeric liquid crystals with a single functional group(eg vinyl group) were polymerized to form a sidechain PLC. Melts of such sidechain polymers retained liquid-crystal textures(nematic, smectic and cholesteric) over a defined temperature range usually in excess of that exhibited by the monomer LC; ie the PLC mesophase relative to the monomeric liquid crystals(MLC) could be 'stabilised' via polymerisation<28>. It seems during that time, sidechain PLCs were synthesised only because they could be prepared by non-synthetically inclined students of physical chemistry, eg cholesterol acrylate, a commercially available MLC, could be heated into its cholesteric phase, allowing the thermally induced polymerisation to proceed; a solid, dimensionally stable, cholesteric polymer film which reflected iridescent colors was obtained<29>. Since these early crude experiments, technologically important end-uses for sidechain PLCs have been identified:(1) cholesteric PLCs function as tuneable wavelength reflectors and notch filters<30>; (2) sidechain copolymers solubilise dichromic dye additives to electro-optic displays<31>; (3) they serve as a noncentrosymmetric host

matrices for hyperpolarisable guest molecules in non-linear optical devices<32>; (4) lyotropic smectic MLCs can be polymerised to stabilise vesicles in drug-delivery schemes<33>. Extensions of the latter to smectic monolayers could stabilise thin organic dielectric layers for microelectronic device fabrication<34>. There have also been efforts to incorporate oblate, disc-like mesogenic cores into thermotropic sidechain PLCs<35>.

During roughly the same period that sidechain PLCs were first synthesised, linear block copolymers prepared from monomers with distinctly different chemical properties were shown to aggregate into liquid crystalline textures in the melt or in the presence of a solvent for one of the blocks<36>. Block copolymer solids with well developed, microphase separated morphologies exhibit unique mechanical properties, and preferentially swollen copolymers yield a variety of morphologies<37>.

The development of linear, mainchain PLCs was more intentional and directed. The potential end uses for linear PLCs (high thermal stability and high tensile strength) focused research on these materials<38>. Expanding on the background provided by research on liquid crystalline phases formed by biological macromolecules<39>, in particular, the anomalously low viscosity of the mesophase<40> relative to the isotropic solution, it would have seemed logical, in retrospect, to design explicitly linear PLCs. Curiously, some polymers subsequently shown to be thermotropic linear PLCs of the semi-flexible polyester type (high aromatic content) were studied in industrial research laboratories in the early

1960s; when ultra-strength materials were being sought. However, the liquid crystalline nature of the fluid phases of these polymers appears to have been overlooked^{<41>}. It was not until Kwolek rationalised the unusually high tensile strengths exhibited by fibres spun from concentrated solutions of the poly(aryl amides) that the critical importance of mesophase formation was recognised^{<42,43>}. Dobb and McIntyre have recently reviewed the development of the industrially important PLCs^{<44>}. The Kevlar(Du Pont) and Arenka(Akzo) poly(aryl amide) lyotropic PLCs have received the most publicity, although commercialisation of thermotropic PLCs has just been announced^{<45>}.

2.4 Classification of Polymer Liquid Crystals

The definition of the liquid crystal state of MLCs' and polymer liquid crystals does not differ. Following the classification of Gray and Winsor^{<46>}, one can distinguish between two types of chemical constitution of liquid crystals (figure 2-1) namely (1) non-amphiphilic LC and (2) amphiphilic LC.

Non amphiphilic LCs can be further differentiated into LC molecules having a cylindrical molecular shape and those having a disc-like shape.

The occurrence of the liquid crystal state of low molar mass substances is, always related to a defined chemical constitution. The idea is obviously to tie up the mesogenic molecule to a macromolecule by a suitable chemical reaction. Assuming the mesogenic structure of the single molecule remains unchanged by polymerisation and can be found in the

MONOMER UNIT	AMPHIPHILIC	NON AMPHIPHILIC	
		CYLINDRICAL	DISCOURIC
MONOMER UNIT			
MAIN CHAIN POLYMER			
SIDE CHAIN POLYMER			

Fig. 2-1 Classification of liquid crystalline polymers.

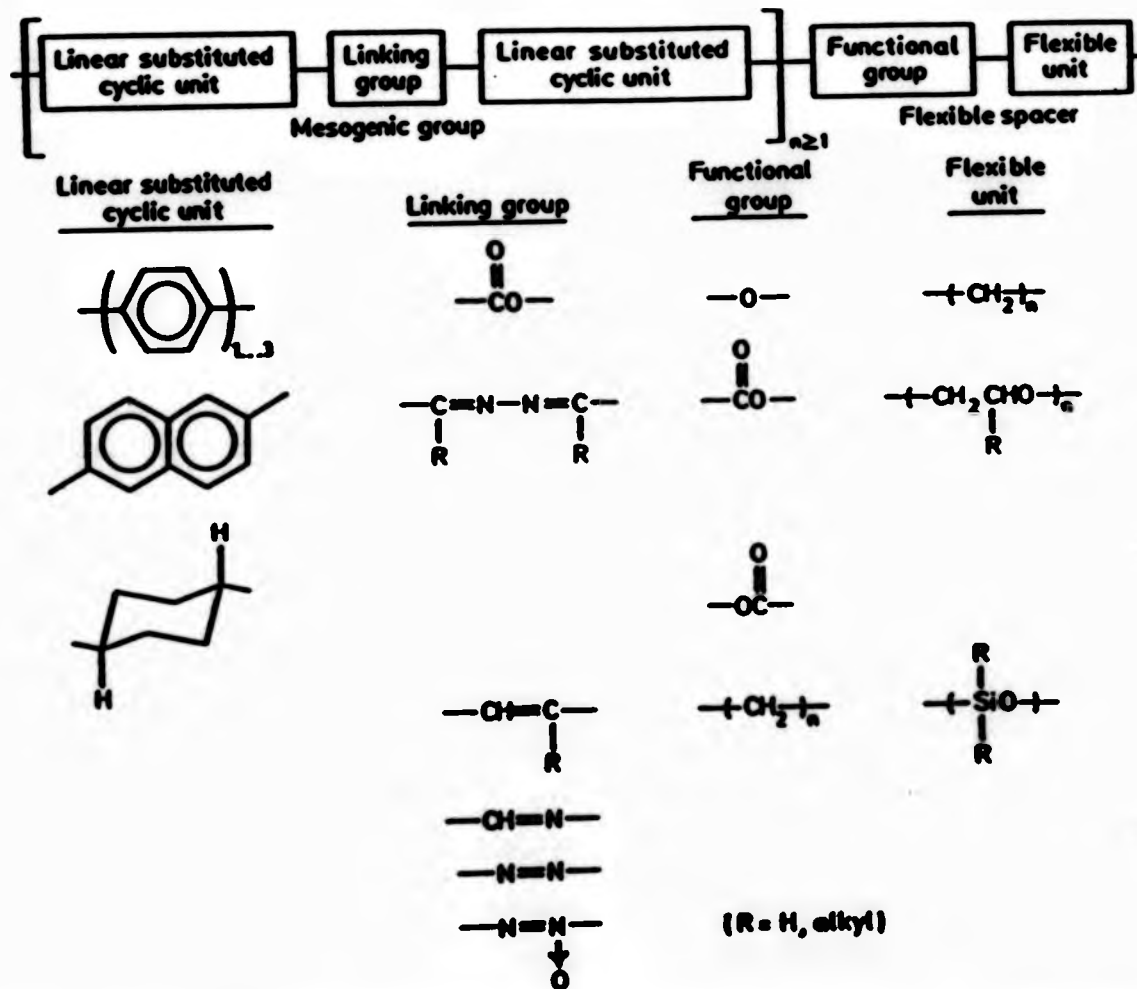


Fig. 2-2 General structure of liquid crystalline polymers having both a linear rigid mesogenic group and flexible spacer in the mainchain.

monomer unit of the polymer, it can be expected that the macromolecules also exhibit the liquid crystalline state.

In principle two different possibilities exist to form a macromolecule from mesogenic reactive monomeric liquid crystals (MLC) (i) mainchain polymer: where the MLCs are tied up by suitable reactive substituents head to tail.

(ii) sidechain polymer: where the MLCs are tied up head to head. This can be performed by using a polymerisable substituent linked to the mesogenic monomer or by addition of a reactive monomer to a polymer backbone.

2.5 Chemical Constitution of Thermotropic

Mainchain LC Polymers

The term 'mesogenic group' is used to refer to the part of the polymer chain that is composed of the rigid, linear segments and the atoms or functional groups which link them together in a linear array, even although these units may or often do not possess intrinsic mesogenic character.

Figure 2-2 is a schematic representation of the general structure of a liquid crystalline polymer having both a linear rigid mesogenic group and flexible spacer in the mainchain. The mesogenic group must consist of at least two aromatic (or cycloaliphatic) rings connected in the para-positions by a short rigid link which maintains the linear alignments of the aromatic rings. In this manner a rigid element is formed which has an overall length that is substantially greater than the diameter of the aromatic group. The linking groups used in LC polymer systems have included imino, azo, azoxy, ester, trans-vinylene and acetylene groups, and a direct link between

aromatic rings may also be used, such as biphenyl and terphenyl units.

CHAPTER THREE

IDENTIFICATION OF MESOPHASES

3.1 Identification of Mesophases Exhibited by Thermotropic Liquid Crystalline Polymers

In 1975, Roviello and Sirigu^{<47>}, prepared new polyalkanoates from p,p'-dihydroxy- α,α' -dimethylbenzalazine and appropriate ^{ba-}acyl chlorides. All the examined polymers melted to give fluid anisotropic phases whose textures and properties appeared quite similar to those observed with conventional liquid crystals, hence the denomination of 'thermotropic liquid crystalline polymers'. Identification of the type of mesophase is thus an important step in the characterization of these materials. The more definitive procedures used for classification of low MWLCs are^{<46,48,49,50>}: (a) Optical pattern of texture observation with a polarizing microscope. There are, however, limitations and a complete classification of smectic phases by texture is not always possible. (b) Differential scanning calorimetry(DSC) can be used to distinguish between thermotropic nematic and smectic phases by the magnitude of the enthalpy change accompanying the transition to the isotropic phase. (c) X-ray investigations. Differences in molecular long range order can be established by small angle X-ray diffraction. Classical X-ray methods only provide information on short range order. (d) Miscibility studies with known liquid crystalline materials. Isomorphous mesophases are considered as equivalent and characterized by the same symbol. (e) Possibility of inducing significant molecular orientations by either supporting surface treatments or application of external fields.

Owing to the high viscosity, broad molecular weight distribution, and the existence of polycrystalline and amorphous materials, the liquid crystalline nature of thermotropic polymers is usually established by a combination of these methods.

3.2 Microscopy

The characterisation of LCs by means of the polarising microscope^{<48,51>} is the most straightforward method available and whenever possible, it should be carried out in the initial stages of an investigation on new polymers. Thermal analyses alone can be misleading. In this procedure, a thin layer of the melt is kept at constant temperature on a hot-stage and observed between crossed polars. Polymeric materials take minutes or hours to show recognisable textures, and in that time period the polymers can decompose.

3.2.1 Nematic Modifications

Several polymers when examined under the polarising microscope exhibit threaded and/or schlieren textures indicative of nematic phases (Plates 3-1 & 3-2)^{<52-57>}.

Upon cooling an isotropic melt, the nematic phase begins to separate at the clearing point typically in the form of droplets which, after further cooling, grow and coalesce to form large domains^{<48>}. Nematic droplets characterise a type-texture of the nematic phase since they occur nowhere else^{<66>}. When observed between crossed polarisers, the schlieren texture shows dark brushes which join at certain points. In some cases, four extinction bands are seen to



Plate 3-1 The threaded texture of the nematic phase

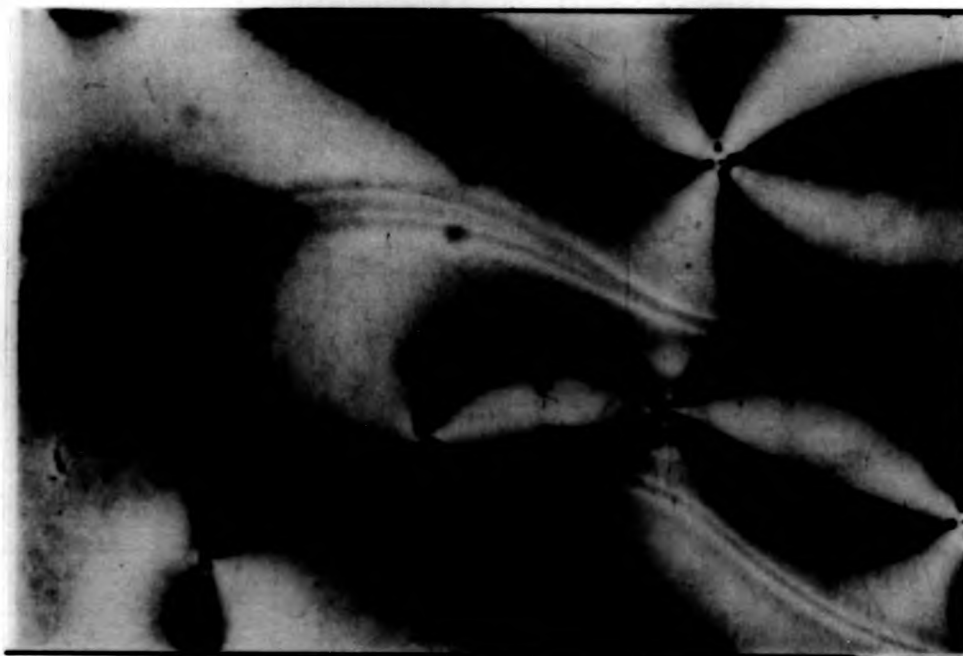


Plate 3-2 The schlieren texture of the nematic phase -



Plate 3-1 The threaded texture of the nematic phase

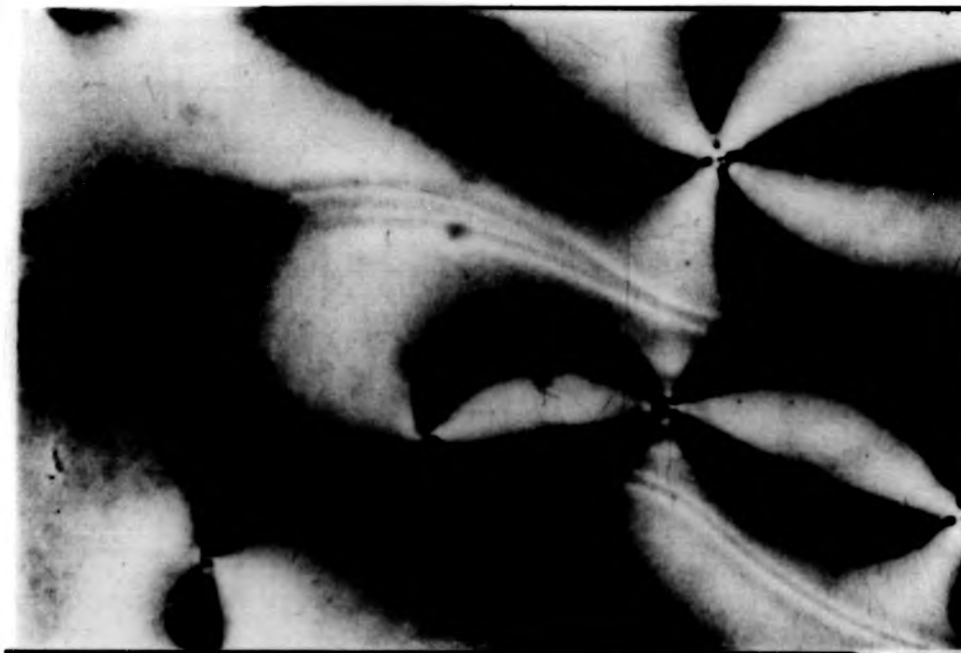


Plate 3-2 The schlieren texture of the nematic phase



Plate 3-1 The threaded texture of the nematic phase

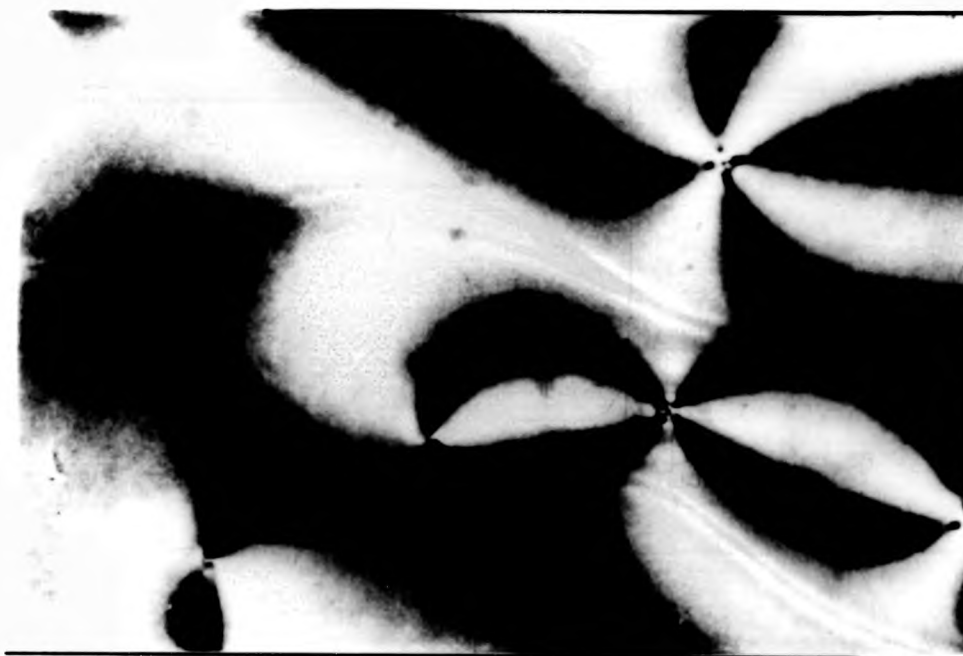


Plate 3-2 The schlieren texture of the nematic phase

radiate from the centre. Such points indicate defects of the structure<52,57,64,65>. However, there are also defects which appear as points at which only two dark brushes meet<52,57,58,64>. From the observation of the latter defects, the mesophase can be unambiguously identified as a nematic phase since these defects occur in no other LC phases<48,66>.

The homogeneous texture occurs in the nematic and only in very special cases of the smectic phase. In this case, the optical axis of the sample lies parallel to the surface boundary of the layer. Sometimes the term planar texture is used in the same meaning. In nematic homogenous textures, a typical example is the marbled texture which exhibit sharp, straight bordered areas that impart a rod-like appearance to the preparation (Plate 3-3)<67>.

Among the more difficult textures to identify is the homeotropic or pseudo-isotropic texture<48,51,60>. By a suitable surface treatment, it is possible to obtain uniformly aligned samples with the optical axis normal to the glass surfaces<62,65,68>. Such samples with a homeotropic texture show no birefringence in orthoscopic observation when viewed vertically. However, if the cover glass is touched, the originally dark field of view brightens instantly, thus distinguishing between a homeotropic and isotropic texture. At high temperatures, perfect layers of this kind, observed between completely crossed polarisers, show a grainy appearance which constantly changes. These scintillation effects are due to a directly observable Brownian motion.

A method of avoiding the formation of the homeotropic texture involves the use of specially treated glass surfaces.



Plate 3-3 The marble texture of the nematic phase

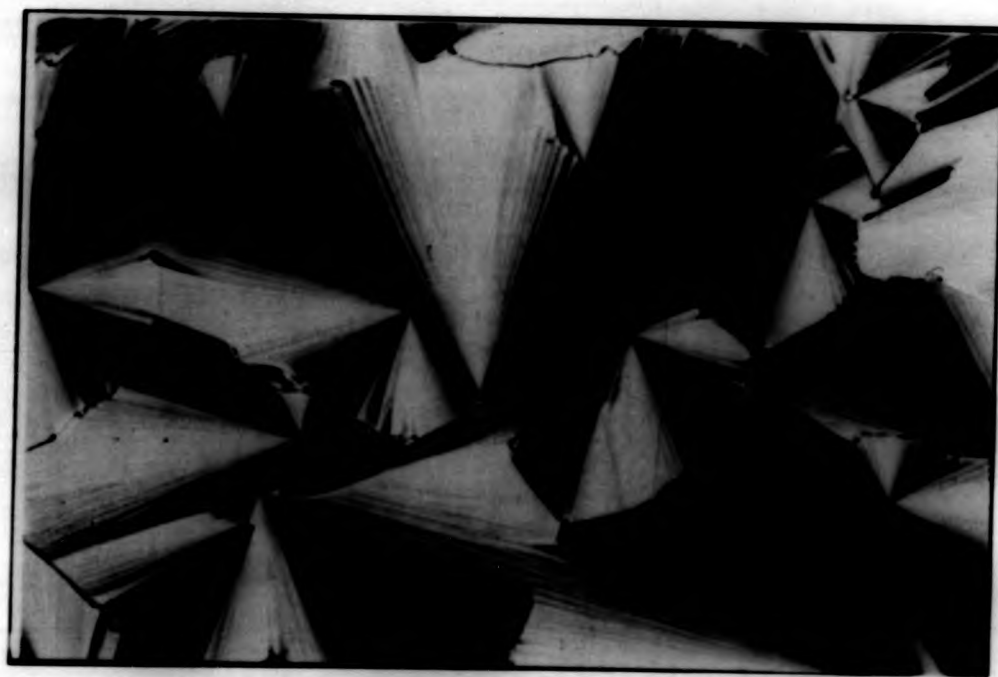


Plate 3-4 The focal-conic fan texture of the smectic A phase

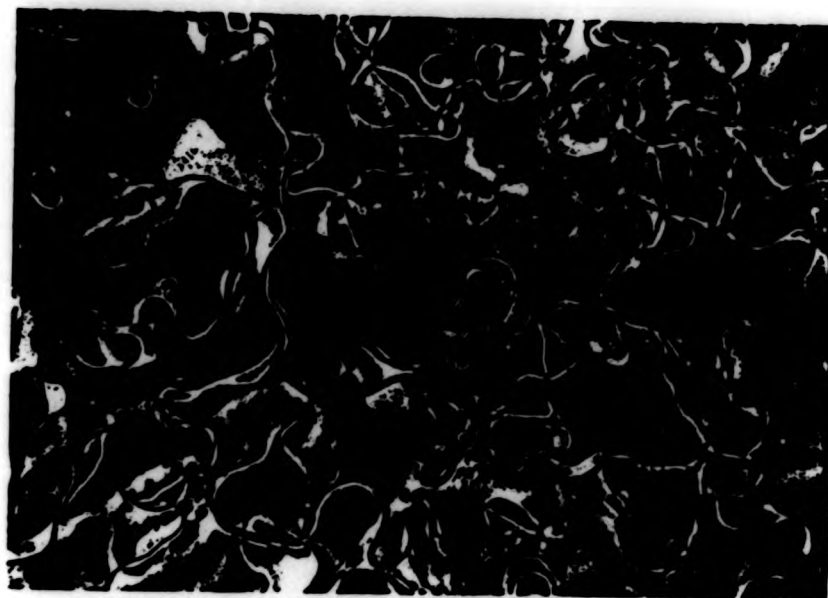


Plate 3-3 The marble texture of the nematic phase

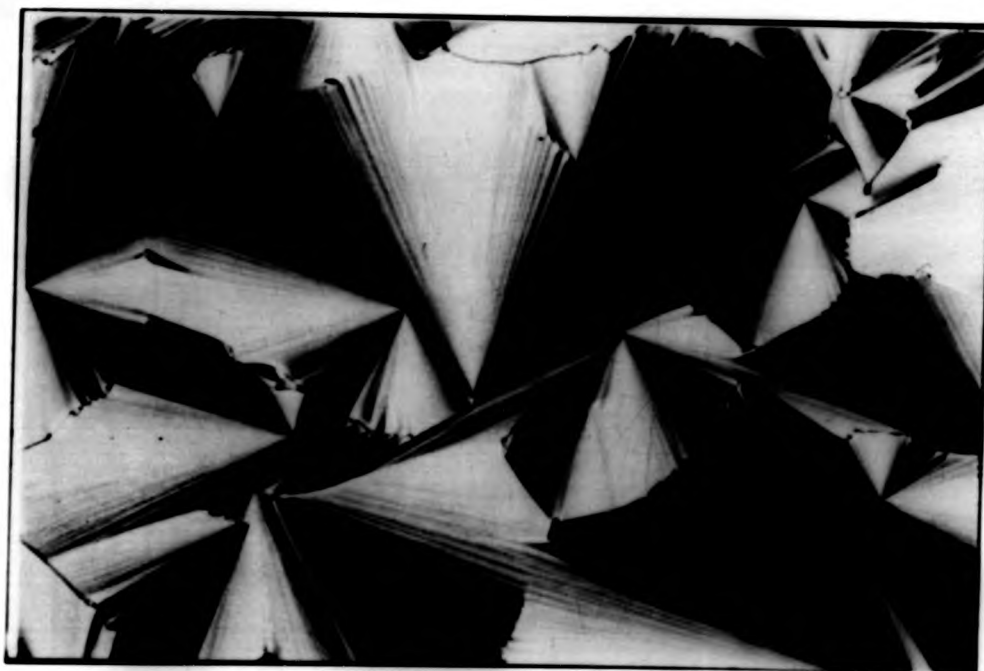


Plate 3-4 The focal-conic fan texture of the smectic A phase

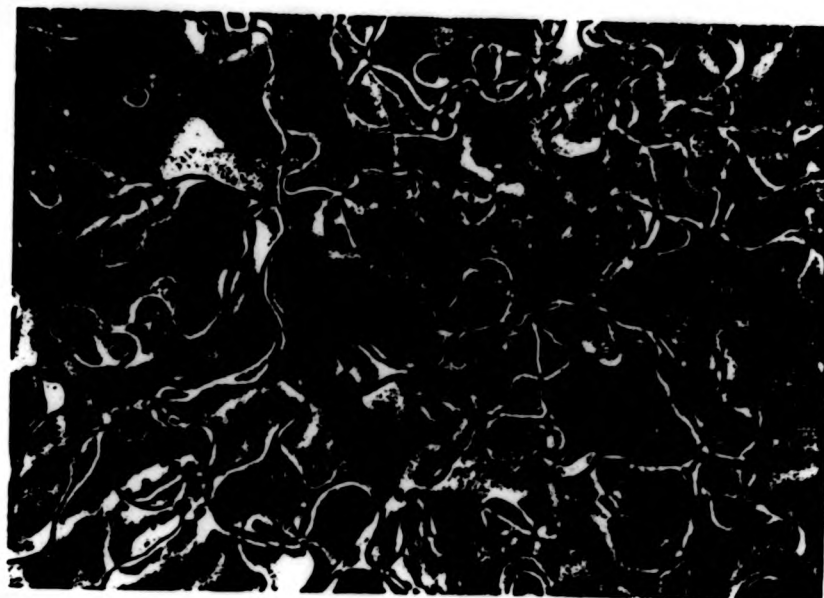


Plate 3-3 The marble texture of the nematic phase

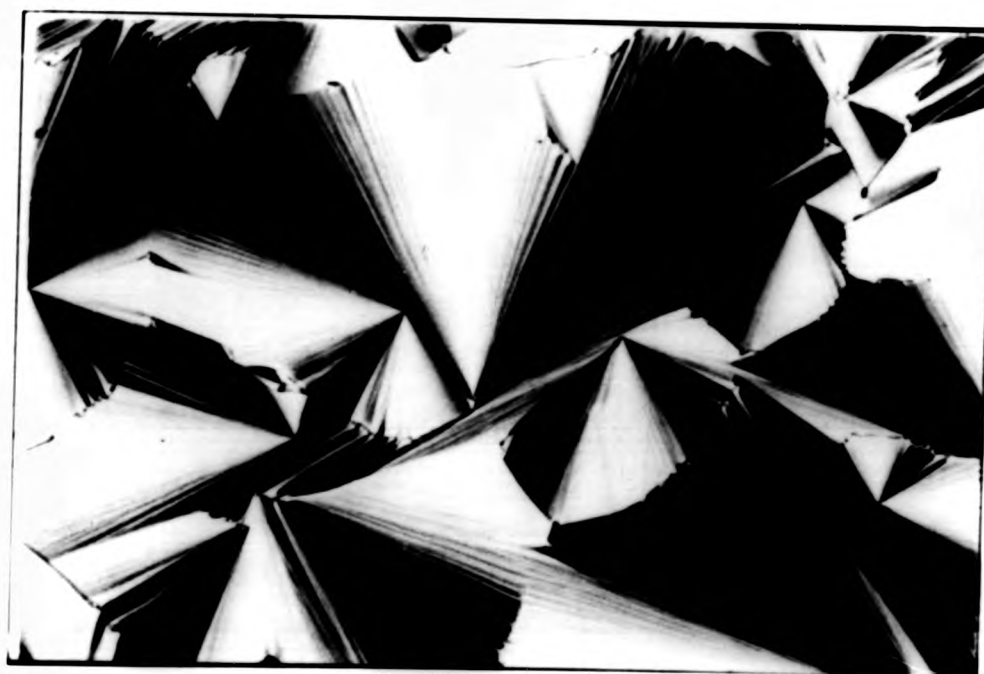


Plate 3-4 The focal-conic fan texture of the smectic A phase

By obliquely evaporating SiO₂ on the glass surface, the new surface causes an alignment of the mesophase at an angle to the incident light<69>.

It is possible to quench the polymers from the nematic phases to room temperature thereby 'freezing in' these nematic-like textures<52,54,56,62,64,65,70,71,72>. In spite of the thermal shock, both the homeotropic alignment and the planar one can be retained in the glassy state.

Identification of mesophases by microscopy is subject to a great deal of subjective interpretation. A more quantitative approach to microscopy involves measuring the depolarised light intensity with a photocell, and plotting this quantity as a function of temperature. This approach is particularly useful in determining the clearing transition when rather broad transitions, quite usual in polymers, are obtained<68>. Unless care is taken to ensure a constant field of view and constant sample thickness, this method should be considered to be only a semi-quantitative measure of depolarised light intensity.

3.2.2 Smectic Modifications

In the case of smectic polymers, observation of specific textures may be difficult. Often textures occur whose characteristics are somewhat obscure and observable only with difficulty even at large magnification. This might be due to the high viscosities of the smectic melts<48>. Coats and Gray have recently written a detailed review on microscopic observation of smectic texture<73>.

Smectic A and C phases, hitherto the most frequently

observed of the presently known smectic phases, are recognised by the typical fan shaped or focal-conic texture. Smectic C phases show the fan texture less distinctly; Sackmann called them 'broken focal-conic' or 'sand-like' textures (Plates 3-4 and 3-5).

In smectic phases, the so called batonnets are closely related to the focal-conic texture. Batonnets are rod shaped with cylindrically symmetrical protrusions and are formed when an isotropic melt cools just before separation of the smectic phase as a whole. Batonnets correspond to the nematic droplets, with regard to formation conditions. The batonnets join together to form larger structures from which the compact focal-conic texture finally forms. Smectic A and nematic phases are similar in their tendency to form homeotropic textures. The homeotropy in an open preparation may persist through a phase transition thus concealing it from microscopic observation(Plate 3-6).

The smectic B phase exhibits the unmistakable mosaic texture. It should be noted that smectic C phases and smectic B phases can also exhibit schlieren textures<74>.

According to publications of Sackmann et al.<66> the smectic textures and phase transitions observed up to now are patterned in the following order:-

Smectic A

Smectic D

Smectic C

Smectic B

Smectic E

Smectic F,G,H.....

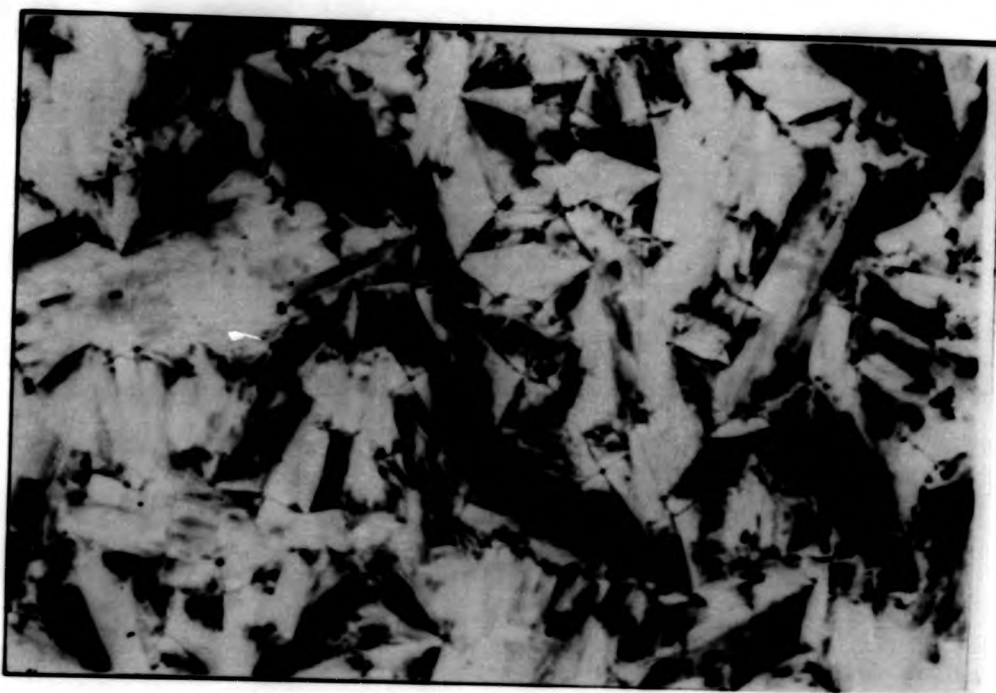


Plate 3-5 The paramorphotic focal-conic fan texture of the smectic C phase formed on cooling the smectic A phase

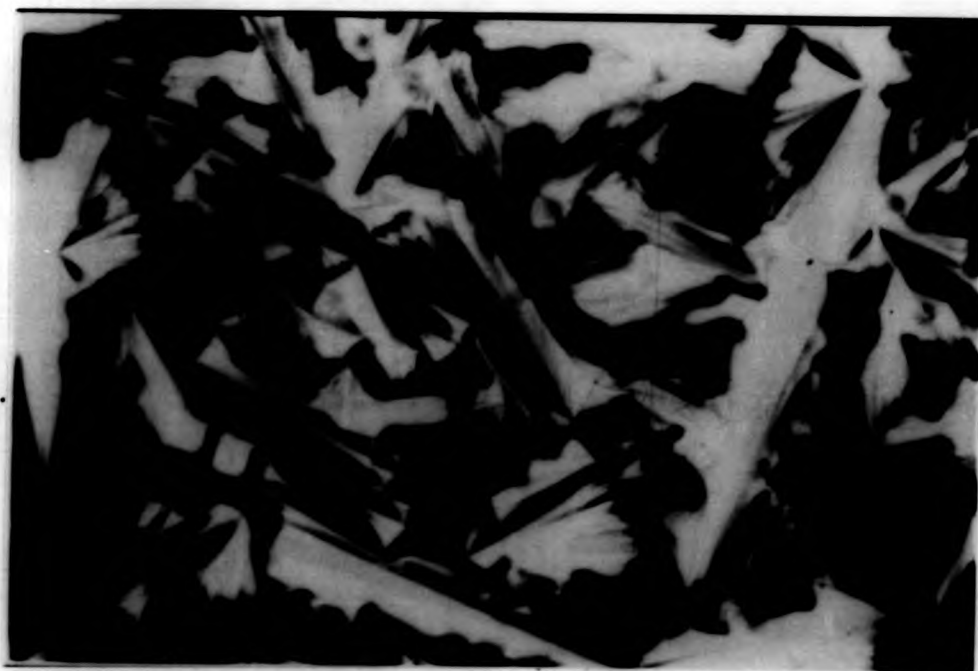


Plate 3-6 The separation of the smectic A phase in the form of batonnets from the isotropic liquid

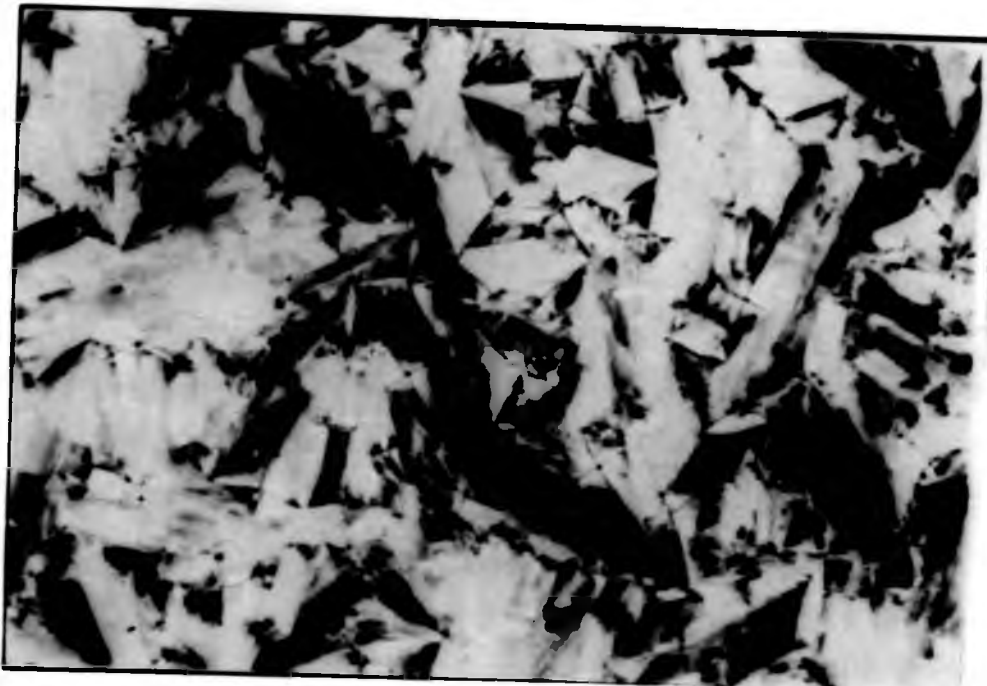


Plate 3-5 The paramorphotic focal-conic fan texture of the smectic C phase formed on cooling the smectic A phase

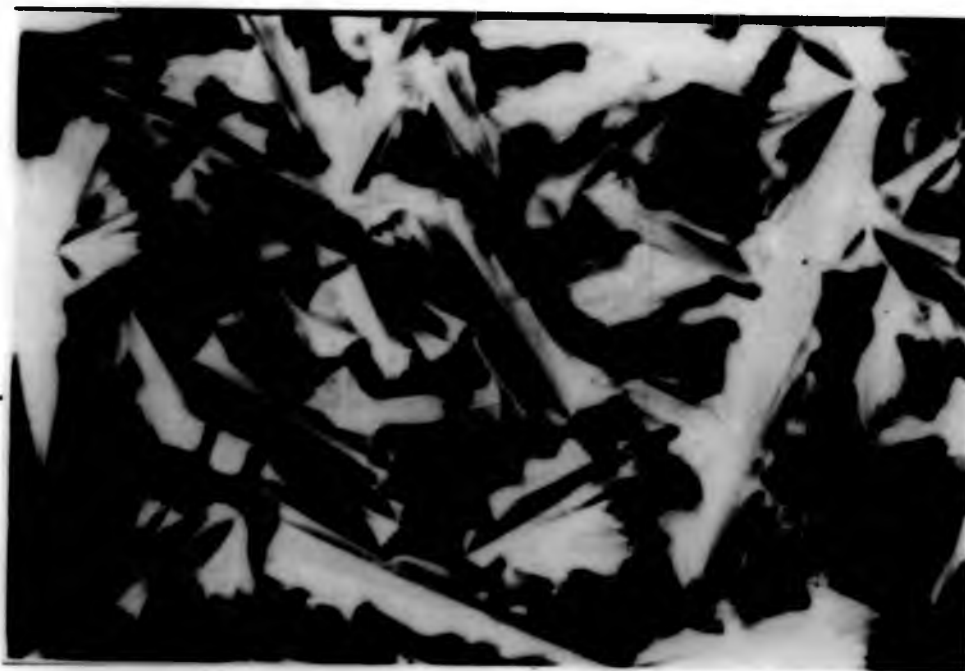


Plate 3-6 The separation of the smectic A phase in the form of batonnets from the isotropic liquid

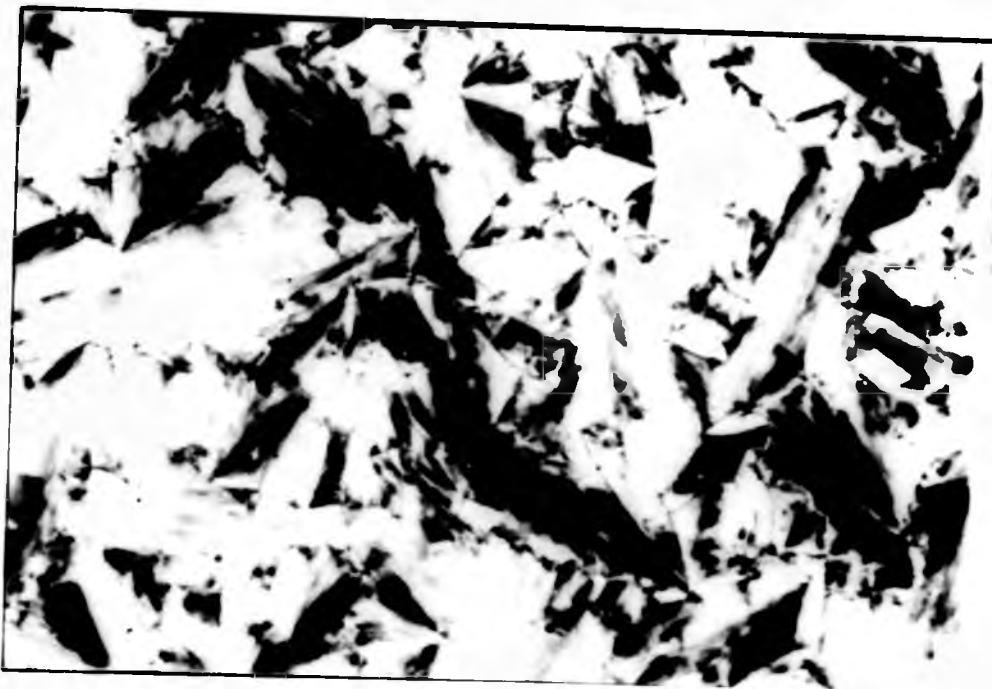


Plate 3-5 The paramorphotic focal-conic fan texture of the smectic C phase formed on cooling the smectic A phase



Plate 3-6 The separation of the smectic A phase in the form of batonnets from the isotropic liquid

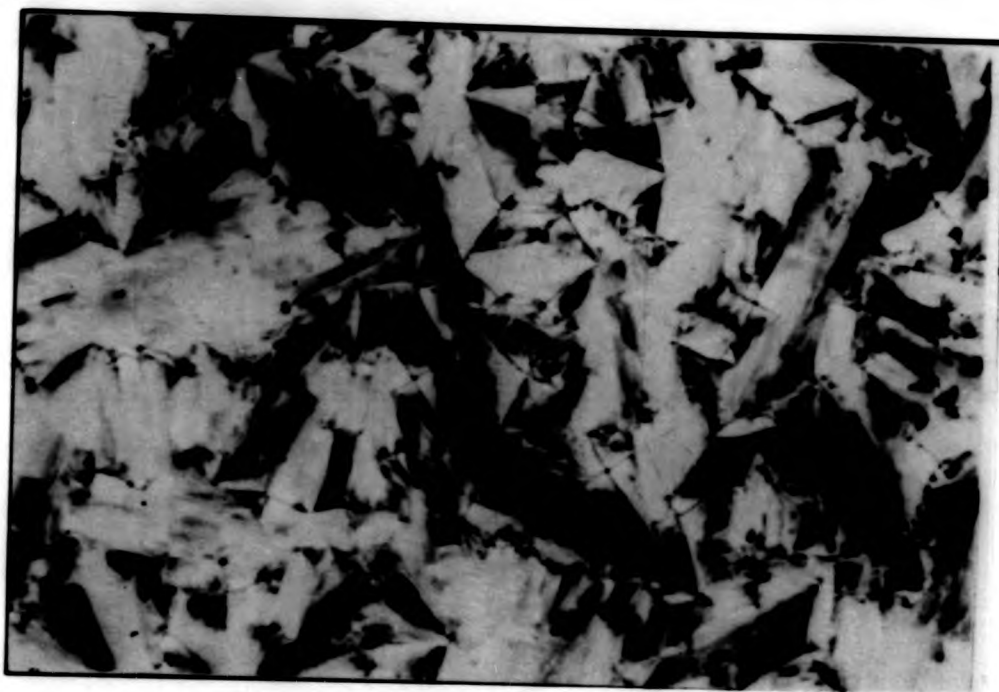


Plate 3-5 The paramorphic focal-conic fan texture of the smectic C phase formed on cooling the smectic A phase

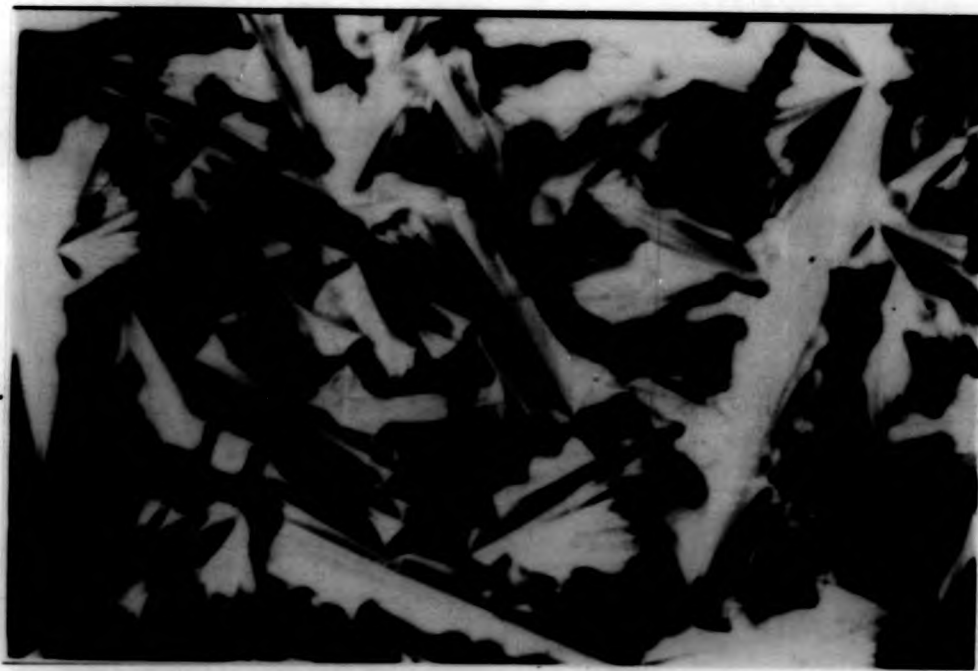


Plate 3-6 The separation of the smectic A phase in the form of batonnets from the isotropic liquid



Plate 3-5 The paramorphotic focal-conic fan texture of the smectic C phase formed on cooling the smectic A phase

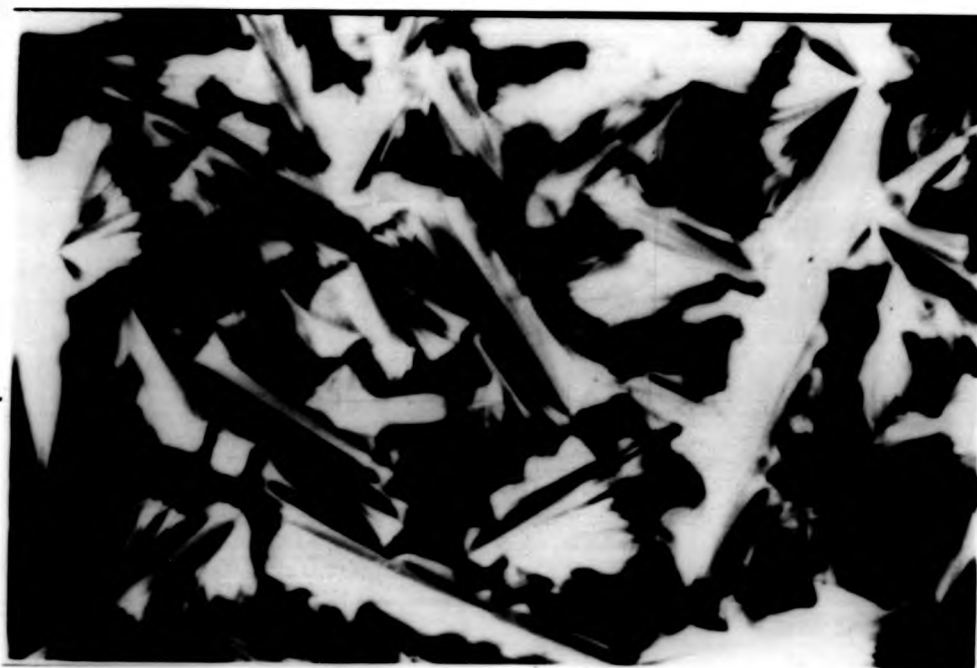


Plate 3-6 The separation of the smectic A phase in the form of batonnets from the isotropic liquid

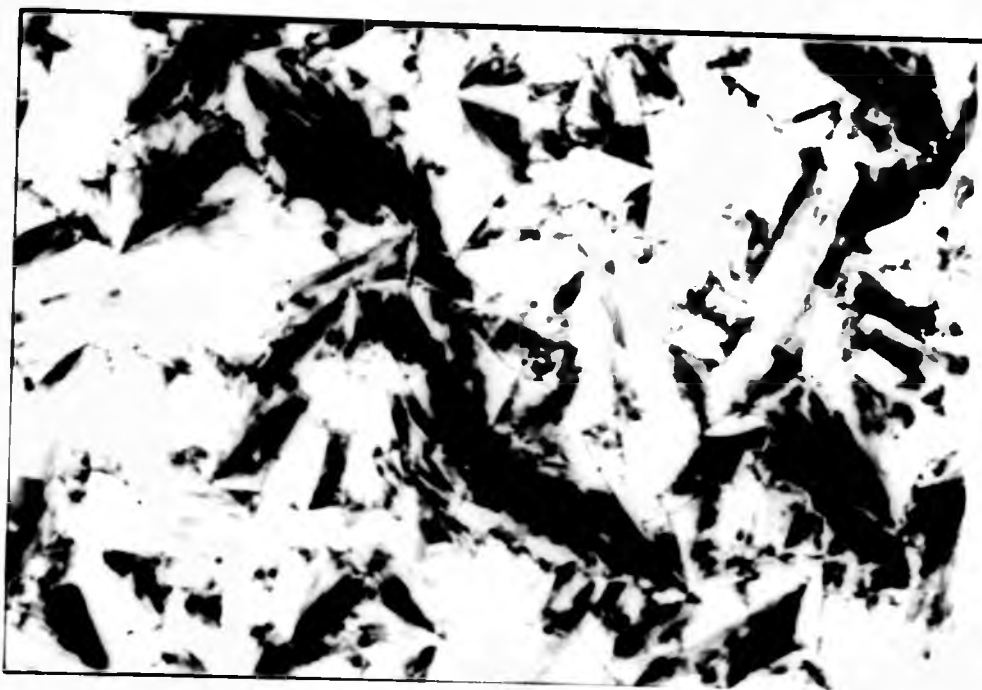


Plate 3-5 The paramorphic focal-conic fan texture of the smectic C phase formed on cooling the smectic A phase



Plate 3-6 The separation of the smectic A phase in the form of batonnets from the isotropic liquid

3.2.3 Cholesteric Modifications

Conventional nematic liquids can be changed into cholesteric ones by doping them with small amounts of optically active materials<49,66>. Chiral compounds on addition to polymers in the nematic state also yield cholesteric liquids<52,53,60,63>. They exhibit typical planar textures with oily streaks, 'Moire fringes' and/or 'Grandjean' lines. In the planar texture, these cholesterics can show bright reflection colours, The wavelength of the light at the centre of the reflection band is, for perpendicular incidence, equal to the length of the pitch multiplied by the mean refractive index(Plate 3-7).

Another possibility is offered by introducing chirality into the molecular structure. Copolymerisation or copolycondensation of a monomer, capable of forming a thermotropic nematic homopolymer, with a chiral compound yields cholesteric copolymers<58,63,75>. The optical properties of these cholesteric copolymers resemble those of conventional cholesteric compounds<70,76,77>.

3.3 Thermal Analysis

As pointed out by Finkleman<70> in his recent review, the essential features of the phase behaviour of liquid crystalline sidechain polymers are relatively well established.

However, the thermal behaviour of LC mainchain polymers is more complicated. In most cases, samples show a glass transition, melting, and mesophase-mesophase and/or



Plate 3-7 Plane texture of the cholesteric phase

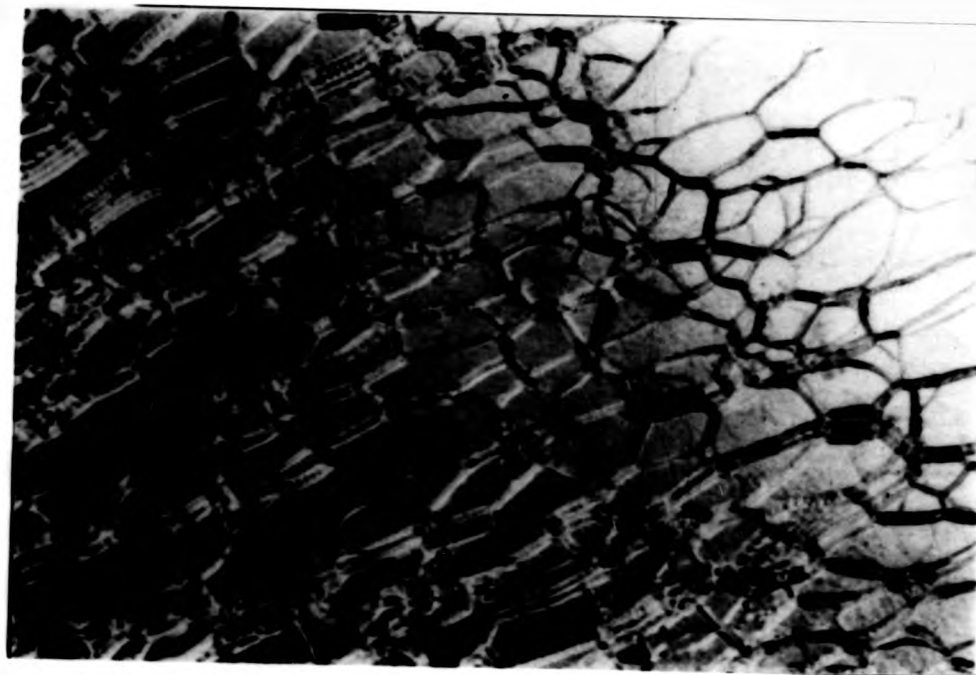


Plate 3-7 Plane texture of the cholesteric phase

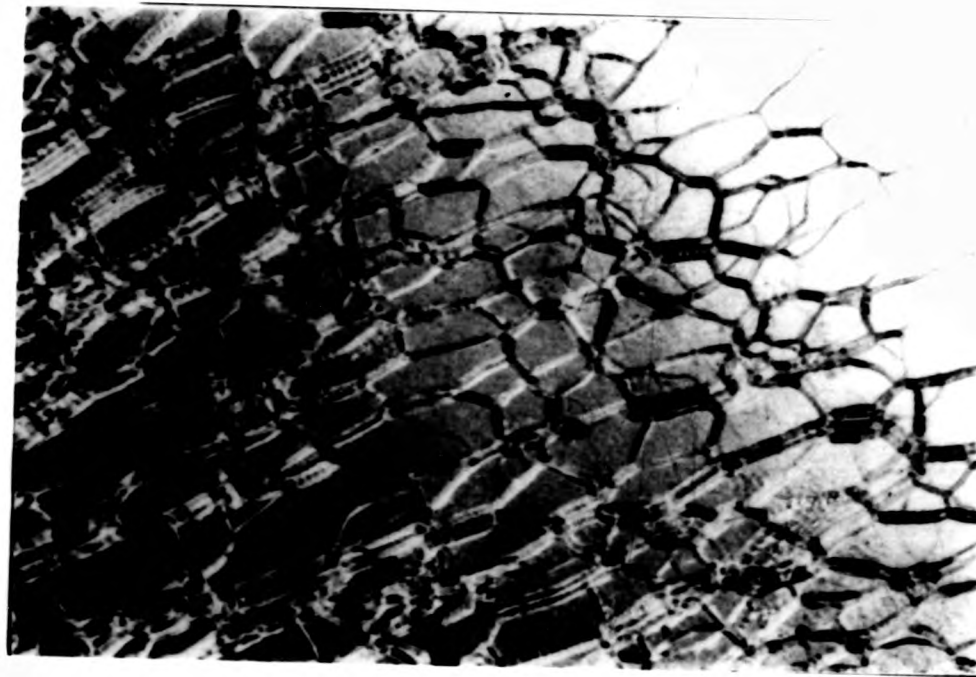


Plate 3-7 Plane texture of the cholesteric phase

mesophase-isotropic liquid transitions. Quickly cooled samples may demonstrate so called 'cold crystallisation' when heated above the glass transition $\langle 52,78 \rangle$. However, as observed by Grebowicz et al. $\langle 79 \rangle$ for low MWLCs, the temperature behaviour depends on the cooling rate: the slower the cooling rate, the smaller are the glass transition and the cold crystallisation exotherm features(Figure 3-1).

Most studies of polymeric and model LC compounds have been performed using the DSC technique.

The melting temperatures of polymeric materials can be greatly affected by the sample history, but it is now commonly agreed that the clearing transition is much less subject to the effects of thermal treatment. If it can be assumed that the clearing transition is an equilibrium process, then the entropy of this transition, ΔS_i , can be calculated from the clearing temperature and from the enthalpy of the transition. Values of ΔS_i give some indication of the order present in the system when the isotropic state is assumed to have equal disorder in all systems.

The enthalpy changes associated with the melting of polymers are usually lower than those determined for small molecules of similar chemical structure $\langle 54,80 \rangle$. This difference reflects the lack of ability of polymers to form crystals having regularity and perfection. Hence the values of the enthalpy of the melting and clearing transitions to be very similar.

Many polymers show clearing entropies larger than those determined for the low MW model compounds $\langle 58,78,80,81,82 \rangle$. Considering the number of possible defects in a polymer

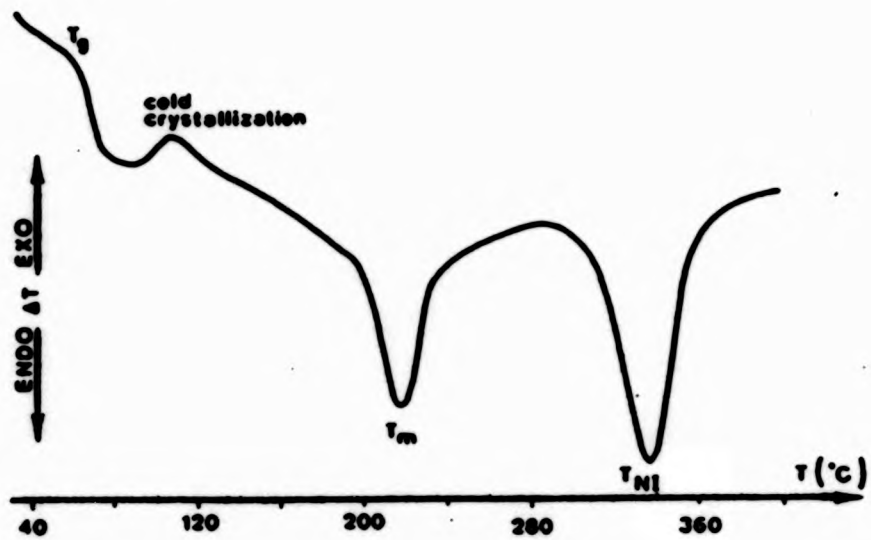


Fig. 3-1 Typical DSC thermogram of thermotropic liquid crystalline polymers.

mesophase from chain entanglements, or from the chains connecting the ordered regions, the possibility of a higher order in the polymer mesophase is surprising. A possible explanation, might be that the higher values of ΔS_i result from the mixing between the spacer and the mesogenic groups at high temperature.

The nematic state is less highly organized than the smectic state, and the difference would be expected to be reflected in similar differences in the entropy of clearing.

3.4 X-Ray Diffraction

X-ray diffraction provides information concerning the arrangement and the mode of packing of molecules and the types of order present in a mesophase. Based on the observations by X-ray diffraction made with small molecules as reviewed by Azaroff<83> a system for identifying the type of mesophase has been developed by DeVries<84>, and this system is now being applied to polymeric liquid crystals.

The diffraction pattern of a polymer sample can be divided into inner rings at small diffraction angle(SAXD) and outer rings at wide angles(WAXD). The inner rings are indicative of longer layer spacings. The outer rings correspond to shorter preferred spacings occurring in the lateral packing arrangement of the molecules. The appearance of a broad halo or a sharp ring furnishes a qualitative indication of the degree of order.

In WAXD, nematic structures produce a diffuse ring(4-5A). This diffuse halo, which is quite similar to that given by the isotropic liquid phase, indicates a lack of periodic lateral

order. In SAXD, nematic patterns may present a diffuse ring, corresponding to a distance close or equal to the repeating unit length which indicates that there is no order in the direction of the molecular long axes.

Cholesteric mesophases in general resemble the nematic mesophase when observed by both SAXD and WAXD.

The smectic mesophase, in contrast, produces both diffuse rings at 4-5A and sharp rings at a distance generally, but not necessarily, equal to the repeat length of the monomer unit, between 15 and 50A. Smectic A and smectic C mesophases, give only one diffuse outer halo which indicates that the lateral arrangement of the molecules is disordered: the distribution of the molecular centres of mass is random. For smectic C phases, diffraction patterns are essentially the same as those for smectic A except that the layer spacings are usually relatively smaller. In a smectic A phase, the director is normal to the layers which are about one repeat unit thick. The accepted structure for smectic C is that the director is tilted with respect to the layers: the lamellar thickness is less than the repeat unit length.

For smectic phases which exhibit three dimensional order: the smectic B and smectic E and their tilted modifications; the smectic G and smectic H, the diffraction patterns show a single or several outer rings which are related to the high degree of order within the layers. The smectic I and smectic F phases are intermediate between these two groups.

X-ray ^{diffraction} patterns obtained from mainchain polymers in the smectic state are characteristic of a disordered lamellar structure. If the sample can be obtained in the form of an

oriented monodomain, it is possible to extract more detailed structural information from its diffraction diagram. Alignment in the sample can be caused by shearing, or application of electric or magnetic fields.

3.5 Miscibility Studies

A complete classification of smectic phases by texture is not always possible. Another technique which uses microscopy is based on the miscibility of compounds with identical mesophases and was first developed by the Halle liquid crystal group for model liquid crystals. Noel has applied this method to mixtures composed of well known model liquid crystals with polymeric liquid crystals^{<63,68>}. Assuming that the method is applicable to mixtures of polymers and low MW compounds, the type of mesophase can be positively identified if the polymer and the model are miscible.

Transition temperatures and the number of transitions can be determined by thermal analysis as performed by Griffin and Havens^{<85>}. By combining the thermal observations with the microscopic observations, a phase diagram can be drawn which indicates whether or not the phases are miscible.

The addition of chiral compounds to their nematic or smectic C phases can be used to convert the mesophases to the cholesteric or twisted smectic C phases, respectively^{<68>}. In this way the possibility of other mesophases being present can be eliminated, and these two mesophases can be differentiated by X-ray diffraction.

The high viscosity of polymer mesophases could possibly prevent the mixing of the mesophases of polymers and certain

model compounds. Therefore, while the miscibility of model compounds with a polymer may be used to identify the type of mesophase, the lack of compatibility does not necessarily suggest that the mesophases are not the same. That is, some model compounds and polymers with the same mesophase may even be inherently incompatible. As a result, some judgement is required in order to make both the proper choice of the model compound and the correct assignment of the mesophase when using this technique.

3.6 Nomenclature and Notation

The various phases and their range of existence can be advantageously indicated by a uniform line notation based on the work of Kelker<49> and Gray<17>. This notation incorporates the following symbols that will be generally used in the following text:

k	crystalline solid
i	isotropic liquid
s	smectic mesophase
n	nematic mesophase
ch	cholesteric mesophase
d	thermal decomposition

According to tradition, the melting point appears to the right of 'k', and the clearing point to the left of 'i'. This disposition brings the transition temperatures rising from the left to the right, as the following example will illustrate:-

k 300K Sc 347K Sa 453K n 500K i

In this case, the crystalline solid melts at 300K to a smectic C phase, at 347K it transforms into a smectic A phase, at 453K

model compounds. Therefore, while the miscibility of model compounds with a polymer may be used to identify the type of mesophase, the lack of compatibility does not necessarily suggest that the mesophases are not the same. That is, some model compounds and polymers with the same mesophase may even be inherently incompatible. As a result, some judgement is required in order to make both the proper choice of the model compound and the correct assignment of the mesophase when using this technique.

3.6 Nomenclature and Notation

The various phases and their range of existence can be advantageously indicated by a uniform line notation based on the work of Kelker<49> and Gray<17>. This notation incorporates the following symbols that will be generally used in the following text:

k	crystalline solid
i	isotropic liquid
s	smectic mesophase
n	nematic mesophase
ch	cholesteric mesophase
d	thermal decomposition

According to tradition, the melting point appears to the right of 'k', and the clearing point to the left of 'i'. This disposition brings the transition temperatures rising from the left to the right, as the following example will illustrate:-

k 300K Sc 347K Sa 453K n 500K i

In this case, the crystalline solid melts at 300K to a smectic C phase, at 347K it transforms into a smectic A phase, at 453K

into a nematic phase, and at 500K into an isotropic liquid.

CHAPTER FOUR
INSTRUMENTATION

4.1 Thermal Analysis

Accurate temperature measuring techniques were all firmly established in Europe by the late 1800s. As a result, it was inevitable that they would soon be applied to the chemical systems at elevated temperatures. In 1964 Watson et al.<86> and O'Neill<87> introduced the the first differential scanning calorimeter(DSC). Most of the commercial systems are described in detail in a monograph by Wendlandt<88>. DSC is an ideal tool for use in polymer characterisation, and parameters such as melting point(T_m), glass transition temperature(T_g), and specific heat measurements etc. can be studied rapidly and conveniently.

DSC is a technique of non-equilibrium calorimetry in which the heat flow into or from a sample and reference is measured as some function of time and temperature(dH/dt).

The system employed was a Perkin-Elmer DSC-2<89>, which was equipped with a low temperature mode accessory and capable of measurements in the temperature range 100-1000K. A schematic diagram of the DSC-2 is shown in Figure 4-1.

Polymer samples with weights of ca. 10 mg were used and studied at a scan rate of 20K/min. The temperature read out of the instrument was calibrated with pure metal standards (Hg, Ga, In & Pb) to $\pm 0.2K$. All experiments were conducted under a dry nitrogen atmosphere.

The measurement of heat capacity is based upon the power expenditure required to heat the empty sample container compared to that required for the sample container with the sample. These two measurements are then compared to a third

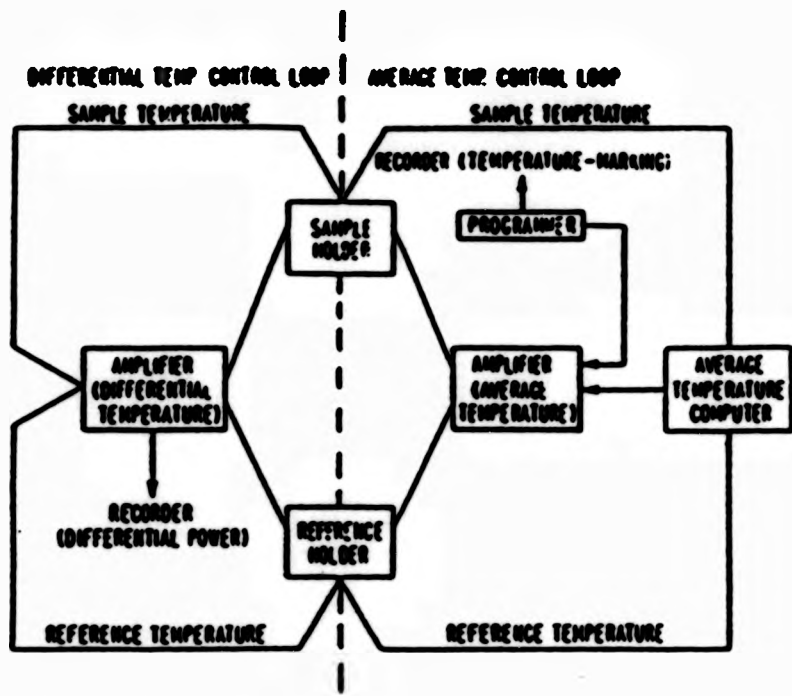


Fig. 4-1 DSC schematic

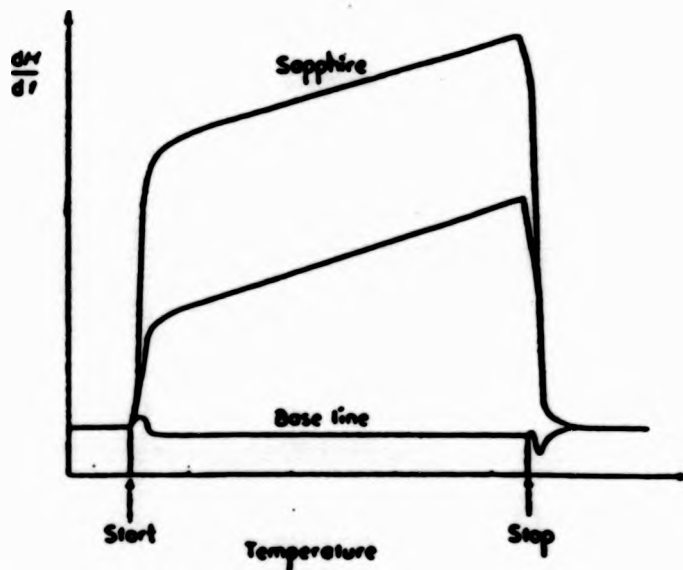


Fig. 4-2 DSC chart recorder traces.
The middle trace is the sample deflection.

measurement over the same temperature range made on a material of known heat capacity. The procedure is described as follows:-

Empty aluminium pans are placed in the sample and reference holders. An isothermal base line is recorded at the lowest temperature chosen and the temperature is then programmed to increase over the required range, at a chosen rate. An isothermal base line is recorded at the higher temperature as indicated in Figure 4-2.

The two isothermal base lines are used to interpolate a reference base line over the scanning section as shown in the same figure. The above procedure is then repeated with a known mass of sample in the sample pan and a trace of dH/dt against time is recorded. There is a recorder deflection due to the absorption of heat by the sample and thus

$$dH/dt = mC_p(dT_p/dt)$$

where m is the mass of the sample and (dT_p/dt) is the programmed rate of temperature increase.

This equation could be used to obtain values of C_p directly, but any errors in recorder read-out of dH/dt and in the programming rate (dT_p/dt) would reduce the accuracy. To minimise these errors the procedure is repeated with a known mass of sapphire in the sample pan, the heat capacity of which is well established, and a new trace is recorded. Thus two ordinate deflections $D(\text{sample})$ and $D(\text{sapphire})$ at any chosen temperature are obtained as shown in Figure 4-2 and yield the ratio of the C_p values of the sample and sapphire. The value of C_p for the sample can then be calculated from the following equation:-

$$C_p(\text{sample}) = \frac{D(\text{sample})}{D(\text{sapphire})} \times \frac{n(\text{sapphire})}{n(\text{sample})} \times C_p(\text{sapphire})$$

4.2 Microscopy

Originally developed to meet the needs of the petrologist and mineralogist, the polarising microscope has become an important tool in liquid crystal studies<51>. A polarising microscope is essentially a compound microscope except that in addition it has a polariser, an analyser and in some cases a slot for compensators used for specific measurements or effects (Figure 4-3).

A Reichert Thermo-var polarising microscope fitted with a hot-stage was employed throughout the studies. Magnification is 100 times in all cases.

4.2.1 Examination Between Crossed Polars

Specimens observed with the polarising microscope can be divided into two types: isotropic and anisotropic. Isotropic materials have identical properties in all directions, that is, they have only one index of refraction. Anisotropic materials, on the other hand, do not have identical properties in all directions, those having two indices of refraction are called uniaxial, while those having three indices of refraction are called biaxial. Hence all anisotropic substances are birefringent.

The analyser is really identical to the polariser in every way except for its position in the light trains. If the analyser is crossed at right angle to the polariser (Figure 4-4-a), an isotropic specimen sandwiched between them will

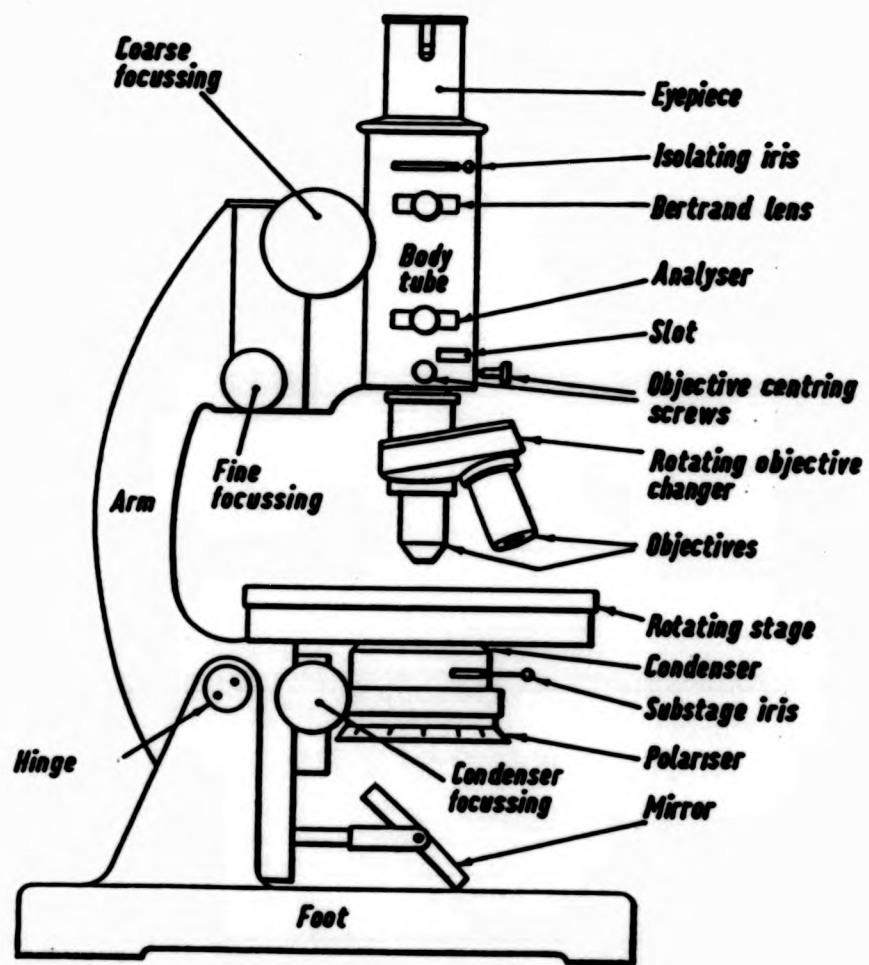


Fig. 4-3 Schematic diagram of polarising microscope

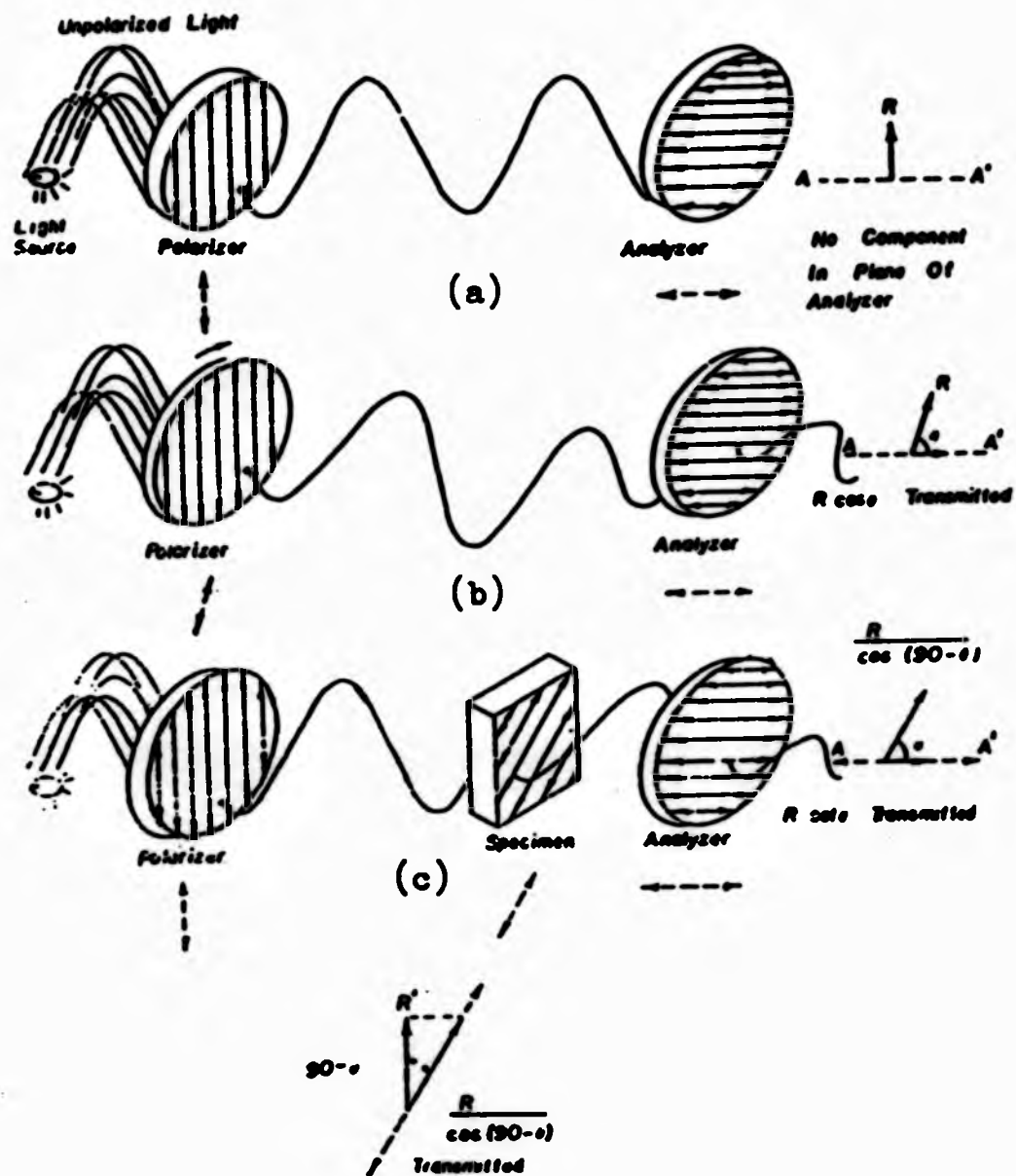


Fig. 4-4-a, b and c

Diagram of the polarised light transmission by the polariser and analyser:

- (a) crossed polaroids. The field of view will be dark because the light transmitted by the polariser (R) has no trigonometric component in the plane of the analyser.
- (b) The polariser has rotated so that the light transmitted by it (R) has a trigonometric component ($R \cos \theta$) in the plane of the analyser. Thus the field of view will be light.
- (c) The plane polarised light from the polariser (R) is rotated by the crystalline specimen and a component ($R/\cos(90-\theta)$) is transmitted to the analyser, whereupon another trigonometric component ($R \cot \theta$) is transmitted producing bright field.

darken the entire field of view. If the analyser or polariser is rotated(Figure 4-4-b), the trigonometrical component from the polariser in the plane of the analyser will be transmitted by the analyser. Similarly if an anisotropic specimen observed between crossed polars rotates the plane polarised light, the trigonometrical component in the plane of the analyser will be transmitted by the analyser(Figure 4-4-c).

In this study, the polymer sample was clipped between two thin glass cover slips and loaded on the hot-stage, the temperature was increased gradually through the melting, mesomorphic and isotropic transitions. There are always discrepancies between transition temperatures obtained using the polarising microscope and DSC, which usually arise because the rubbery state of the polymer before melting impedes formation of the homeotropic texture.

CHAPTER FIVE

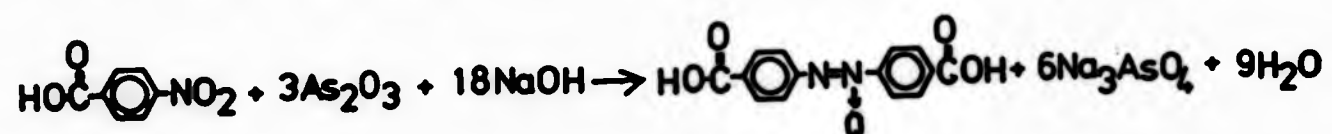
EXPERIMENTAL

5.1 Synthesis of 4,4'-Azodibenzoic Acid<90>



To the mixture of p-nitrobenzoic acid(100g,0.598Mol), methanol(750ml) and 250ml NaOH solution(95.73g,2.39Mol) was added zinc dust(78.24g,1.197Mol) with stirring and left overnight. The mixture was filtered while hot, and the precipitate was washed with warm methanol(500ml) to remove residual p-nitrobenzoic acid, then washed with warm 2% HCl solution to remove zinc salts. After filtration, the orange solid was dissolved in 10% NaOH solution, filtered and neutralised with 10% HCl. The product precipitated instantly, it was filtered and dried at 100C. Yield: 43%, mp>300C, (M/e:270)

5.2 Synthesis of 4,4'-Azoxydibenzoic Acid<91>



Sodium arsenate was prepared by dissolving powdered arsenious oxide(44.39g, 0.224Mol) made into a paste with a little water in 117ml NaOH solution(53.8ml). This solution diluted with 117ml of water was added to p-nitrobenzoic acid(50g,0.299Mol), stirred and refluxed for 10 hours.

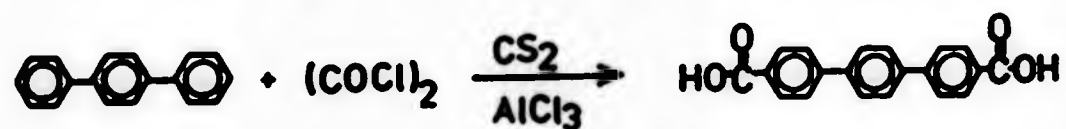
The reaction mixture was cooled and filtered. The yellow solid was washed with hot methanol and warm 5% HCl solution respectively. The crude product was then dissolved in 10% KOH solution, filtered and precipitate with 10% HCl. The yellow

powder was filtered and dried at 100C. yield: 52%, mp >300C,
(M/e:286)

5.3 Synthesis of 4,4'-Stilbenedicarboxylic Acid<92>

A mixture of p-toluic acid(40g, 0.294Mol) and sulphur(9.4g, 0.294Mol) was heated in a three necked flask equipped with an air cooled condenser, stirrer and thermometer. The mixture was refluxed at about 275C for 2 hours; during the reaction, the mixture darkened and hydrogen sulphide was evolved. When evolution of H₂S ceased, the mixture was cooled to 140C, and 200ml of hot xylene was added. The solution was refluxed 30 minutes, filtered hot, and the cake washed with hot xylene. After evaporation of the solvent, the filtered cake was extracted with 200ml of hot dioxane and dried. The crude product was dissolved in slight excess of 30% hot aqueous KOH, and the potassium salt of the stilbenedicarboxylic acid crystallized from the solution. The free acid was precipitated from the hot salt solution by adding an excess of HCl. This procedure was repeated twice. The final product was dried at 100C. Yield:23%, mp >350C,
(M/e:268)

5.4 Synthesis of 4,4'-Terphenyldicarboxylic Acid<93>



A mixture of terphenyl(45g, 0.195Mol), oxalyl chloride(150g, 1.18Mol) and carbon disulphide(300ml) was treated with stirring with 40g of anhydrous powdered aluminium

chloride. The mixture immediately turned dark brown/black. It was stirred in an ice bath for one hour, then an additional 30g of anhydrous aluminium chloride was stirred in and the ice bath removed. Stirring was continued overnight at room temperature, then the mixture was poured onto cracked ice to decompose the complex. The carbon disulphide was evaporated with a stream of nitrogen and the residual solid was filtered, washed repeatedly with dilute HCl and dried. A pale yellow solid was obtained. Yield:45%, mp >400C.

5.5 Synthesis of 4,4'-Terphenyldicarbonyl Chloride

For conversion to the acid chloride, 20g of the crude product was refluxed with 150g of thionyl chloride and 6 ml of pyridine. Part of the dicarboxylic acid gradually went into solution, the excess thionyl chloride was evaporated and the crude acid chloride was dissolved in boiling benzene. The solution was filtered free from undissolved material, treated with a small amount of decolourising charcoal and filtered again. On cooling, the benzene deposited yellow leaflets. Yield:25%, mp 216C

5.6.1 Synthesis of 4,4'-Dihydroxyazoxybenzene<94>

5.6.1.1 Synthesis of 4-Nitrosophenol

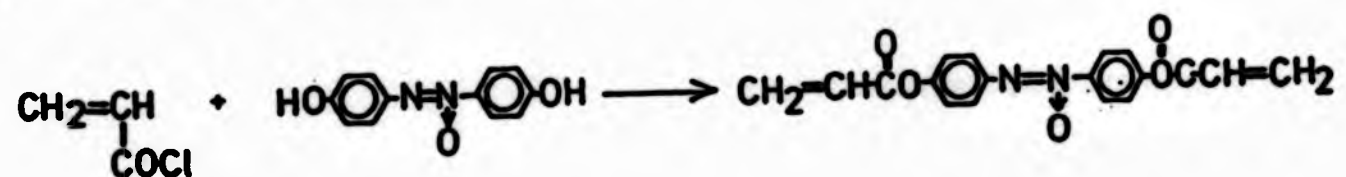
To a cooled(ice bath) solution of phenol(10g,0.106Mol), NaOH(4.5g, 0.112Mol) and sodium nitrite(9.02g, 0.13Mol) in 250ml of water, was added dropwise a solution of sulphuric acid(25g) in water(70ml), while keeping the temperature of the reaction mixture below 0C. The solution was then stirred at 0C for an additional 2 hours. The yellow precipitate which had

appeared was filtered off, washed with cold water(30ml) and dried in vacuum at room temperature over P2O5. Yield:66%.

5.6.1.2 Synthesis of 4,4'-Dihydroxyazoxybenzene

4-nitrosophenol(10g, 0.081Mol) and toluene-4-sulphonyl chloride(13g,0.068Mol) in pyridine(70ml) were stirred at room temperature for 12 hours. The solution was then refluxed for 20 minutes and, after cooling down to room temperature , was poured into a cold solution of sulphuric acid(75g) in water(300ml). After extraction into diethyl ether, followed by washing of the organic phases with water and drying over anhydrous NaSO₄, the solvent was distilled off to leave a yellow solid which was recrystallised from an ethanol/water mixture(80:20). Yield:22%, mp 234C

5.6.2 Synthesis of 4,4'-Azoxydi-phenylene Diacrylate<95>



A solution of acryloyl chloride(6.66g,0.074Mol) in anhydrous tetrahydrofuran(22.5ml) was added dropwise with vigorous stirring to a solution of 4,4'-dihydroxyazoxybenzene(6g, 0.03Mol), triethylamine(8.55g, 0.084m) and 2,6-di-t-butyl-4-methylphenol(0.15g) in 150ml of the same solvent. The temperature was maintained at 0-5C by means of an ice bath for 1 hour. The reaction mixture was then filtered, and the solution evaporated to dryness in vacuo. The residue was recrystallised from ethanol twice. Yield:65%,
Tm:142C, Ti:172C

5.7.1 Synthesis of 4-Carboxyloxy Phenol (I)

(see reaction scheme 5-7)

Benzyl alcohol (20g, 0.088Mol) was added dropwise to a solution of p-ethoxycarbonyl benzoyl chloride (9.46g, 0.088Mol), pyridine (8g, 0.1Mol) and 1,2-dichloroethane (20ml). The reaction mixture was left overnight at room temperature for 10 hours and then gradually brought to reflux for 30 minutes. The solution was poured into 5% HCl (1 litre), washed with water and recrystallised from ethanol twice. Yield: 57%, mp: 98-100C.

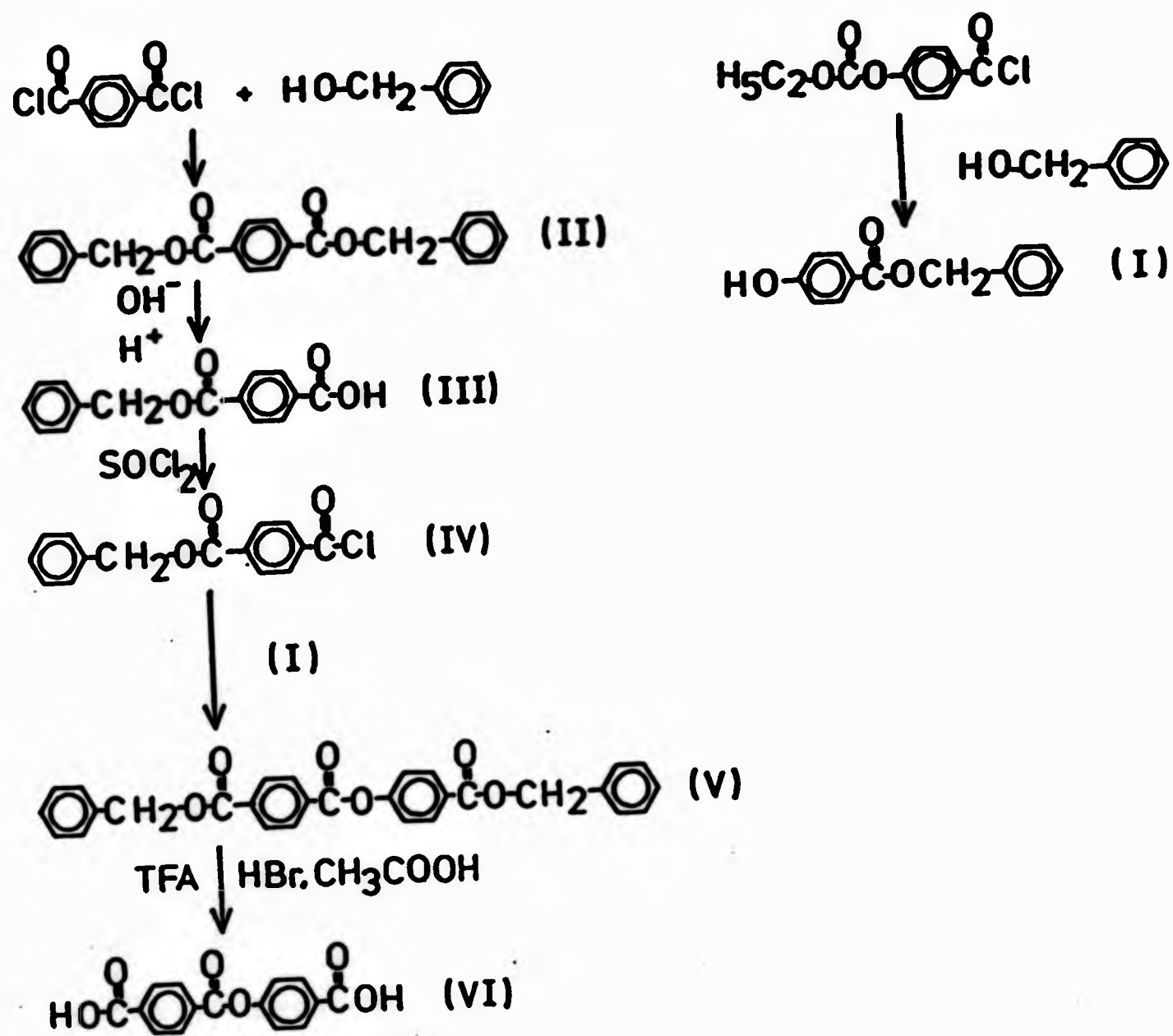
5.7.2 Synthesis of 4,4'-Dibenzyl-Terephthalate (II)

Benzyl alcohol (106.54g, 0.985Mol) was added dropwise to a solution of terephthaloyl chloride (100g, 0.493Mol) and anhydrous pyridine (100g, 1.266Mol). The reaction mixture was kept at 60C for 4 hours. After cooling, the mixture was poured into 5% HCl (1 litre), the precipitated dibenzyl terephthalate was washed with water and dried under vacuum at 50C. The crude product was recrystallised from toluene twice. Yield: 70%, mp: 74C.

5.7.3 Synthesis of 4-Carbobenzoyl Benzoic Acid (III)

<96,97>

Compound II (86.6g, 0.25Mol) was dissolved by warming in 350ml benzyl alcohol. At the same time, 14g of KOH was dissolved portionwise by warming in 250ml benzyl alcohol. Both solutions were cooled rapidly to 30C and mixed with stirring. After a portion of the ester had separated out, 400ml benzene was added and temperature brought to 50C over a period of 1



Reaction scheme 5-7
 Synthesis of 4-Carboxyphenyl Hydrogen Terephthalate

hour. As soon as the reaction mixture was neutral, it was filtered and the K⁺ half ester salt was freed of excess benzyl alcohol with warm benzene. The K⁺ half ester salt was then dried under vacuum at 120C overnight. The salt is very soluble in water and cannot be recrystallied from it. Yield:96%.

The crude K⁺ half ester salt was dissolved in distilled water(1 litre) and with 0.02M HCl titrated until pH=5.3, whereby an crude monosubstituted terephthalic acid precipitated out. After 2 hours, extra HCl was added until pH=5.25, the mixture was cooled to 0C and left overnight, then the precipitate(half acid) was filtered and dried.

The product so obtained was taken up in potassium bicarbonate solution and after half an hour again filtered to remove insoluble material. It was then reprecipitated using HCl to adjust to pH=5.25. The product was then freed from the diester(water insoluble) and also from the terephthalic acid which does not precipitate out until pH=4.7. Solution and precipitation was repeated to ensure that eventually any terephthalic acid that coprecipitated with the product was completely separated. Yield:20%, mp: 180C.

5.7.4 Synthesis of 4-Carbobenzoxy Benzoyl Chloride (IV)

To compound III (4.1g, 0.016Mol) was added thionyl chloride(3.8g, 0.032Mol) together with two drops of DMF and the temperature was brought to reflux until all the acid dissolved. Excess thionyl chloride was distilled off and recrystallised from dry toluene. Yield:93%.

5.7.5 Synthesis of Benzyl 4-(Carbobenzoxy)phenyl

Terephthalate (V)

To a solution of I (12.04g, 0.044m) in 95ml of dry pyridine was added IV (11.65g, 0.051m). The mixture was heated at 60C for 4 hours, stirred at ambient temperature for two days, and poured into 500ml of 2M HCl. The precipitate was filtered, dried, and crystallised in 95% ethanol. Yield: 35%, mp: 96-97C.

5.7.6 Synthesis of 4-Carboxyphenyl Hydrogen terephthalate

(VI) <98>

Benzyl-blocked diacid V (10g, 0.021m) was dissolved in 150ml of CF₃COOH, 5ml of 33% solution of HBr in CH₃COOH was added, and the mixture was allowed to stir for 4 hours. A precipitate formed after about 15 minutes, and the stirring became more difficult. The reaction was stopped by addition of acetone, and the product was filtered, washed with acetone, dried under vacuum, and then crystallised from a CH₃COOH/water(5:1) mixture. Yield: 45%, mp > 300C.

5.8 Synthesis of Cis-1,5-cyclooctane bis(p-hydroxybenzoate)

5.8.1 Synthesis of p-Ethoxycarbonyloxybenzoic Acid(I) <99>

Ethyl chloroformate(50ml) was added portionwise to a chilled solution of p-hydroxybenzoic acid(50g, 0.434 mol) and sodium hydroxide(38g, 0.955Mol) in 900 ml of distilled water. The reaction mixture was then acidified with 2M HCl and the precipitate was filtered and washed with excess water. The product was recrystallised from an acetone/water mixture. Yield: 90%; mp 158C.

5.8.2 Synthesis of p-Ethoxycarbonyloxybenzoyl Chloride(II)

The above compound(20g,0.095Mol) was refluxed with thionyl chloride(15g,0.126 Mol) in the presence of three drops of DMF. The excess thionyl chloride was distilled off, and the crude product was recrystallised from hexane. Yield:80%

5.8.3 Synthesis of Cis-1,5-cyclooctane

bis(p-ethoxycarboxyloxybenzoate)(III)

Cis-1,5-cyclooctane(6.3g,0.028Mol) was added to a solution of II(2g,0.014Mol) in 20 ml of 1,2-dichloroethane. The mixture was refluxed with stirring overnight under a nitrogen atmosphere. The mixture was then cooled, and poured into 50 ml of 0.5M NaOH solution in ice water. The product was extracted into toluene. After drying with MgSO₄, the solvent was evaporated and dried under vacuum and recrystallised in ethanol. Yield:70%; mp 90C. H nmr:(CDCl₃ & TMS) 1.5(t;-CH₃-), 1.95(m;cyclic-CH₂-), 4.25(q;-CH₂-), 5.10(s;-CH-) and 7.05,7.85(d;-Ar-) ppm.

5.8.4 Synthesis of Cis-1,5-cyclooctane

bis(p-hydroxybenzoate)(IV)

Compound III(6g, 0.011Mol) was dissolved in ethanol(20ml) and treated with 2M NaOH(12ml) on a steam bath for 30 min. The ethanol was removed by rotary evaporation. The residue was then adjusted to pH 7 with 10% acetic acid, filtered, vacuum dried and recrystallised from ethanol/water(50:50) mixture. Yield:46%; mp 197C. H nmr:(d-acetone & TMS) 1.90(m;cyclic-CH₂-), 5.10(s;-CH-) and 6.75,7.75(d;-Ar-) ppm.

5.9 Synthesis of Diaza-18-crown-6-ether

Bis(p-hydroxybenzoate)

Diaza-18-crown-6-ether (0.6g, 2.28mMol) was added to a solution of p-ethoxycarboxyloxybenzoyl chloride (1.15g, 5.03mMol) in chloroform (15ml) with triethylamine (0.508g). The reaction mixture was left at room temperature overnight under a nitrogen atmosphere and then poured into 100ml of hexane. The precipitate was filtered, washed with distilled water and dried under vacuum. The solid obtained was dissolved in 50 ml of 10% ammonium hydroxide solution for 4 hours. The final product was filtered, dried and recrystallised from ethanol. Yield: 25%, mp=257C. H nmr: (d-DMSO & TMS) 3.4(m; -CH₂CH₂O-), and 6.60, 7.10(d; -Ar-) ppm.

5.10 Synthesis of Polymers

5.10.1 Polyesters

All polyesters in this study were prepared using the same method, and a typical example is shown below.

Monomer IV (3.127g, 8.13mMol) was dissolved in a minimum amount of anhydrous pyridine, and to this was added a solution of adipoyl chloride (1.417g, 8.13mMol) in 1,1,2,2-tetrachloroethane (30ml). The mixture was stirred at room temperature under a nitrogen atmosphere for 24 hours and then poured into 200ml methanol. The precipitated polymer was washed with methanol. The polymer was then digested with 20% sodium carbonate solution for 2 hours, filtered, washed with diluted HCl, washed, and finally dried in a vacuum oven at 60C. Yield: 87%

5.10.2 Polyamides

4,4'-Azoxydibenzoyl chloride(0.3736g,1.16mMol) was dissolved in 15ml of chloroform, and to this was added a solution of Diaza-18-crown-6-ether (0.3032g,1.16mMol) in 15ml of chloroform with small amount of triethylamine(0.2339g,2.31mMol). The mixture was stirred under a nitrogen atmosphere for 24 hours and then poured into 200ml of hexane. The precipitated polymer was washed with water, ammonium hydroxide, diluted HCl, and water respectively. The polymer obtained was vacuum dried. Yield: 97%.

5.10.3 Polvurethanes and Polyureas

Cis-1,5-cyclooctanediol(1.5g,10.4mMol) in 20ml of anisole was added to a solution of 3,3'-dimethyl-4,4'-biphenylene diisocyanate(2.746g,10.4mMol) with 50ml anisole. The temperature of the reaction mixture was brought to 120C for 10 hours under a nitrogen atmosphere. Polymeric material started to precipitate at the early stage of reaction. The reaction mixture was poured into 300ml of acetone and dried. Yield: 94%.

5.10.4 Polv(B-aminoester)

4-(4-Acryloyloxybenzylideneamino)phenyl acrylate(0.6448g,1.91mMol) and Diaza-18-crown-6-ether(0.5g,1.91mMol) were dissolved in 10ml of anhydrous 1,4-dioxane. The polymerisation mixture was stirred at room temperature for 24 hours and then poured into a large excess of diethyl ether. The polymeric material was purified by several precipitations from chloroform solution.

5.11 Notation of Monomers and Nomenclature of Polymers

The monomer structures and corresponding notation are shown in Figure 5-1.

Polymers are notated by the composition of the monomers unless otherwise specified, eg.

Polymer COHB-10

Polymer prepared from monomers 11 and 8(n=10)

Polymer AZO-CO

Polymer prepared from monomers 1 and 12

(1)		AZO
(2)		AZOXY
(3)		STIL
(4)		TER
(5)		TA
(6)		BTA
(7)		NTA
(8)		n = 2,3,4,---10
(9)		MAA
(10)		CPHT
(11)		COHB
(12)		CO
(13)		AZA-IB-CNB
(14)		AZA-IB-C
(15)		APDA
(16)		DBPDI
(17)		BPOSC
(18)		HDI
(19)		PD

Fig. 5-1 Notation of monomers

CHAPTER SIX

FLEXIBLE SPACER IN MAINCHAIN LIQUID CRYSTALLINE POLYMERS

6.1 Introduction

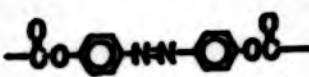
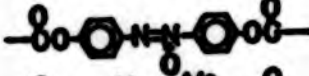
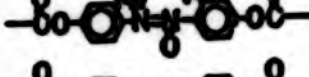
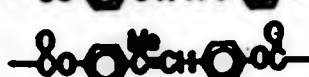
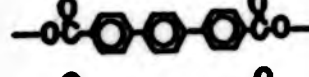
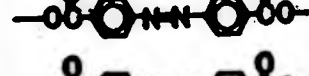
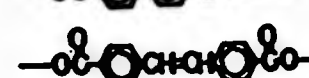
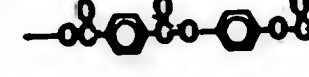
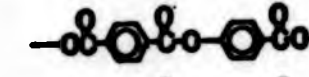
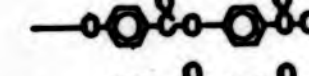
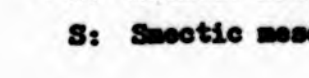
Since the conversion from the nematic to isotropic phase is a first order transition, a random copolymer would be expected to exhibit a biphasic region in which both nematic and isotropic phases coexist. If mechanical properties are of interest, such a biphasic system is undesirable because the isotropic portion may not achieve the desired orientation during flow. A wide biphasic region can be avoided while still maintaining some control over the transition temperatures, by alternating rigid and flexible residues in the repeating unit as suggested by de Gennes^{<100>}. Representative structures of this kind of semi-flexible polymer are shown in table 6-1. Both nematic and smectic mesophases have been reported.

Table 6-2 lists the polyesters synthesised, also their intrinsic viscosities and transition temperatures. All of the polymers based upon cis-1,5-cyclooctane bis(p-hydroxybenzoate) are designated by the letters COHB, followed by the number of the methylene units in the aliphatic dibasic acid.

Intrinsic viscosities (η) of these polyesters were determined at 25°C in chloroform. A Cannon-Ubbelohde viscometer was used without a kinetic energy correction since the solvent flow time exceeded 100 seconds. The values of (η) varied from 0.1 to 0.2 except polymer COHB-10(0.5).

The polyesters under study here were prepared by a low temperature solution polymerisation method. Melt transesterification reactions can also be used, however, this method is somewhat limited in use because it often leads to polymer structures of poorly defined sequence^{<101>}. The molecular weights of these polyesters were relatively low as

Table 6-1 Liquid crystalline properties of polymers containing decamethylene spacer

No.	Mesogenic Structure	Approx Length (Å)	T _m (K)	T _{ni} (K)	ΔT	Ref.
1		13.5	498 (N)*	518	20	162
2		13.5	489 (N)	538	49	58
3		13.5	391 (N)	435	42	58
4		13.5	469 (N)	491	22	58
5		16.0	490 (N)	515	25	167
6		13.5	473 (N)	495	22	126
7		19.0	475 (?)	498	23	104
8		15.5	538 (S)	584	55	54
9		13.5	483 -	-	0	162
10		13.5	473 -	-	0	162
11		11.0	427 (?)	433	6	54
12		13.5	470 (N)	473	3	54
13		19.0	493 (S)	540	47	99
14		19.0	503 (N)	538	35	148
15		13.0	413 -	-	0	98
16		19.0	510 (N)	567	57	57
17		18.0	509 (N)	538	29	57
18		10.0	476 (S)	530	54	117
19		12.0	423 (S)	474	51	110

* N: Nematic mesophase
S: Smectic mesophase

<u>methylene unit</u>	<u>yield</u>	<u>intrinsic viscosity</u>	<u>heating T_g (K)</u>	<u>heating T_m (K)</u>	<u>heating T_{ni} (K)</u>	<u>cooling T_{in} (K)</u>	<u>T_{ni}-T_{in} ΔT</u>
3	0.89	0.135	-	335	366	357	29
4	0.92	0.100	342	393	417	388	24
5	0.95	0.130	310	352	358	350	8
6	0.86	0.130	304	366	389	365	23
7	0.94	0.190	309	349	375	370	26
8	0.90	0.105	-	338	348	333	10
9	0.87	0.175	300	341	355	352	14
10	0.96	0.500	301	367	396	378	7

Table 6-2 Physical properties of the COHB series polymers.

reflected by their low viscosities. The yield of polymerisation was reasonably good (ca 90%).

Columns 4, 5, 6 and 7 of Table 6-2 list the transition temperatures of the series of polymer COHBs measured by DSC. The peak temperature of the highest endotherm observed during the second heating cycle (20K/min) was labelled T_{ni} (mesophase to isotropic transition), while the endotherm in the lower temperature region from the first heating cycle was taken as T_m (crystal to mesomorphic transition). T_{in} (isotropic to mesomorphic transition) was recorded from the second cooling cycle which was normally the first exotherm to appear. Scans after the first heating cycle were virtually identical unless otherwise specified.

Microscopic studies showed that both nematic and smectic mesophases were exhibited by this series of polymers.

Multiple melting endotherms were detected after annealing at an appropriate temperature eg polymer COHB-4 and polymer COHB-10. A similar phenomenon has also been reported in non-liquid crystalline polymers like poly(ethylene terephthalate) (PET) due to multistage crystallisation $\langle 102, 111 \rangle$. However, that seems very unlikely to happen here as the 'melt' was still viscous and pressable. Careful microscopic observation revealed that there was no sign of formation of crystallites instead was typical smectic textures like those found in low MW mesogens were seen.

6.2 Smectic Polymers

6.2.1 Polymer COHB-4

The DSC thermograms of polymer COHB-4 are shown in Figure

6-1. On the first heating scan (curve 1), a small and broad melting transition appeared at about 393K followed by a much larger endothermic transition in the temperature range of 400K to 430K for the mesophase to isotropic transition. Subsequent scans gave almost identical patterns as the first scan. On cooling (curve 3), the isotropic to mesomorphic transition appeared at 388K and there was no indication of a crystallisation transition. The clearing transition (T_{in}) obtained from cooling was 36K lower than when heating which was possibly due to a supercooling effect. This phenomenon was also observed by some other research workers <103,104,117>. However, after annealing the sample at 400K for 4 hours, an enhanced melting transition and also a better resolved mesophase to isotropic transition were detected (curve 2) which clearly show two distinct transitions at 405K and 417K. A glass transition was found at 342K. The small exotherm appearing just below 406K was attributed to cold crystallisation. The melting transition of polymers is related to the degree of crystallinity. The crystallisation process in polymers is not instantaneous, and rapid quenching of samples when heated above the glass transition may induce recrystallisation. However as observed by Grebowicz and Wunderlich <79>, the slower the cooling rate the smaller are the T_g and the cold crystallisation features.

Microscopic observation showed the existence of two different mesophases. When the isotropic melt was cooled to about 410K, strong stir-opalescence was observed. By further cooling to 405K, elongated particles reminiscent of the batonnets seen in low MW mesogens started to appear and then the homeotropic background gradually changed to a mosaic

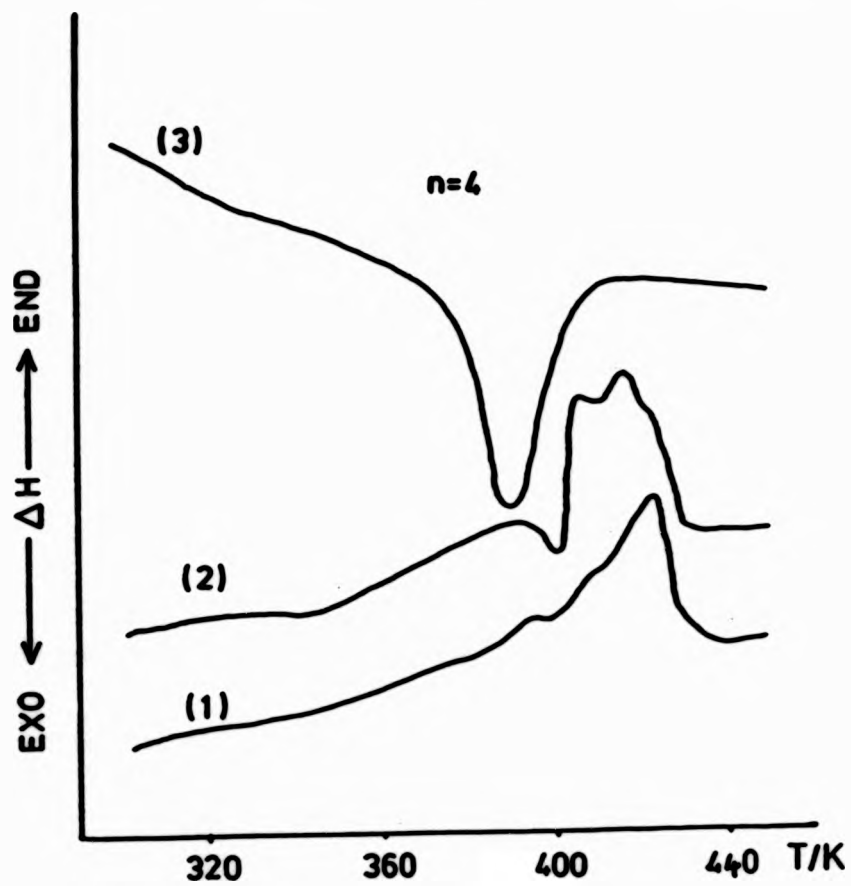


Fig. 6-1 DSC thermograms for polymer COHB-4
 (1) 1st heating scan, (2) 2nd heating scan,
 (3) cooling scan.

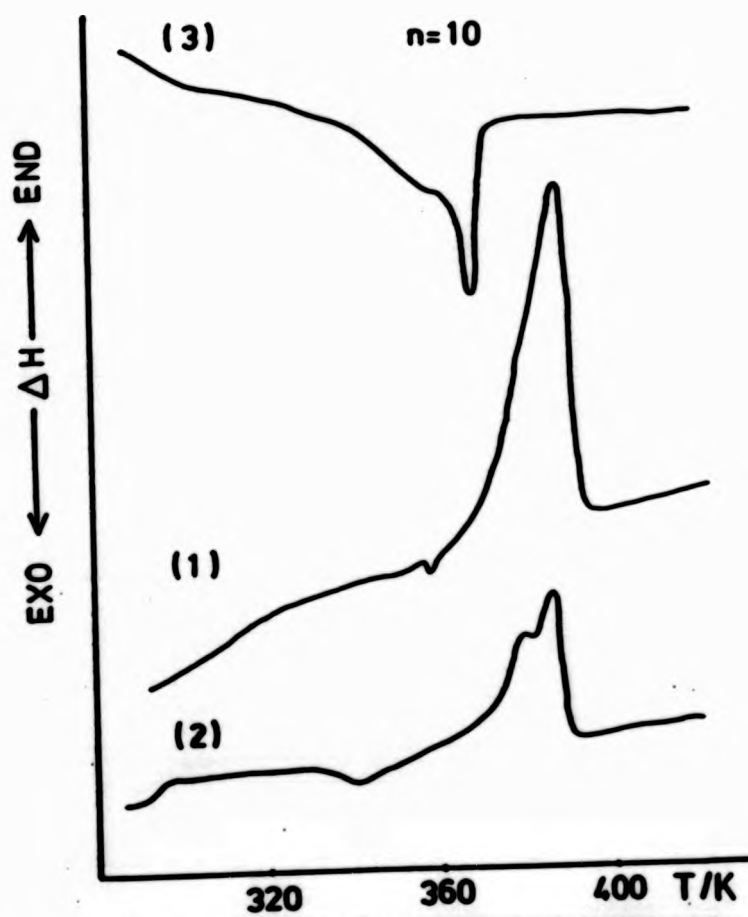


Fig. 6-2 DSC thermograms for polymer COHB-10
 (1) 1st heating scan, (2) 2nd heating scan,
 (3) cooling scan.

texture as shown in Plate 6-I. In low MW liquid crystals, only nematic, smectic A and smectic B phases exhibit this pseudoisotropic texture. In a smectic A phase, batonnets are usually formed from the preceding phase. If this does not occur the isotropic liquid will itself grow to a focal-conic fan texture. Smectic B phase distinguishes itself from other phases by the unmistakable mosaic texture. Smectic A and smectic B endotherms are usually quite large and first order in nature. Hence, the mesomorphic order of polymer COHB-4 was assigned as:-

g 339K k 393K Sb 406K Sa 417K i.

6.2.2 Polymer COHB-10

Figure 6-2 displays the DSC thermograms of polymer COHB-10, its features are similar to those of polymer COHB-4. The second heating scan (curve 2) exhibited a sharp peak at 396k and a small shoulder at 318K even without thermal treatment. Cold crystallisation and supercooling effects were again detected, T_g and T_m were found at 301K and 367K respectively. In fact, studying under crossed polarisers showed the same kind of textures as those observed in polymer COHB-4, i.e. the coexistence of both smectic A and smectic B phases. Plate 6-II shows the batonnets surrounded by a mosaic texture during a phase transition. Hence, the mesomorphic order was concluded to have the following sequence:-

g 300K k 367K Sb 381K Sa 396K i.

The highly ordered structures of smectic A and smectic B phases make the sample very difficult to shear. It is remarkable that textures in liquid crystalline polymers can be



Plate 6-I The batonnet and mosaic texture of polymer COHB-4



Plate 6-II The batonnet and mosaic texture of polymer COHB-10



Plate 6-I The batonnet and mosaic texture of polymer COHB-4



Plate 6-II The batonnet and mosaic texture of polymer COHB-10



Plate 6-I The batonnet and mosaic texture of polymer COHB-4



Plate 6-II The batonnet and mosaic texture of polymer COHB-10

frozen in the glassy state but this may be due to the relatively high viscosities. In low MW mesogens, only the lowest mesomorphic order can be retained and once this state has been reached, then in most cases, crystallisation will subsequently occur.

Before moving to the last smectic polymer found in this series of polyesters, one has to emphasise again that both DSC and microscopic studies only give an incomplete picture of the mesophase of the specimens being studied; additional information can be obtained by using techniques like X-ray diffraction and the miscibility method. Indeed, some of the ^{textures} are almost undetectable by DSC, for instance, the smectic C phase. In this case, the appearance of the mesophase is quite often featureless and very much dependent upon the preceding phase; the word 'paramorphic' is sometimes used to describe these inherited textures.

6.2.3 Polymer COHB-3

A large endothermic transition between 360K and 415K with a maximum at 406K was detected in the first heating scan of polymer COHB-3 (Figure 6-3, curve 1). In the second heating scan (curve 2), the highest peak dropped about 40K to 366K, that is towards the lower temperature region. It was because of this enormous change that the heating scan was repeated for another three times, and no sign of alteration in the thermogram was observed. A glass transition was not detected and T_m was assigned at 335K after repeated scanning. The supercooling effect was milder in this case with T_{in} at 357K.

Polymer COHB-3 was heated on a hot-stage polarising

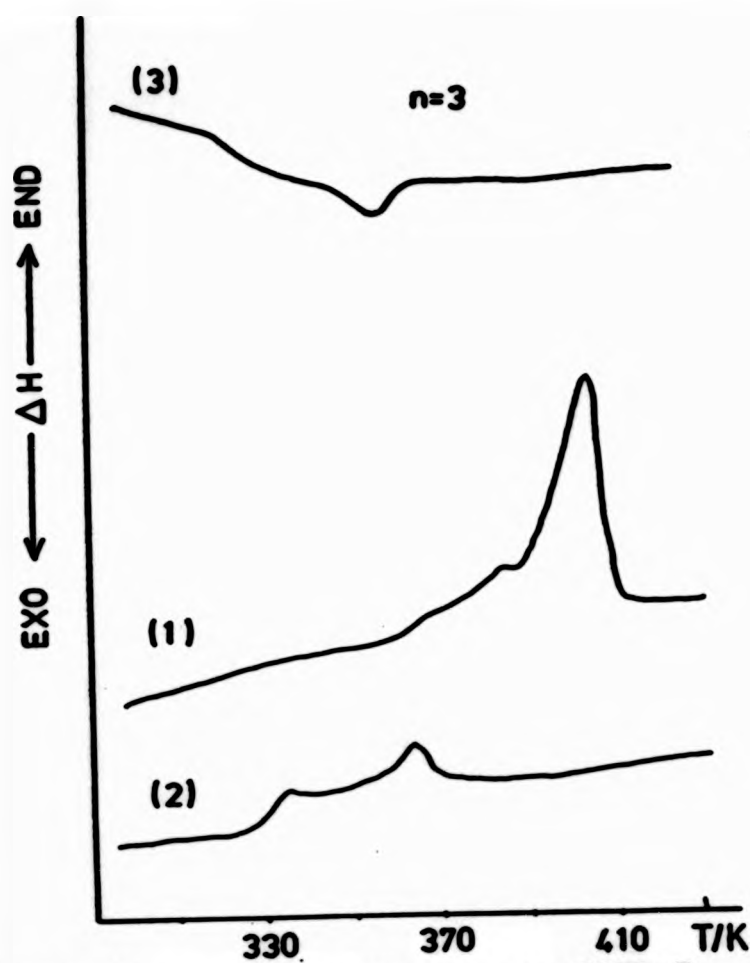


Fig. 6-3 DSC thermograms for polymer COHB-3
 (1) 1st heating scan, (2) 2nd heating scan,
 (3) cooling scan.

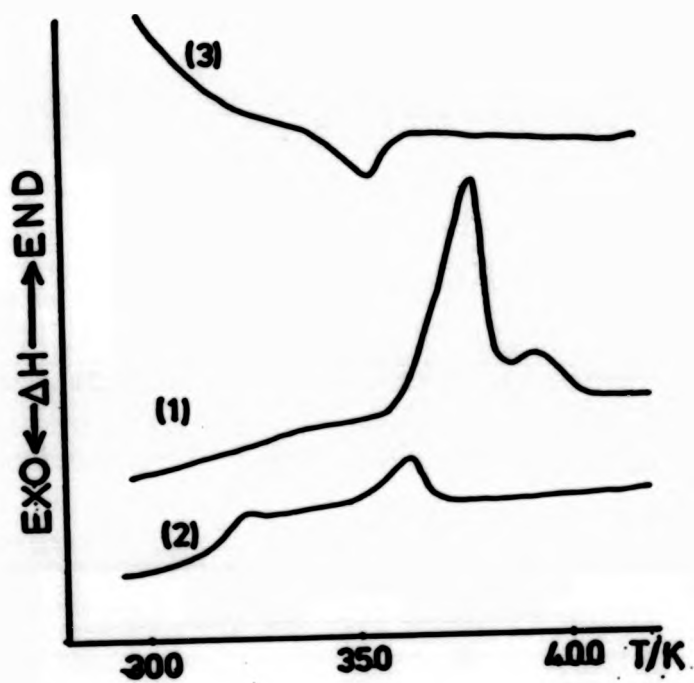


Fig. 6-4 DSC thermograms for polymer COHB-MAA
 (1) 1st heating scan, (2) 2nd heating scan,
 (3) cooling scan.

microscope about 20K above its isotropic transition and cooled slowly to 363K. By annealing the sample at this temperature for 24 hours, a focal-conic texture was developed. Since no mosaic texture was observed, the focal-conic texture which developed from a homeotropic phase can only be referred to as smectic A phase. The sample was then heated up to 400K and quenched to 358K, and maintained at this temperature for two hours. A blurred schlieren (sand-like) texture was developed (Plate 6-III). It is well known that in low MW mesogens when a smectic C phase is cooled from a homeotropic smectic A phase, usually a schlieren texture will be obtained. A smectic C phase can only be obtained from nematic, smectic A and smectic D phases. Further evidence of the existence of the smectic C phase was the change of the birefringence colours from a pale-grey yellow colour to a rust-blue colour on cooling. This colour change phenomenon contrasts with those observed in a twisted nematic phase (cholesteric) in which only heating yields a bathochromic change. Indeed, this birefringence colour change of both phases is a result of changing the tilt angle between adjacent layers of the molecules. This angle is generally strongly temperature dependent. Based on the above evidences, the sequence of the mesomorphic order of polymer COHB-3 was assigned as

k 335K Sc 358K Sa 366K i.

There was no evidence of a nematic phase in any of the aforementioned polymers.

6.2.4 Discussion

The identification of a particular smectic mesophase is a



Plate 6-III The blurred schlieren (sandlike) texture of polymer COHB-3



Plate 6-IV The nematic schlieren texture of polymer COHB-5



Plate 6-III The blurred schlieren (sandlike) texture of polymer COHB-3



Plate 6-IV The nematic schlieren texture of polymer COHB-5



Plate 6-III The blurred schlieren (sandlike) texture of polymer COHB-3



Plate 6-IV The nematic schlieren texture of polymer COHB-5

difficult undertaking, even for small mesogens. The mutual miscibility, or contact method, developed for this purpose by Sackmann, Arnold and Demus<66,105> involves construction of the phase diagrams of pairs of low molecular weight mesogens. Identification of the mesomorphic modification rests upon the postulate that chemically dissimilar mesophases of the same type will be mutually immiscible in all proportions. According to this criterion there is only one type of nematic phase, and smectic mesophases Sa through Si were assigned in the chronological order of their identification. The preferred texture seen in the polarising microscope and the sequential order of the appearance of the mesophases with increasing temperature provide useful supplemental information. The binary phase diagrams may turn out to be simple or quite complex. In the latter case, errors in the identification of small molecule smectic mesophases have occurred, even in the hands of experienced workers<106>. Turning to polymeric mesophases, there is no a priori reason to believe that the basic postulate of the mutual miscibility method would be applicable. Even if it is, the low solubility and the high viscosity of the binary systems involving polymeric components may make determination of the phase diagram difficult. In view of these reservations, it is encouraging to note that the mutual miscibility method has been successfully applied to identify polymeric nematic and smectic phases by Fayolle et al.<60> and to identify polymeric nematic phases by Griffin and Havens<85>. More recently, Watanabe et al.<107> and Jung et al.<108> have studied mesogenic polymer mixtures. However, the application of this procedure to more highly ordered

polymeric smectic phases has yet to be demonstrated.

The relationship between the molecular structure of the mesogenic unit and the type of mesophase it forms is still not well understood. It is believed that the dipolar effects, the planarity and the rigidity of the mesogenic unit, and the length to width ratio are the major structural factors which influence the properties of the mesophase. These factors are difficult to quantify either absolutely or relatively. Hence, by comparing the properties of polymers with different mesogenic units but of the same spacer, these influences may be perceived. Table 6-1 lists the transition temperatures and the temperature ranges of mesophase stability ΔT of different LC polymers in which a common flexible spacer is present, the decamethylene spacer. This spacer gives polymers with melting temperatures in a range very convenient for study.

According to Table 6-1, in view of the frequent occurrence of polymorphism among small molecule mesogens, it is surprising that most of the LC polymers examined today have shown only one type of mesophase. Indeed, only five cases had been reported which exhibited smectic mesophases. Ober et al. (99), based on optical studies, found that the triad ester (polymer no. 13, Table 6-1) exhibited a smectic A phase, Krigbaum et al. (109) using 4,4'-dihydroxybiphenyl prepared polymer no. 18 and reported a smectic H phase from X-ray diffraction, Meurisse et al. using terphenyl dicarboxylic acid observed a smectic texture (polymer no. 8), and Al Dujaili et al. (110) using 4,4'-dihydroxydiphenylacetylene prepared polymer no. 19 which they claimed a smectic phase was observed.

None of the above mentioned smectic polymers have their

spacers connected to the mesogenic unit through an ether linkage. Although, Shaffer and Percec<112> reported smectic textures for a series of polythioethers based on 4,4'-dithiobiphenyl and dibromoalkanes having methylene units between 2 to 12. However, the photomicrographs shown were reminiscent of highly ordered spherulites. The same authors<113> also synthesized polyketones based on biphenyl and fluorene combined with aliphatic dibasic acids using a decamethylene spacer; they revealed a smectic texture which exhibited batonnets.

Only one example can be found in the literature which displayed a smectic texture with a carboxy-terminated spacer<117>. Ozcayir and Blumstein<115> have just recently reported a series of diacetylene LC polymers prepared using linear dibasic acids, however, they could not identify the mesophase with $n=10$. Bear in mind, spacers in polymer COHB-3, 4 and 10 are all carboxy-terminated..

The characteristics of the mesophases present in polymers are to some extent dependent upon the molecular weight and the properties of the chain ends, this aspect will be discussed briefly in the next chapter. Nevertheless, the occurrence of a smectic B phase has never been reported, although, polymorphism has been observed quite often in sidechain LC polymers<30,114>.

In general, the longer the aromatic segment the higher the melting temperature<55>. The other factors such as the rigidity and the polarity of the mesogenic group are also

important, but these have a much greater effect on the clearing temperature of the mesophase than on the melting point.

When different classes of polymers are compared, however, the correlation in length is not so straightforward. Polymers no. 13 and 14 with ester triads which have a mesogenic length of approximately 19A, melt and clear at lower temperatures than the shorter but more rigid terphenyl polymer, polymer no. 8. The shorter azo and azoxy mesogenic groups give polymers no. 9 and 10 with lower melting temperatures and no mesophase, while the shorter biphenyl polymer has an even lower melting temperature and no mesophase (polymer no. 11). Apparently the planarity and the rigidity of the terphenyl and biphenyl groups are very important for the mesophase formation.

Comparing, finally, the polymers made from diphenolic compounds and linear dibasic acids, the Schiff base structure in polymer no. 5 and the methylstilbene structure in polymer no. 6 gave polymers with about the same range of mesophase stability, but the polymer with the shorter stilbene unit has a lower melting temperature. However, the azo and azoxy polymers, polymers no. 1 and 2, which have mesogenic structures of the same size as the stilbene unit possess high melting temperatures, and the azoxy polymer has a wider range of mesophase stability. Evidently, the polarity of the azoxy and azo polymers is very important in both aspects of mesophase behaviour.

Liquid crystalline behaviour can also be modified by the addition of lateral substituents. The substituents can have

either one of two effects: either (1) they increase the intermolecular attractions through changes in the molecular dipole moment and/or polarisability, or (2) they act to separate the long axes of the mesogens through steric interactions. Of course, these factors depend on the size and type of substituent and the mesogen involved. The position of the substituent is also important, and in certain cases an added substituent can either create a mesogen from a non-mesogen or destroy the liquid crystallinity^{<116>}.

Asrar et al.^{<117>} had demonstrated that a smectic phase could be destabilized by disrupting the regularity along the backbone chain; a cholesteric phase was observed when the linear spacer was diluted with (+)-3-methyl adipic acid(MAA). Meurisse et al.^{<54>} also found that using branched flexible spacers had the effect of broadening the molecules, and increasing the separation of the long axes of the neighbouring molecules.

For this reason, polymer COHB-MAA was prepared which has the same number of carbon atoms between the mesogenic unit as polymer COHB-4, but different in that MAA which is methyl-substituted and optically active. Thermal analysis revealed that polymer COHB-MAA had a glass transition(T_g) at 327K, a melting transition(T_m) at 376K and a mesophase to isotropic transition(T_{ni}) at 388K (Figure 6-4). As anticipated there was a pronounced decrease in T_g ($dT=15K$), T_m ($dT=17K$) and T_{ni} ($dT=24K$). There is also a change in mesophase; polymer COHB-MAA(see Plate 8-VI) exhibited a twisted nematic phase compared with the smectic A and B phases exhibited by polymer COHB-4.

The features of various textures are caused by the existence of different kinds of defects. Defects occurring in the solid state usually have sub-microscopic dimensions, whereas in liquid crystals, various defects are visible under the microscope at low magnification (ca 100x). This is obviously due to the fact that the energy necessary to stabilise the defects is much lower in the liquid crystals than in solid crystals, and thus, there may occur stronger distortions corresponding to defects of larger domain. Defects also occur during all growth processes of liquid crystals or are caused by a violent disturbance of the liquid crystal, eg mechanical stress.

6.3 Nematic Polymers

6.3.1 Polymer COHB-5

Plate 6-IV shows the nematic schlieren texture of polymer COHB-5 when cooled from the isotropic melt to 353K. This texture observed between crossed polarisers, displayed dark brushes (schlieren) which have irregular curved shapes. At some points, two dark brushes meet and at others clusters of four brushes meet. The black brushes originating from the points are thought to be similar to the dislocations in crystals and are called 'disclinations' by Frank^{<118>}. The significance of these schlieren textures was first understood by Lehmann^{<119>} and Friedel^{<10>} but the mathematical treatment of the actual configuration around the disclinations was given by Oseen^{<120>} and Frank^{<118>}. A more complete discussion of the theory of schlieren textures is due to Nehring and Saupe^{<121>}. From the observation of points at which only two dark brushes meet, the

mesophase can be identified unambiguously as a nematic phase since these 'disclinations' occur nowhere else. Indeed, in contrast with nematic schlieren textures in which points with two or four schlieren are possible, the textures of smectic C, B, and D display points with only four brushes $\langle 48, 66, 122 \rangle$.

The DSC thermograms of polymer COHB-5 are depicted in Figure 6-5. The first heating cycle (curve 1) displayed two endothermic transitions of different size at 352K and 367K respectively, the former one was assigned as the melting transition. The melting transition vanished after reheated and left only the mesophase to isotropic transition at 358K (curve 2). No changes could be detected in the subsequent scans. The second order transition at 310K revealed the change of state from amorphous to rubbery, and the supercooling effect was modest (8K).

6.3.2 Polymer COHB-6

When polymer COHB-6 was quenched from the clearing temperature to 373K, tiny multicoloured droplets were first to appear (Plate 6-V-a) and after further growing coalesced to larger domains (Plate 6-V-b), and eventually formed a threaded schlieren texture (Plate 6-V-c). This sequence of texture development is typical for a nematic phase. The nematic droplets differ from the batonnets found in a smectic A phase in that they are rather shapeless and coalesce to a planar texture instead of focal-conic. The threaded schlieren texture gave flashes when the top cover slip was slightly touched, this phenomenon does not happen in smectic C schlieren texture.

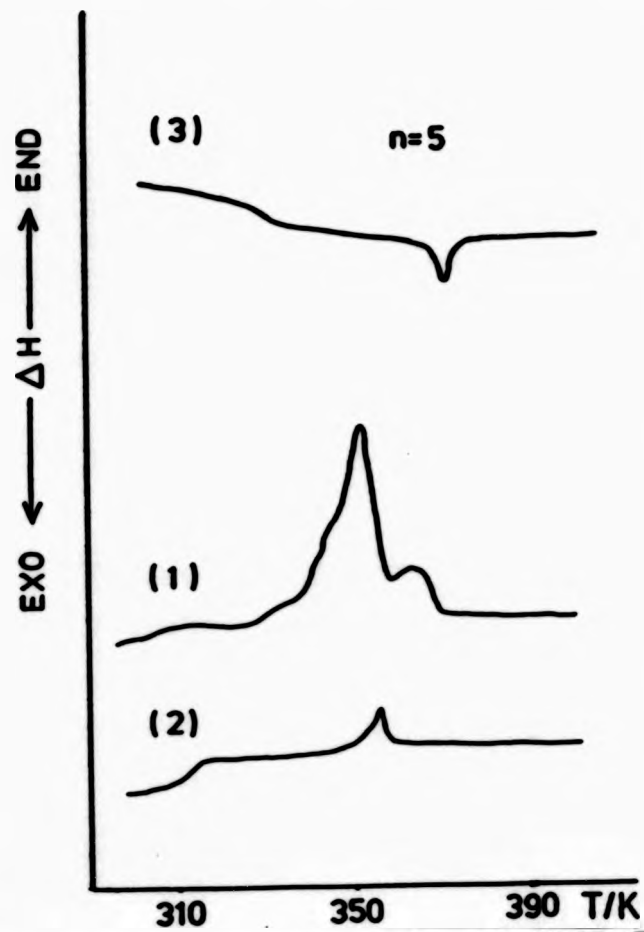


Fig. 6-5 DSC thermograms for polymer COHB-5
 (1) 1st heating scan, (2) 2nd heating scan,
 (3) cooling scan.

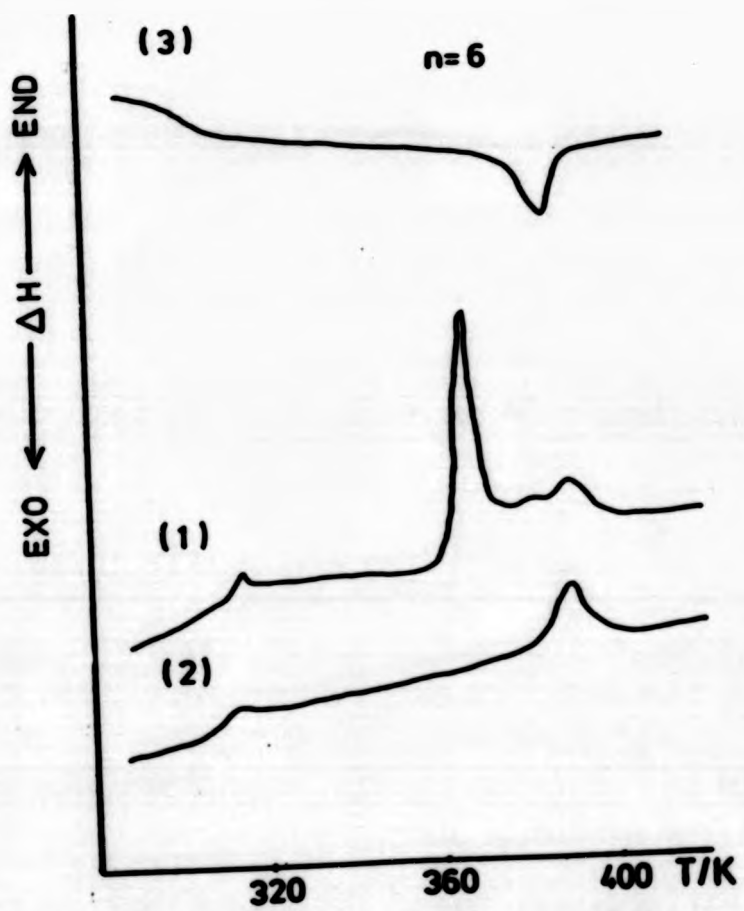


Fig. 6-6 DSC thermograms for polymer COHB-6
 (1) 1st heating scan, (2) 2nd heating scan,
 (3) cooling scan.



Plate 6-V-a The appearance of nematic droplets from the isotropic phase of polymer COHB-6



Plate 6-V-b The coalescence of nematic droplets of polymer COHB-6

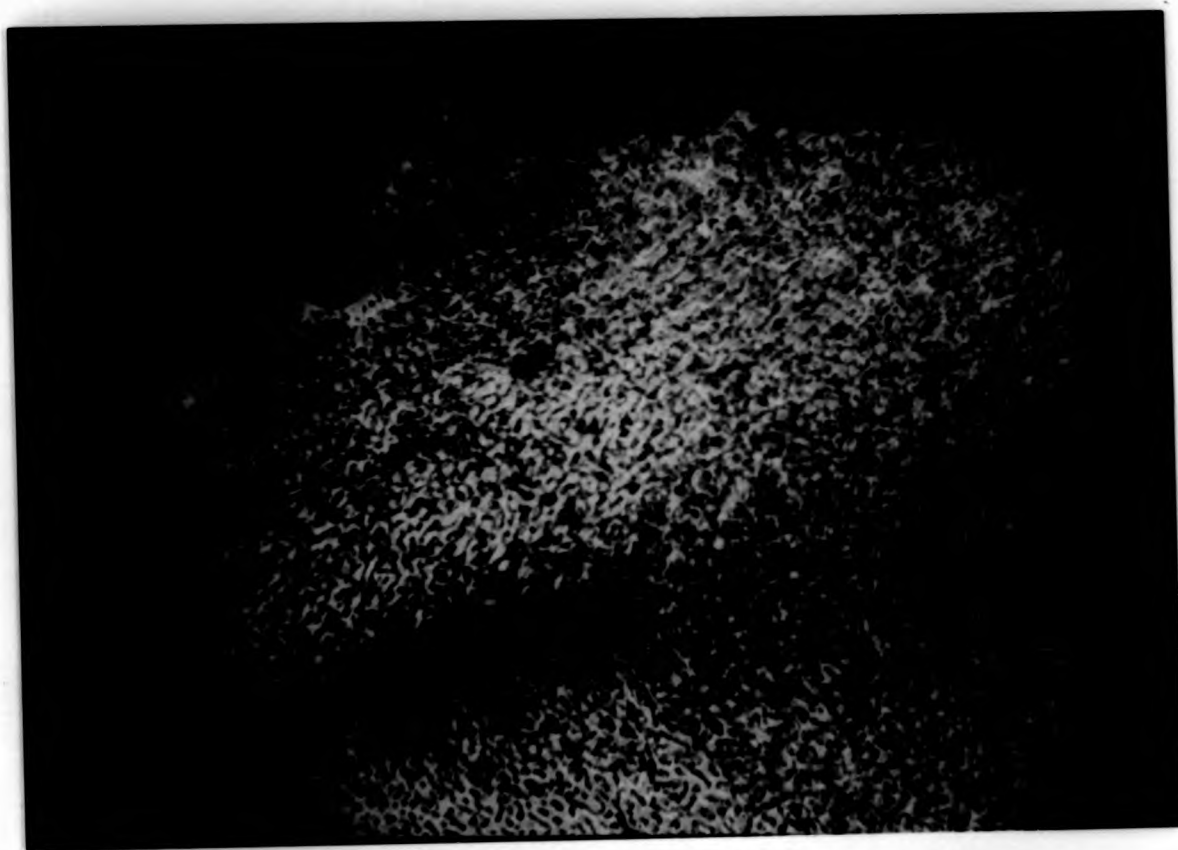


Plate 6-V-a The appearance of nematic droplets from the isotropic phase of polymer COHB-6



Plate 6-V-b The coalescence of nematic droplets of polymer COHB-6



Plate 6-V-a The appearance of nematic droplets from the isotropic phase of polymer COHB-6



Plate 6-V-b The coalescence of nematic droplets of polymer COHB-6



Plate 6-V-c The schlieren nematic texture of polymer COHB-6



Plate 6-VI-a The threaded nematic texture of polymer COHB-7 -



Plate 6-V-c The schlieren nematic texture of polymer COHB-6



Plate 6-VI-a The threaded nematic texture of polymer COHB-7 -

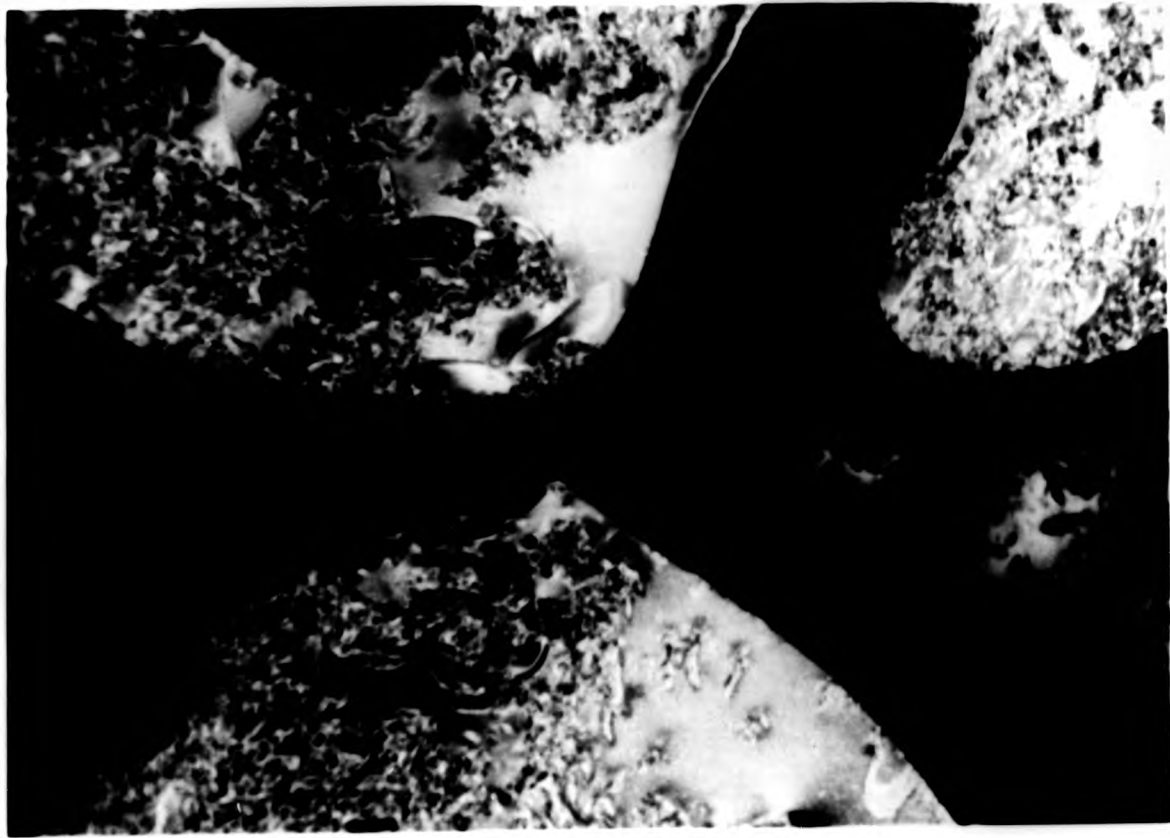


Plate 6-V-c The schlieren nematic texture of polymer COHB-6

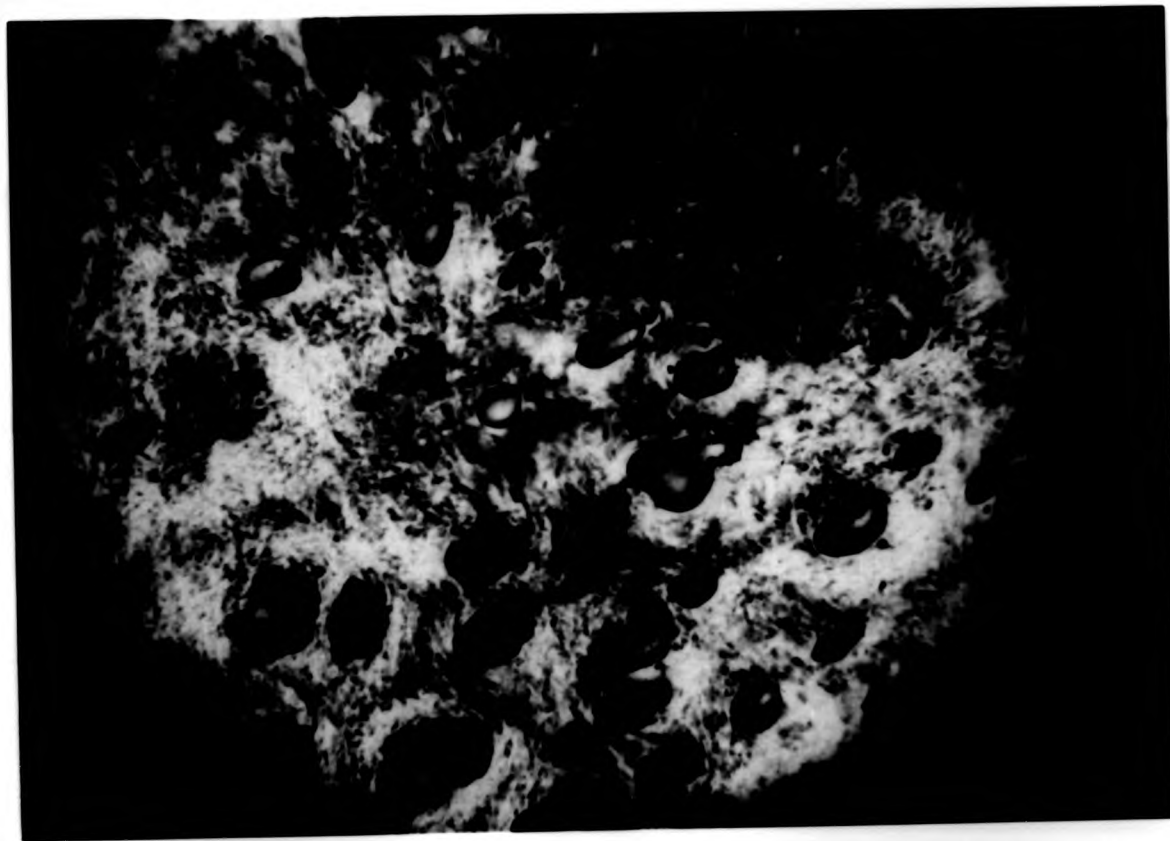


Plate 6-VI-a The threaded nematic texture of polymer COHB-7 -

The occurrence of schlieren or threaded textures in a nematic liquid is dependent upon the specimen preparation, thicker layers favour the formation of a threaded texture while thinner layers induced by shearing usually display a schlieren texture with dark brushes.

The DSC traces of polymer COHB-6 (Figure 6-6) were reminiscent of the preceding homolog. Apart from the first heating cycle, the polymer was enantiotropic i.e. the mesomorphic structure can be detected by both heating and cooling. In some other cases^{<98>}, especially when the flexible spacer is short the polymer is monotropic i.e. textures only observable when cooling. According to Figure 6-6, T_g , T_m , and T_{ni} were identified at 303K, 366K and 389K respectively. The supercooling effect was substantial (25K).

6.3.3 Polymer COHB-7

Moving to the next homolog, polymer COHB-7, two endothermic transitions of almost equivalent size were detected by DSC when the virgin sample was scanned (Figure 6-7, curve 1). The one appearing in the lower temperature region was assigned as T_m (349K). The small difference between T_{ni} (375K) and T_{in} (370K) indicates that thermal treatment had little effect on the mesophase to isotropic transition or vice versa (curves 2 & 3). The glass transition was at 309K. Optical observations of defects in polymeric nematic phases exhibiting threaded textures showed that a mass organisation of macromolecules occurs as the temperature is raised. For example, immediately after the melting of polymer COHB-7 between two cover slips, a large number of threads were observed (Plate 6-VI-a). When the

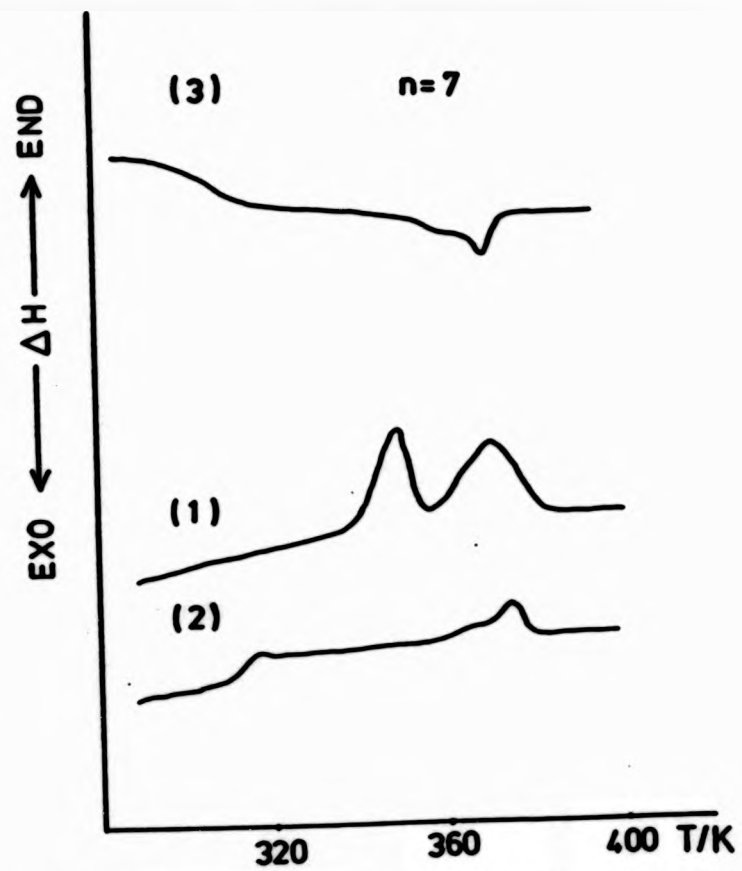


Fig. 6-7 DSC thermograms for polymer COHB-7
 (1) 1st heating scan, (2) 2nd heating scan,
 (3) cooling scan.

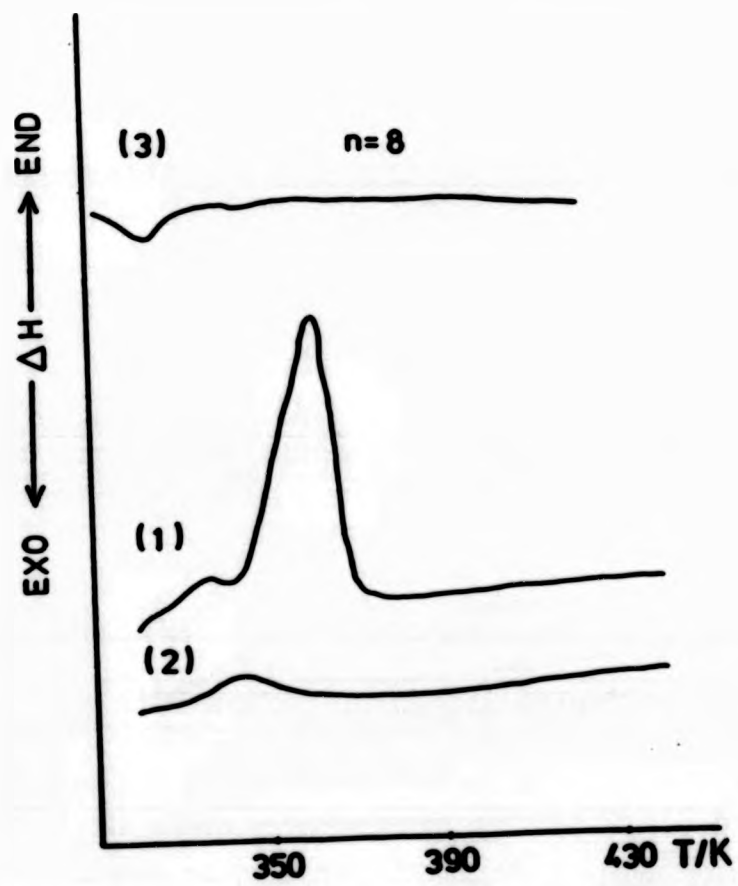


Fig. 6-8 DSC thermograms for polymer COHB-8
 (1) 1st heating scan, (2) 2nd heating scan,
 (3) cooling scan.



Plate 6-VI-b The homogenous nematic texture of polymer COHB-7 when sheared



Plate 6-VII The threaded nematic texture of polymer COHB-8



Plate 6-VI-b The homogenous nematic texture of polymer COHB-7 when sheared



Plate 6-VII The threaded nematic texture of polymer COHB-8



Plate 6-VI-b The homogenous nematic texture of polymer COHB-7 when sheared



Plate 6-VII The threaded nematic texture of polymer COHB-8

temperature of the melt was increased, the number of threads diminished. Simultaneously, the threads became loose and shrunk. At a higher temperature most of them formed closed loops. They were unstable and after some time they became smaller and smaller and to a great extent disappeared. When the temperature was near T_{ni} , the sample contained no threads and slight pressure produced a homogeneous greenish blue colour across large areas between the crossed polarisers (Plate 6-VI-b). Similar observations have been reported by Millaud et al. <123> for the lyotropic nematic phase of poly(p-phenylene terephthalimide).

6.3.4 Polymer COHB-8

Polymer COHB-8 exhibited the same nematic texture as COHB-7 (see Plate 6-VII). The melting endotherm (338K) was very small compared with the mesophase to isotropic transition when the freshly prepared sample was scanned (Figure 6-8, curve 1). The following scan gave a rather broad peak roughly at 348K which was assigned as T_{ni} (curve 2). No glass transition was detected at ambient temperatures. As with the preceding homologs, the area of the exotherm (T_{in}) was about the same size as the endotherm (T_{ni}). At this stage it is pertinent to comment that one may possibly notice a tendency for the supercooling effect to weaken as the spacer lengthens; in this case it was about 15K (curve 3). The enormous size of the mesophase to isotropic transition in curve 1 can probably be attributed to the stepwise melting of crystallites of various dimensions, this phenomenon will be explained in the next sample.

6.3.5 Polymer COHB-9

Untreated sample of polymer COHB-9 exhibits two endothermic transitions as illustrated in Figure 6-9, curve 1. Once the virgin sample was heated above 385K, cooling and heating then produced a different thermogram as shown in curves 2 & 3. In these cases the transitions at 340K and 370K have disappeared. $T_{ni}(355K)$ of the once melted sample was about 10K higher than the corresponding transition of the virgin sample.

At first it was thought that the extra endotherm at 371K was due to a marked reduction in molecular weight during dissolution and precipitation. Hence, the polymer was annealed at 330K in a vacuum oven for 10 hours and the viscosity was measured. There was a slight increase in viscosity(6%) which was possibly due to transesterification during annealing, as this happens quite often in polyesters<124>. This result indicated that the molecular weight was not the determining factor for the existence of the extra endotherm. The present polymer under study is an alternating polymer, the possibility of randomisation of a block sequence distribution by ester interchange reactions in the melt like some of the copolyesters can be excluded. Annealing the virgin sample at 342K for 4 hours seemed to give slightly better resolved endotherms between 330K to 360K with no change of the endotherm at 371K(curve 4). It is well known that in poly(ethylene terephthalate) the melting transition is dependent upon thermal treatment. Finally, careful observations of the birefringence can also be used as an explanation. Part of the virgin sample of polymer COHB-9

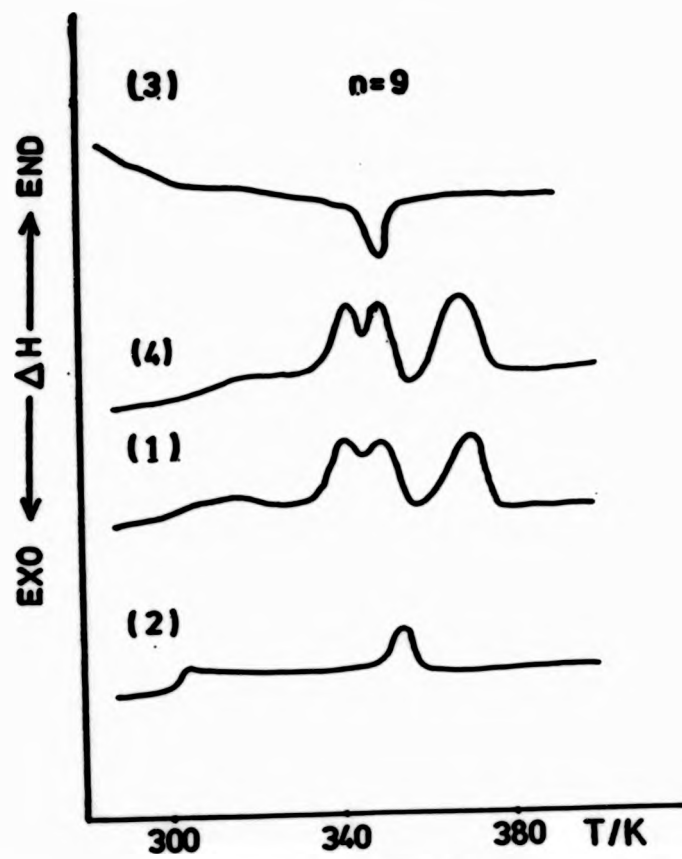


Fig. 6-9 DSC thermograms for polymer COHB-9
 (1) 1st heating scan, (2) 2nd heating scan,
 (3) 3rd heating scan, (4) cooling scan.

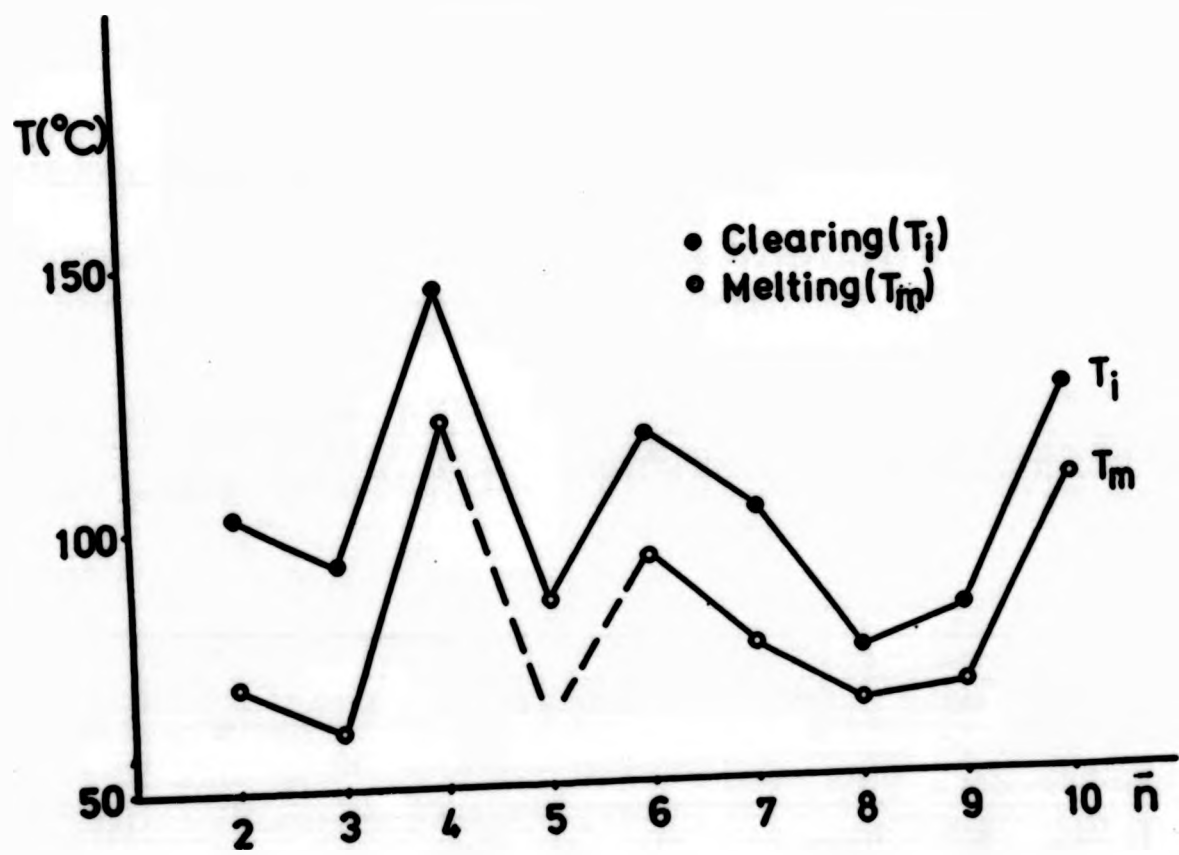


Fig. 6-10 Plot of the mesophase range for the COHB series polymers.

melted to the isotropic state at 340K, while the remainder of the crystallites were more perfect and finally melted at 371K. Lader and Krigbaum^{<125>} observed a similar phenomenon in .co(Poly(ethyleneterephthalate)-p-Oxybenzoate). The glass transition was observed at 300K.

Microscopic studies revealed the existence of a rather blurred homogenous nematic texture(Plate 6-VIII) when sheared at about 353K.

6.4 The Odd-Even Effect

The effect of an increasing polymethylene flexible spacer length on the properties of mainchain LC polymers has been well documented in a number of publications ^{<47,85,104,111,126,127>}. Essentially three effects can be observed in all such series: (1) reduction of the transition temperatures(both melting and clearing) with increased spacer length, (2) an odd-even relationship for the transition temperatures, in which polymers with an even number of atoms in the spacer generally have higher transition temperatures than those in the same series with an odd number of atoms, and (3) in some cases, a smectic mesophase is formed by polymers containing very long spacers. All of these effects are illustrated in Figure(6-10).

The virtually universal odd-even behaviour of both melting and clearing temperatures for the liquid crystalline polymers having polymethylene spacers has not yet been explained theoretically, but similar trends have also been observed for low molecular weight LC compounds with alkyl terminal groups. Nevertheless, odd-even effects are well known for the melting



Plate 6-VIII The blurred homogenous nematic texture of
polymer COHB-9 when sheared at 353K



Plate 6-VIII The blurred homogenous nematic texture of
polymer COHB-9 when sheared at 353K

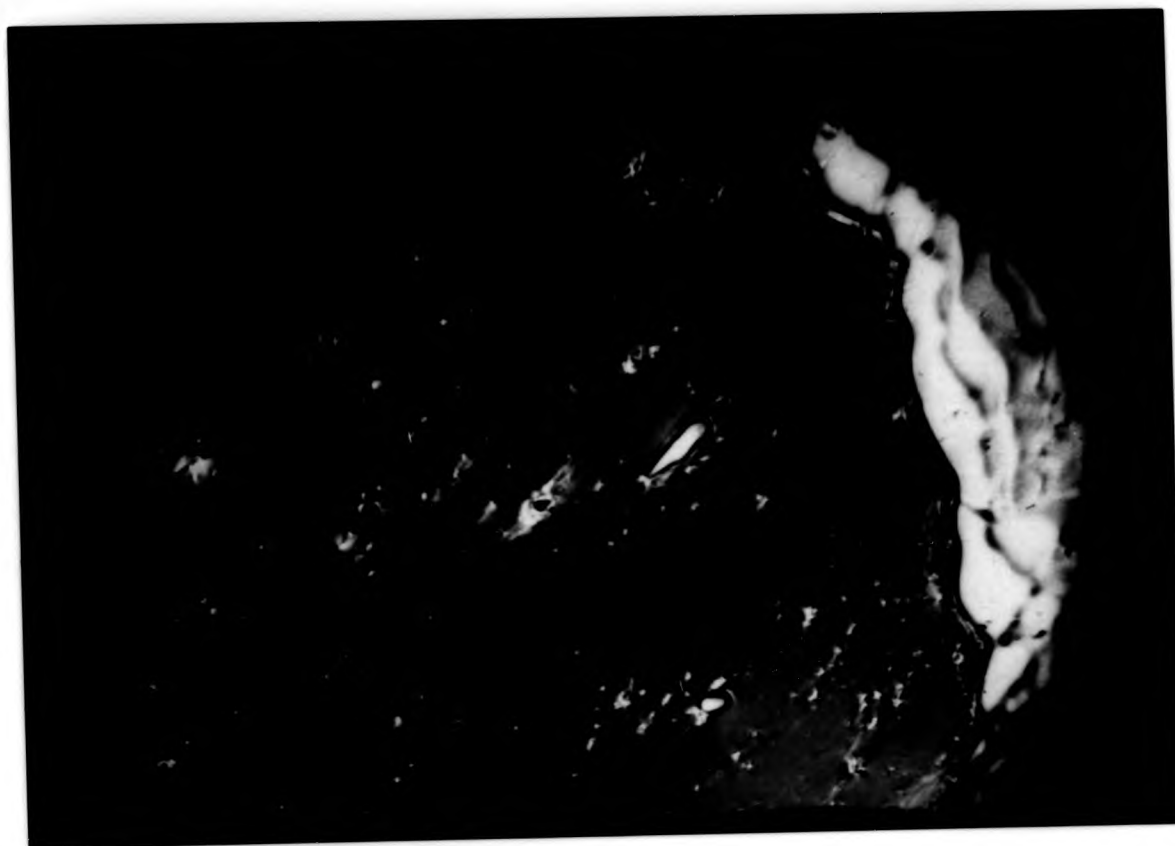


Plate 6-VIII The blurred homogenous nematic texture of
polymer COHB-9 when sheared at 353K

points of both low molecular weight compounds and polymers with polymethylene structures<17,128>.

The liquid crystalline state of bulk polymers presents challenging scientific problems as well as novel technological applications. The molecular or structural factors controlling its stability over the isotropic state of random chains are directly related to the fundamental question of the packing of long chain molecules to a high density in the condensed state. It is now well established that polymer chains with sufficient flexibility and negligible orientation dependent (anisotropic) interactions assume unperturbed random coil configurations in the undiluted amorphous state, which are unaffected by intermolecular interactions<129>. In this regard, polymer liquid crystals are a clear reminder of the critical importance of intermolecular interactions for chains with incomplete flexibility and/or appreciable anisotropic interactions.

Liquid crystalline polymers comprising of rigid units connected by flexible spacer groups have been studied most prominently in recent years, mainly owing to the presence of well defined isotropic liquid crystalline transitions in these polymers<128>. The rigid groups which normally contain aromatic units introduce both limited flexibility and anisotropic interactions. For this class of thermotropic polymer it is well established that the spacer groups play critical roles in determining the stability of the liquid crystalline state over the isotropic state.

The transition temperatures as a function of the number of methylene units in the spacer for the crystal to mesophase

transition(T_m) and the mesophase to isotropic transition(T_i) are shown in Figure(6-10). One may notice that there is a progressive decrease of both transition temperatures up to the value of n equal to 8, followed by an increase up to n equal to 10. An odd-even effect is also observed.

In low molecular weight liquid crystals, explanations of these trends have been based on changes in either molecular polarisability<130,131> or conformational effects resulting from the lengthening of the alkyl end groups and passing from the odd to even terminal chain length<132,133,134>.

Most models assume that the mesogen behaves as a rigid cylinder, and any change in geometry caused by rotation of bonds that leads to violation of the cylindrical shape results in formation of an isotropic phase. That is, the explanation for a reduction of clearing temperature with increased spacer length is generally based on the effect of increasing the number of possible conformations available to the long spacers with the resulting distortion of the cylindrical shape of the mesogen<131>. According to the rigid rod theory an all trans conformation, as illustrated in Figure(6-11) favours the liquid crystalline state, so the increased addition of gauche bonds would reduce the mesophase order.

At high enough temperatures, the large number of gauche conformations present in the terminal groups of the low molecular weight LC compounds distort the cylindrical shape of the mesogen and destroy the liquid crystalline order<131>.

The odd-even effect is induced by changes in the molecular polarisability of the mesogen in its normal and perpendicular components<130>. The polarisability along the molecular axis

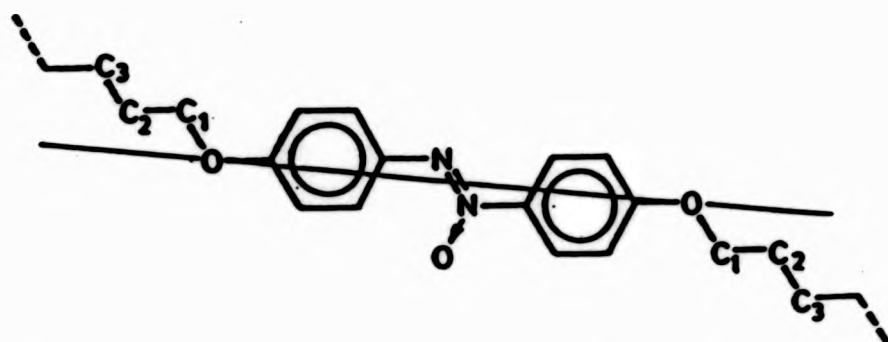


Fig. 6-11 Trans conformation of a mesogenic unit

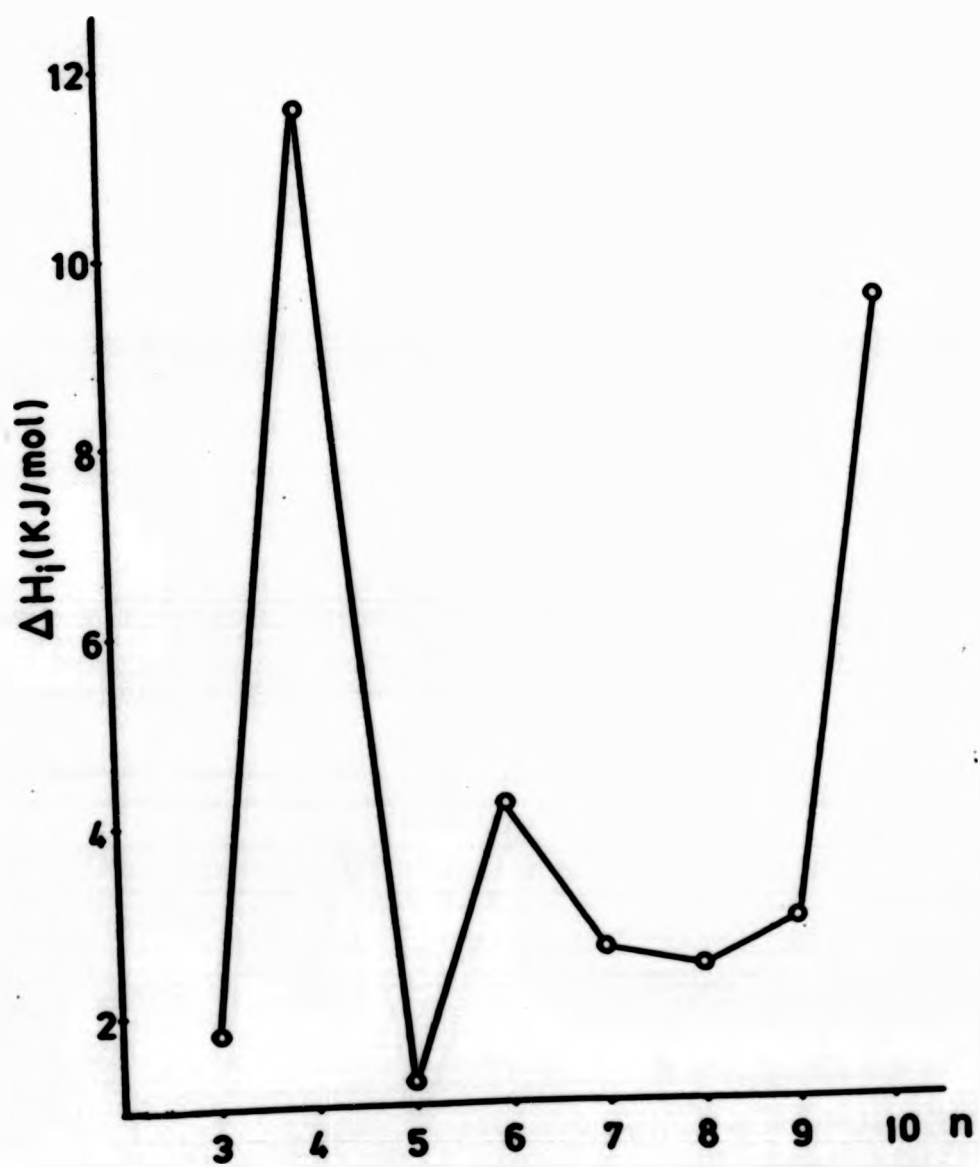


Fig. 6-12 Plot of the enthalpy for the COHB series polymers.

is greater than that perpendicular to the axis for even chains, but is about equal for all odd chains if an all trans conformation is assumed. Stronger attractions exist between mesogens with even end groups, and consequently these compounds have higher clearing temperatures.

Such reasoning could logically be extended to liquid crystalline polymers with the added consideration that rather than having free end groups, the mesogenic units act to constrain the spacers and therefore to reduce the number of possible conformations that the spacer groups might have.

Many liquid crystalline polymers do not possess liquid crystalline moieties, however, the predisposition towards rod like character results in very large axial ratios (length to diameter). Long flexible spacers not only play the role of 'solvent', but also participate actively in the ordering process in the mesomorphic state.

The thermodynamic parameters for the isotropic transition of polymer COHBs are listed in Table 6-3. The values of dH_i were obtained from the measured peak areas and the transition temperatures were obtained from the position of the peak maxima in the DSC scans. By assuming that the mesophase to isotropic transition is an equilibrium process, entropy changes (dS_i) for these transitions can easily be obtained from the following relation:

$$dS_i = dH_i / dT_i$$

Discussion is restricted to polymers of the same mesophase at this stage. Based on optical observation and DSC studies, polymers COHB-5, 6, 7, 8, and 9 all possess nematic mesophase.

As shown in Figures 6-12 and 6-13, the values of dH_i and

<u>methylene unit</u>	<u>Mol. Wt. of repeating unit</u>	<u>Cp (Tni) J/g</u>	<u>ΔH_{ni} kJ/mol (kcal/mol)</u>	<u>ΔS_{ni} kJ/molK (cal/molK)</u>	<u>Tni (K)</u>
3	478	3.77	1.80 (0.43)	1.18 (0.28)	366
4	492	23.52	11.57 (2.77)	6.64 (1.58)	417
5	506	2.45	1.24 (0.30)	0.84 (0.20)	358
6	520	8.02	4.17 (1.00)	2.57 (0.61)	389
7	534	4.97	2.65 (0.64)	1.71 (0.42)	375
8	548	4.46	2.44 (0.58)	1.67 (0.40)	348
9	562	5.20	2.92 (0.70)	1.97 (0.47)	355
10	576	16.40	9.45 (2.26)	5.71 (1.36)	396

Table 6-3 Calorimetric data of the COHB series polymers.

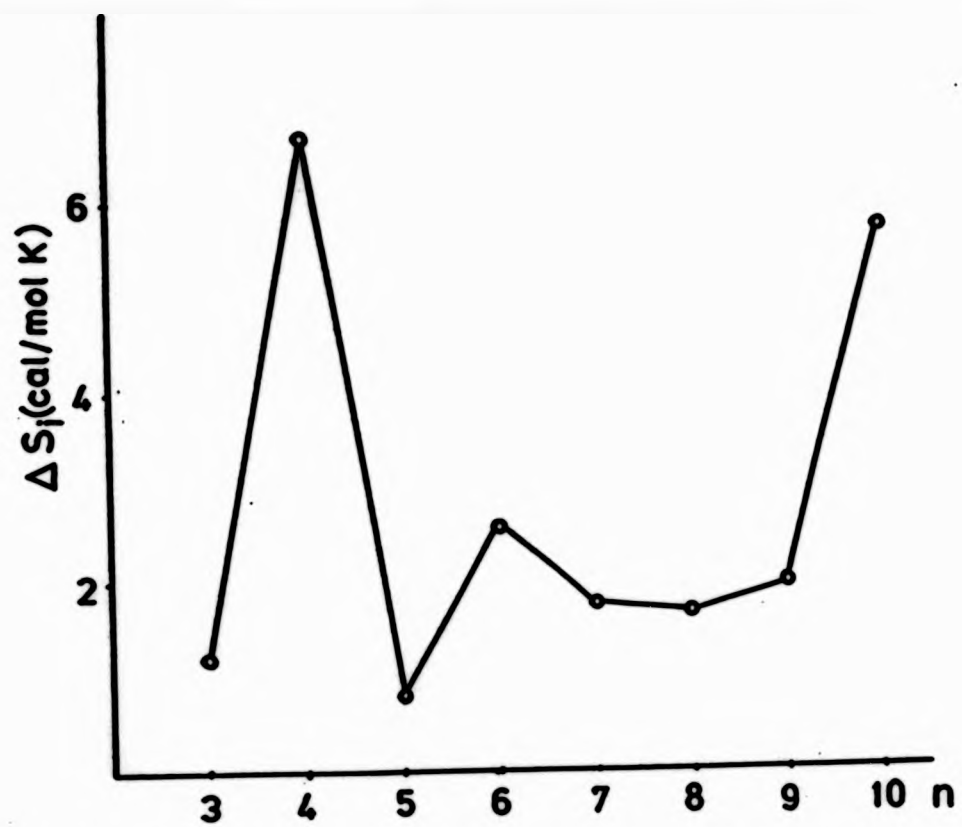


Fig. 6-13 Plot of the entropy for the COHB series polymers

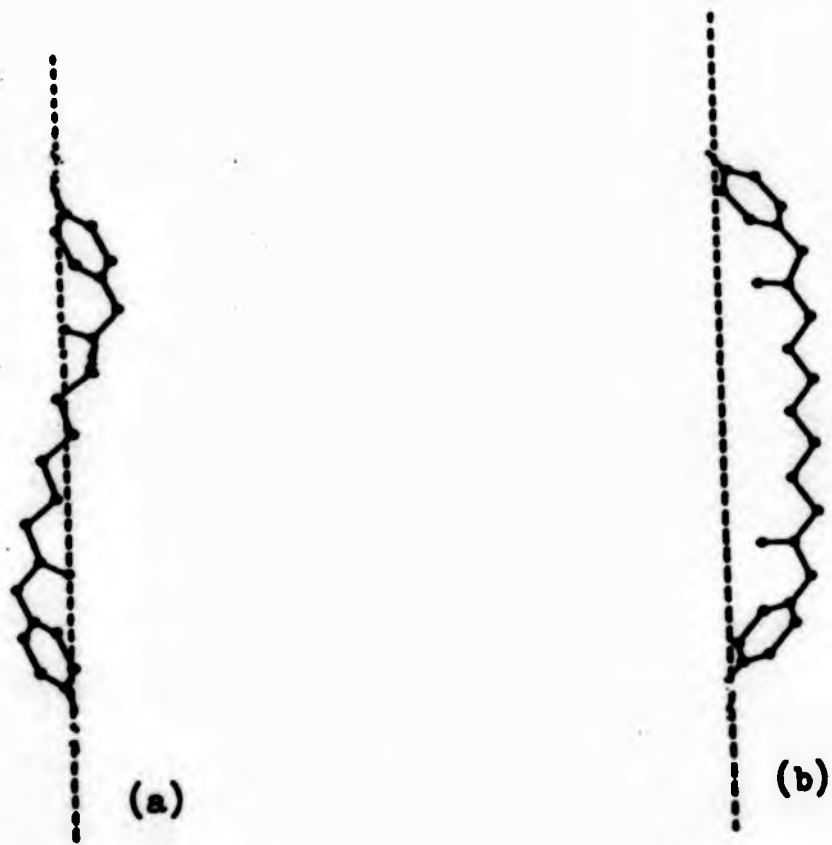


Fig. 6-14 The fully extended conformation of polymers
(a) COHB-6 (b) COHB-7

d_{Si} generally increased with n even though T_i steadily decreased (discounting the odd-even effect). Haller and coworkers^{<135>}, in a study on a homologous series of aldonitrones, made a similar observation that the change in d_{Si} , between the mesomorphic and isotropic states of N -(p -alkoxyphenyl) - α -(p -methoxyphenyl)nitrones increased smoothly with n . The increase of d_{Si} with n indicates that, for polymer molecules with longer polymethylene spacers, the conformations of these chains and the placement of the mesogenic units were increasingly more ordered for the mesophase related to the isotropic phase.

According to Ronca and Yoon^{<136>}, the total partition function of a bulk system of chain molecules may be factorized into three contributions: the steric repulsion, the anisotropic attractions and the degrees of freedom of configuration.

The ordered state is driven by the favourable steric and anisotropic interactions, while sacrificing the configurational degrees of freedom, over the disordered state. Maximisation of the steric repulsion requires minimizing the angle of distortion of the chain segments of rigid and flexible groups to the major orientation axis. This implies that highly anisotropic (extended) configurations will be favoured for the steric packing consideration.

The anisotropic configuration here is defined as the axis along which the total projection of the rigid groups appended at the ends of a spacer group is maximised. The extension of chain sequence along this axis is therefore a proper measure of the anisotropy of spatial configurations, which is most

critical to packing.

On the other hand, the anisotropic attractions can be maximised by aligning only the rigid groups; the detailed configurations of the intervening spacer groups are less critical in this regard.

For polymer COHB-6 and polymer COHB-7, both steric repulsion and anisotropic attractions can be considered as almost identical as the difference between them is merely a -CH₂- unit. The entropies of polymer COHB-6 and polymer COHB-7 are 2.57 and 1.71 cal/molK respectively (mole here refer to one mole of repeating unit). The higher entropy of polymer COHB-6 than polymer COHB-7 reflects that the former polymer must be in a higher state of order.

The enthalpies of polymer COHB-6 and polymer COHB-7 are 4.17 and 2.65 kJ/mol respectively. Hence, the average ΔH_i per methylene unit for polymer COHB-6 and polymer COHB-7 is 0.695 and 0.379 kJ/mol respectively. If one assumes that the entropy per -CH₂- is due to conformational entropy, it becomes possible to estimate roughly the extent of packing. Taking from the literature the value for the gauche to trans energy per -CH₂-, estimated to be 2-3 kJ/mol^[137], the experimental ΔH_i per -CH₂- of polymer COHB-6 represents an increase of the population of trans conformer between 23% ($0.695/3=0.23$) to 35% ($0.695/2=0.35$) at the nematic to isotropic transition. While for polymer COHB-7, it was about 13% ($0.379/3=0.13$) to 19% ($0.379/2=0.19$). In both cases, this should lead to a significant extension of the flexible spacer. The value of this extension is uncertain, due to the lack of knowledge about the respective populations of trans/gauche conformers in

the pre-transition state. It is however, likely that in the pre-transitional state, this ratio exceeds 0.5. This would suggest that in the nematic state the population of trans conformers could well exceed 80%.

The fully extended conformations of polymer COHB-6 and polymer COHB-7 are compared in Figure(6-14).

According to Figure 6-14, in polymer COHB-6, every second bond starting from the $-OC(=O)-CH_2-$ is in the trans state. Owing to the tetrahedral bond geometry involved, this conformer not only allows the successive rigid groups to align with each other, but also separates them at the same(maximum) extension along this alignment axis regardless of the conformations of the intervening bonds. Also, the trans arrangement of the carbonyl dipoles would be expected to contribute to the stability of the crystalline phase of the even membered series.

On the other hand, in polymer COHB-7, the fully extended conformer results in the two rigid groups at the ends of a spacer being tilted by 30 degree from the major extension axis. This may lead to a less favourable packing arrangement, as was demonstrated by its smaller entropy.

By following the same concept, polymer COHB-8 would be expected to have a higher transition temperatures than its immediate neighbours, polymers COHB-7 and COHB-9. However, T_i and T_m of polymer COHB-8 turns out to be anomalously low..A similar phenomenon was also observed by Ober et al.<99>(see Figure 6-15 symbol \square), these authors suspected that this was

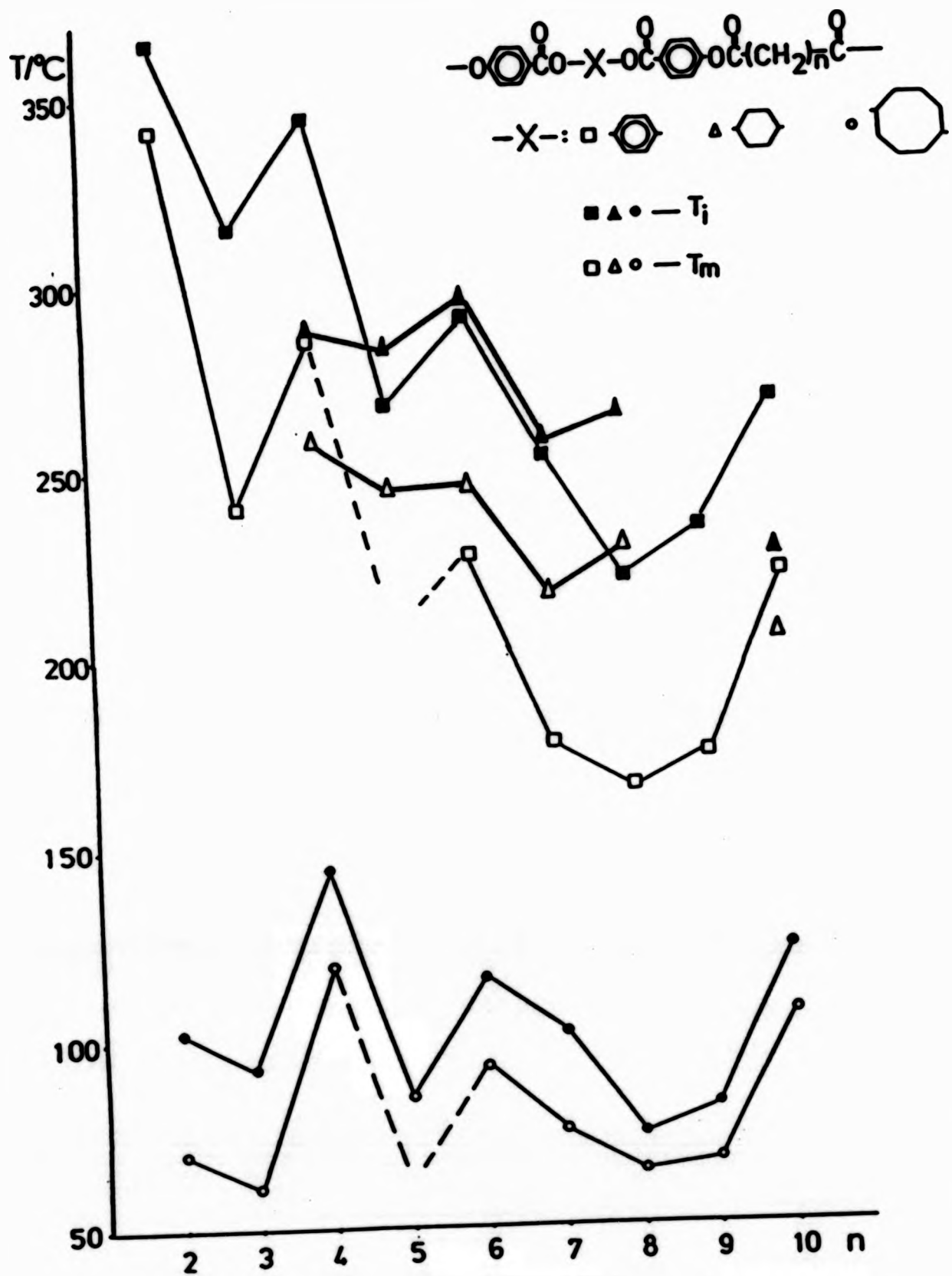


Fig. 6-15 Comparison of three series of structurally similar polymers containing viz. phenyl, cyclohexyl and cyclooctyl moieties.

due to the formation of a smectic phase, but such a phase could not be observed by them using other characterisation methods. For polymer COHB-8, only a threaded nematic texture was observed and there was no indication of any smectic phase like those found in polymers COHB-3, 4 and 10. The absence of an ordered smectic phase was also reflected by the low calorimetric data with $dH_i=2.44\text{kJ/mol}$ and $dS_i=1.67\text{cal/molK}$. More recently, Braun and Schulke^{<104>} prepared a series of polyesters which are structurally similar to polymer COHBs except the cyclooctyl unit was replaced by a cyclohexyl unit, the mesophase was not disclosed, but a consistent odd-even effect from $n=4$ to $n=8$ was observed(see Figure 6-15 symbol Δ).

No explanation can be provided for the abnormality of polymer COHB-8 at this stage, the discrepancies from the Ober and Braun series may be attributed to the intrinsic structural differences because of different type of mesogenic units. For low molecular weight liquid crystals, it is well known that structural variations in the mesogenic units can give rise to substantial changes in the thermal behaviour of the mesophases^{<138>}.

As expected, polymer COHB-5 also follows the odd-even trends, and the relatively lower thermodynamic data obtained with $dH_i=1.24\text{kJ/mol}$ and $dS_i=0.84\text{cal/molK}$ was compatible with the nematic mesophase observed.

Literature values are now available for the clearing enthalpies(dH_i) of several hundred nematic compounds. Marzotko and Demus^{<139>} found that these values fall in the region of 0.02-2.30 kcal/mol, with a typical value of slightly less than 0.50 kcal/mol. Despite the slightly lower value for polymer

COHB-5(0.3 kcal/mol), the average value of dH_i from $n=6$ to $n=9$ is 0.73 kcal/mol which is 23% higher than the typical low molecular weight LC compounds. Entropies for the nematic to isotropic transition show a similar comparison. This observation suggests that the order present in polymeric mesophase is higher than is found in low MW liquid crystals.

Descending from the homologues, the odd-even effect is still noticeable, however, the mesophase begins to alter from nematic to smectic when the value of n is below 5. The nematic state is less organized than the smectic state, and this difference would be expected to be reflected in the entropies of clearing. In fact, the entropic value of polymer COHB-4, ($dS_i=1.58$ cal/molK), is almost 8 times higher than polymer COHB-5($dS_i=0.2$ cal/molK).

The abrupt change of mesophase from $n=5$ (nematic) to $n=4$ (smectic) is difficult to explain. A possible explanation of this phenomenon may be that there are reduced degrees of freedom of configuration because of the shorter spacer length. The probability of one mesogenic core imposing a dipole-dipole interaction on the one in the immediate vicinity is greatly increased. As a consequence, the rigid units are able to pack more easily into layers as shown in Figure 6-16.

The mesomorphic sequence of polymer COHB-4 as determined by microscopic studies and DSC analysis is found to be from a smectic B phase to a smectic A phase.

At higher temperatures, the increased incidence of gauche bonds still allows the the alignment of the chain molecules along the major orientation axis, however, the vigorous molecular motion of the flexible spacer groups would certainly

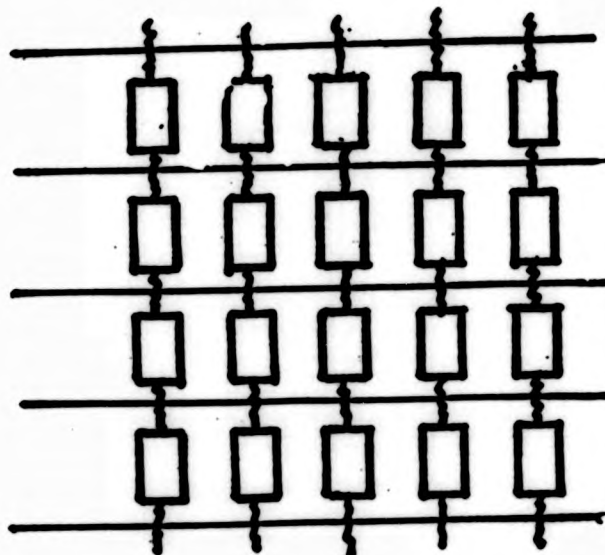


Fig. 6-16 Typical molecular alignment of polymer in smectic mesophase

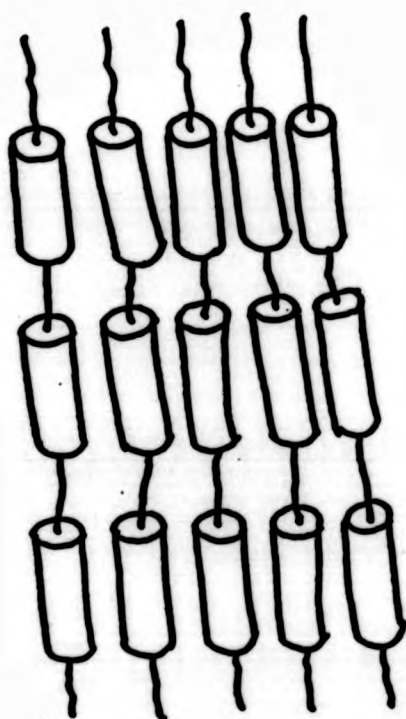


Fig. 6-17 The proposed molecular alignment of the smectic A phase for polymer COHB-4

distort regular packing of the mesogenic units embedded in a discrete layer. As a result, the lateral distribution of the segments within each layer will probably be in a random state and rotate freely. This kind of molecular arrangement is typical of the smectic A phase of low molecular weight liquid crystals. A schematic diagram of the smectic A phase of polymer COHB-4 is depicted in Figure 6-17.

For mesogens exhibiting several polymorphic smectic phases, the highly ordered ones will appear at the low end of the mesomorphic temperature range. When temperature decreases, the rotation of the segments in the layers will be constrained by the more favourable trans conformers, and eventually the units are frozen into a highly ordered array, the smectic B phase. Also, the trans arrangement of the carbonyl dipoles would be expected to assist the formation of the smectic B phase. In low molecular weight liquid crystals, X-ray diffraction shows that the molecules are arranged in layers with the molecular centres positioned in a hexagonally close-packed array $\langle 122 \rangle$. However, the molecules are still able to rotate about their molecular long axes, although, these rotations tend to be very much slower compared to the smectic A phase. The enormously large entropy demonstrated the solid-like structure of smectic B phase. A simplified structure of the smectic B phase of polymer COHB-4 is shown in Figure 6-18.

As mentioned for polymer COHB-4, there is a tendency of formation of the smectic phase due to the reduced degrees of freedom of configuration, therefore, it is no surprise to find polymer COHB-3 also exhibits smectic phases. However, as the odd membered spacer gets shorter, glutaric acid residue($n=3$),

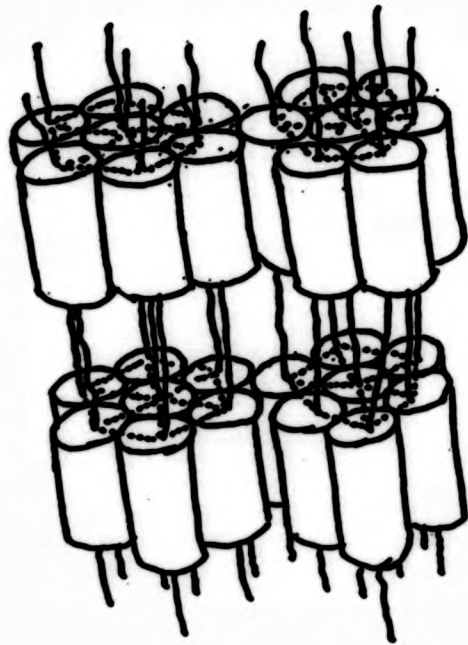


Fig. 6-18 The proposed molecular alignment of the smectic B phase for polymer COHB-4

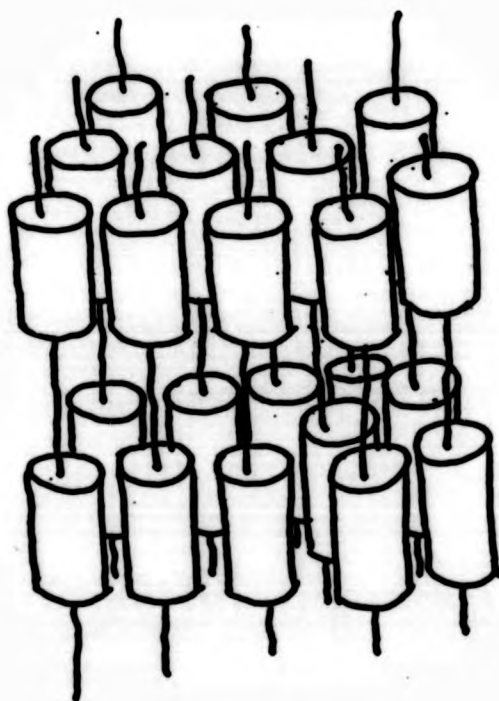


Fig. 6-19 The proposed molecular alignment of the smectic A phase for polymer COHB-3

short range interactions between the terminal ester groups occur when the two internal C-C bonds are in the g+g- or g-g+ conformation. In other words, a larger proportion of trans conformers would be preferred. For polymer COHB-3, the mechanism of formation of smectic A phase at higher temperature will be similar to that of polymer COHB-4. However, when the temperature was decreased, the relatively extended conformers (mostly trans) resulted in the rigid unit at the ends of the spacer being tilted about 30 degree from the long molecular axis. Consequently, the rigid segments confined within each layer will tilt at an angle θ (say 30 degrees) to the layer normal. This tilted arrangement is typical of a smectic C phase in low MW liquid crystals <122>. The possible alignments of polymer COHB-3 during a mesomorphic transition from smectic A phase to smectic C phase is depicted in Figures 6-19 & 6-20.

The enthalpic value for the clearing transition in polymer COHB-3 is 1.80 kJ/mol which is very much smaller compared with polymer COHB-4. Apart from the odd-even effect which should be taken into account, the main cause is that the enthalpies associated with the transition from smectic C phase to smectic A phase is very small and sometimes almost undetectable by DSC (Figure 6-3).

The argument for formation of smectic mesophases based on the reduced degrees of freedom of configurations for the shorter spacer polymers COHB-3 and COHB-4 becomes debatable when the spacer length gets longer. However, a smectic mesophase was observed in polymer COHB-10; what is the reason for this phenomenon?

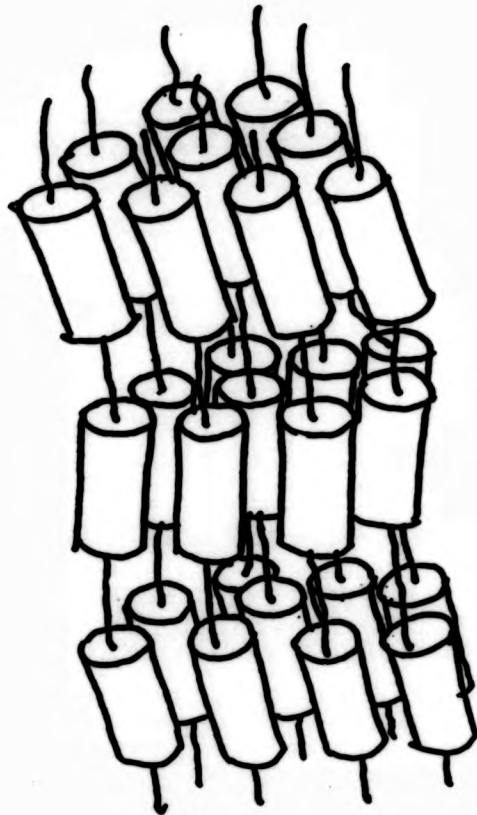


Fig. 6-20 The proposed molecular alignment of the smectic C phase for polymer COHB-3

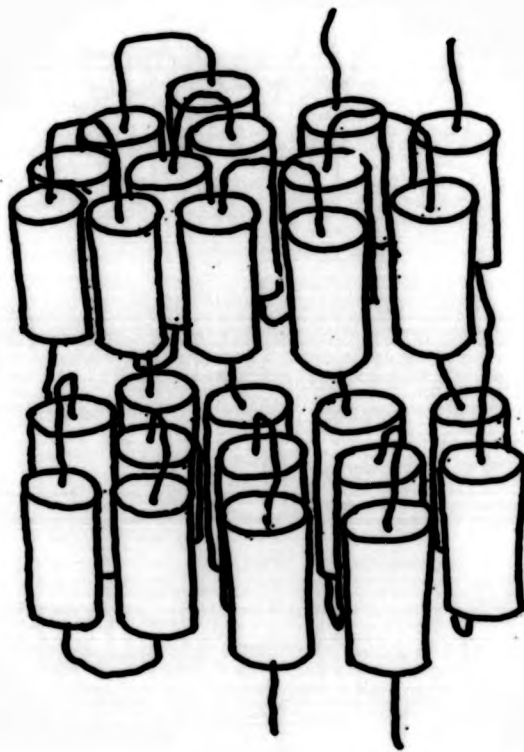


Fig. 6-21 The proposed molecular alignment of the smectic A phase for polymer COHB-10

In a perfectly crystalline polymer, all the chains would be incorporated in regions of three dimensional order, called crystallites. Perfectly crystalline polymers are not encountered in practice and instead polymers may contain varying proportions of ordered and disordered regions in the sample. These semi-crystalline polymers usually exhibit both T_g and T_m . When the polymer is in the melt state, the behaviour of the chains is largely influence by the proximity of the neighbouring chains and the secondary forces which act between them. These factors determine the orientation of the chains relative to each other.

Electron microscopy studies revealed that polymer single crystals are made up of thin lamellae of thickness about 10-20nm. The observation raises the dilemma of how a chain many times longer than the layer thickness and of non-uniform length, as chains usually are in the polymer, can be confined within the lamellae. The chains must fold back and forth at the regular intervals so that the lattice geometry between the straight stems is preserved.

This famous 'chain folded model' <140> could be logically extended to offer an explanation of the formation of a smectic liquid crystalline phase with very long spacers like polymer COHB-10.

The possible structural arrangements of polymer COHB-10 when changed from smectic A to smectic B phase is illustrated in Figures 6-21 and 6-22. The calorimetric data obtained was similar to polymer COHB-4, with $dH_i = 9.45 \text{ kJ/mol}$ and $dS_i = 5.71 \text{ cal/mol/K}$.

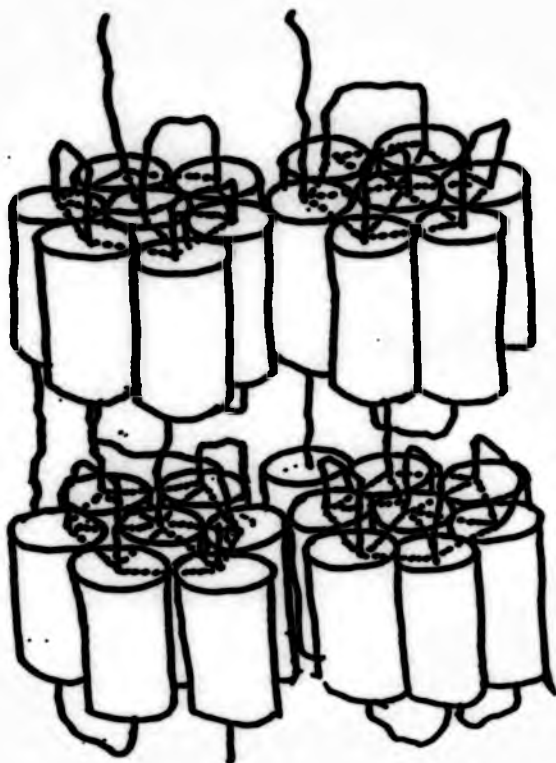


Fig. 6-22 The proposed molecular alignment of the smectic B phase for polymer COHB-10

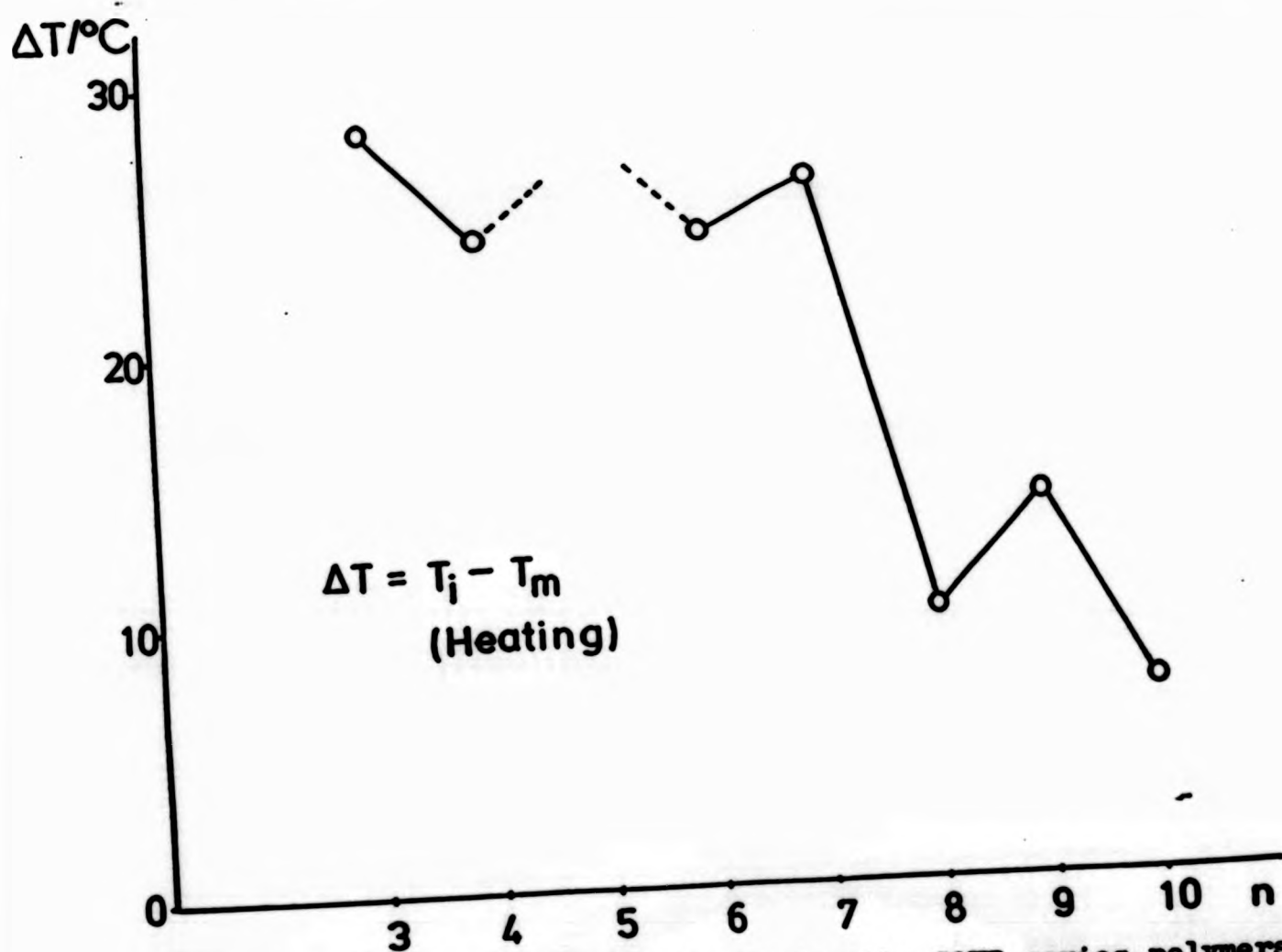


Fig. 6-23 The mesophase stability for the COHB series polymers

The mesophase stabilities of COHB polymers are illustrated in Figure 6-23. This parameter (dT) is defined as the difference between the clearing and the melting temperature. As shown in Figure 6-23, dT oscillates in an odd-even fashion. The temperature range over which the mesophase existed was consistently broader for the polymers with an odd n value as compared with those with an even n . A similar phenomenon was also observed by Ober et al. <99>. These authors attributed this to the ability of the variation in length of the spacer groups to have a greater effect of decreasing T_m than T_i , particularly among the polymers with odd numbered polymethylene spacers. Their argument was based on the higher enthalpy and entropy values of the odd membered series, despite the fact that both the clearing and melting transitions of the 'evens' are higher than the 'odds'. However, it needs to be mentioned that the thermodynamic parameters reported are generally in agreement with the COHB series in the way, dH_i and dS_i of even members are higher than the odd members <81,47>.

Bear in mind, for COHB polymers, the melting transition (T_m) was recorded from the first heating cycle, while the clearing transition (T_i) was taken from the second heating scan. Looking back to the DSC thermograms, some of the melting transitions for freshly prepared samples were either overlapped with the clearing transition or too ambiguous to be determined with confidence, although effort has been made to keep the thermal history constant. It is for this reason that the calorimetric values for melting were not measured. Iimura et al. <141> reported that higher molecular weight compounds have a wider

temperature range of mesophase stability. By referring to Table 6-2, the viscosities of the even numbered polymers are slightly lower than those of the odd numbered ones. While the thermal history was kept as constant as possible this could affect the observed trends. Also as the molecular weight and the molecular weight distribution were not clearly defined, their effects on mesophase stability is undetermined. The occurrence of a supercooling phenomenon accompanied by the odd-even effect is illustrated in Figure 6-24.

Most of the literature reviews indicate that a supercooling effect in liquid crystalline polymers is generally detected in the mesophase to crystal transition. There is now more evidence that this effect can also happen from the isotropic to mesomorphic transition^(104,117). There are two kinds of theory to explain this phenomenon, equilibrium and kinetic. Equilibrium theory is based on lattice dynamics and envisages a state of minimum free energy corresponding to a particular extension of the lattice along the chain direction⁽¹⁴²⁾. In the kinetic theory, based on the rate of crystallisation, supercooling occurs when the cooling rate is faster than the maximum rate of crystallisation⁽¹⁴²⁾.

One of the remarkable properties of liquid crystalline polymers is that the mesomorphic order can be locked into the glassy state. Such pre-transitional order induced by this mechanical shock might be one of the contributing factors to this unusual supercooling effect from the isotropic to the mesomorphic transition.

According to Figure 6-24, there is a consistent decrease in supercooling effect when the spacer length increases. Also,

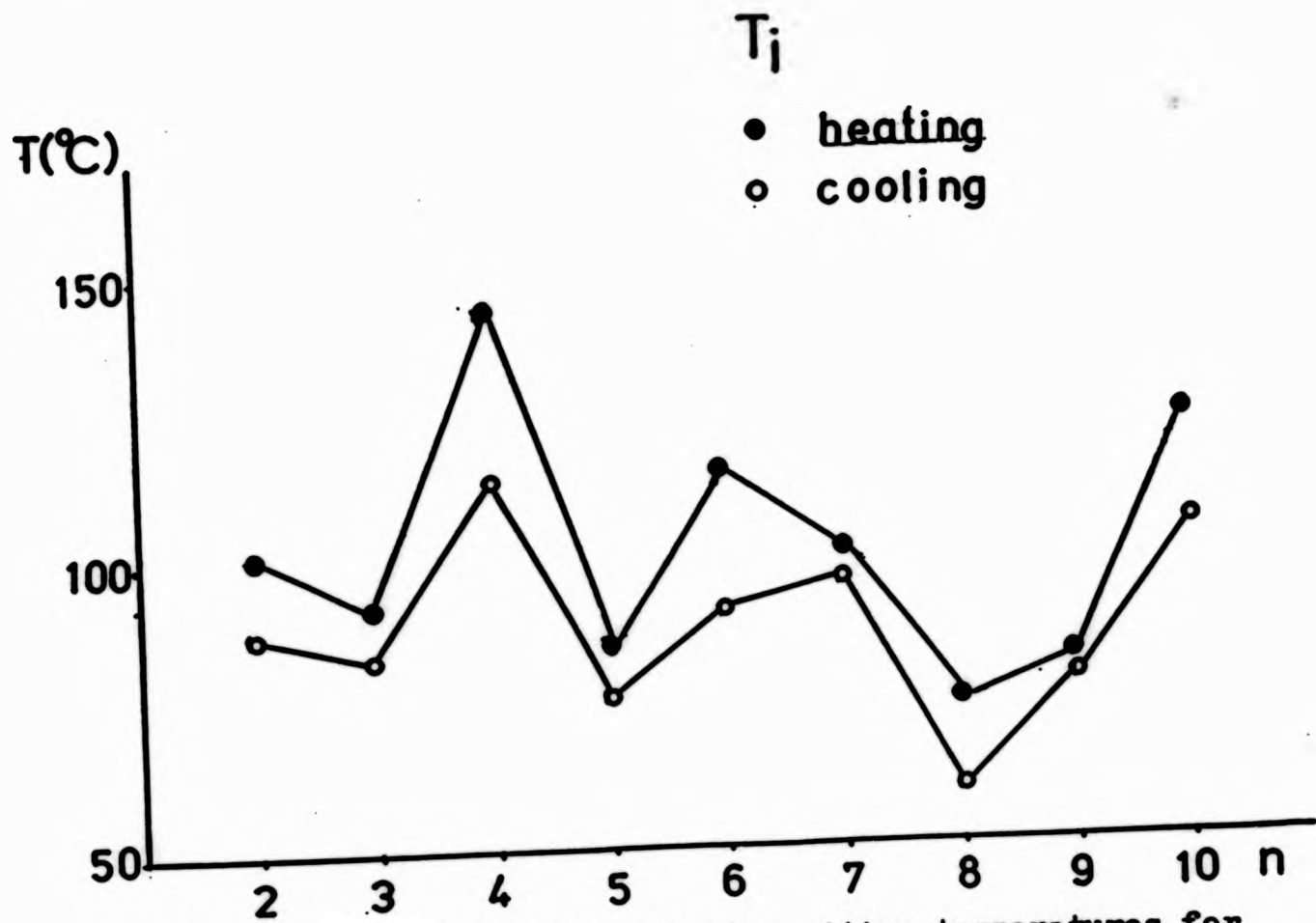


Fig. 6-24 Plots of the isotropic transition temperatures for the COHB series polymers obtained from heating and cooling.

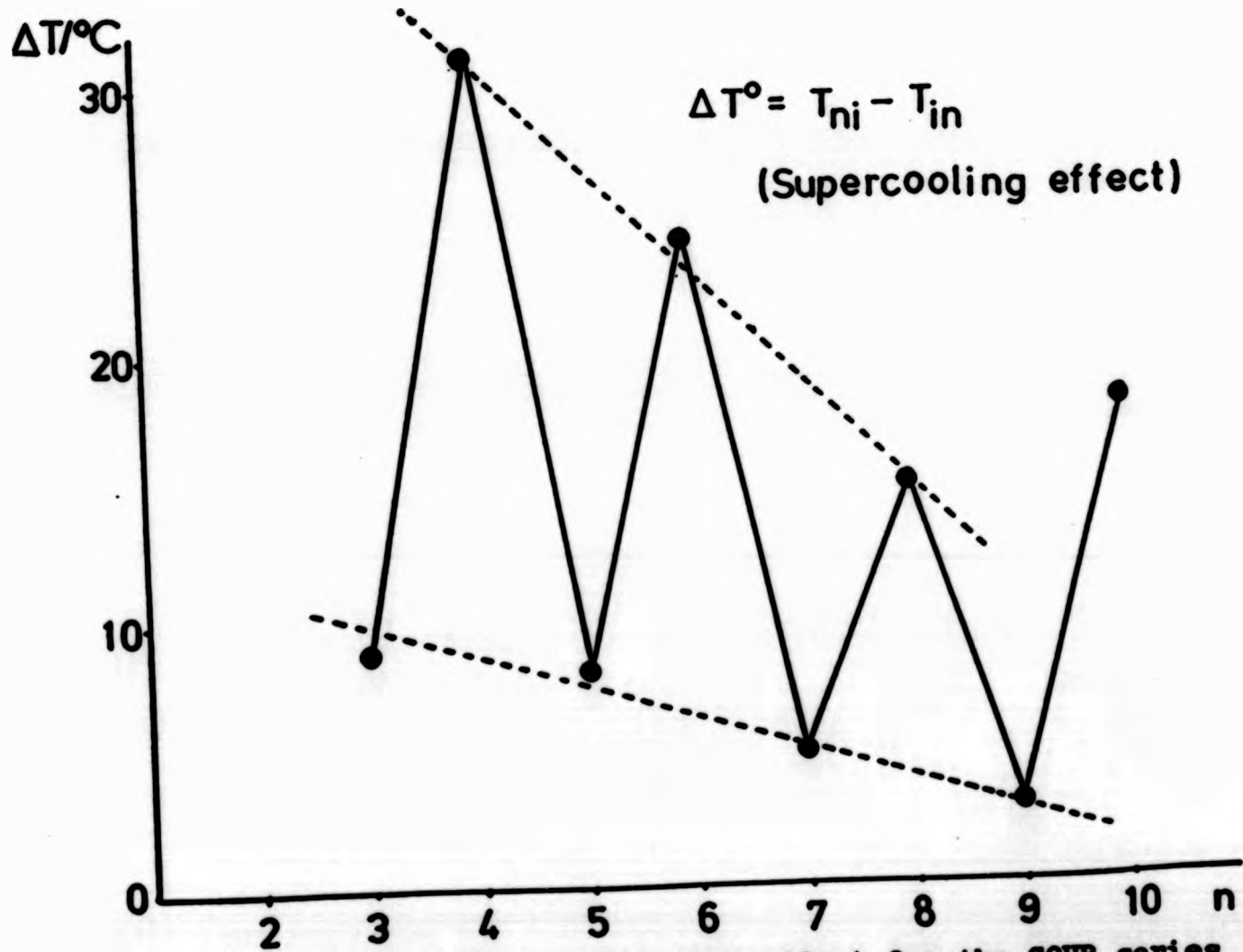


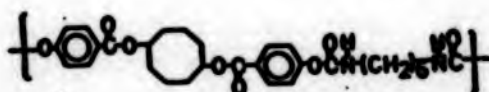
Fig. 6-25 Plot of the supercooling effect for the COHB series polymers.

this effect is more prominent for the even numbered series (Figure 6-25).

In the isotropic state, order does not exist, and chain entanglements will hinder the diffusion of chains into suitable orientations. The even numbered series when compared with the odd numbered series, at constant cooling rate, will have a larger proportion of gauche conformers at higher temperatures. On the other hand, the odd numbered series have their mesophases in a relative lower temperature region, and will be more ready to adopt the thermodynamically more stable trans conformers. As a result, it will take a longer time for the even numbered series to exhibit the liquid crystalline behaviour, hence, a larger supercooling effect is observed.

As the spacer lengths decrease, the mesophase to isotropic transitions also decrease; this reduced supercooling effect when ascending the homologous series could reasonably be explained by the above thermodynamic argument.

Finally, to demonstrate the importance of the linking group, polymer COHB-HDI with the following structure was prepared



The DSC thermogram is depicted in Figure 6-26. T_g was found at 337K and T_m at 509K with decomposition. The number of atoms between the two carbonyl carbons is equivalent to polymer COHB-8, however, no liquid crystalline behaviour could be observed. It is obvious that hydrogen bonding is a detrimental factor to the formation of a mesophase and should be avoided in designing the structure of thermotropic LC polymers.

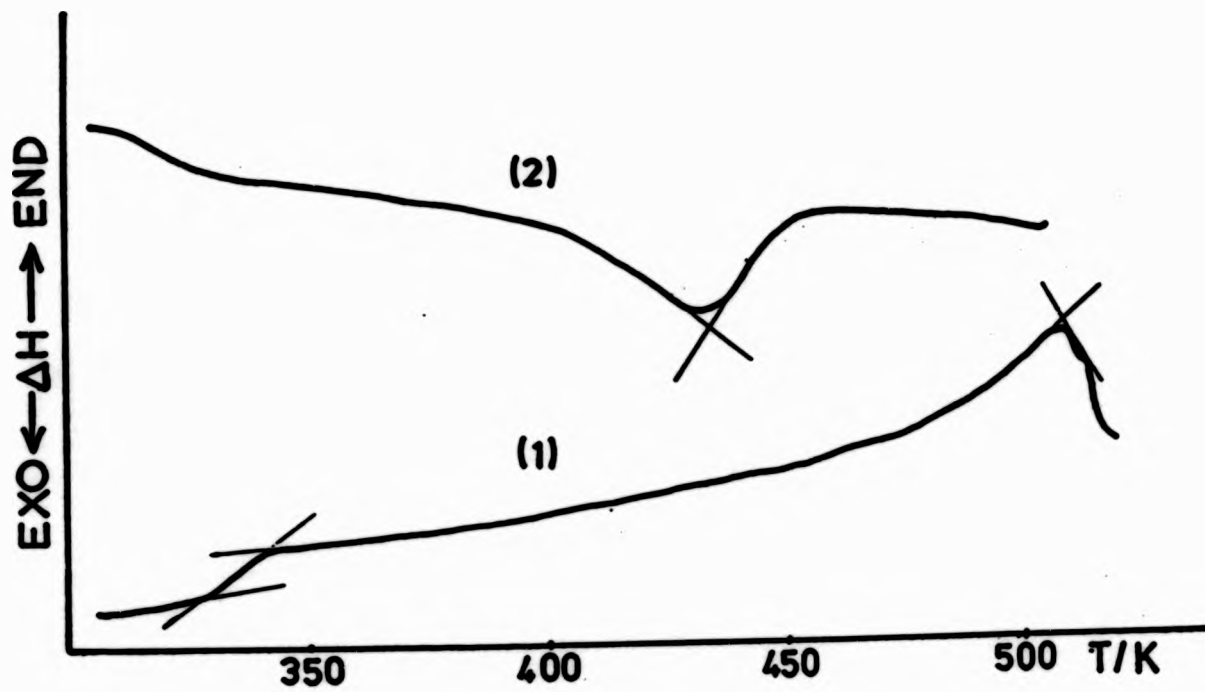


Fig. 6-26 DSC thermograms for polymer COHB-HDI
(1) heating
(2) cooling

EXO-VII - EWD

CHAPTER SEVEN
EFFECT OF SUBSTITUENTS

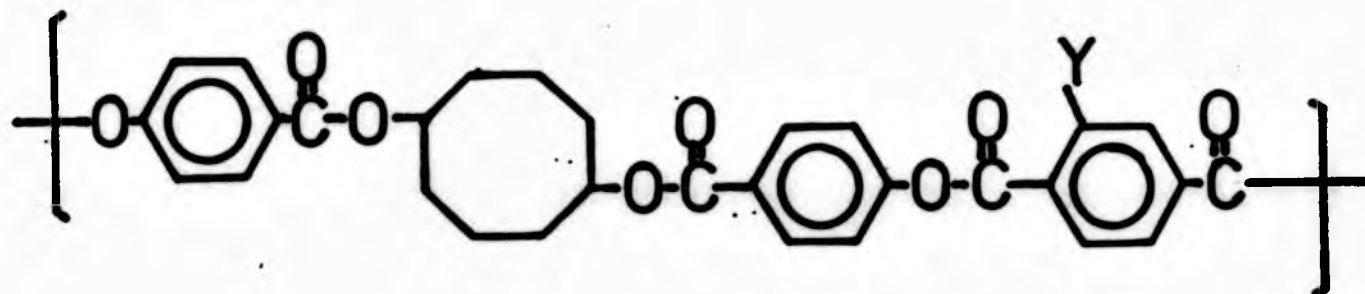
It is well known that in low molecular weight liquid crystals, substituents can act to reduce the coplanarity of adjacent mesogenic groups and increase the diameter or decrease the axial ratio of the mesogens^{<143,144>}. In addition, the ordering of neighbouring mesogenic groups becomes more difficult because the side groups force the molecules apart in order to meet their own steric requirements. However, an increase in dipolar interactions between neighbouring polar substituents can also occur and it may be helpful, while the other effects may be detrimental, to the thermal stability of the liquid crystalline phase. The position of the substitution also influences the type of mesophase exhibited^{<144>}.

In completely rigid and extended linear polymers, such as poly(p-phenylene terephthalate) and related aromatic polyesters, the melting temperatures are usually above 800K, so decompositions start to occur before the appearance of liquid crystalline behaviour. Therefore, it is crucial to depress the melting temperatures of these polymers if they are to be spun in their liquid crystalline state. These high melting points can be decreased by several types of structural modification including (i) the introduction of a flexible spacer group in the main chain, (ii) the placement of lateral substituents on the repeating units, (iii) the introduction of molecular kinks or bends in these units, (iv) by copolymerisation with other rodlike comonomers^{<128,146>}.

Because of the difficulty of introducing various substituents into the mesogenic units of LC polymers, few such systematic studies have been made.

One of the earliest studies on the effect of substituents on lowering the melting and clearing temperatures of main chain thermotropic LC polymers is that described in patents issued to du Pont<147>. Most of the work on substituted polyesters was done by Lenz et al.<57,148,149>. Both steric and polar effects of the substituents had been studied<149>.

In the present study, three polyesters were prepared. Substituted terephthalic acids were used to polymerise with monomeric diol 'COHB'. The general structure of these polyesters is illustrated schematically as below:-



Y = H, Br, and NO₂

These polymers are named according to the diacids incorporated in the structure, viz: polymers TA-III, BTA and NTA. The liquid crystalline properties of these three polyesters are recorded in Table 7-1.

7.1 Polymer TA-III

Figure 7-1 shows the DSC thermograms of polymer TA-III. Both crystal to mesophase transition(T_m) and mesophase to isotropic transition(T_{ni}) were obtained from the first heating scan because the sample decomposed at high temperature if held for long. The glass transition(T_g) was determined from the second heating cycle. The cooling scan was virtually

<u>Polymer</u>	<u>T_g (K)</u>	<u>T_m (K)</u>	<u>T_{m1} (K)</u>	<u>ΔT</u>
TA	358	442	517	75
BTA	353	457	550	93
NTA	351	430	505	75

Table 7-1 Liquid crystalline transitions for polymer TA, polymer BTA and polymer NTA

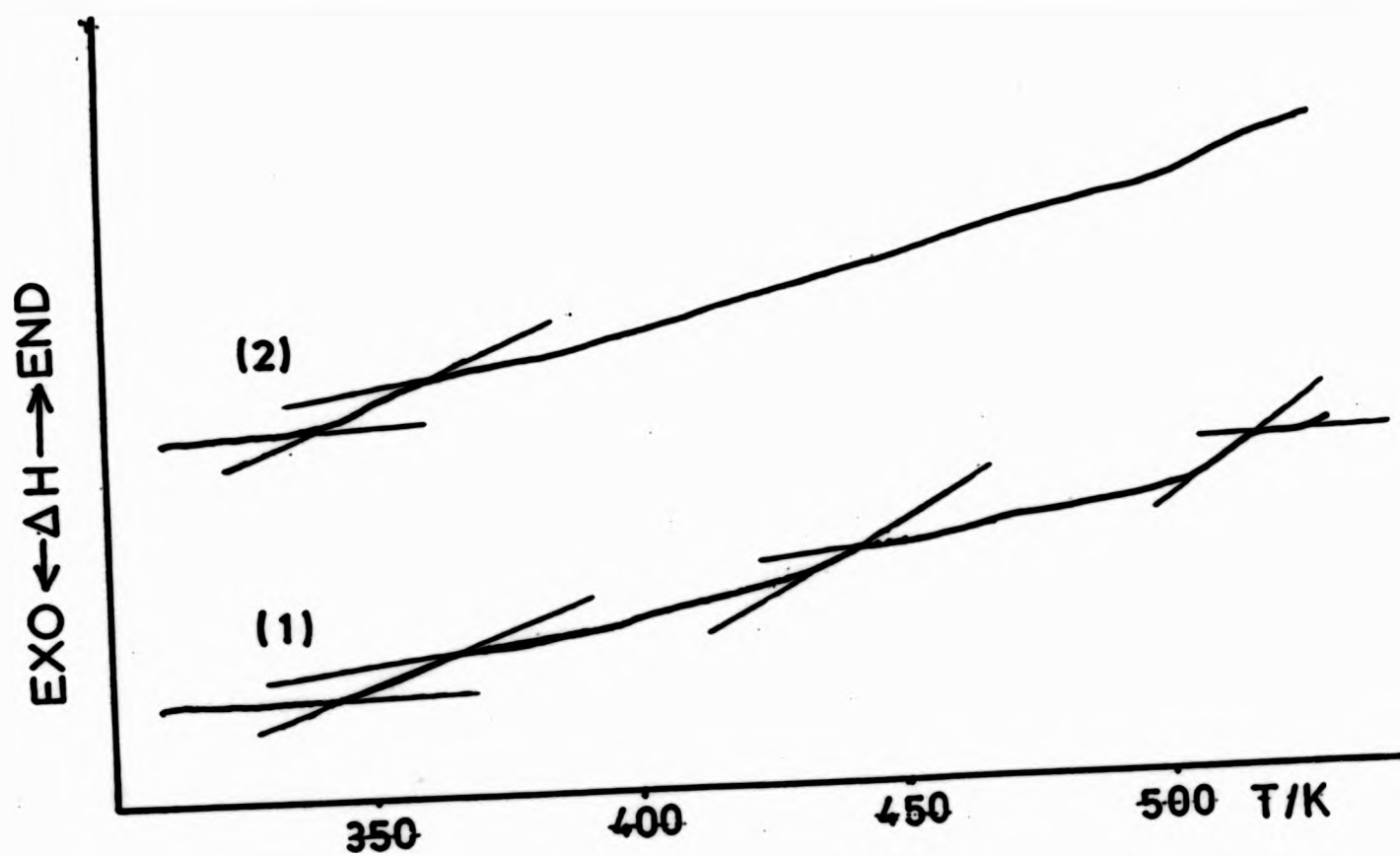


Fig. 7-1 DSC thermograms for polymer TA-III
 (1) 1st heating scan
 (2) 2nd heating scan

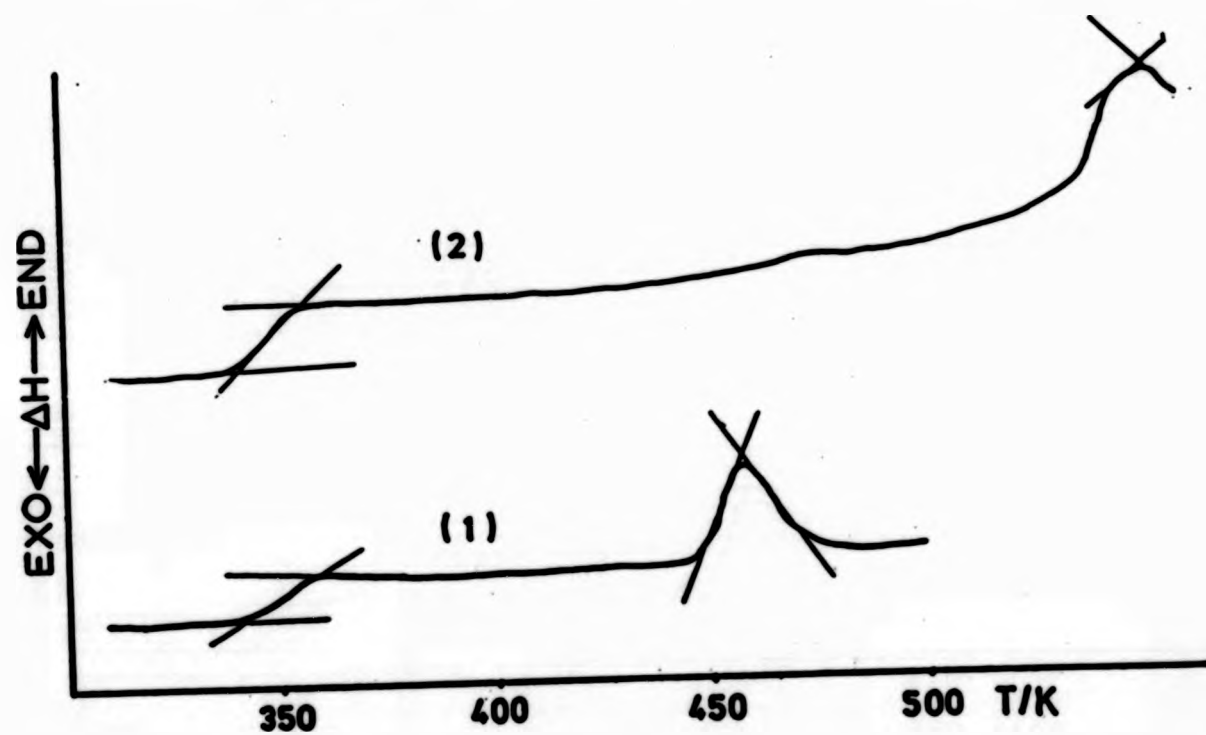


Fig. 7-2 DSC thermograms for polymer BTA
 (1) 1st heating scan
 (2) 2nd heating scan

non-informative. T_g , T_m and T_{ni} are at 358K, 442K and 517K respectively.

The mesophase stability of polymer TA-III is about 75K based on the DSC measurement. However, studies under the hot-stage microscope revealed the existence of a biphasic region which is probably due to the broad molecular weight distribution. The last anisotropic phase observed by hot-stage microscope vanished at about 600K.

Microphotographs of polymer TA-III are shown in Plate 7-I and 7-II. The sample was heated until it cleared (ca 600K) and then gradually cooled to 500K, photographs were taken at this temperature. On the top left hand side of Plate 7-II, the appearance of tiny droplets in a homeotropic background revealed the existence of a nematic phase. When the temperature was decreased to 490K and annealed for about 20 minutes, nematic droplets began to coalesce (Plate 7-I), while the brownish charred region was due to decomposition at high temperature.

Rigid polymers like poly(p-phenylene terephthalate) have a melting temperature above 800K, by replacing the phenylene group with cyclooctyl unit leads to a significant depression of melting temperature.

7.2 Polymer BTA

The DSC thermograms of polymer BTA are displayed in Figure 7-2. The crystal to mesophase transition was at 457K based on the first heating scan. In order to avoid decomposition, the sample was only heated up to 500K in the first scan. After cooling, the sample was scanned at 20K/min until decomposition

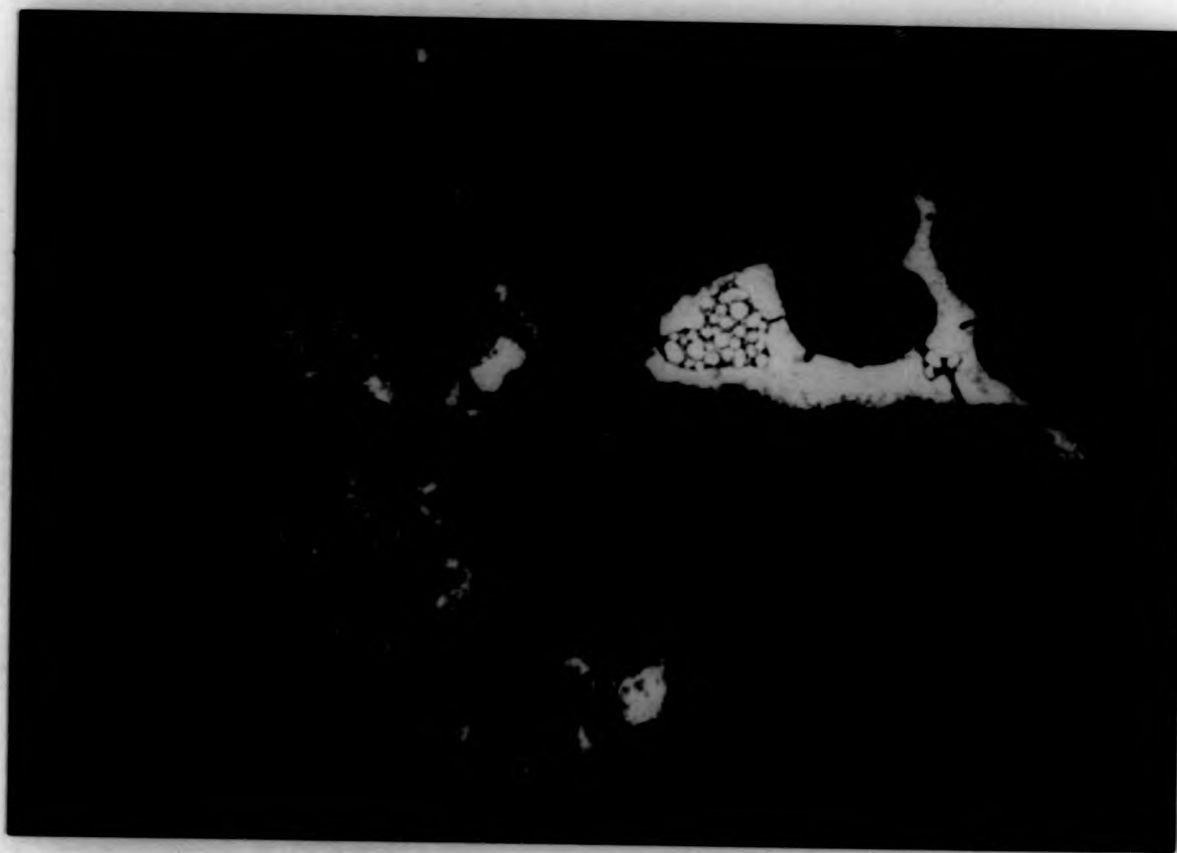


Plate 7-I The appearance of nematic droplets from the isotropic phase of polymer TA-III



Plate 7-II The coalescence of nematic droplets of polymer TA-III

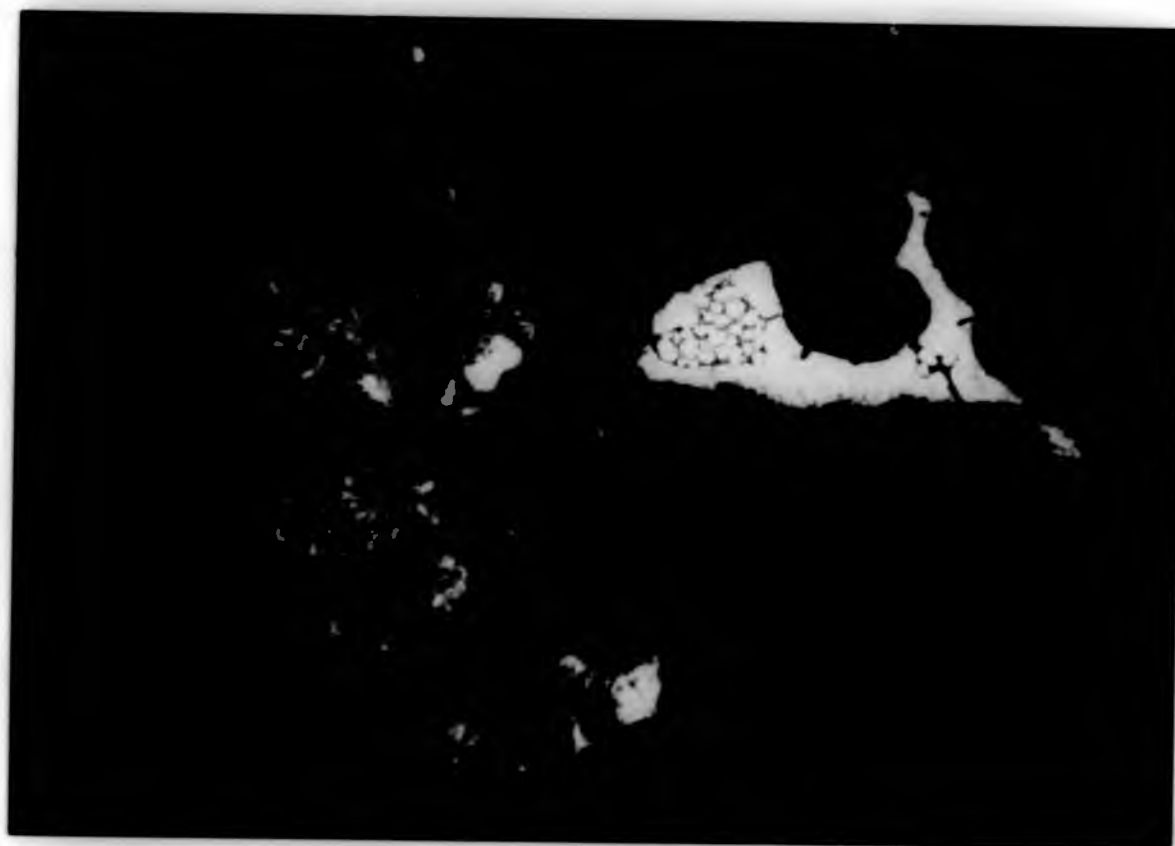


Plate 7-I The appearance of nematic droplets from the isotropic phase of polymer TA-III



Plate 7-II The coalescence of nematic droplets of polymer TA-III

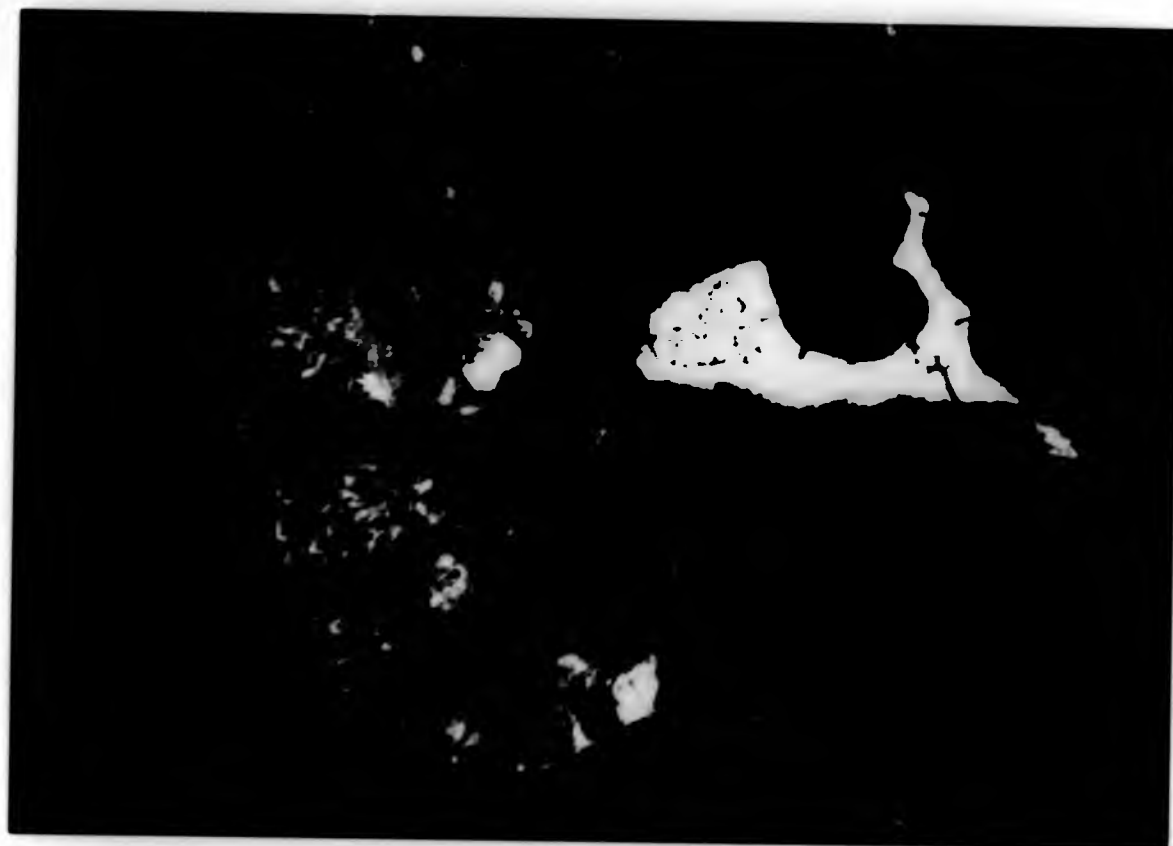


Plate 7-I The appearance of nematic droplets from the isotropic phase of polymer TA-III

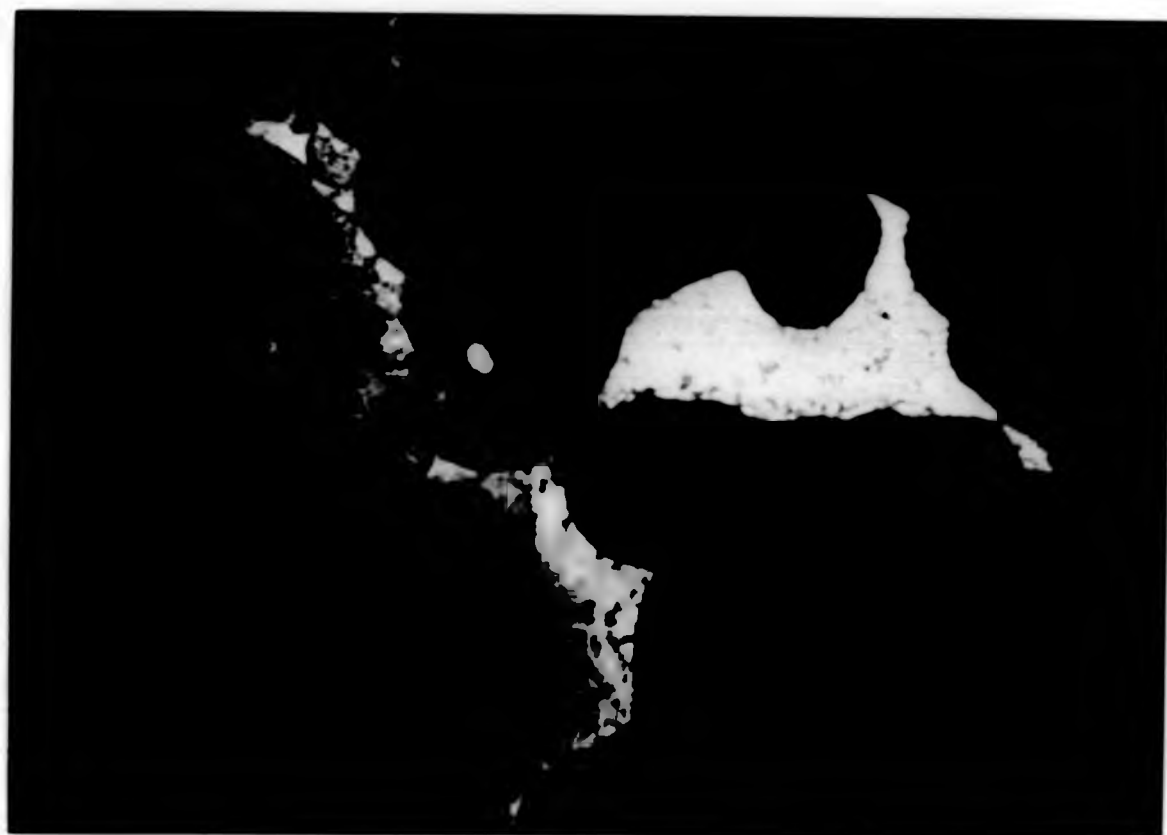


Plate 7-II The coalescence of nematic droplets of polymer TA-III

occurred. The glass transition and the isotropic transition were found at 353K and 550K respectively.

When polymer BTA was cooled from the isotropic melt to 530K, a blurred schlieren texture began to develop (Plate 7-III). After annealing at this temperature for 30 minutes, large coloured domains started to irradiate from the centre of the anisotropic melt (Plate 7-IV). A fully developed nematic schlieren texture (Plate 7-V) was obtained after prolonged annealing (3 hours).

The mesophase stability of polymer BTA according to DSC is 93K. Compared with polymer TA-III, the effect of the bromo-group seems not only to increase the mesophase stability (ca 18K) but also to increase both melting and isotropic temperatures.

7.3 Polymer NTA

The DSC thermograms of polymer NTA are depicted in Figure 7-3. When the sample was observed under the hot-stage microscope, at about 510K, decomposition began to occur. In order to avoid this happening during the heating scan, the highest temperature for the first two scans was restricted at 490K. After that, the sample was heated up until the mesophase to isotropic transition began to appear. Based on this workout, the glass transition and the melting point were found at 351K and 430K respectively from the second scan, while the mesophase to isotropic transition along with some degree of degradation was recorded at 505K from the third scan. An exotherm representing cold crystallisation was detected just below the melting point. This phenomenon was not found in

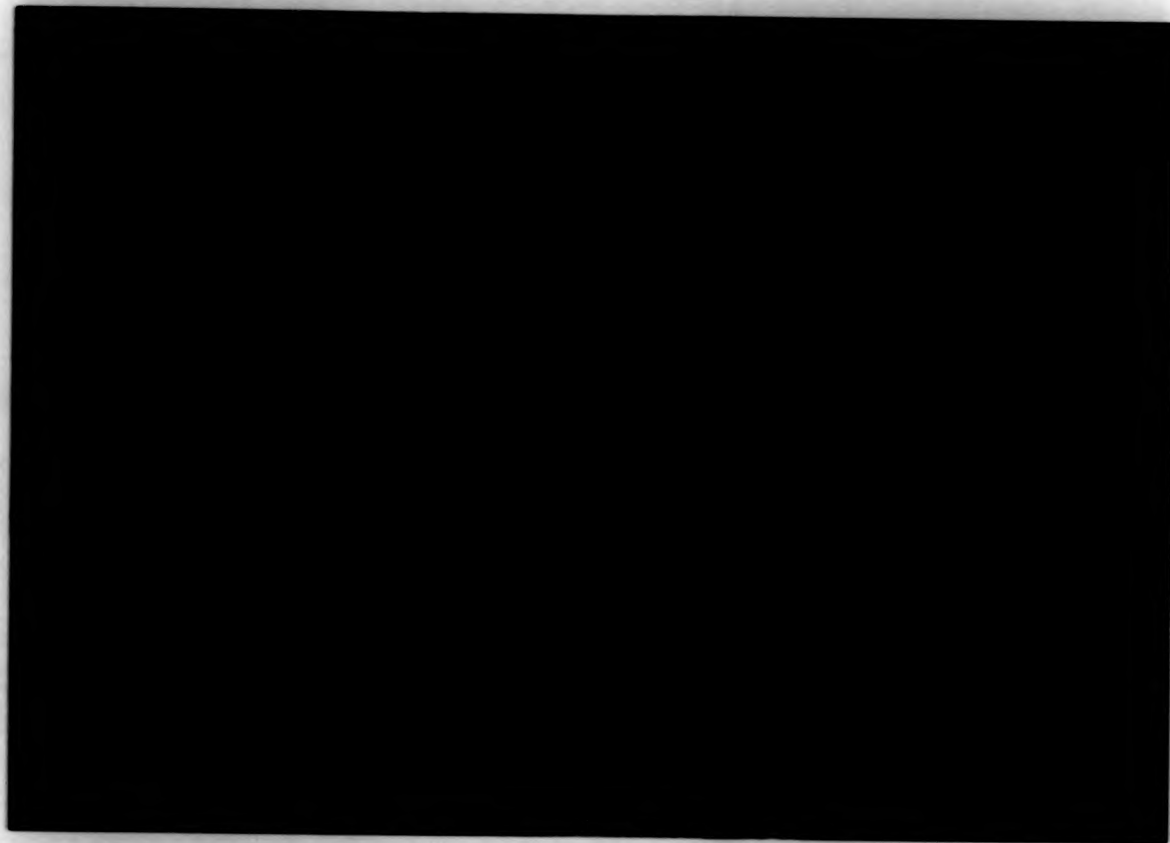


Plate 7-III The blurred schlieren texture of polymer BTA

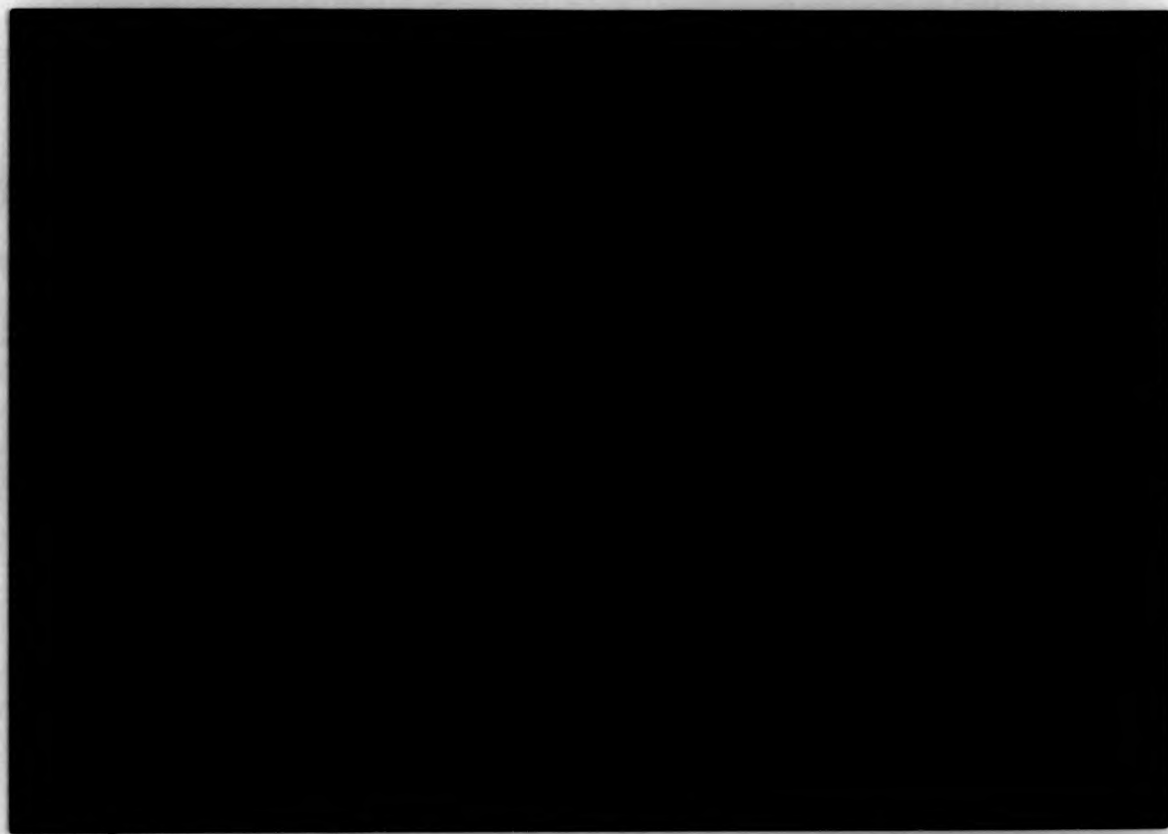


Plate 7-IV Polymer BTA after annealing at 530K for 30 minutes

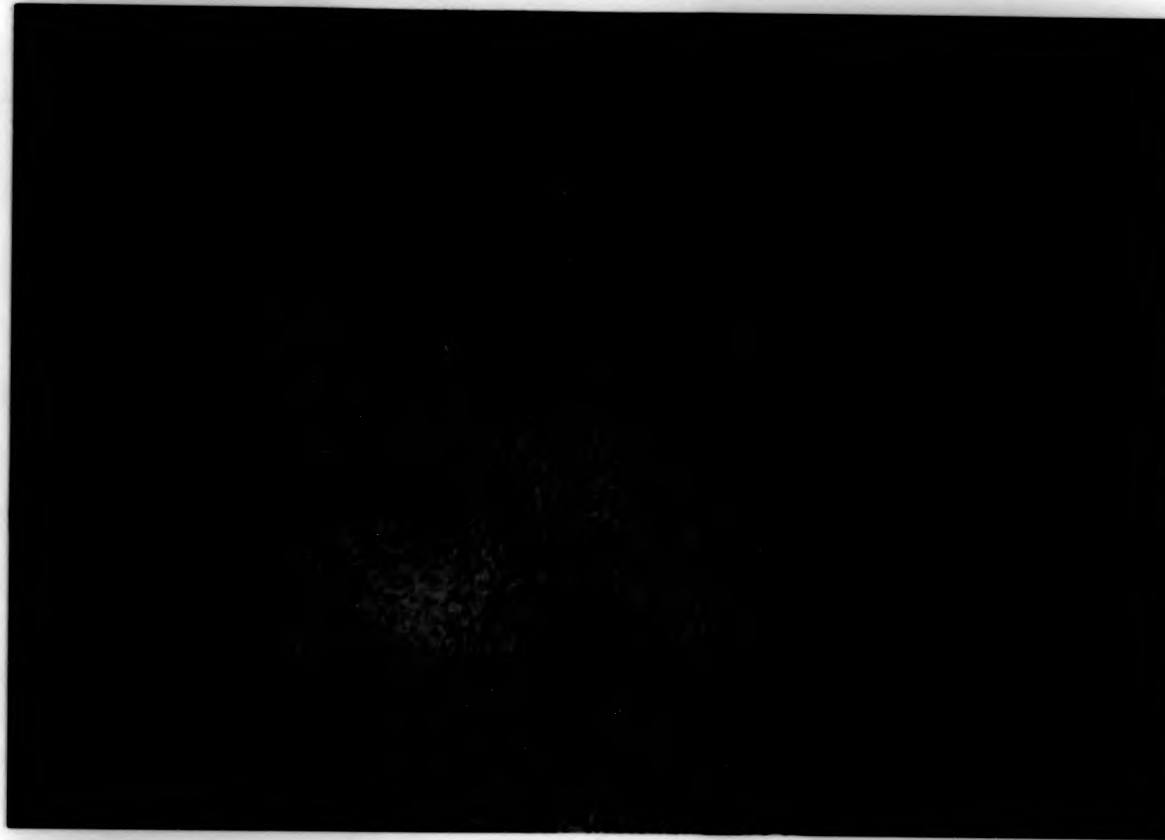


Plate 7-III The blurred schlieren texture of polymer BTA

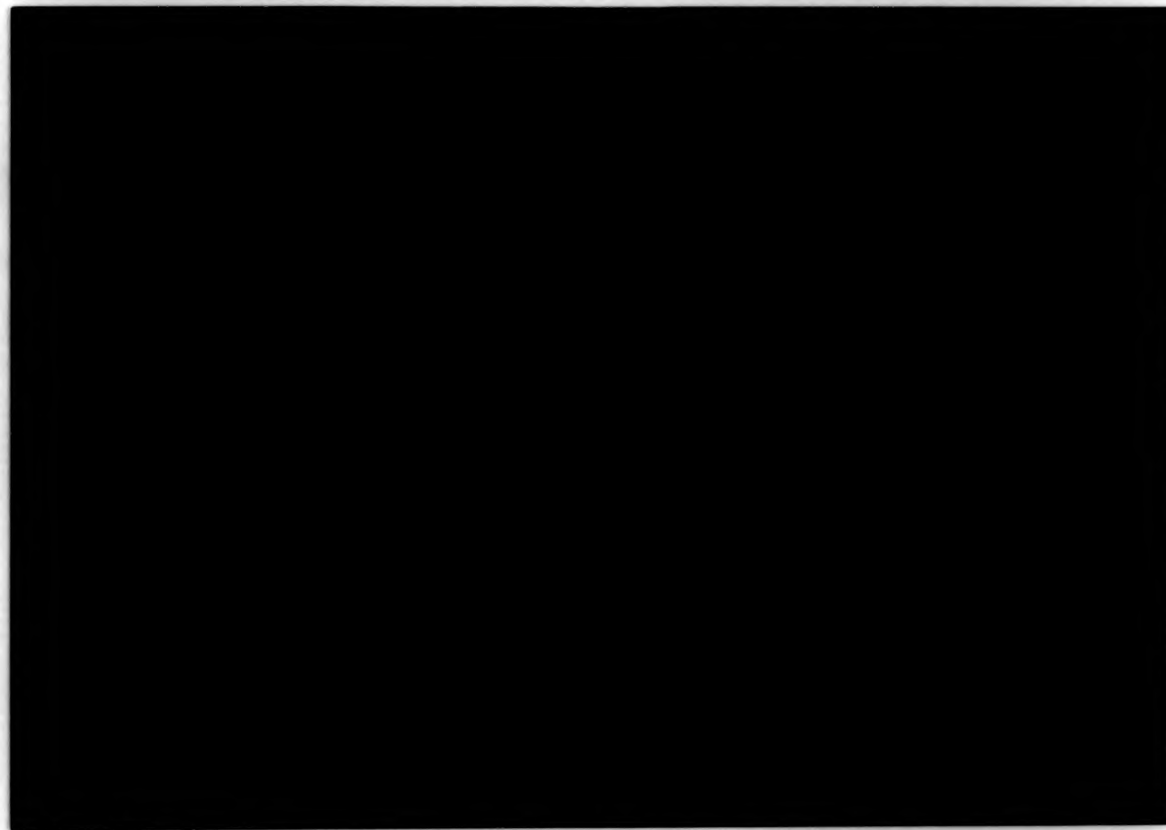


Plate 7-IV Polymer BTA after annealing at 530K for 30 minutes

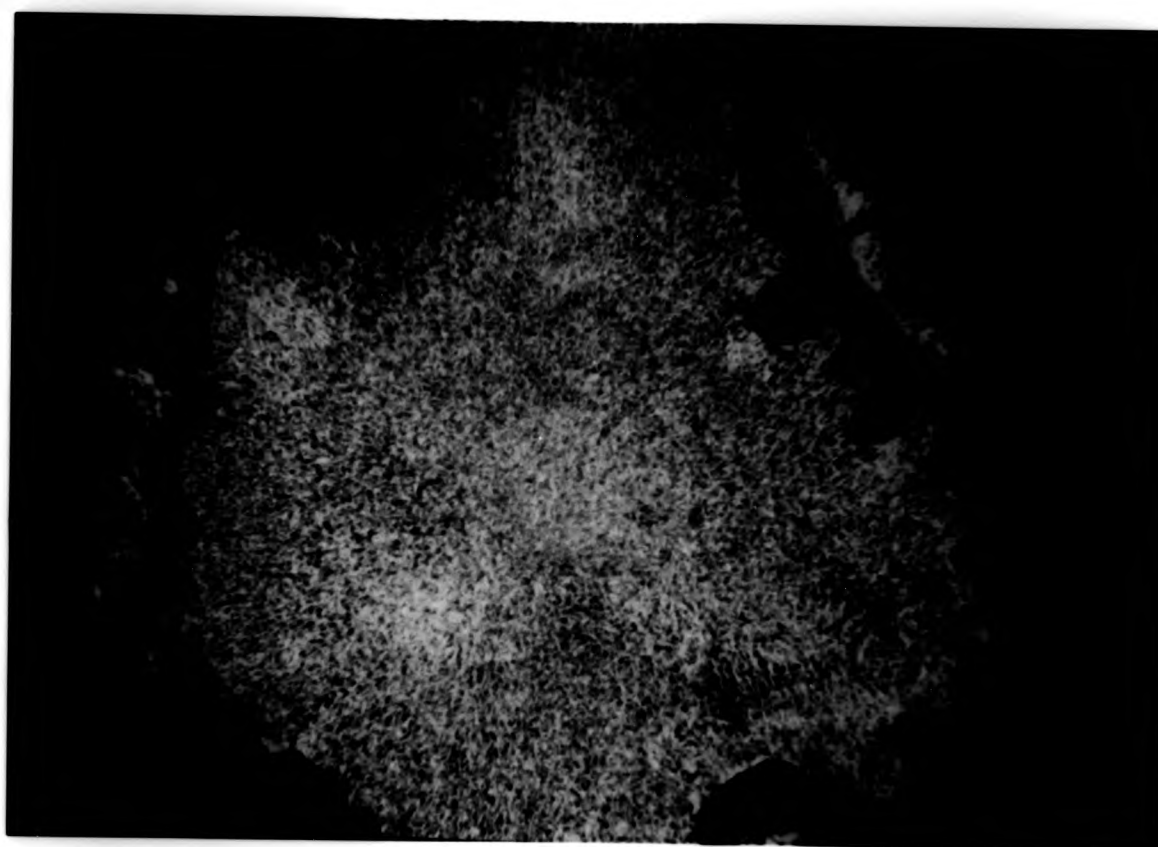


Plate 7-III The blurred schlieren texture of polymer BTA



Plate 7-IV Polymer BTA after annealing at 530K for 30 minutes

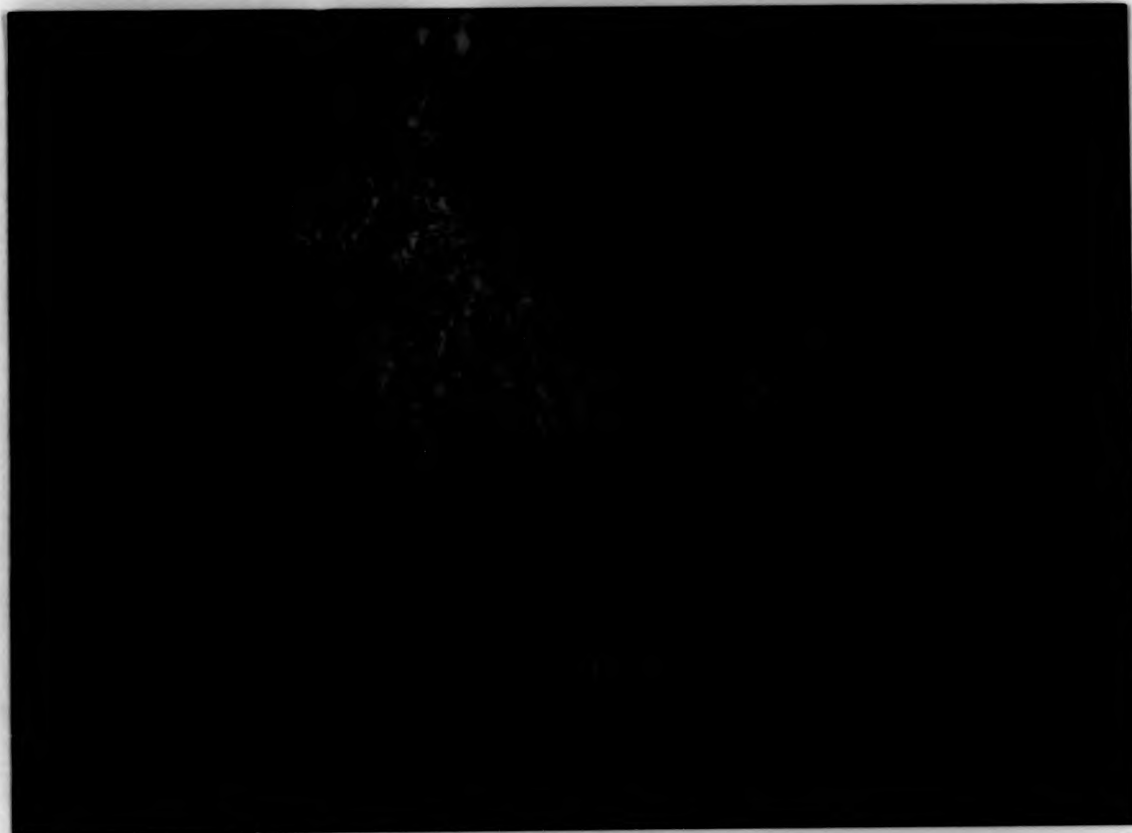


Plate 7-V The fully developed nematic schlieren texture of polymer BTA

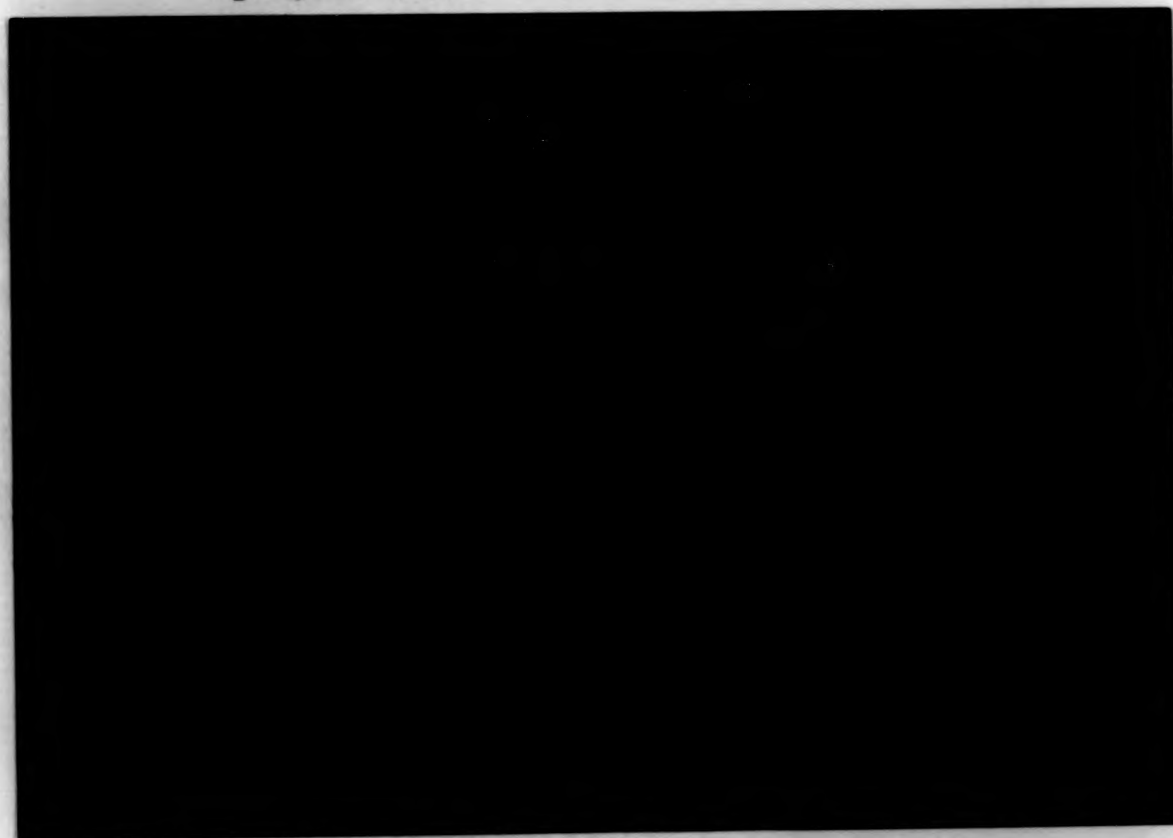


Plate 7-VI The threaded nematic texture of polymer NTA



Plate 7-V The fully developed nematic schlieren texture of polymer BTA



Plate 7-VI The threaded nematic texture of polymer NTA

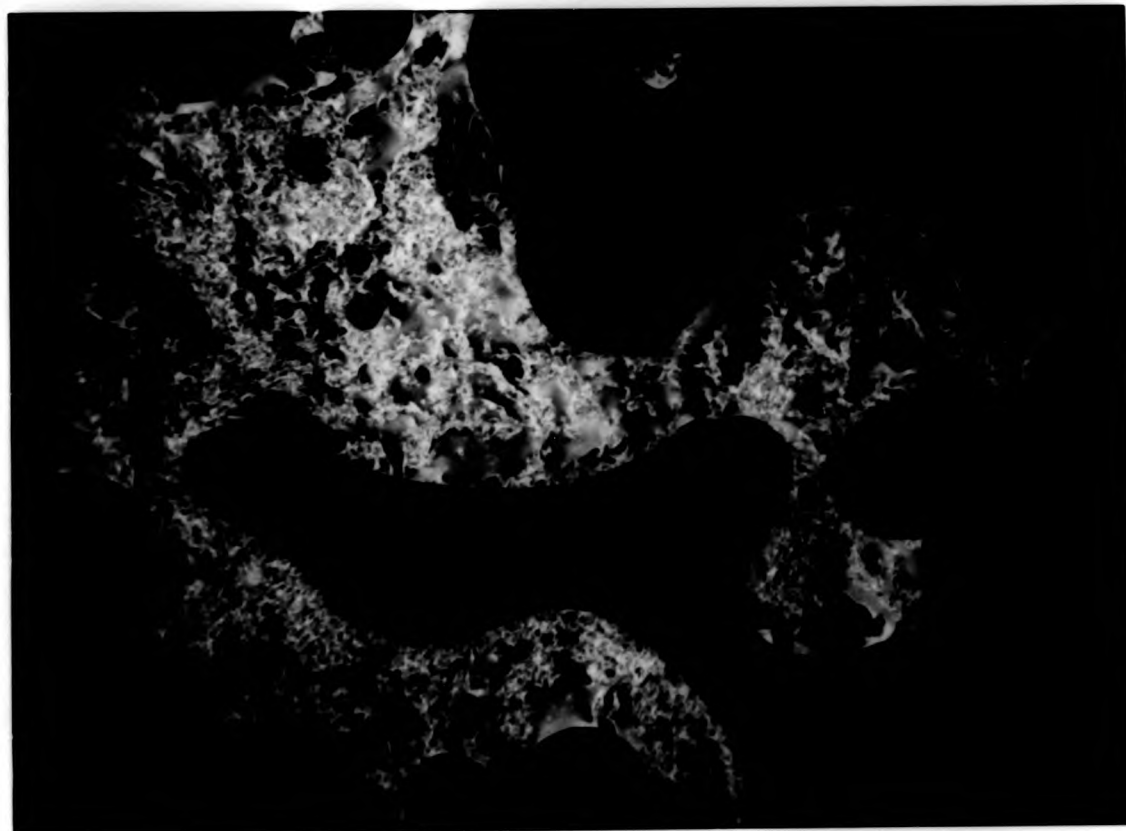


Plate 7-V The fully developed nematic schlieren texture of polymer BTA

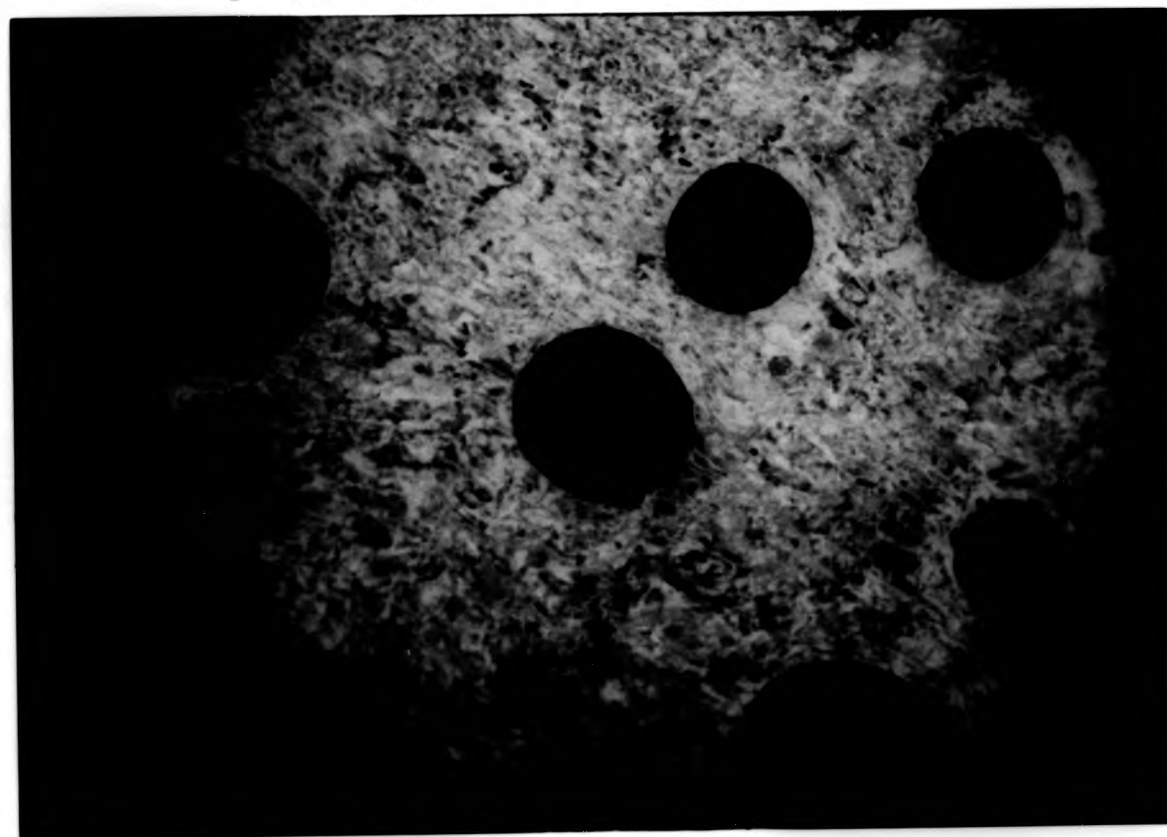


Plate 7-VI The threaded nematic texture of polymer NTA

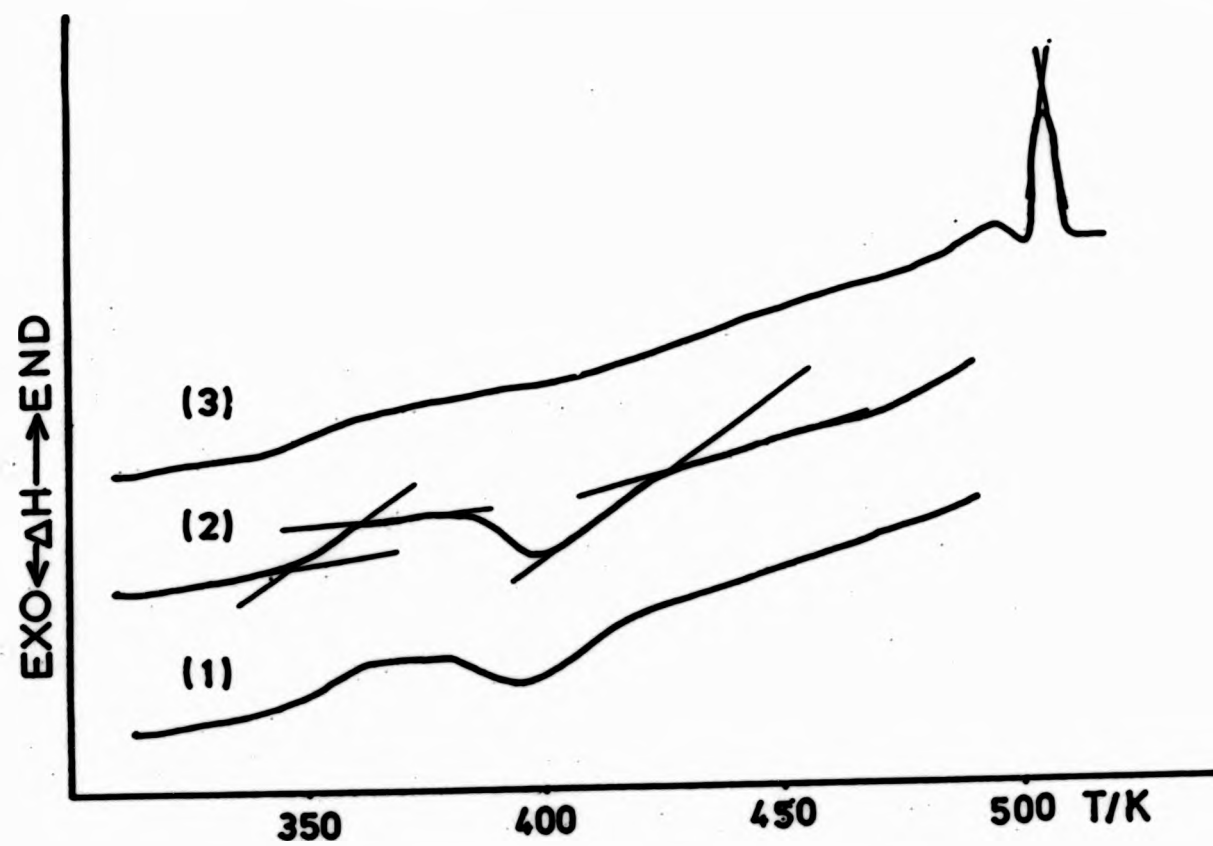


Fig. 7-3 DSC thermograms for polymer NTA
(1) 1st heating scan
(2) 2nd heating scan
(3) 3rd heating scan

polymer TA-III and BTA although the scanning rates were kept the same. It appears that the more bulky nitro-group retards the rate of crystallisation more effectively. A typical threaded nematic texture was observed in the mesomorphic state of polymer NTA (Plate 7-VI). Mesophase stability is about 75K which is narrower than polymer BTA.

7.4 Comparison of Polymers of Different Substituents

The effect of substituents on the mesophase stabilities of these polymers is shown in Figure 7-4. No sign of depression of either melting or isotropic temperatures can be noticed. Instead, in the case of polymer BTA there was actually an increase in both transition temperatures and the mesophase range, while for polymer NTA there was nearly no change at all. These observations were based on DSC measurements.

As mentioned earlier in this section, all of these polymers under study exhibit biphasic phenomenon and this phenomenon is particularly significant in polymer TA-III. If the mesophase stability was defined as the difference between T_{ni} (clearing temperature obtained by microscope) and T_m , then, the effect of substituents would agree with the general observation on bulky side groups, i.e. depression in both melting and clearing temperatures.

It is generally believed that size and polarity of the substituent are important factors in deciding the mesomorphic transition temperatures. The size of the nitro-group and the bromo-group based on van der Waals volumes are 16.8 and 14.4 cm²/mole respectively <150>. There is only a minor difference in size between these two, hence, the effectiveness in

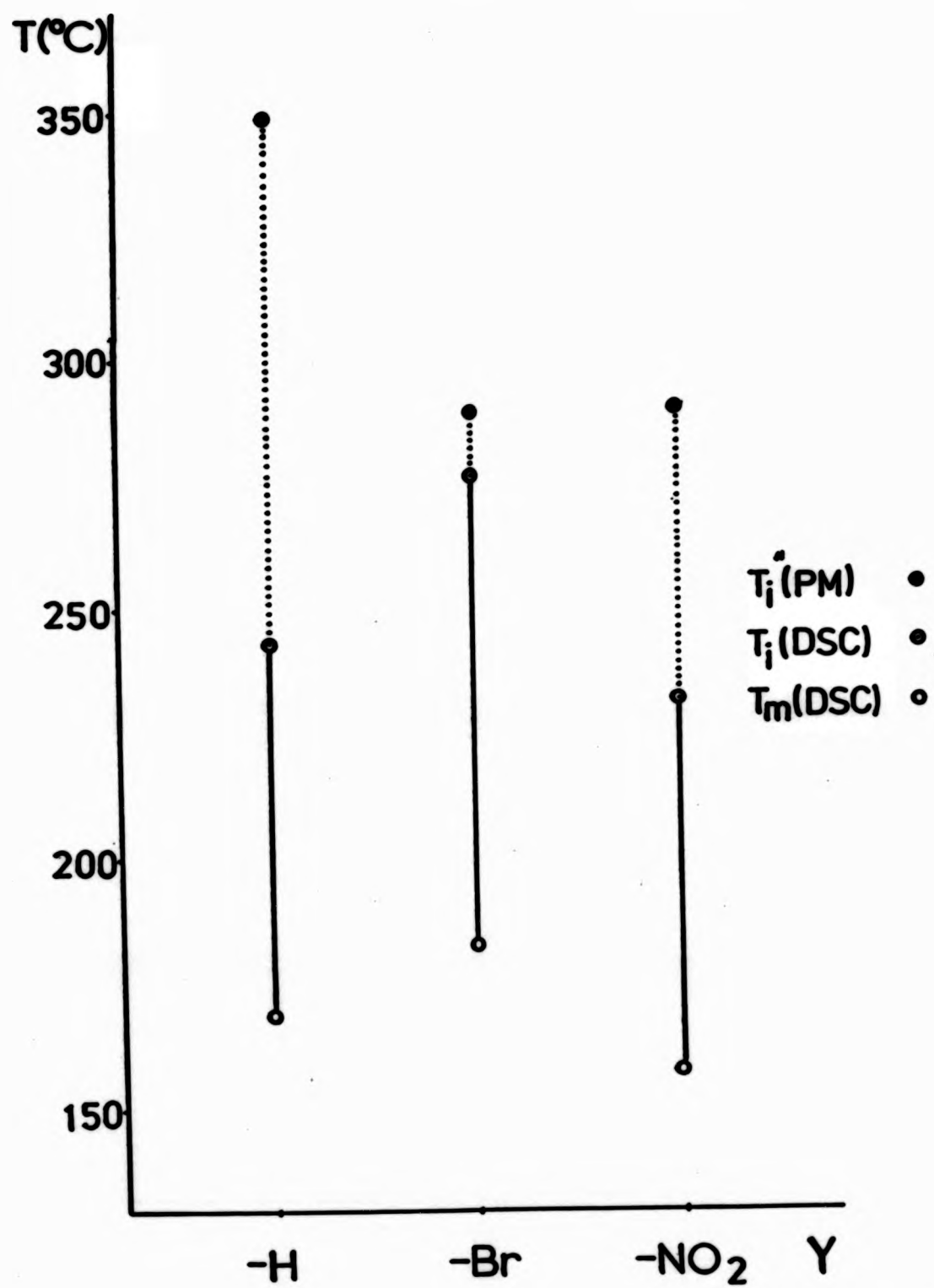


Fig. 7-4 Plots of mesophase range for polymer TA-III, polymer BTA and polymer NTA.

depressing the melting and the clearing temperatures must rest on the difference in polarity. The dipole moments of nitrobenzene and bromobenzene are 4.27×10^{-18} and 1.7×10^{-18} esu respectively^{<151>}. The nitro-group is nearly two and half times more polar than the bromo-group. The reduced mesophase stability of polymer NTA is probably a result of the strong repulsion exerted by the more polar nitro-group.

CHAPTER EIGHT

CHIRAL LIQUID CRYSTALLINE POLYMERS

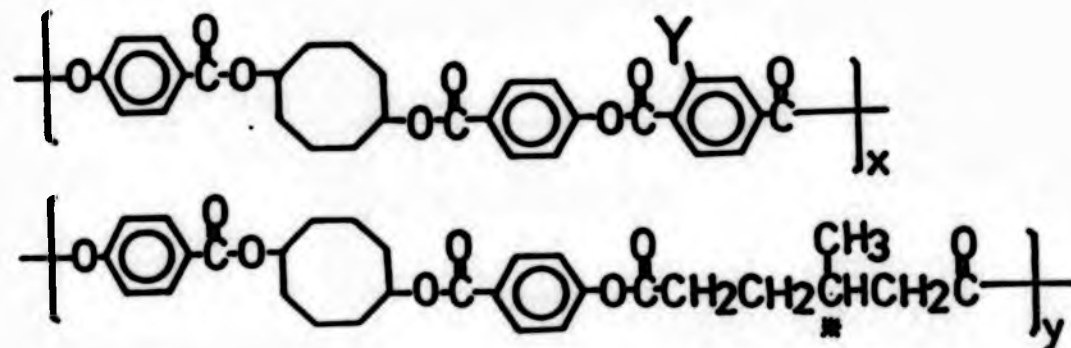
The uniaxial alignment characteristic of a nematic phase is ideal for the production of high modulus fibres, since the resulting distribution of molecules about the fibre axis is very narrow. A perfect biaxial orientation, with every molecule lying parallel to a plane, would be the corresponding 'ideal' orientation for a film. Such an ideal structure could be prepared as a composite from uniaxially orientated films by rotating the direction of preferred orientation of successive layers by a fixed angle. However, since each uniaxial film has highly anisotropic properties, it may be difficult to obtain the permanent adhesive bond necessary for such a composite. A molecular composite would appear to offer a more attractive route to biaxially oriented films. A thin cholesteric mesophase with 'Grandjean' texture would have all of the helical axes perpendicular to the plane. If such a texture could be conserved during solidification, the resulting film should have the optimum modulus if tested along any arbitrarily selected direction in the plane of the film.

It is well known that in sidechain LC polymers the copolymerisation of optically active monomers with mesogenic monomers, in the same manner as the mixing of optically active compounds with nematic low molecular weight compounds, can induce the formation of a cholesteric mesophase^(76,77,152). Therefore, it is expected that the inclusion of chiral spacers in the mainchain LC polymers, which would be nematic in the absence of the chiral centres, will lead to cholesteric products.

The properties of polymeric cholesteric phases have been mainly investigated for the lyotropic mesophases of

polypeptides<19,156> and cellulose derivatives<153,154,155>. The first examples of chiral thermotropic LC polyesters date back to 1980 and appeared almost simultaneously in the contributions of Strzelecki et al.<75> and Vilasagar et al.<157>. Systems containing the same commercially available (+)-3-methyladipic acid(MAA), as the chiral component, have been reported by other research groups<58,63,128,158,159>. A large variety of dihydroxylated benzenoid mesogens with an unsaturated or an oxycarbonyl group bridging two para-substitued aromatic nuclei were used in both polyesters and copolyesters<58,63,75,117,128,157,158,159>. Polyesters containing an aromatic triad mesogen consisting of a terephthaloyl residue bridging two hydroquinone units has been prepared<160>. Series of copolyesters containing the same mesogenic cores and variable mixtures of MAA and C6-C12 unbranched aliphatic diacids have also been investigated<161>.

Three series of cholesteric copolyesters based on COHB as the mesogenic core were synthesised. The bisphenol counterparts used included terephthalic acid(TA), bromo-terephthalic acid (BTA), nitro-terephthalic acid(NTA) and (+)-3-methyladipic acid(MAA). The general structure of these copolyesters is shown as below:-



Results are listed in Tables 8-1, 8-2 and 8-3 which illustrate the polymer compositions and transition

<u>composition</u>	<u>Yield</u>	<u>T_g (K)</u>	<u>T_m (K)</u>	<u>T_{m1} (K)</u>	<u>T_{m1}" (K)</u>	<u>ΔT</u>
100:0	0.70	358	442 (493)	517	(623)	
75:25	0.64	336	(460)	493	(526)	33
50:50	0.54	335	(410)	475	(540)	65
25:75	0.65	327	(408)	433	(458)	25
0:100	0.96	327	376	388		

Table 8-1 Liquid crystalline transitions for the TA-MAA series copolymers

() data based on polarising microscope

<u>composition</u>	<u>yield</u>	<u>T_g (K)</u>	<u>T_m (K)</u>	<u>T_{ni} (K)</u>	<u>T_{ni}" (K)</u>	<u>ΔT</u>
100:0	0.74	353	457 (388)	550	(563)	
75:25	0.58	343	(368)	486	(561)	75
50:50	0.65	341	(363)	476	(543)	67
25:75	0.68	330	(358)	433	(488)	55
0:100	0.96	327	376	388		

Table 8-2 Liquid crystalline transitions for the BTA-MAA series copolymers
() data based on polarising microscope

<u>composition</u>	<u>yield</u>	<u>T_g (K)</u>	<u>T_m (K)</u>	<u>T_{ni} (K)</u>	<u>T_{ni}" (K)</u>	<u>ΔT</u>
100:0	0.76	351	430 (413)	505	(566)	
75:25	0.65	350	(408)	376	(553)	77
50:50	0.68	347	(399)	442	(528)	86
25:75	0.60	323	(368)	404	(457)	47
0:100	0.96	327	376	388		

Table 8-3 Liquid crystalline transitions for the NTA-MAA series copolymers
 () data based on polarising microscope

temperatures.

The transition temperatures of these polymers were studied using both the hot-stage polarising microscope and DSC. All of the copolyester systems exhibited a biphasic region in which the isotropic and liquid crystalline phases coexist. This phenomenon was also observed by other research workers on cholesteric polymers⁶³. The crystal to mesophase transition (T_m) was determined as usual by DSC, the mesophase to isotropic transition (T_{ni}) was assigned from the peak of the highest endotherm. The highest temperature which the mesophase disappeared was T_{ni}'' which was determined by the polarising microscope. Thus, as the temperature is increased from T_{ni} to T_{ni}'' , the isotropic phase grows in the expense of the anisotropic phase. The difference between T_{ni} and T_{ni}'' is defined as the biphasic region.

8.1 Copolymer TA-MAAs

The DSC thermograms of copolymer TA-MAA(75:25) (the numbers in the bracket represent the molar feed ratio of TA to MAA) are shown in Figure 8-1. A well defined glass transition (T_g) was detected at 336K, followed by two very broad and small endotherms at 460K (T_m) and 493K (T_{ni}). All these transitions were obtained from the second heating scan. By comparing the first and the second heating scan, there is an apparent diminishing of the higher endotherm, repeated scans still gave the same pattern as the second scan. It seems that there is also a possibility of the existence of two melting endotherms with one of them (the higher one) overlapping with the biphasic region. The cooling scan was unremarkable, and

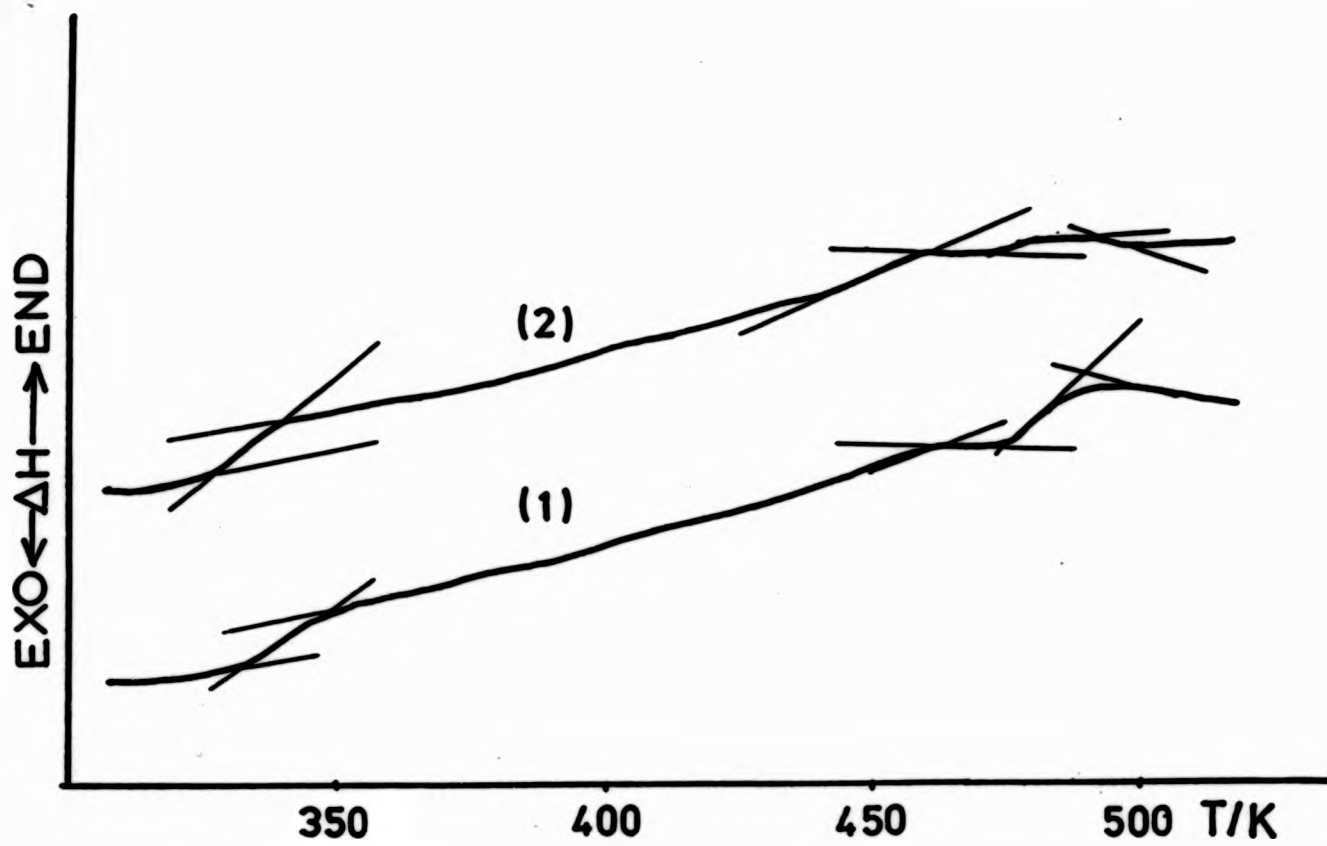


Fig. 8-1 DSC thermograms for copolymer TA-MAA(75:25)
 (1) 1st heating scan
 (2) 2nd heating scan

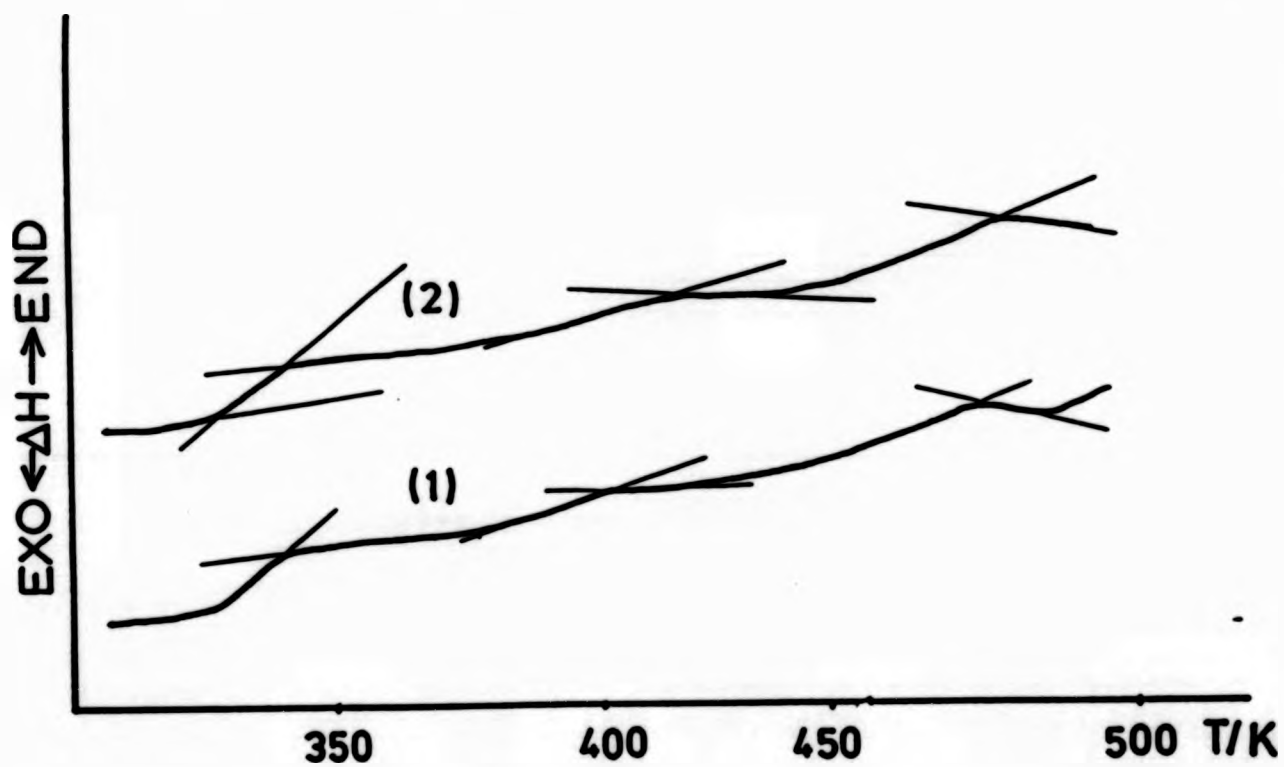


Fig. 8-2 DSC thermograms for copolymer TA-MAA(50:50)
 (1) 1st heating scan
 (2) 2nd heating scan

non-informative.

The transition temperatures of copolymer TA-MAA(50:50) are at 335K(T_g), 410K(T_m) and 475K(T_{ni}). The endotherms were still broad and widely separated(Figure 8-2). Copolymer TA-MAA(25:75), with an increased content of flexible spacer(MAA), exhibited a narrow mesophase stability, as expected; T_g , T_m and T_{ni} are at 327K, 408K and 433K respectively(Figure 8-3).

Figure 8-4 depicts the phase diagram of copolymer TA-MAAs with the transition temperatures plotted against the copolymer compositions.

All these polymers show typical copolymer effects in improving solubility properties(soluble in all chlorinated solvents). The mesophase stabilities are dependent upon the copolymer composition ranging from 408K to 493K. The greatest mesophase stability is reached for copolymer TA-MAA(50:50) is 65K. The randomness of different residues in the polymer backbone and the methyl-substituent in the flexible spacer help to disrupt the three dimensional order of polymer segments, which resulted in a relatively large depression in melting temperature particularly when the concentration of MAA is equal or above 50%. By contrast, the isotropic temperature appears to be affected to a lesser extent. For example, there is only a 24K decrease in T_{ni} for copolymer TA-MAA(25:75), while T_m , in fact, is 22K higher than the corresponding 'homopolymer' TA-MAA(100:0). On the other hand, when the concentration of MAA dropped below 50%, there was little effect on the melting temperature, the difference between copolymer TA-MAA(50:50) and copolymer TA-MAA(25:75) is merely

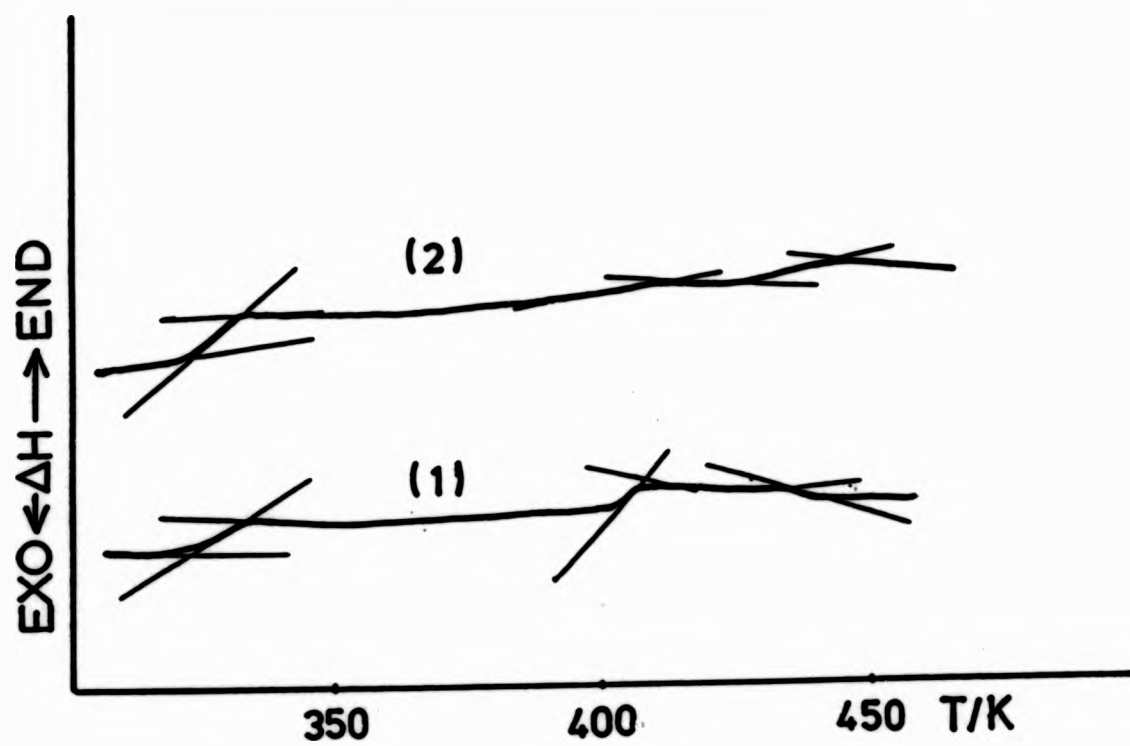


Fig. 8-3 DSC thermograms for copolymer TA-MAA(25:75)
 (1) 1st heating scan
 (2) 2nd heating scan

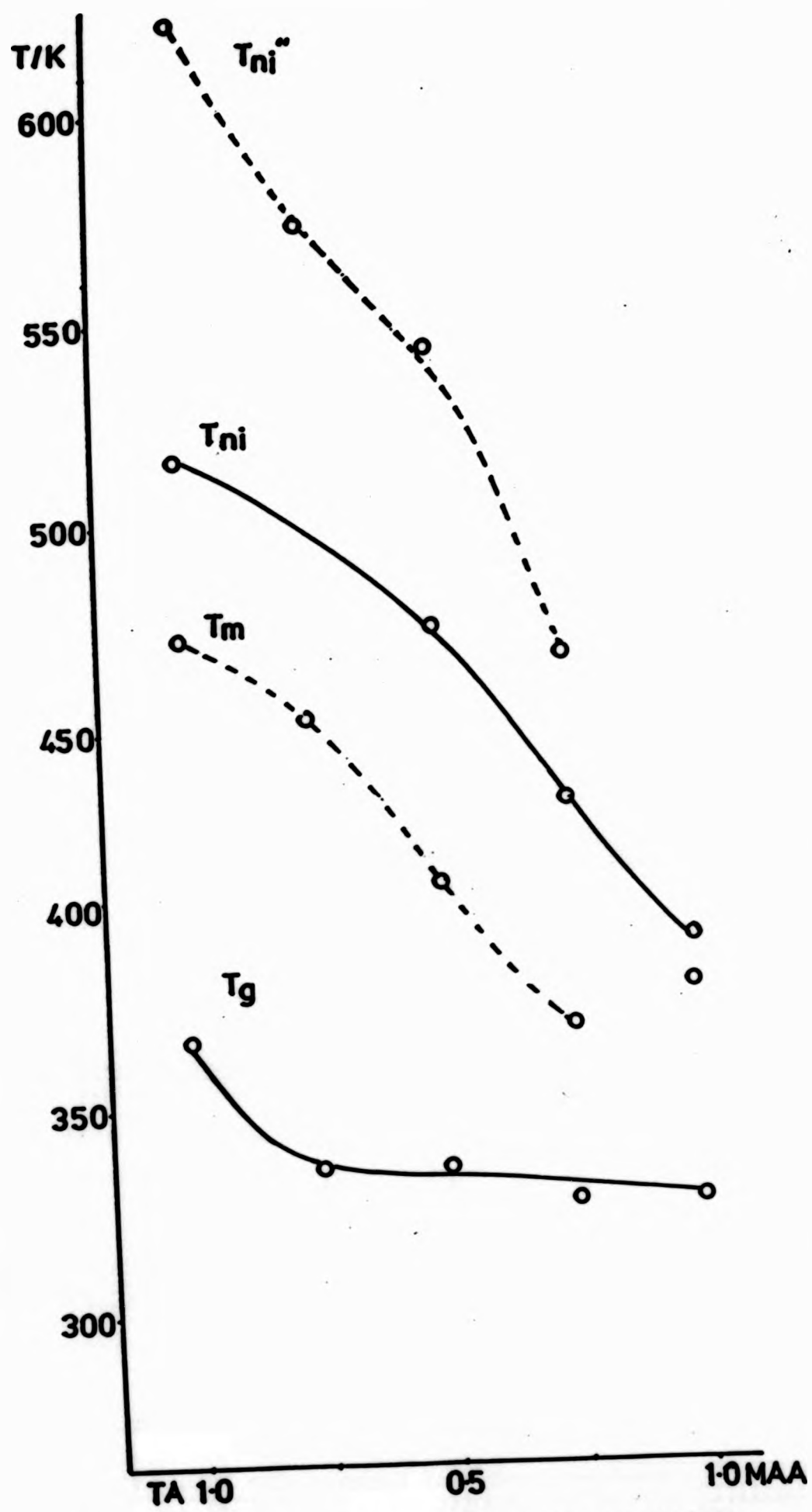


Fig. 8-4 Phase diagram for copolymer TA-MAAs

2K, while there is a substantial fall in the isotropic temperature by 42K.

The copolymer effect is further demonstrated by the change in glass transition temperature. There was a drastic decrease in glass transition temperatures even with as little as 25% MAA, after that, the increase in the content of MAA seems not to have any obvious effect.

Addition of substituents to terephthalic acid disrupts the molecular packing considerably as has already been shown in Chapter Seven. Whether on top of this effect the flexible spacer(MAA) will cause any changes is intriguing. Another two series of cholesteric copolyesters were prepared, the copolymers were designated by the letters BTA-MAA and NTA-MAA for bromo-terephthalic acid and nitro-terephthalic acid respectively.

8.2 Copolymer BTA-MAAs

For copolymer BTA-MAAs, again, biphasic regions were observed. Apparently due to the bulky bromo-group, the three dimensional order was disrupted significantly, as a consequence, the polymers are quite amorphous. The melting transitions were either undetected or only appeared as an obscure endotherm in the first heating scan. Therefore, the melting transitions were estimated by using hot-stage polarising microscope, and Table 8-2 shows the results which were obtained. The definition of T_{ni} and T_{ni}'' is no different from that of copolymer TA-MAAs.

The DSC thermogram of copolymer BTA-MAA(75:25) is displayed in Figure 8-5. T_g and T_{ni} were assigned at 343K and 486K

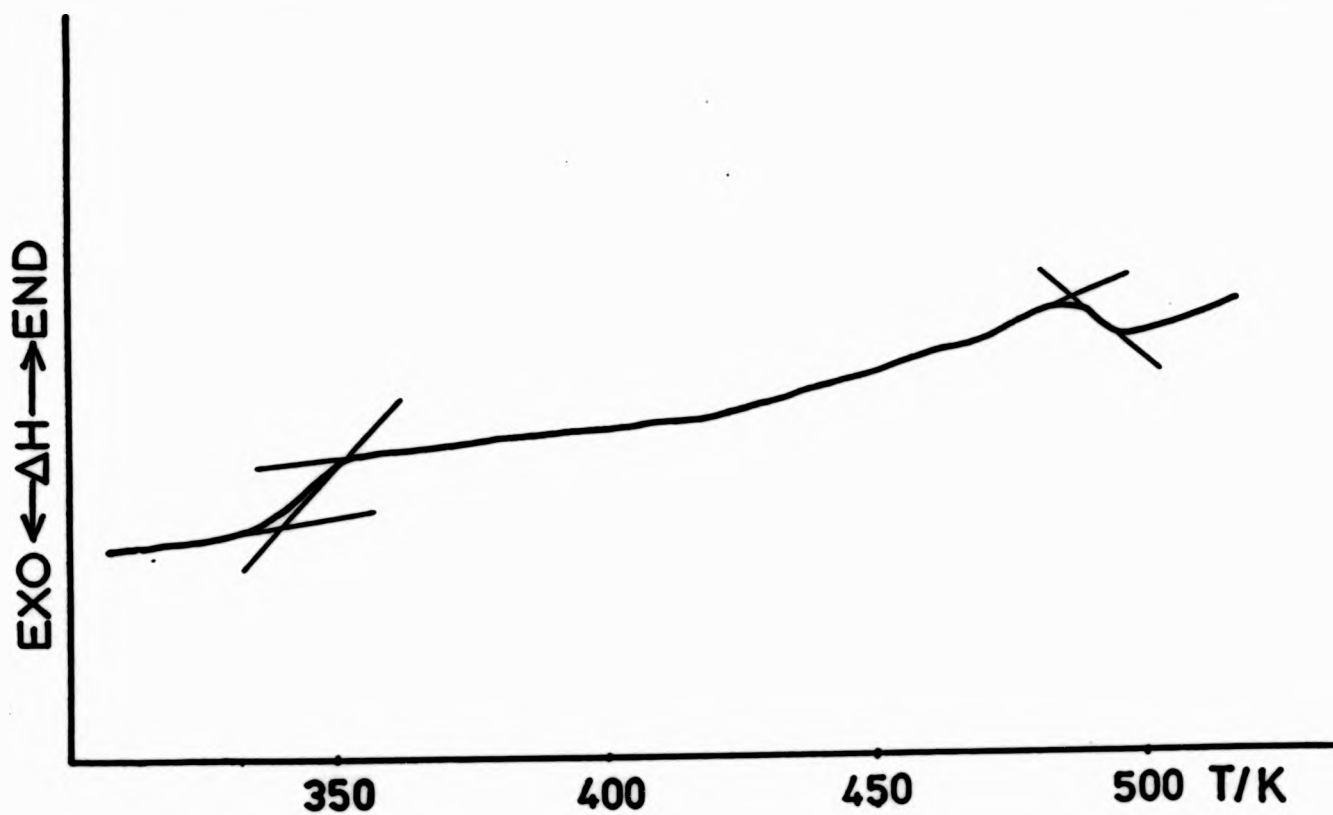


Fig. 8-5 DSC thermogram for copolymer BTA-MAA(75:25), heating

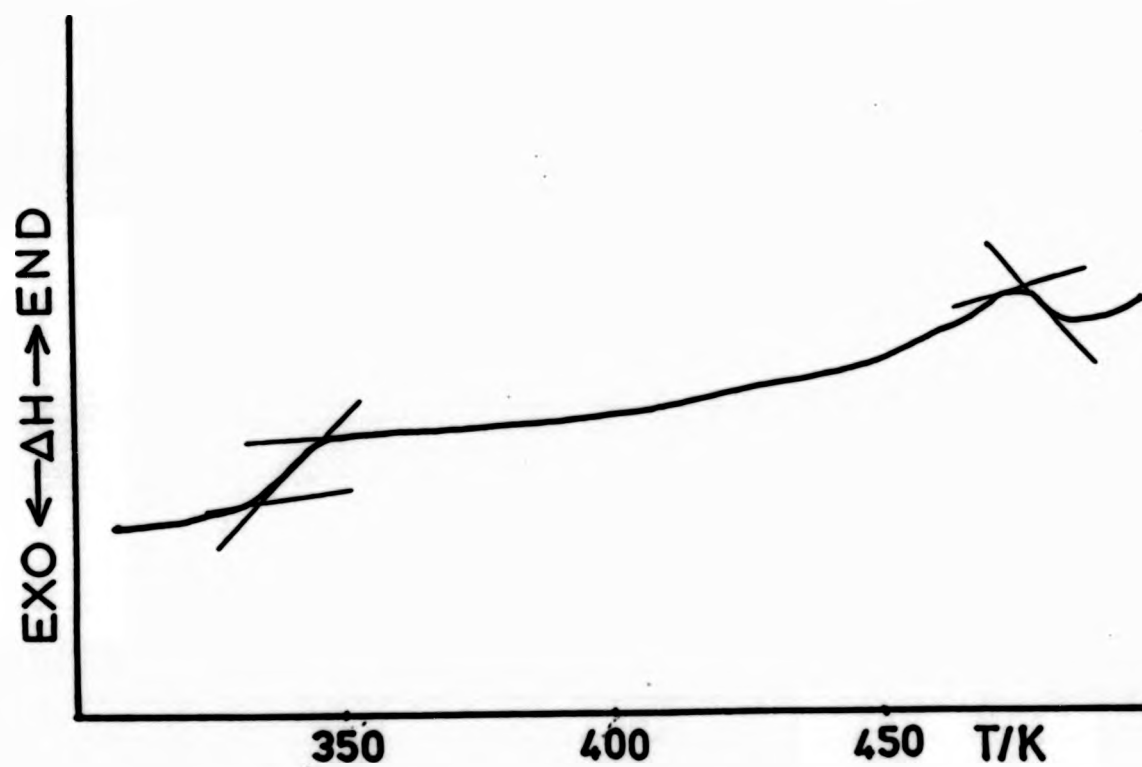


Fig. 8-6 DSC thermogram for copolymer BTA-MAA(50:50), heating

respectively. The estimated T_m (368K) by optical microscopy was 20K lower than polymer BTA-MAA(100:0) while the isotropic transition(T_{ni}) based on DSC was 64K lower. The large deviation in isotropic transition was attributed to the biphasic phenomenon. The temperature determined by optical microscopy at which the anisotropic phase completely vanished was, in fact, virtually unchanged compared to polymer BTA-MAA(100:0), i.e. 560K. Therefore, addition of 25% MAA has little influence on the clearing temperature; this phenomenon was also observed in the terephthalic acid(TA) series.

When copolymer BTA-MAA(75:25) was cooled from the isotropic melt, tiny droplets which were both light blue and yellow in colour began to form(Plate 8-I). The cooler peripheral area allowed the droplets to coalesce into larger domains. The cholesteric character of the mesophase was highlighted by Plate 8-II, such homogenous schlieren texture was obtained when the sample was subjected to shearing. This texture can be locked into the glassy state by quenching so that the light blue iridescent colour is still visually observable.

A typical biphasic region from 410K to 480K was demonstrated in Figure 8-6: the DSC thermogram of copolymer BTA-MAA(50:50). The maximum at 476K was taken as the isotropic transition(T_{ni}). The glass transition is at 341K and there is little change in T_{ni} in comparison with the copolymer containing 25% MAA, however, the decrease in T_{ni} (ca 10K) illustrated that the copolymer effect is beginning to show.

The texture of copolymer BTA-MAA(50:50) was similar to copolymer BTA-MAA(75:25), but the colour is much more intense(Plate 8-III). This effect is attributed to the



Plate 8-I The appearance of chiral nematic droplets from the isotropic phase of copolymer BTA-MAA(75:25)

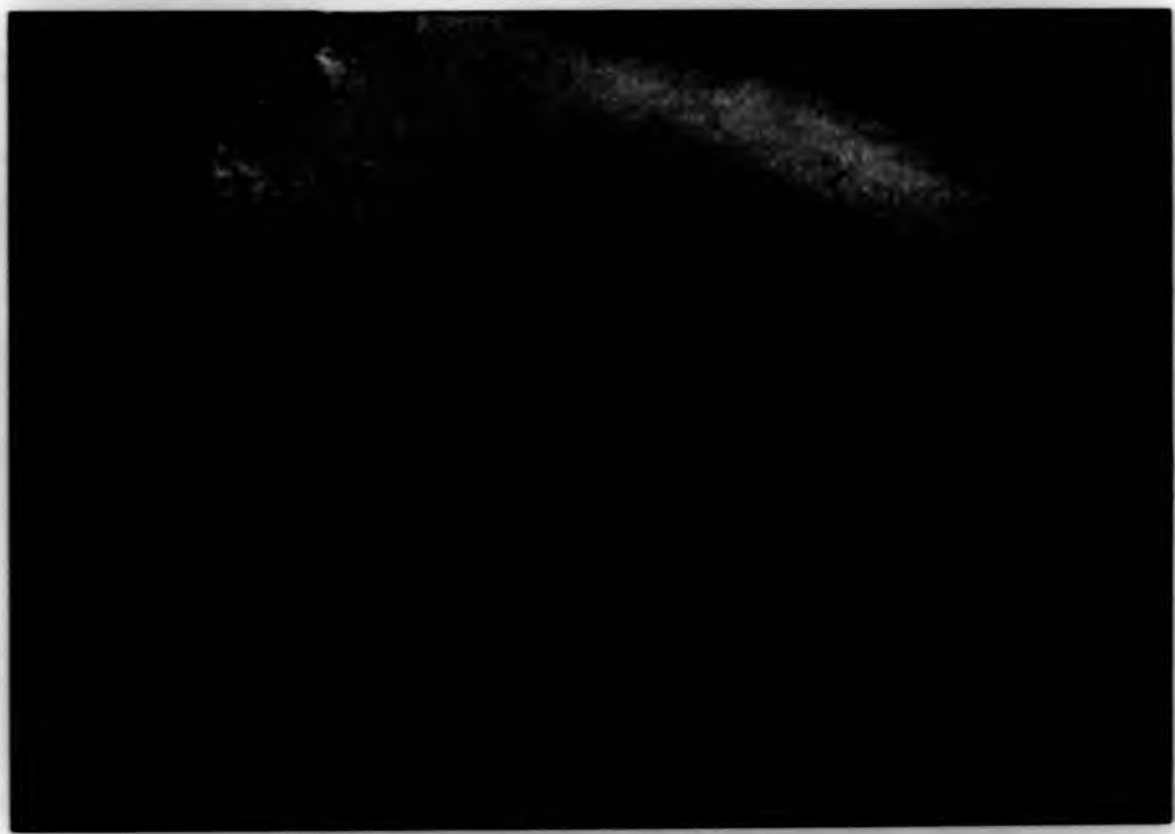


Plate 8-II The homogenous schlieren texture of the cholesteric phase of copolymer BTA-MAA(75:25) when sheared

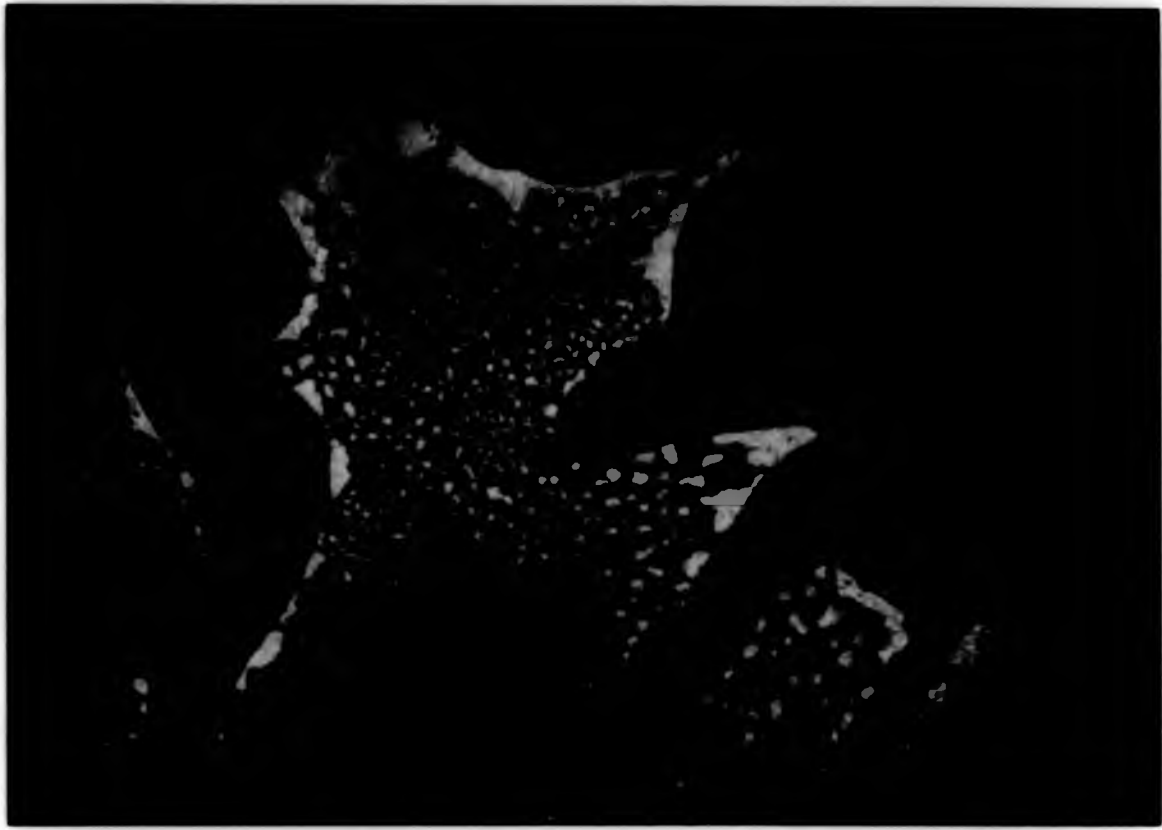


Plate 8-I The appearance of chiral nematic droplets from the isotropic phase of copolymer BTA-MAA(75:25)

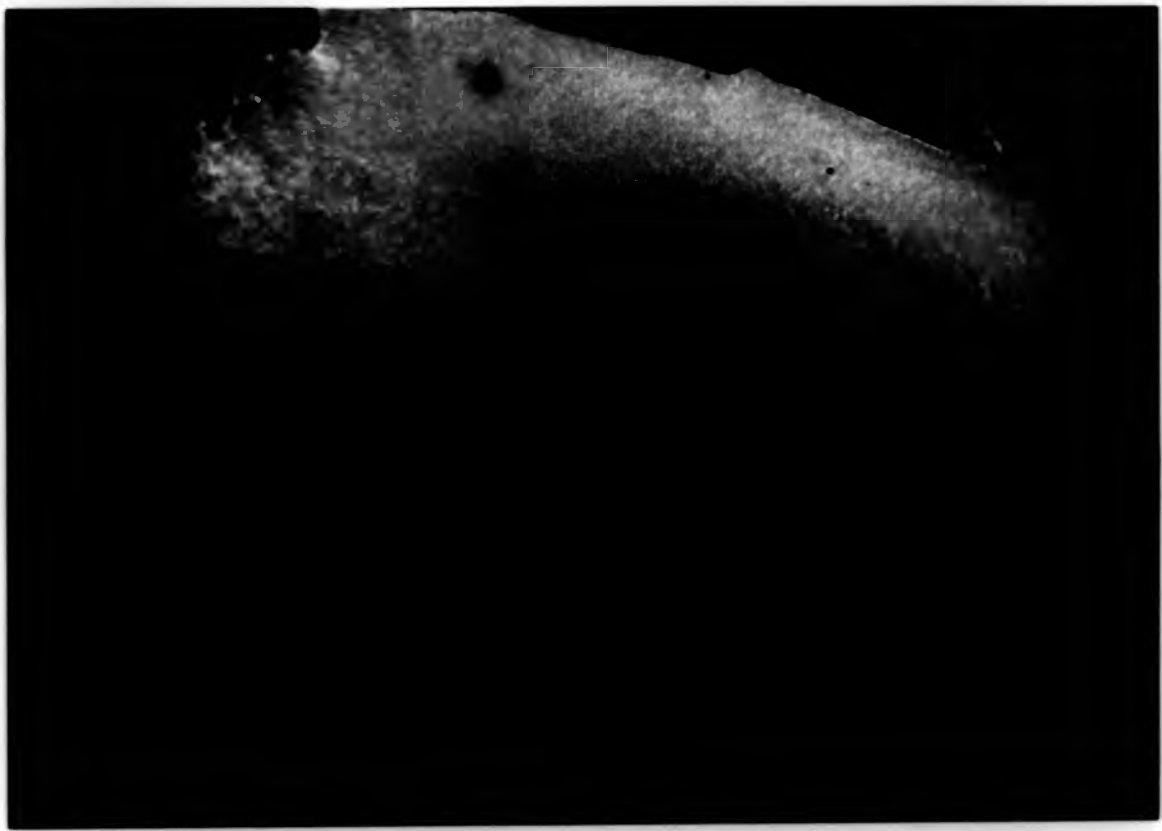


Plate 8-II The homogenous schlieren texture of the cholesteric phase of copolymer BTA-MAA(75:25) when sheared

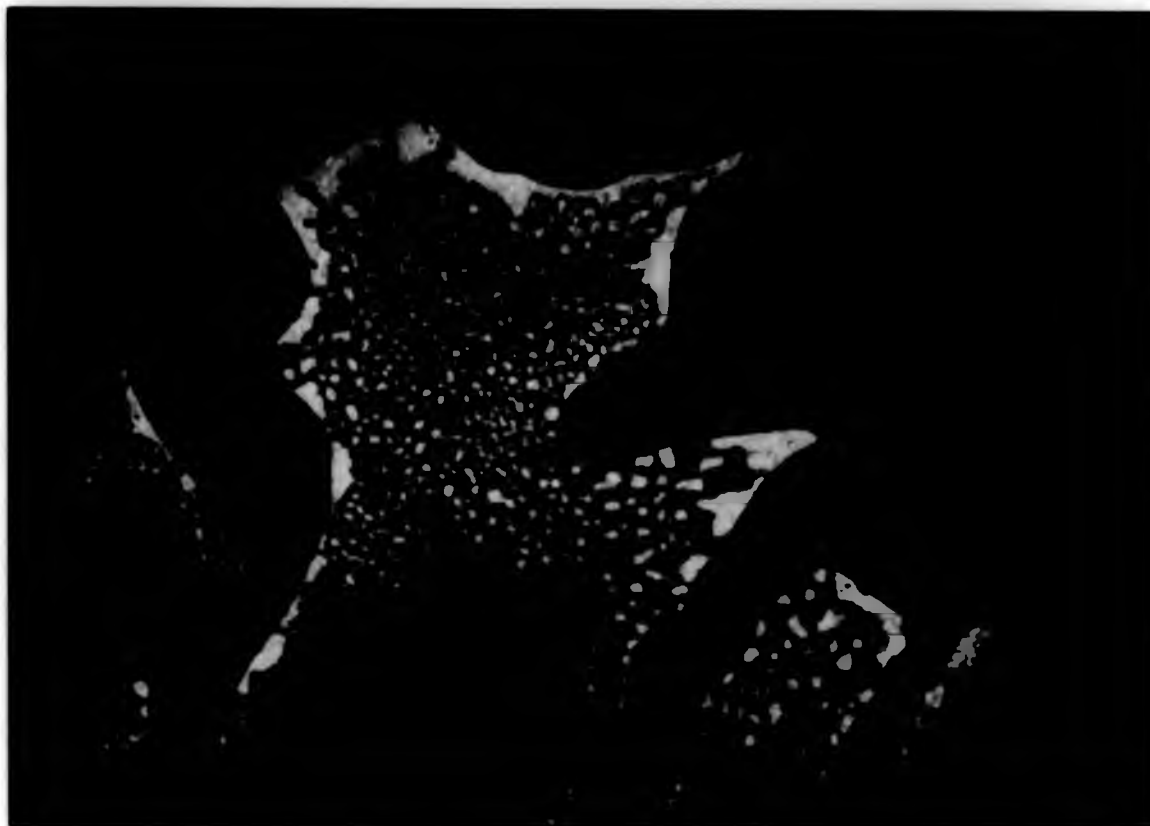


Plate 8-I The appearance of chiral nematic droplets from the isotropic phase of copolymer BTA-MAA(75:25)

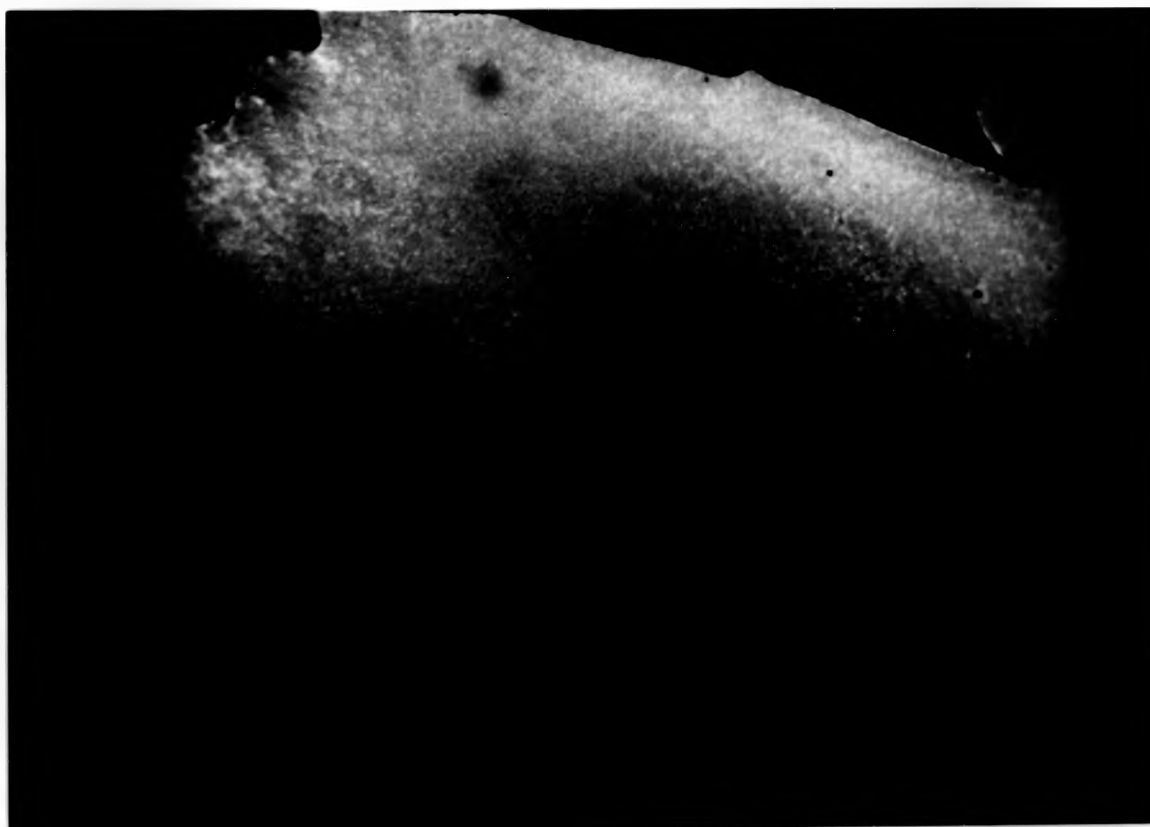


Plate 8-II The homogenous schlieren texture of the cholesteric phase of copolymer BTA-MAA(75:25) when sheared

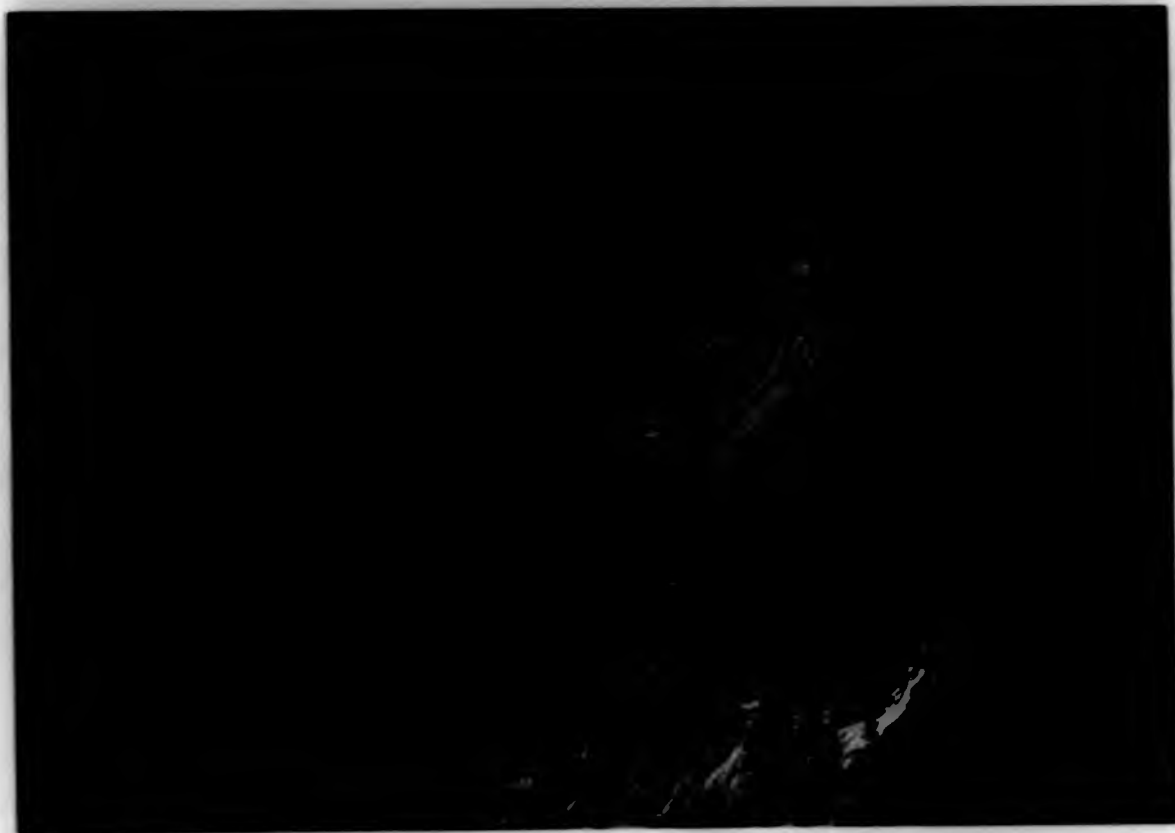


Plate 8-III The cholesteric schlieren texture of
copolymer BTA-MAA(50:50)

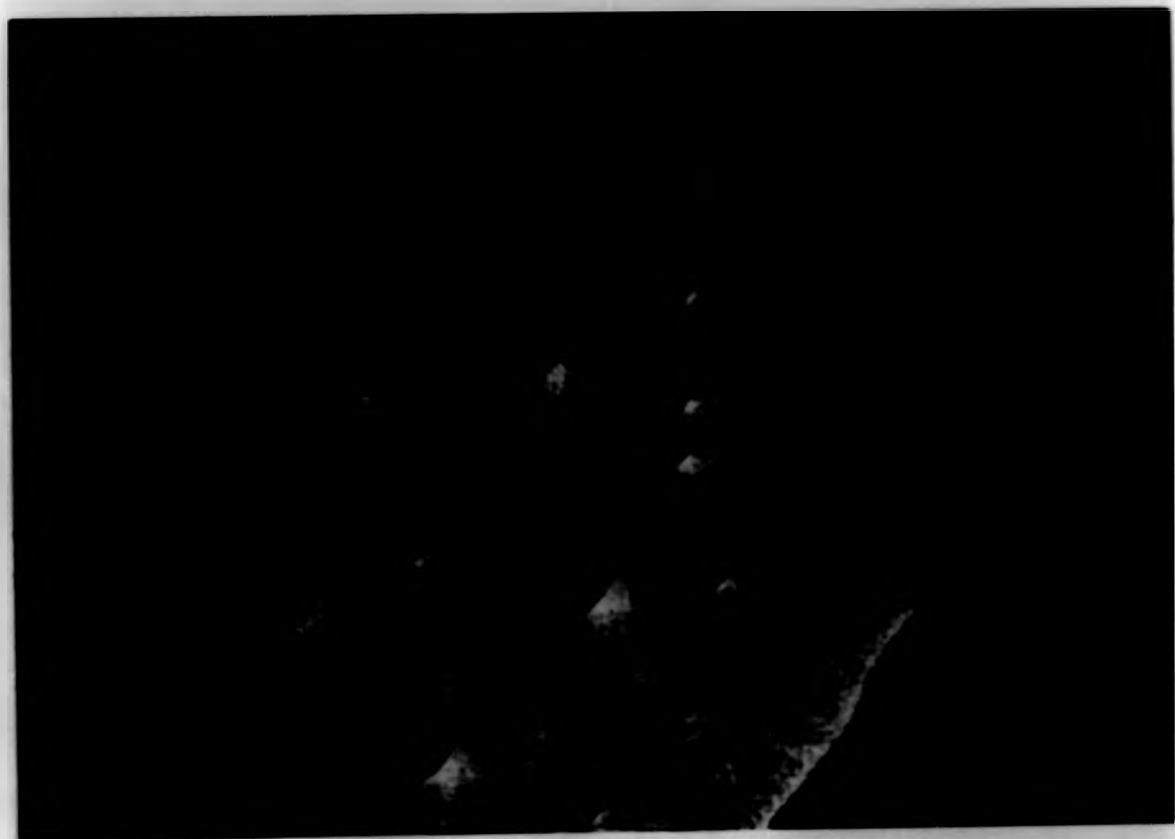


Plate 8-IV The planar texture of copolymer BTA-MAA(25:75)
when sheared

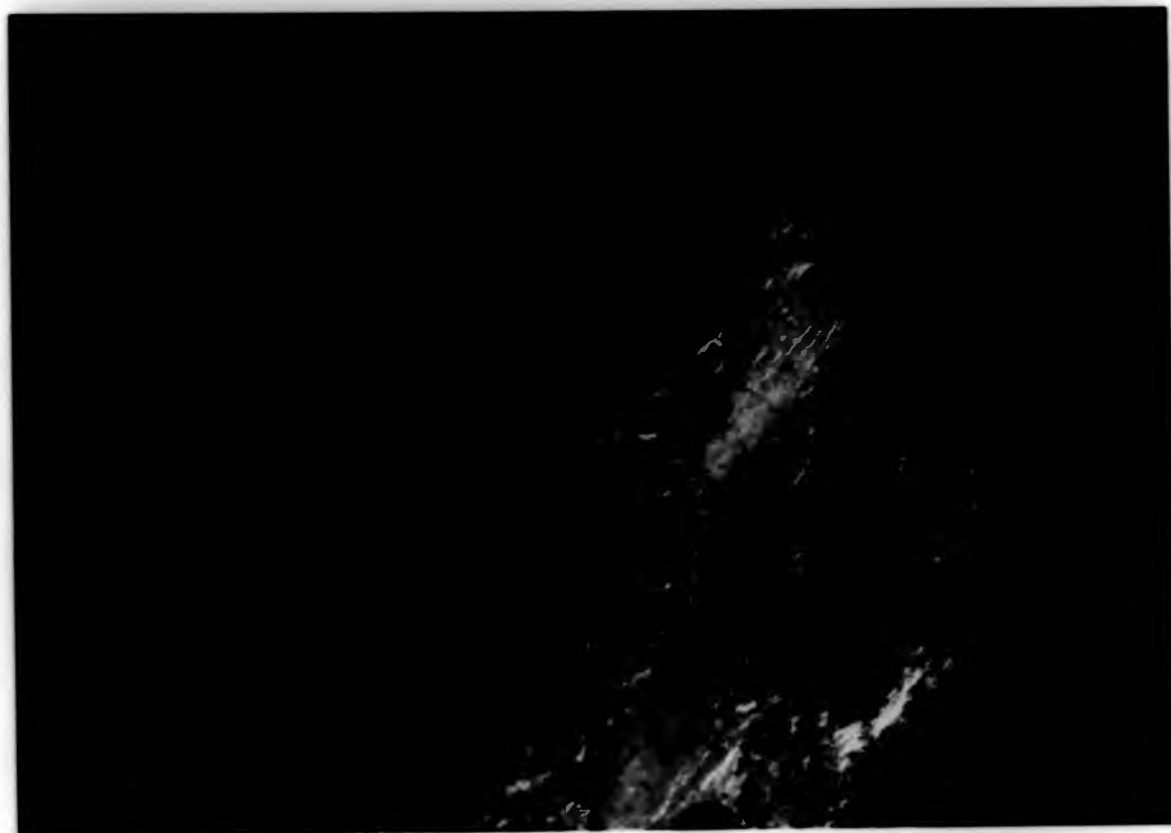


Plate 8-III The cholesteric schlieren texture of
copolymer BTA-MAA(50:50)

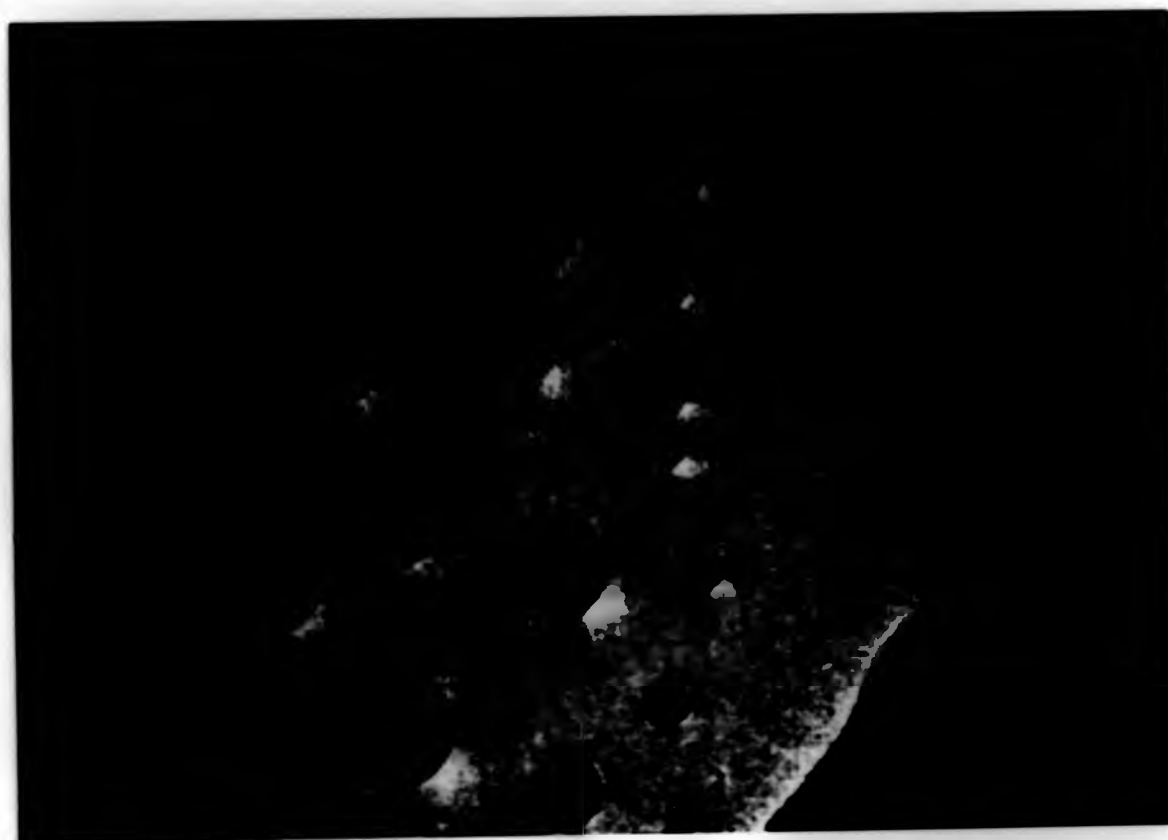


Plate 8-IV The planar texture of copolymer BTA-MAA(25:75)
when sheared

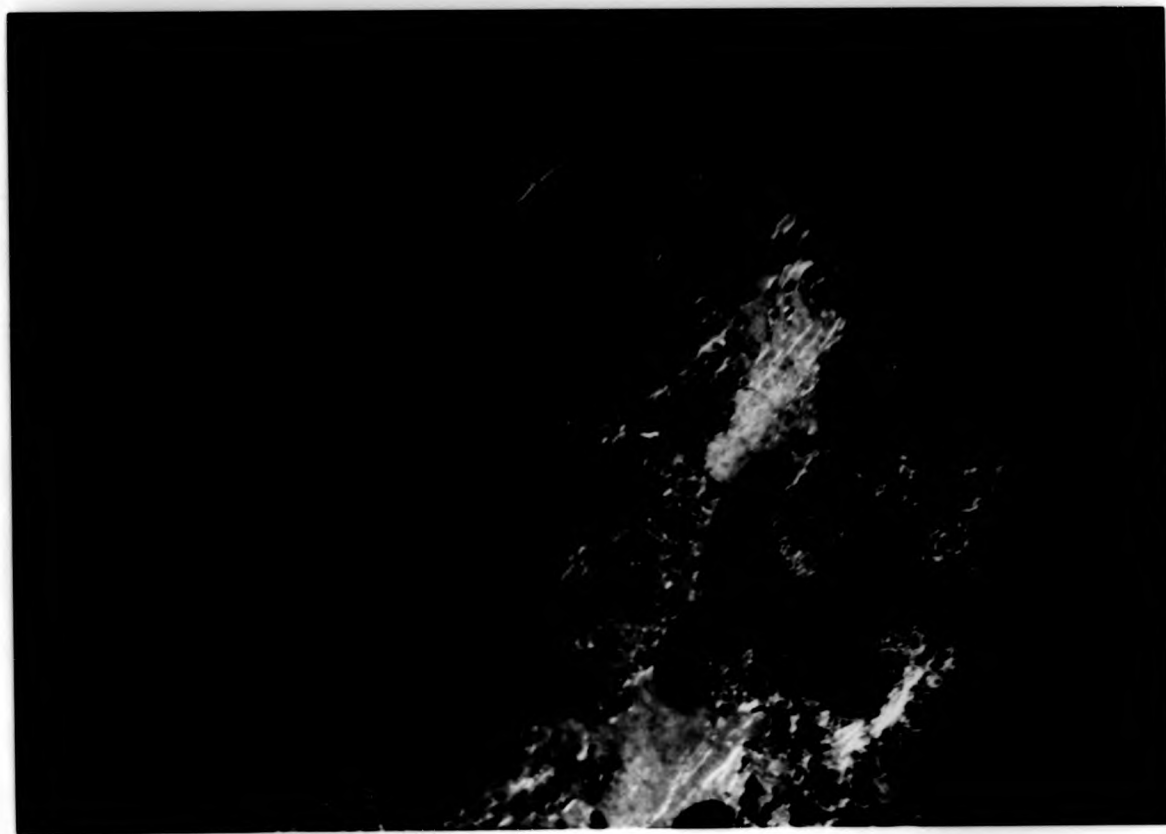


Plate 8-III The cholesteric schlieren texture of
copolymer BTA-MAA(50:50)



Plate 8-IV The planar texture of copolymer BTA-MAA(25:75)
when sheared

increase of optical active monomer which altered the pitch of the cholesteric phase. This ability to control the pitch of the cholesteric phase makes it possible to prepare polymeric films in a range of colours without the need for added pigments or dyes.

As would be expected, further increase of flexible spacer contents to above 50% resulted in a rapid drop in isotropic transition temperature. For copolymer BTA-MAA(25:75), T_g at 330K and T_{ni} at 433K were detected by DSC as shown in Figure 8-7.

The higher proportion of MAA in copolymer BTA-MAA(25:75) makes the polymer very sensitive to temperature and mechanical changes. A light blue planar texture can still be obtained by simply shearing the sample (Plate 8-IV). Without any treatment, the texture (Plate 8-V) was closer to polymer COHB-MAA (see Plate 8-VI). According to Figure 8-8, mesophase stability can be retained up to an equimolar composition of BTA and MAA, mainly because of maximum structural randomness and the biphasic phenomenon.

Samples of LC polymer crystallised from a biphasic system would probably have inferior mechanical properties since the portions existing in the isotropic phase would not achieve the desired orientation. Thus, a biphasic region over a wide temperature range is undesirable. This can hardly be avoided for random copolymer, which represents a disadvantage of this procedure for lowering the melting temperature. Without considering the melting temperatures, comparing Figures 8-4 and 8-8, one can see that bromo-group has no effect on T_{ni} and T_{ni} nor T_g . This observation is certainly not the case in

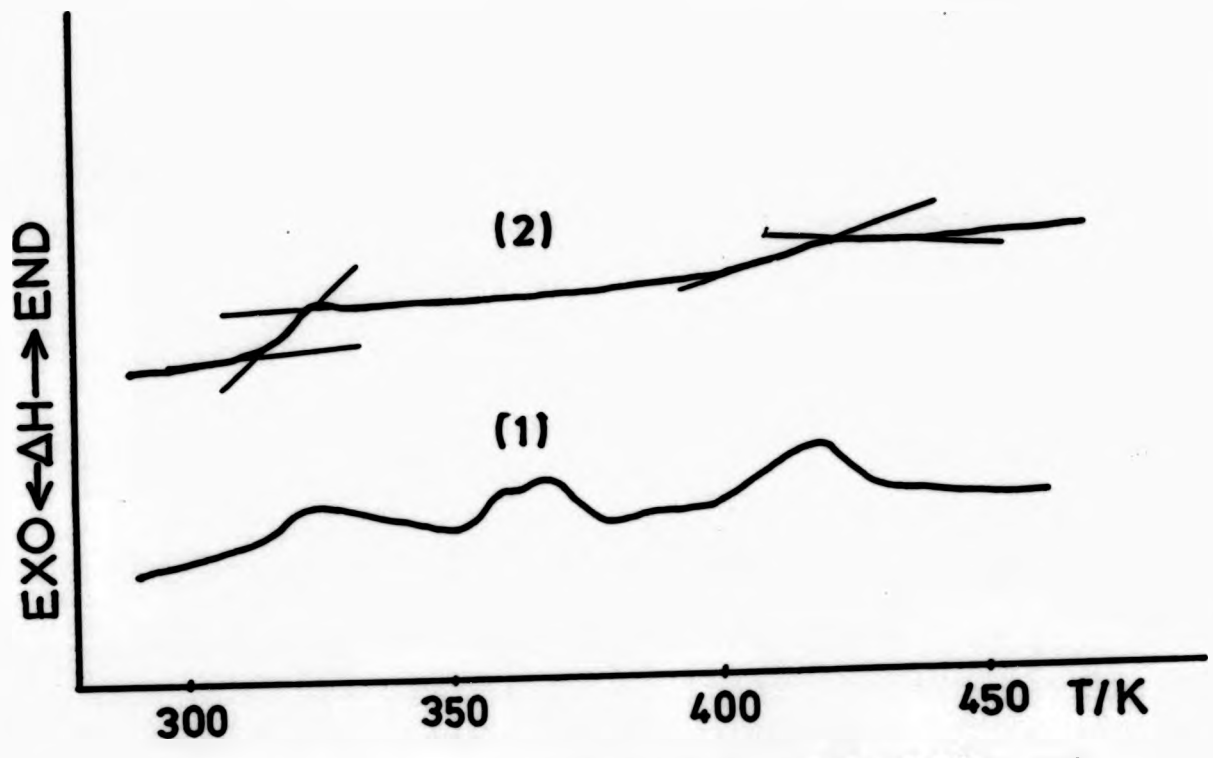


Fig. 8-7 DSC thermograms for copolymer BTA-MAA(25:75)
(1) 1st heating scan
(2) 2nd heating scan



Plate 8-V The schlieren texture of copolymer BTA-MAA(25:75)
without shear



Plate 8-VI The cholesteric texture of polymer COHB-MAA
without any treatment

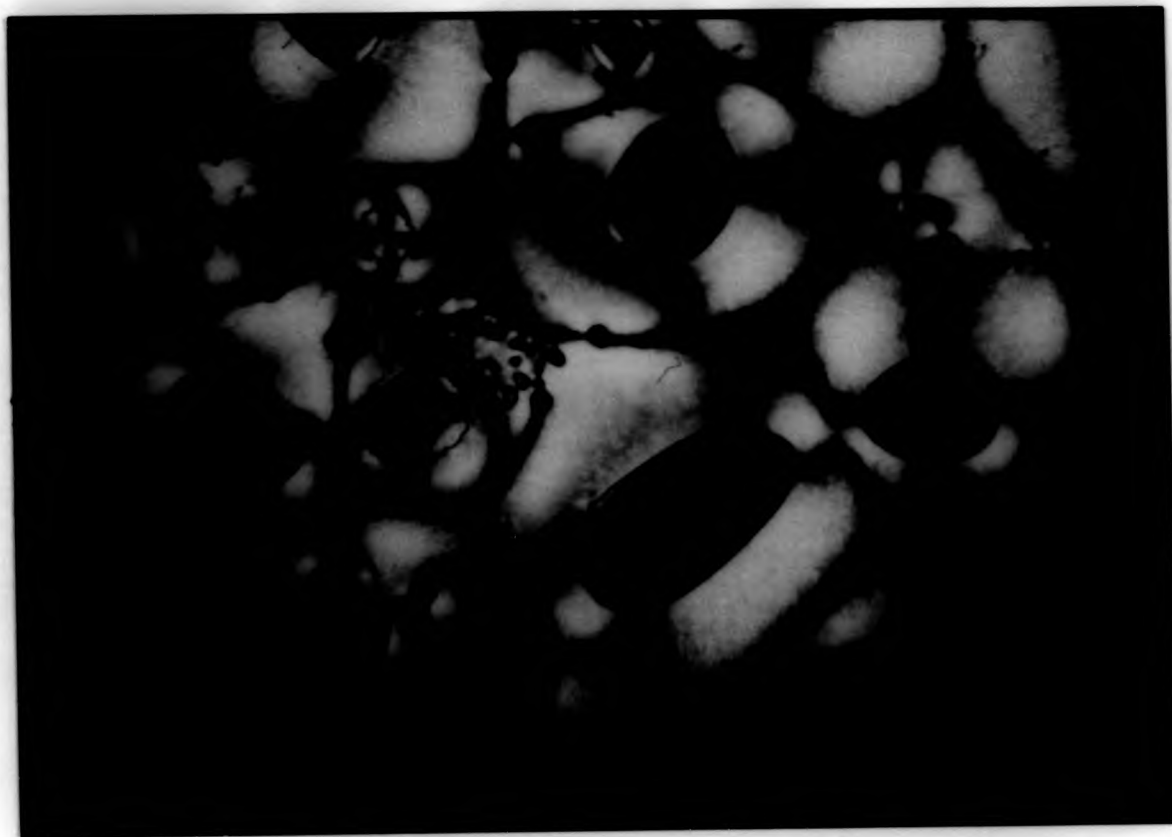


Plate 8-V The schlieren texture of copolymer BTA-MAA(25:75)
without shear



Plate 8-VI The cholesteric texture of polymer COHB-MAA
without any treatment

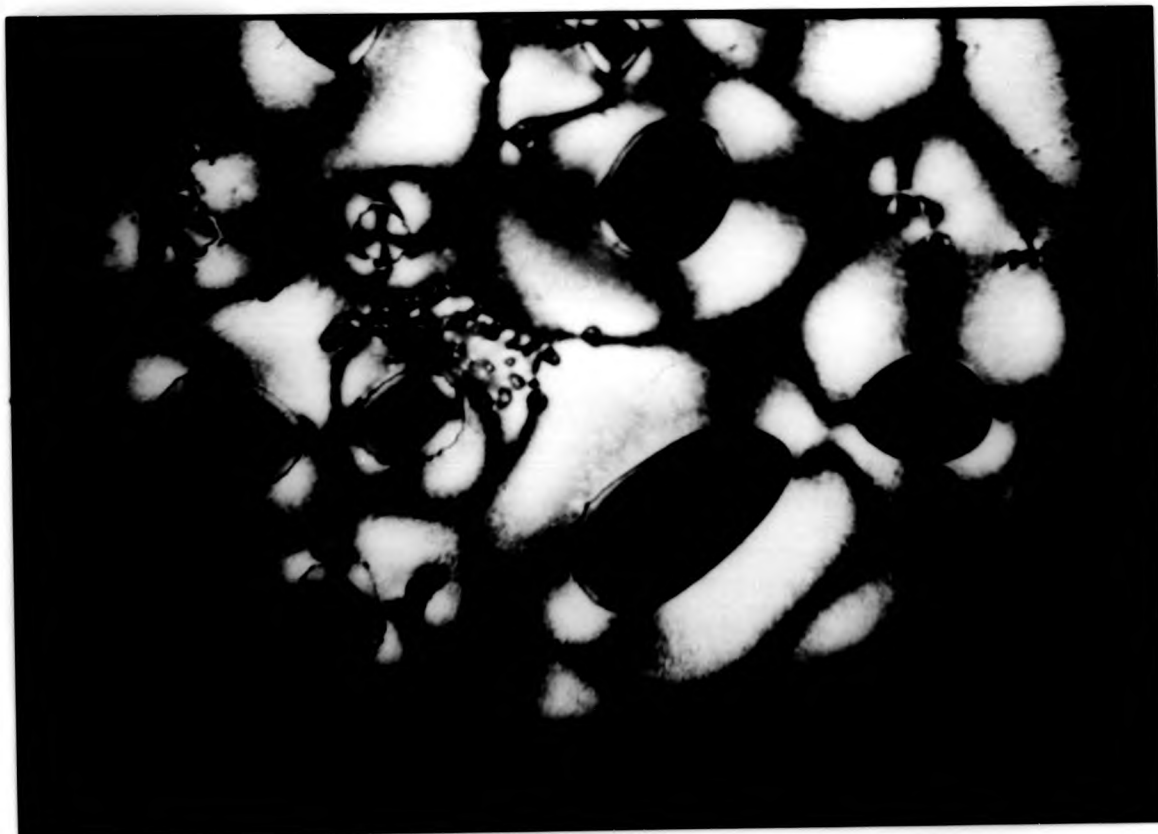


Plate 8-V The schlieren texture of copolymer BTA-MAA(25:75)
without shear

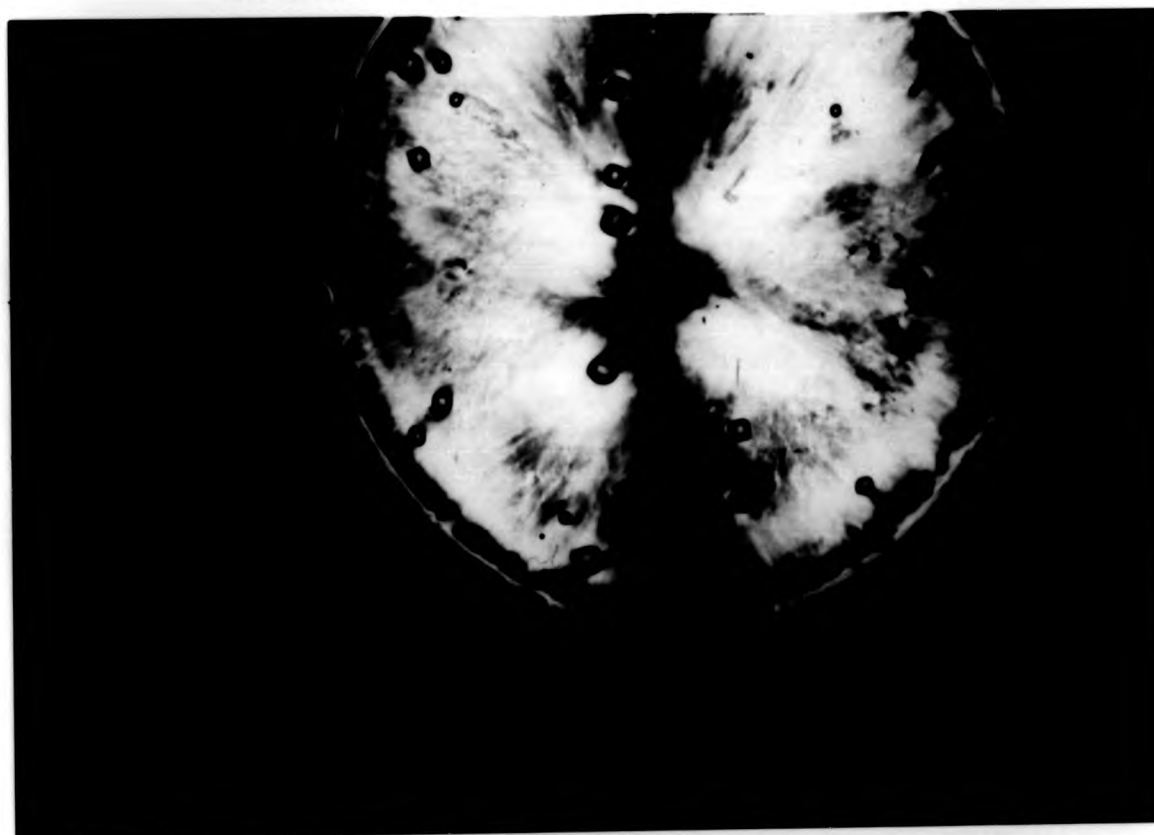


Plate 8-VI The cholesteric texture of polymer COHB-MAA
without any treatment

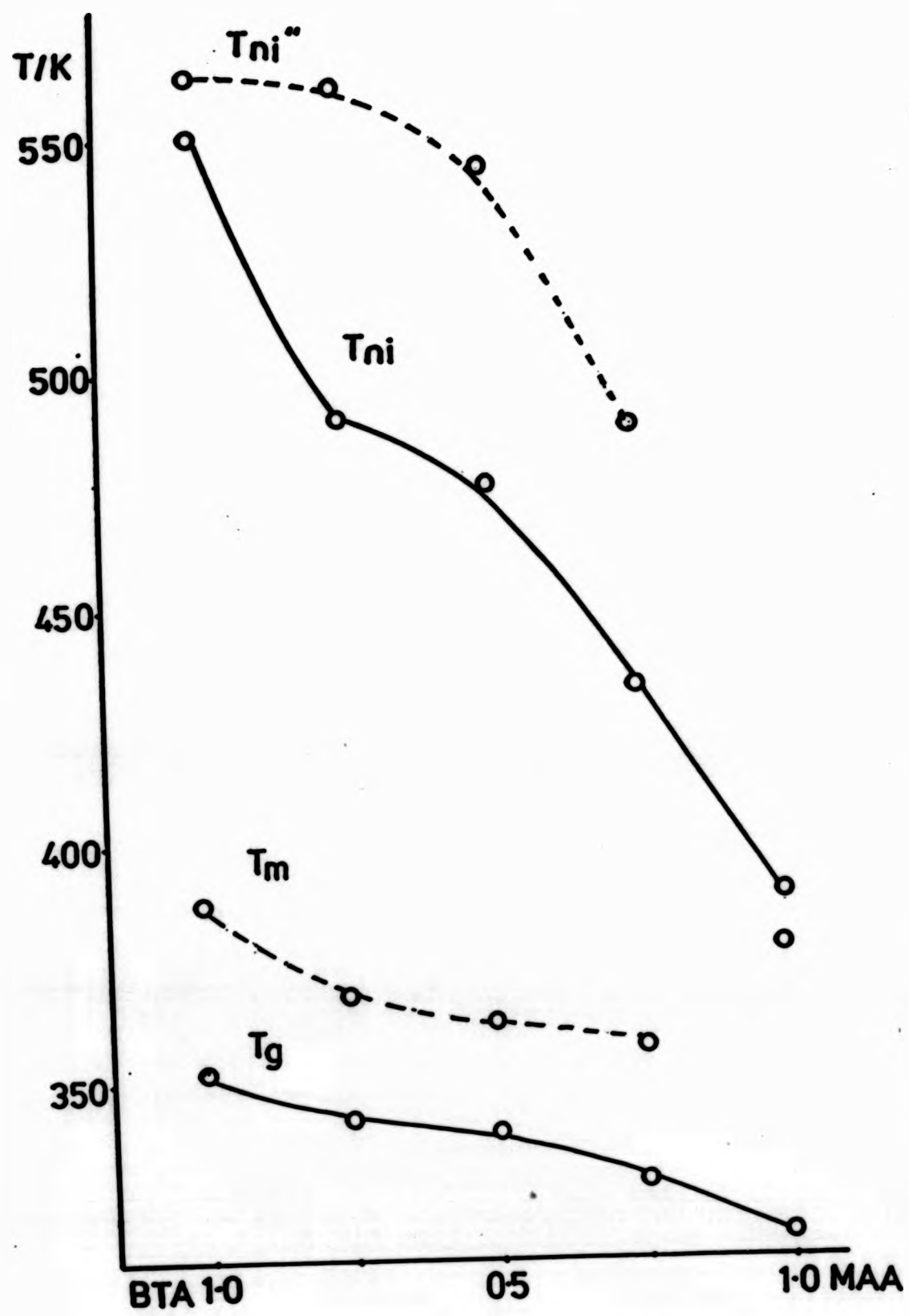


Fig. 8-8 Phase diagram for copolymer BTA-MAAs

polymer TA and polymer ETA. The bromo-substituent seemingly was rendered ineffectual by the highly flexible spacer.

8.3 Copolymer NTA-MAAs

The effect of a bulky substituent attached to the aromatic nuclei is further demonstrated by the next series of copolyesters. Figure 8-9 shows the phase diagram of copolymers 'NTA-MAA'. Results of calorimetric and optical studies are listed in Table 8-3.

Figure 8-10 displays the DSC thermogram of copolymer NTA-MAA(75-25) which clearly indicates T_g at 350K and T_{ni} at 376K. Microphotographs taken at these transitions are shown in Plate 8-VII and 8-VIII. At a higher temperature, with shear, the sample exhibited a homogenous planar texture of light blue colour (Plate 8-VII). However, when the sample was cooled a few degrees lower, the twisted nematic phase reflected deep blue light (Plate 8-VIII). At even higher temperatures, along the edges of the air bubbles, a yellow colour was observed.

The isotropic transition (T_{ni}) of copolymer NTA-MAA(50:50) was taken from the highest endotherm at 442K (Figure 8-11), and the glass transition temperature (347K) was based on the second heating scan.

In low molecular weight cholesterols, their sensitivity to temperature alteration has made them particularly valuable in colour display technology. It is surprising to note that in cholesteric polymers, this colour changing phenomenon is also noticeable, although of a much slower speed because of higher viscosity. This effect is demonstrated by Plate 8-IX and 8-X. At high temperature, without any thermal treatment, copolymer

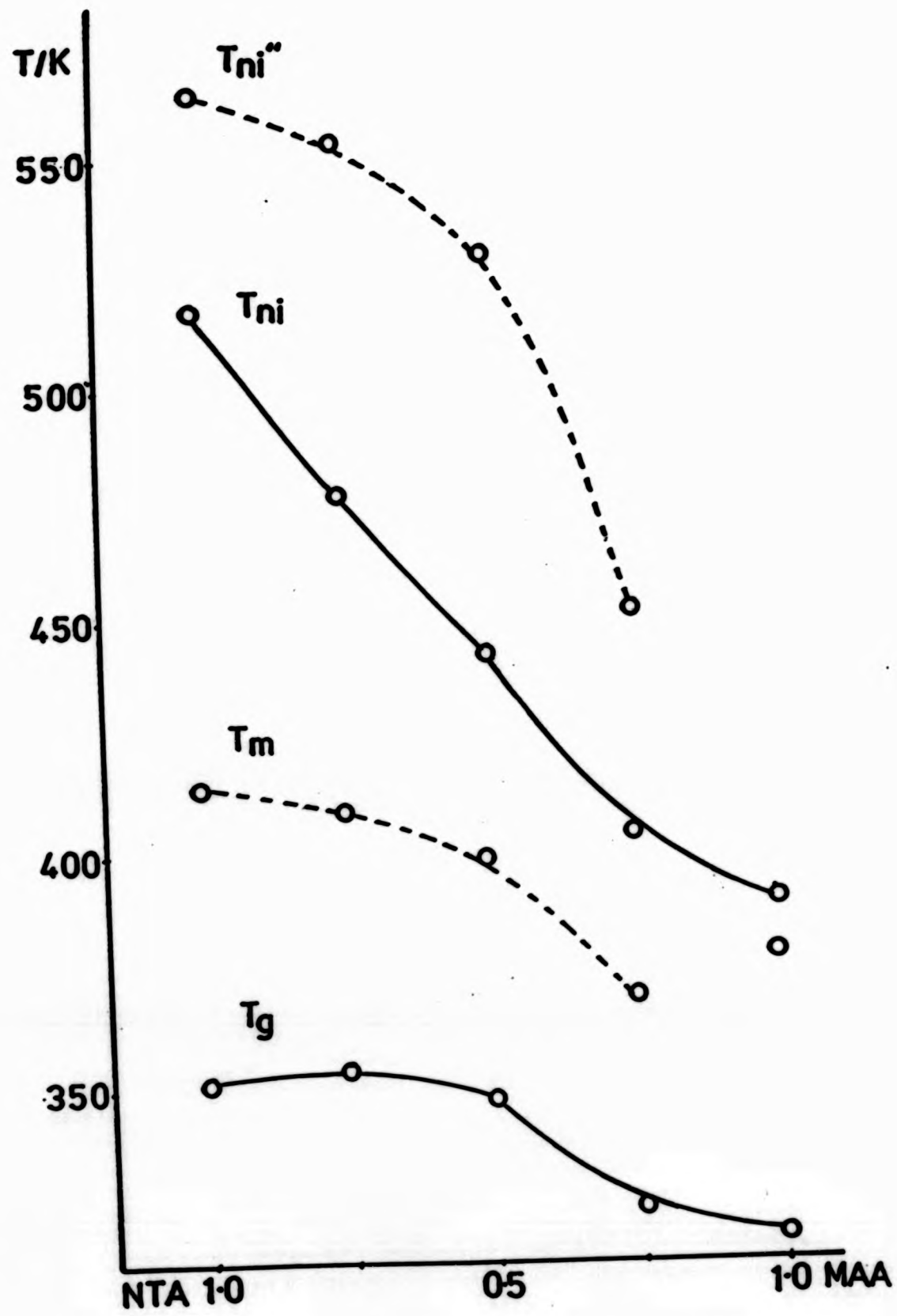


Fig. 8-9 Phase diagram for copolymer NTA-MAAs

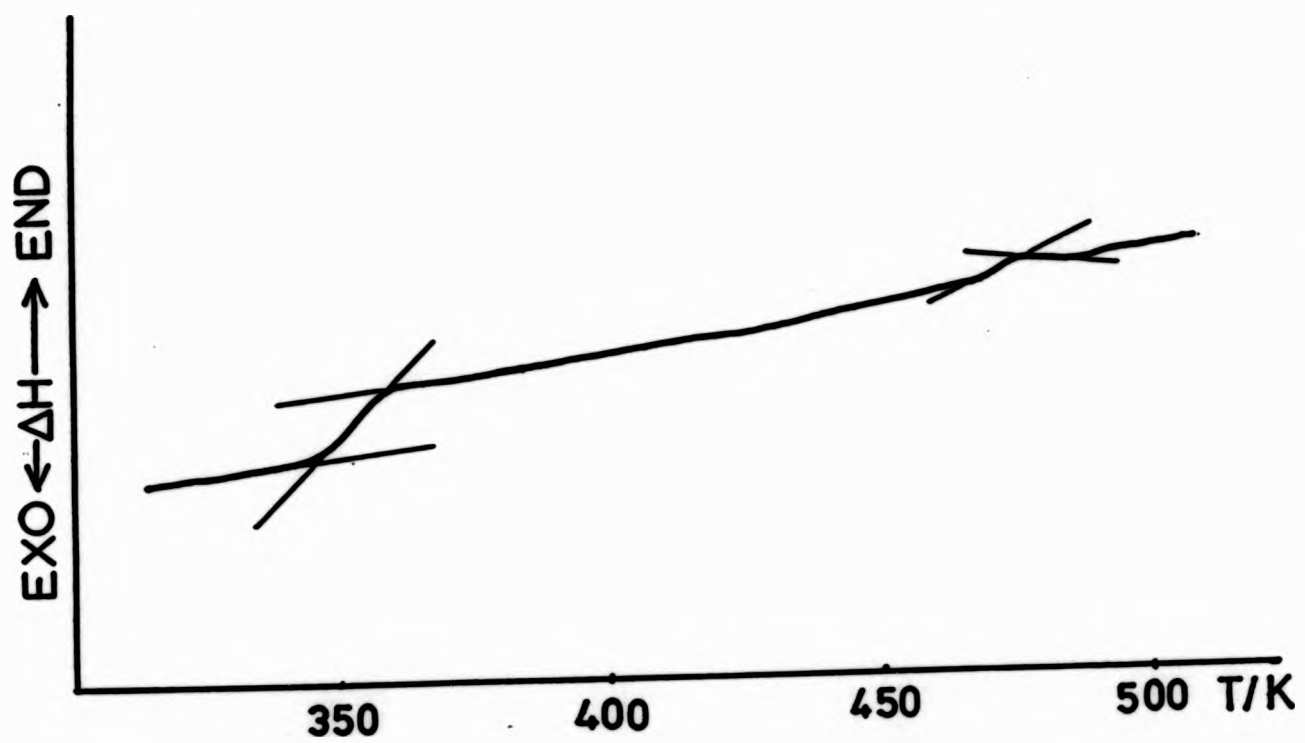


Fig. 8-10 DSC thermogram for copolymer NTA-MAA(75:25), heating

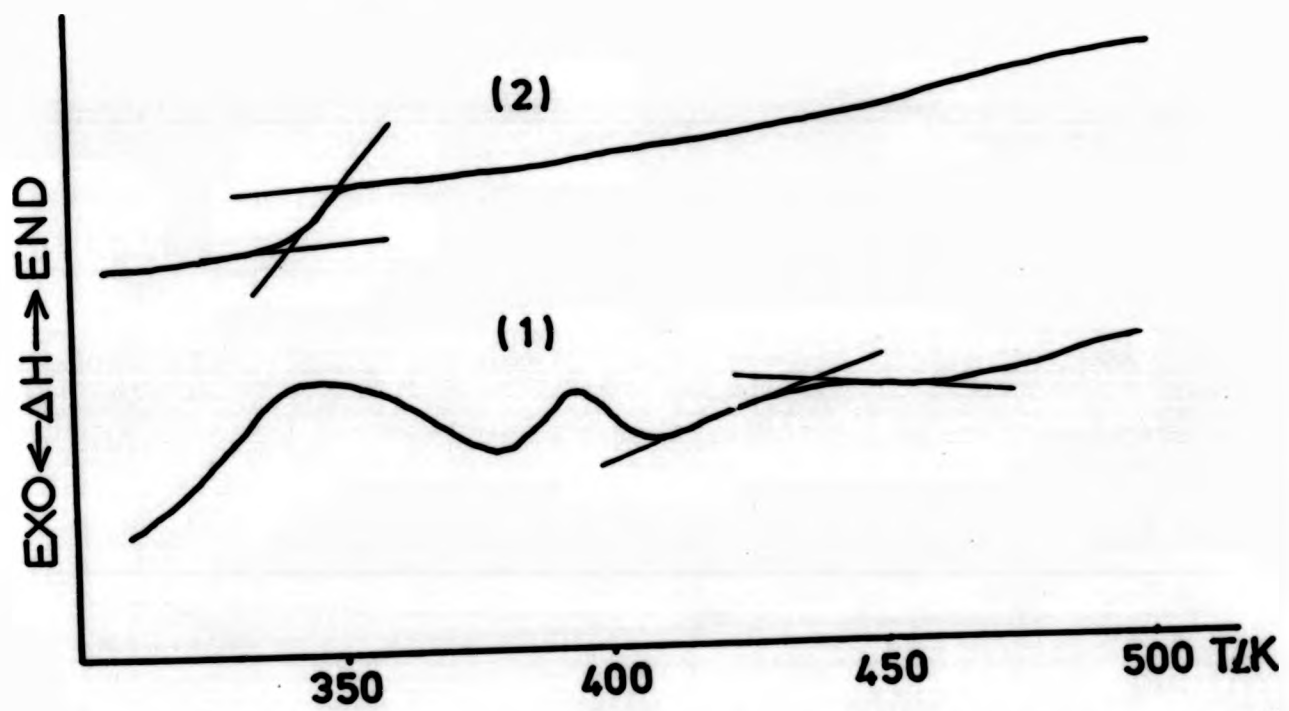


Fig. 8-11 DSC thermograms for copolymer NTA-MAA(50:50)
 (1) 1st heating scan
 (2) 2nd heating scan

EXO ← ΔH → END

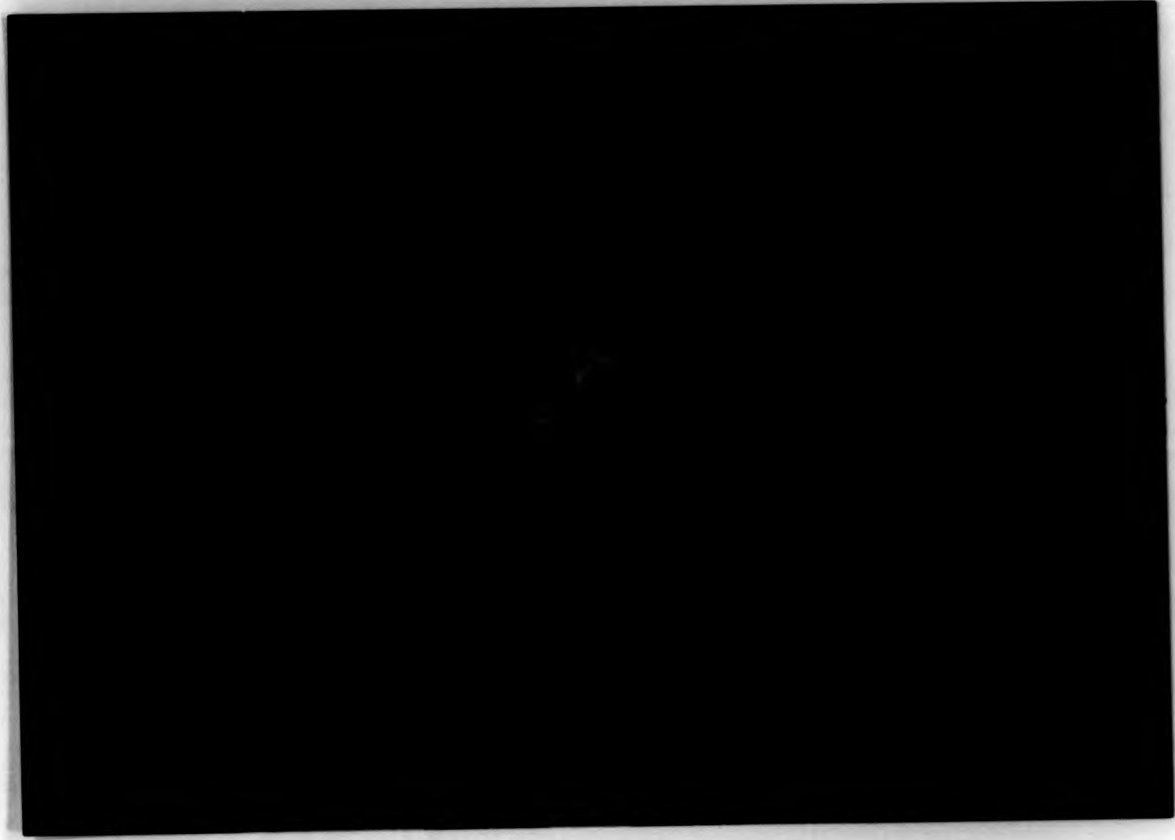


Plate 8-VII The homogenous planar texture of copolymer
NTA-MAA(75:25) at 376K

EXO ← ΔH → END



Plate 8-VIII The planar texture of copolymer NTA-MAA
(75:25) at 360K

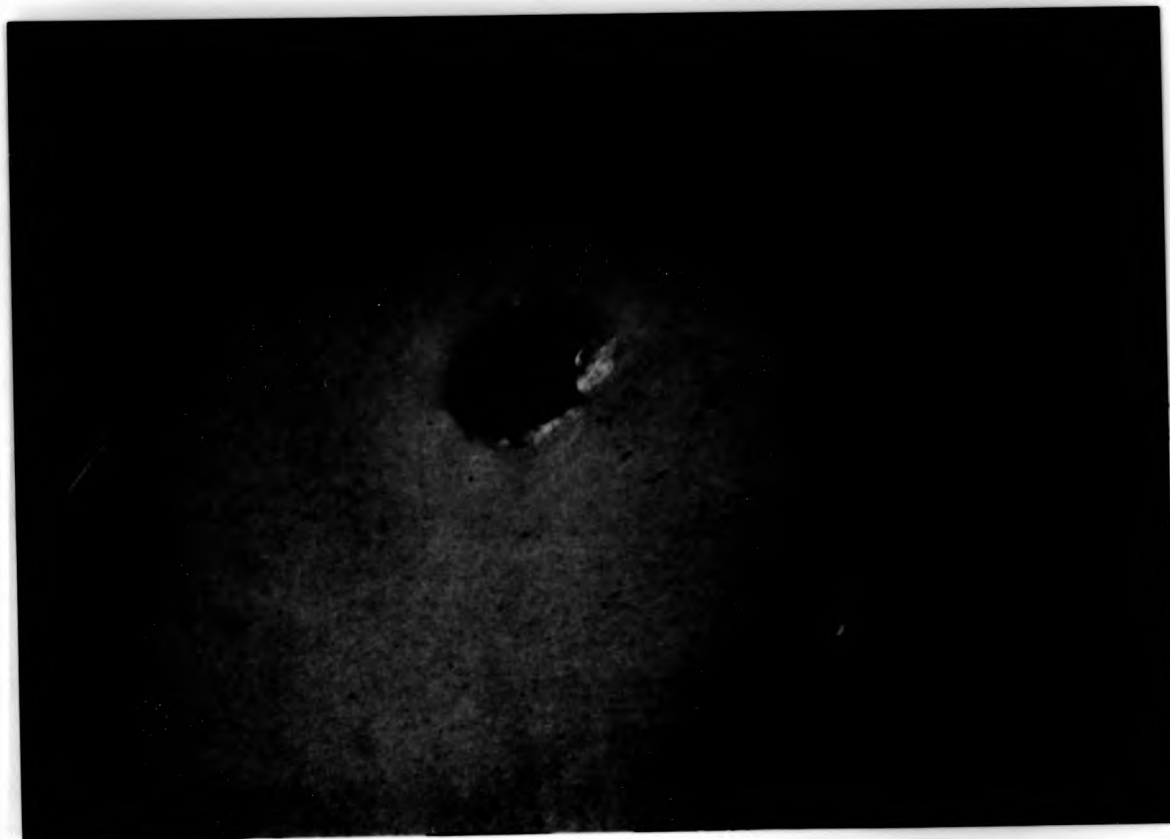


Plate 8-VII The homogenous planar texture of copolymer
NTA-MAA(75:25) at 376K



Plate 8-VIII The planar texture of copolymer NTA-MAA
(75:25) at 360K

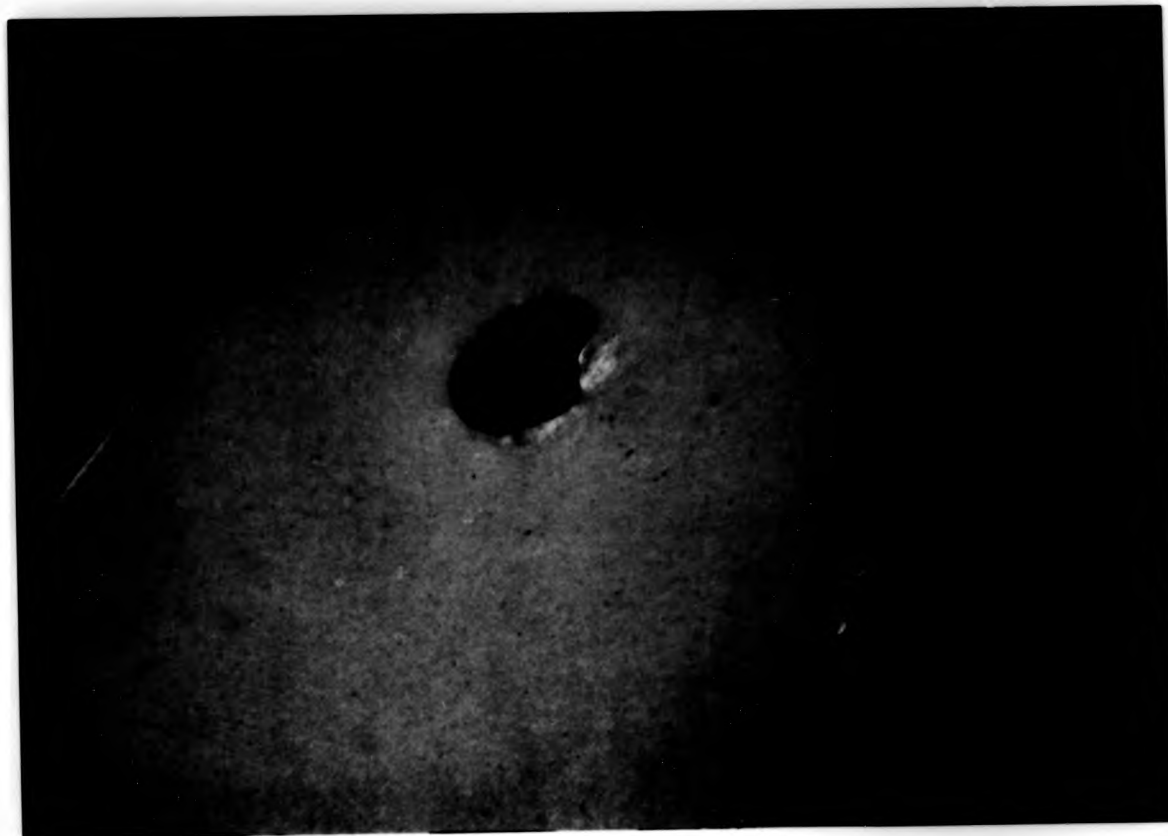


Plate 8-VII The homogenous planar texture of copolymer
NTA-MAA(75:25) at 376K



Plate 8-VIII The planar texture of copolymer NTA-MAA
(75:25) at 360K



Plate 8-IX Copolymer NTA-MAA(50:50) shows intense blue colour
at 440K

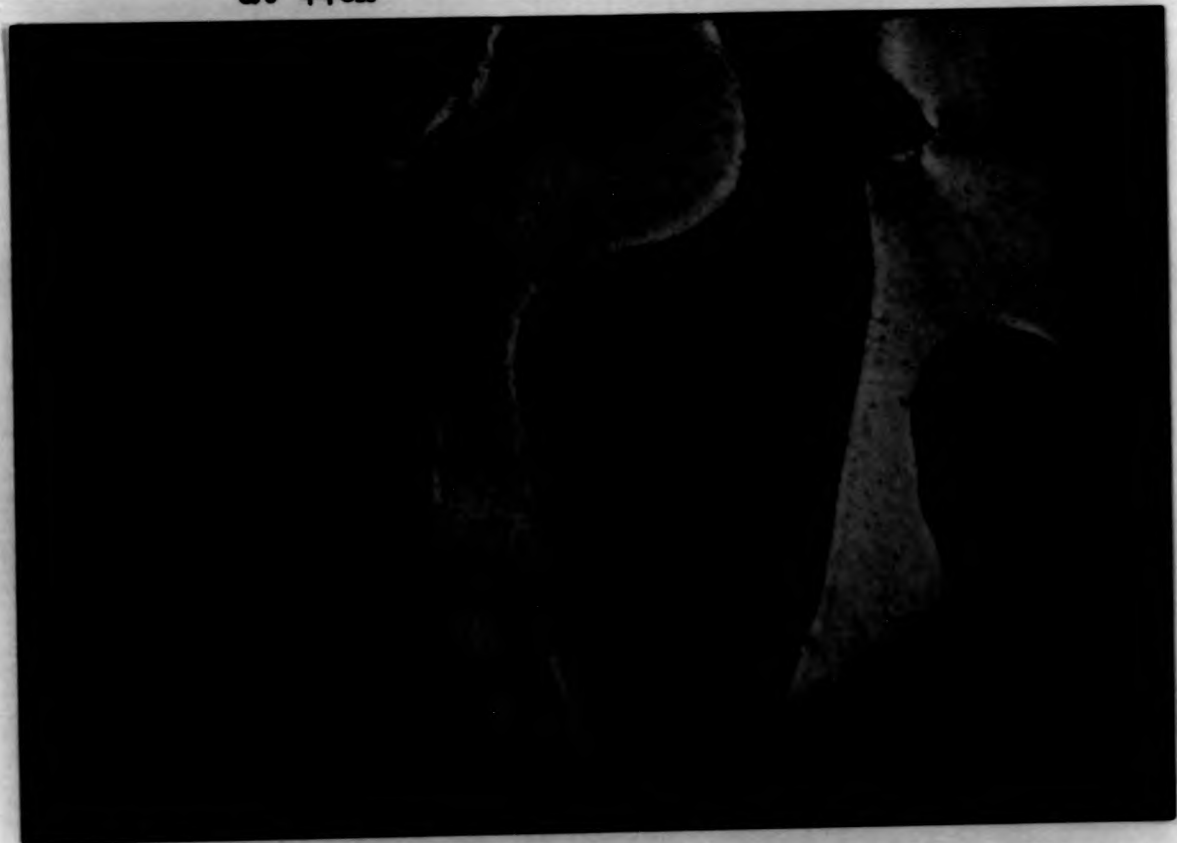


Plate 8-X Copolymer NTA-MAA(50:50) shows reddish yellow colour
at 430K when subjected to shear

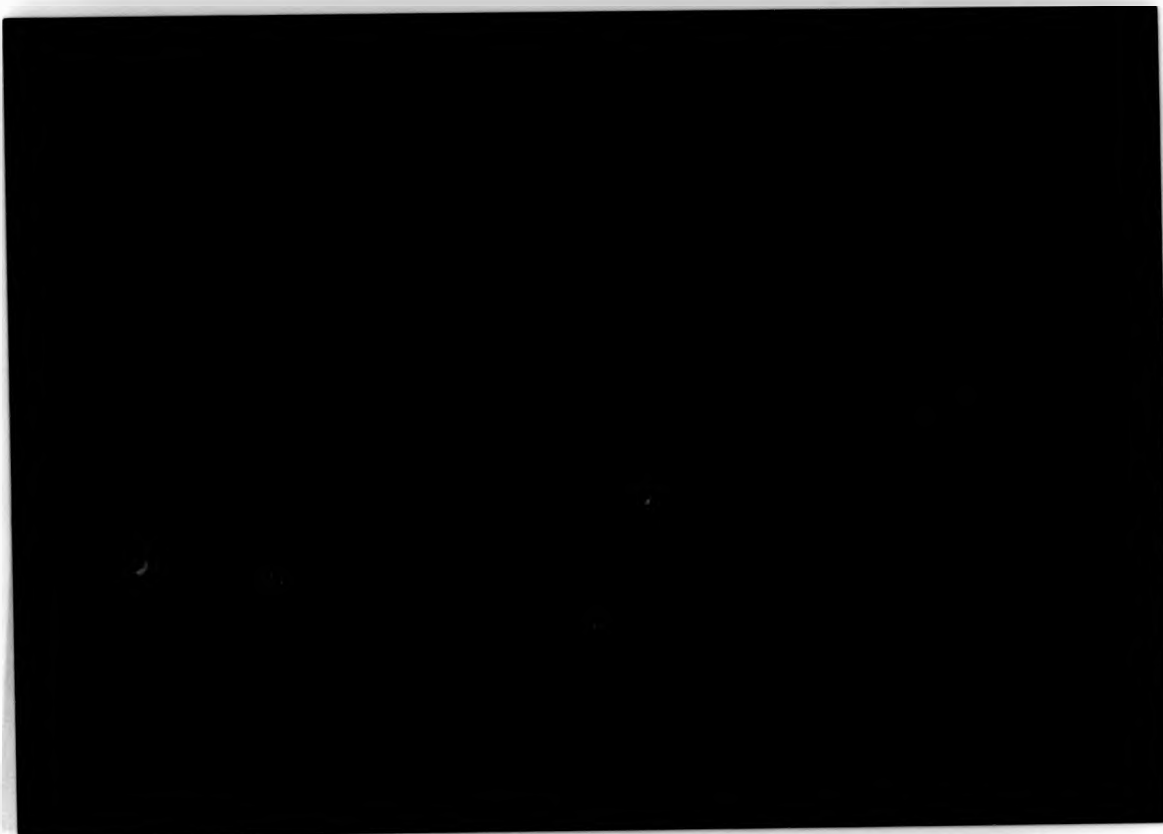


Plate 8-IX Copolymer NTA-MAA(50:50) shows intense blue colour
at 440K



Plate 8-X Copolymer NTA-MAA(50:50) shows reddish yellow colour
at 430K when subjected to shear

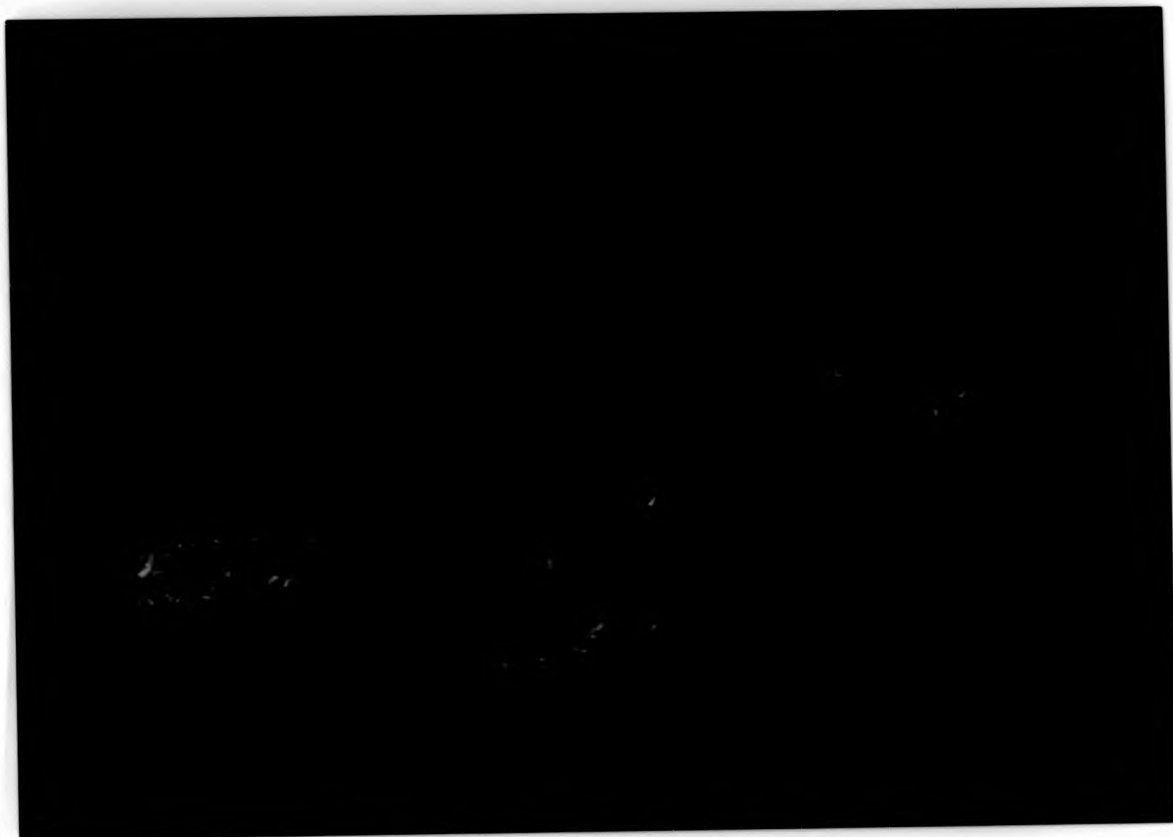


Plate 8-IX Copolymer NTA-MAA(50:50) shows intense blue colour
at 440K



Plate 8-X Copolymer NTA-MAA(50:50) shows reddish yellow colour
at 430K when subjected to shear

NTA-MAA(50:50) displayed an intense blue colour(Plate 8-IX). A shear was then applied, when the temperature was decreased by about 10K, a dramatic change of colour was observed(Plate 8-X). This change of colour from blue to reddish yellow is typical of a twisted nematic phase in low molecular weight liquid crystals when the temperature is decreased.

The DSC thermograms of copolymer NTA-MAA(25:75) are shown in Figure 8-12, T_g and T_{ni} were found at 323K and 404K respectively. A microphotograph of the phase is shown in Plate 8-XI. The mesophase was composed mainly of a greyish blue region with some diffuse yellow domains due to differences in thickness. A weak yellow iridescent colour can only be seen visually when great care is taken.

8.4 Comparison of Cholesteric Polymers with Different Substituents

The phase diagram of copolymer NTA-MAA is shown in Figure 8-9. Like the other series of copolyesters, there is a consistent decrease in the isotropic transition temperature(T_{ni}) as the content of flexible spacer increases. $T_{ni}(s)$ are approximately 30K lower than the corresponding copolymer BTA-MAA(s) with an equivalent composition. This phenomenon is also found in the 'homopolymers'.

In the BTA and NTA series, the substituent was always attached to the mainchain. Both steric and dipole-dipole attractive interactions are generally short range effects which require the substituents to come close together in order to interact effectively. As the content of the flexible spacer increases, the steric effect arising from the bulky

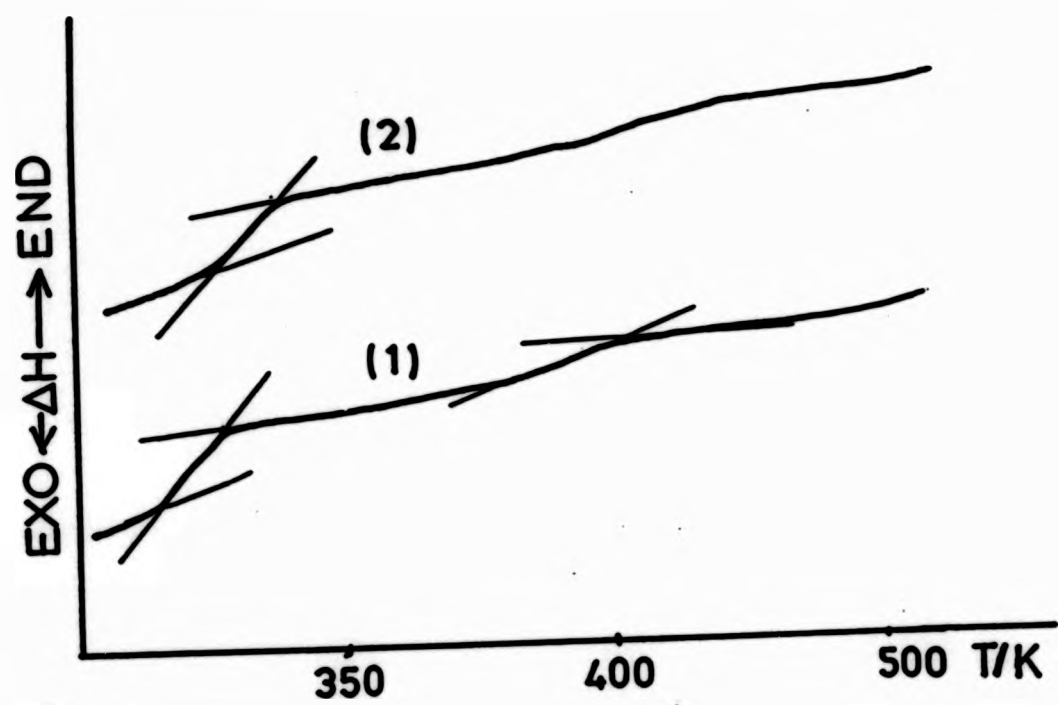


Fig. 8-12 DSC thermograms for copolymer NTA-MAA(25:75)
(1) 1st heating scan
(2) 2nd heating scan



Plate 8-XI The greyish blue homogenous texture of
copolymer NTA-MAA(25:75)

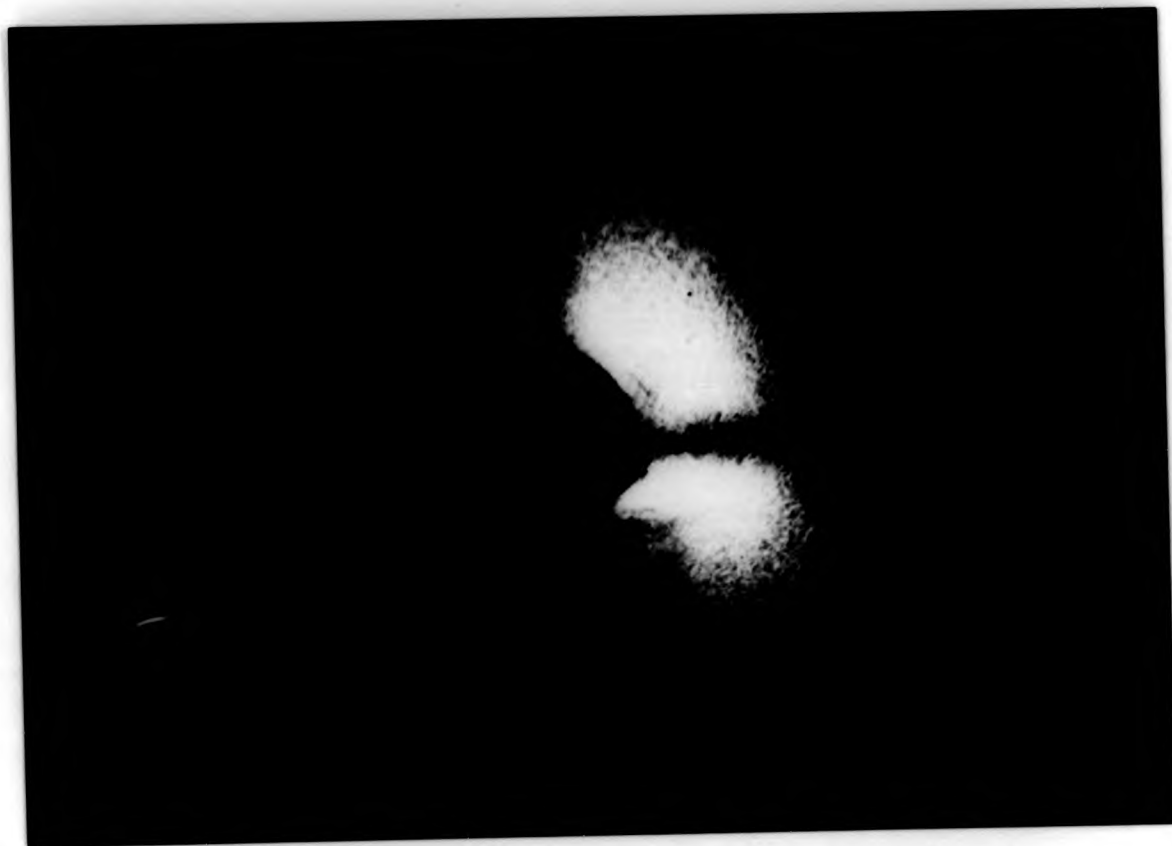


Plate 8-XI The greyish blue homogenous texture of
copolymer NTA-MAA(25:75)

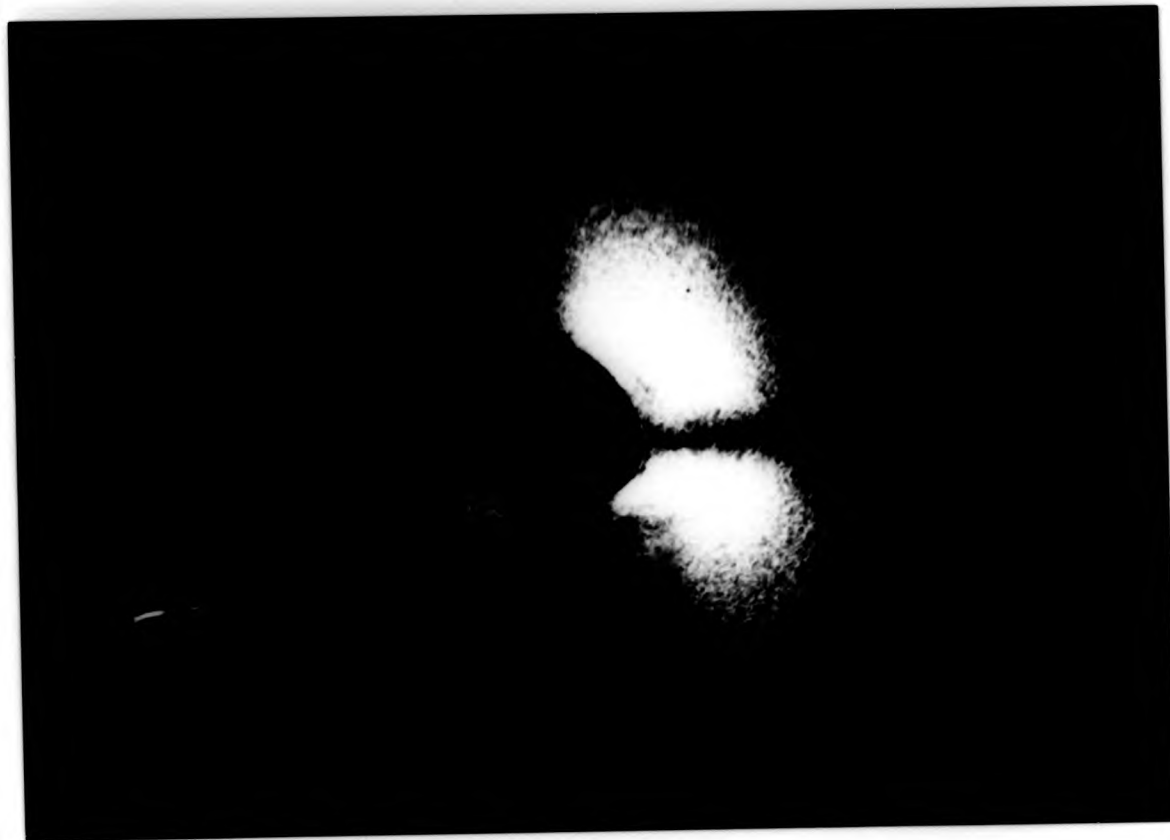


Plate 8-XI The greyish blue homogenous texture of
copolymer NTA-MAA(25:75)

substituent becomes insignificant; this probably explains why there is only a small difference in isotropic temperature (T_{ni}) between copolymer TA-MAAs and copolymer BTA-MAAs.

The van der Waals volumes of -Br and -NO₂ are very similar with -NO₂ slightly larger than -Br (150). In addition, the nitro-group has greater polarity than the bromo-group, hence, the repulsion exerted by the nitro-group should be greater. It is the larger size of the nitro-group and the stronger repulsion which impairs the isotropic temperatures of copolymer NTA-MAAs.

The glass transition is more susceptible to the change of polymer composition. The highest mesophase stability is again found for polymer of maximum randomness, i.e. copolymer NTA-MAA(50:50).

CHAPTER NINE

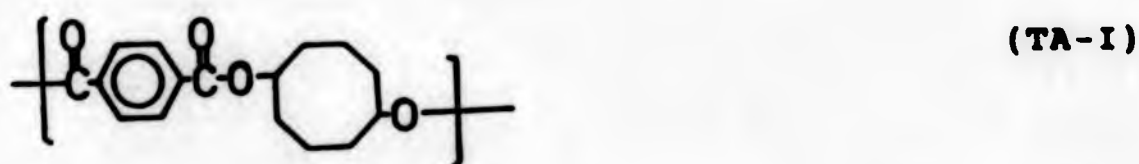
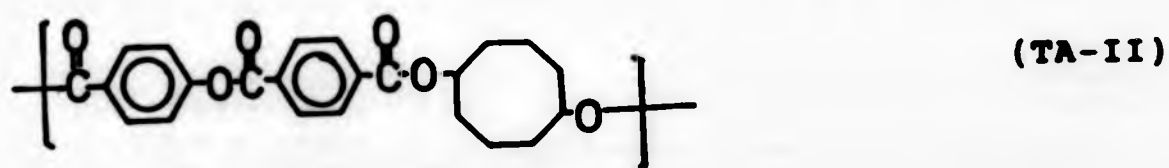
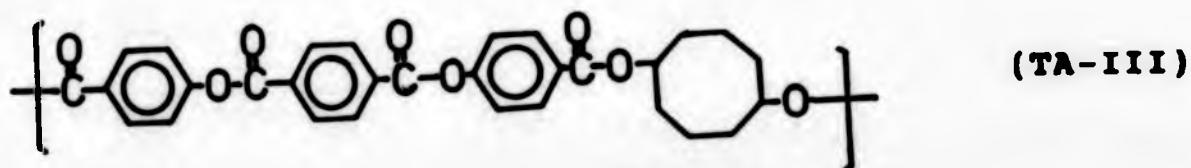
EFFECT OF MESOGENIC UNIT LENGTH

The ester mesogenic structures reported to date generally contain either two or three aromatic units^{<56,57,98,99,103>}. These structures have been synthesised using mainly terephthalate, p-oxybenzoate and hydroquinone units in either their substituted or unsubstituted forms. Linkage to the spacing group in the terminal para positions of these mesogenic group ester diads and triads may be either ester or ether linkages, and the former link can be formed in two different orientations.

In the present study an attempt has been made to find out the effect of the mesogenic unit length to the properties of thermotropic LC polymers.

Polymers containing a common spacing group but mesogenic groups of various length were prepared. The spacing unit employed was an eight membered ring (cis-1,5-cyclooctanediol) while the mesogenic groups consisted of one, two and three aromatic units.

Structures of these three polymers are shown as below:-



9.1 Polymer TA-III

The properties of polymer TA-III have already been described in Chapter Seven.

9.2 Polymer TA-II

The DSC thermograms of polymer TA-II are shown in Figure 9-1. Two endotherms were detected between the temperature range 370K to 420K (curve 1). The higher endotherm at 408K was assigned as the mesophase to isotropic transition while the one at lower temperature (385K) was probably the melting transition. After the first heating scan, subsequent scans were rather featureless apart from an obscure glass transition at about 330K (curve 2). The cooling scan did not provide any information. However, optical observations revealed that there was a mesomorphic transition between 390K to 410K. As a result, the sample was cooled from 420K to 390K and annealed at this temperature overnight. Next day, the sample was cooled at the normal rate (20K/min) to 300K and then reheated to 420K. Two endotherms were again obtained, with one at 406K and the other at 375K (curve 3). There was little change in clearing temperature (ca 2K) while the melting temperature obtained from the annealed sample was about 10K lower than the virgin sample. Apparently, thermal treatment at 390K gave the polymer molecules sufficient time to align themselves in the anisotropic state. This supposition agreed with optical observations.

When heated on a hot-stage microscope, the sample began to melt at about 370K and the last crystallite disappeared at 400K. After that, the sample transformed into a homeotropic

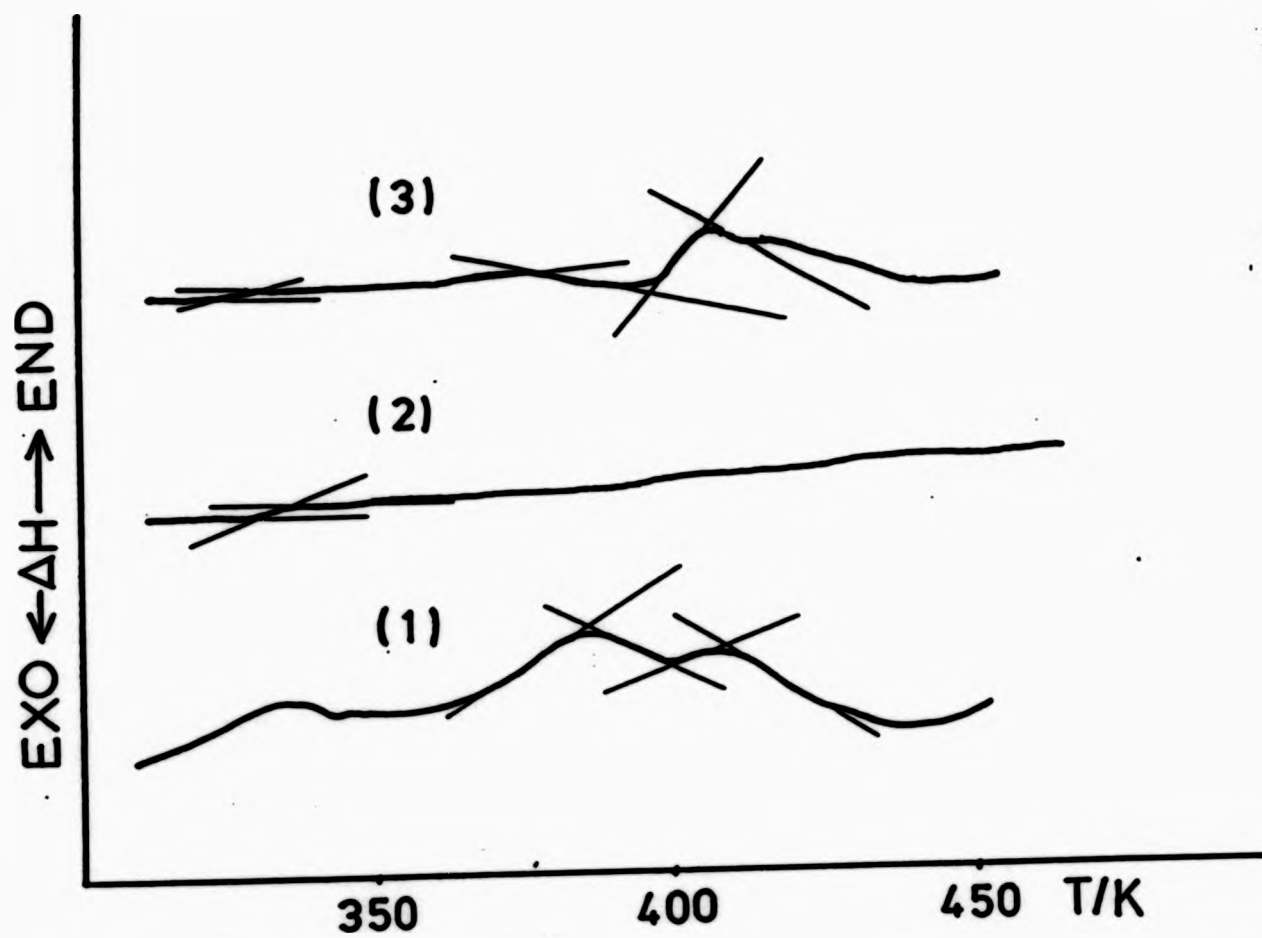


Fig. 9-1 DSC thermograms for polymer TA-II
 (1) 1st heating scan
 (2) 2nd heating scan
 (3) 3rd heating scan after annealing at 390K overnight

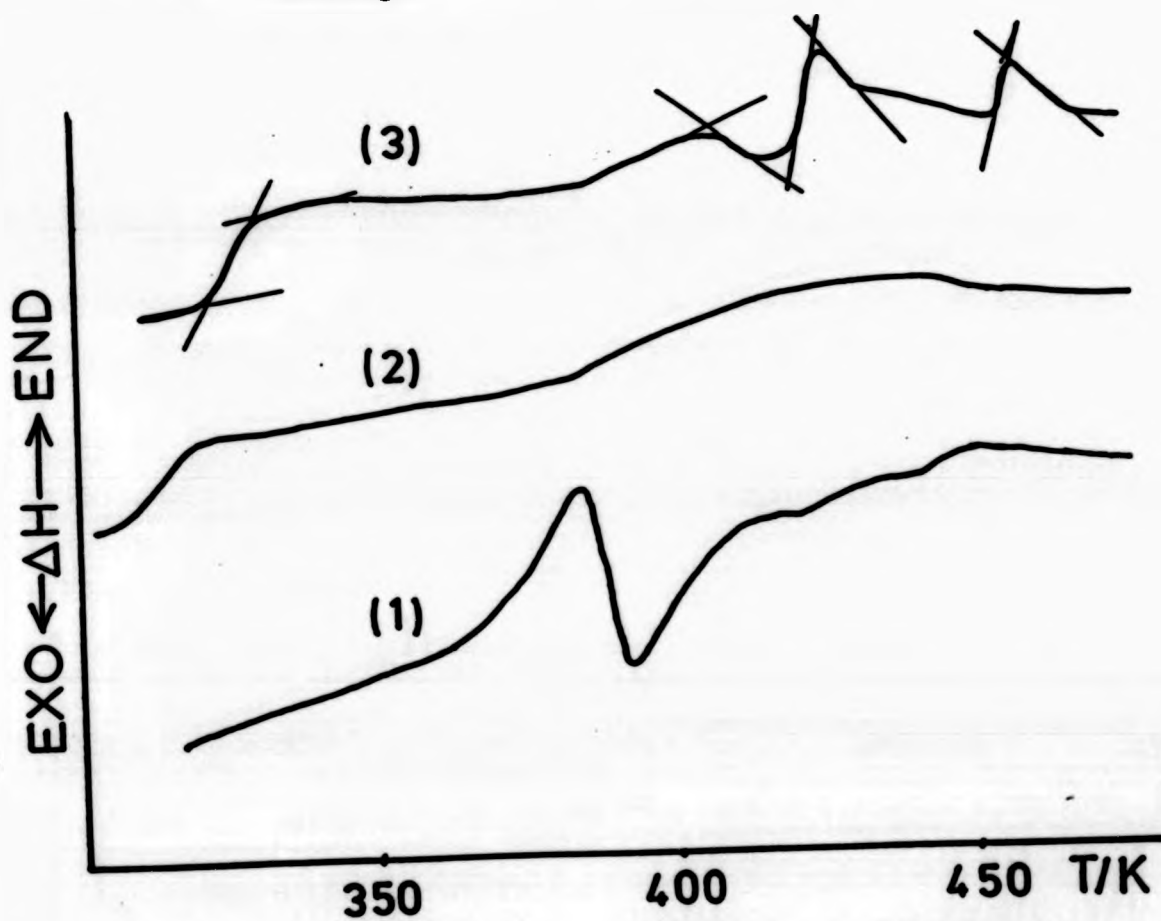


Fig. 9-2 DSC thermograms for polymer TA-II-MAA(75:25)
 (1) 1st heating scan
 (2) 2nd heating scan
 (3) 3rd heating scan after annealing at 415K for one hour

texture and the stir-opalescence effect vanished at 420K. When quenched from the isotropic melt rapidly to room temperature, no identifiable texture was observed, instead the sample was transparent. This phenomenon is common in liquid crystalline polymers in that the mesophase can be locked in the glassy state. As a result, the sample was heated 20K above its clearing temperature followed by cooling to 390K and kept at this temperature for 24 hours. A yellow fan-like texture began to develop after two hours at the expense of the homeotropic phase. Four hours later, a spherulite-like texture started to appear. The sample was shearable before the formation of the spherulites. Plate 9-I shows the coexistence of a fan-like texture and spherulites. The fan-like texture developed from a homeotropic phase is usually observed in the smectic A phase of low molecular weight liquid crystals. The origin of the spherulites is not known, although Shaffer and Percec⁽¹¹²⁾ observed a similar texture in a series of polythioethers. These authors concluded that this spherulite-like texture was a highly ordered smectic mesomorphism based on DSC and optical observations.

It is possible to disrupt a crystal lattice or highly ordered smectic phase by incorporating substituted flexible units as has been demonstrated in Chapter Six on the 'effect of flexible spacers'. It is a matter of interest to find out whether a small amount of flexible spacer has any effect on this spherulite-like texture.



Plate 9-I The fan-like texture of polymer TA-II
with spherulite background

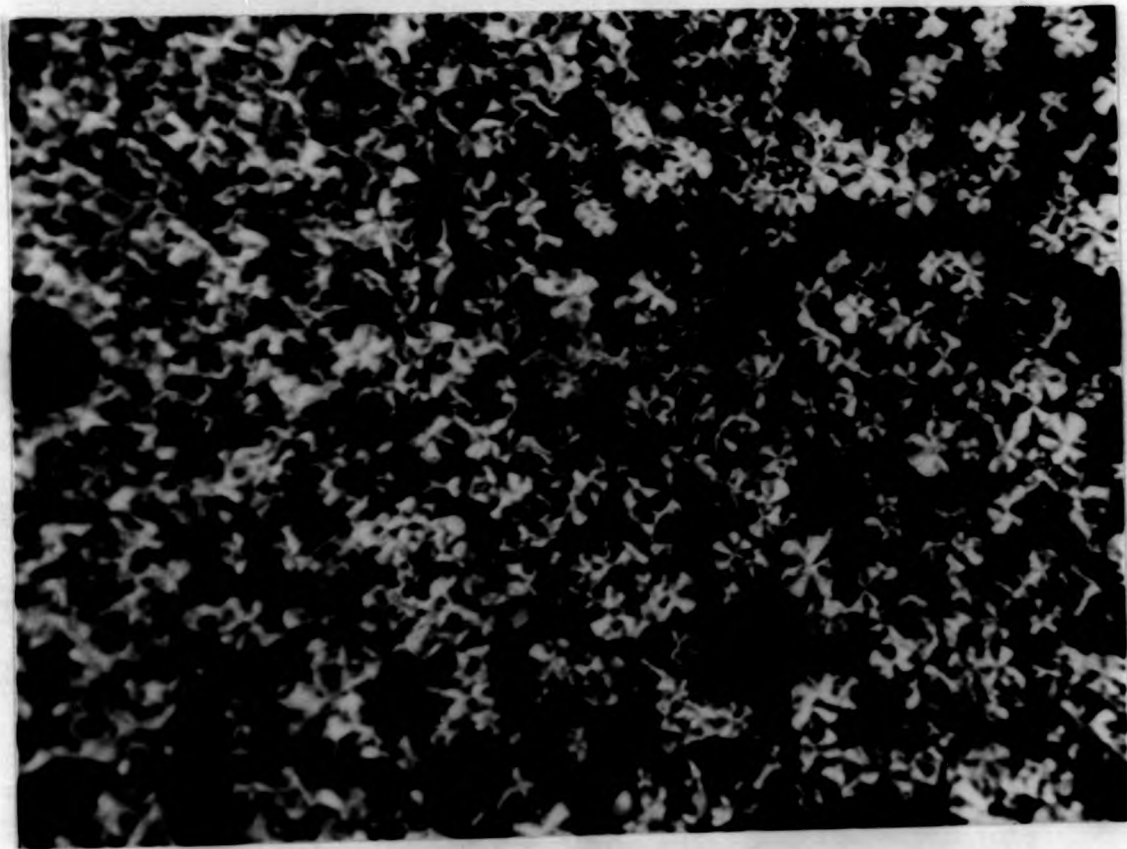


Plate 9-II The focal-conic smectic texture of copolymer
TA-II-MAA(75:25)



Plate 9-I The fan-like texture of polymer TA-II
with spherulite background

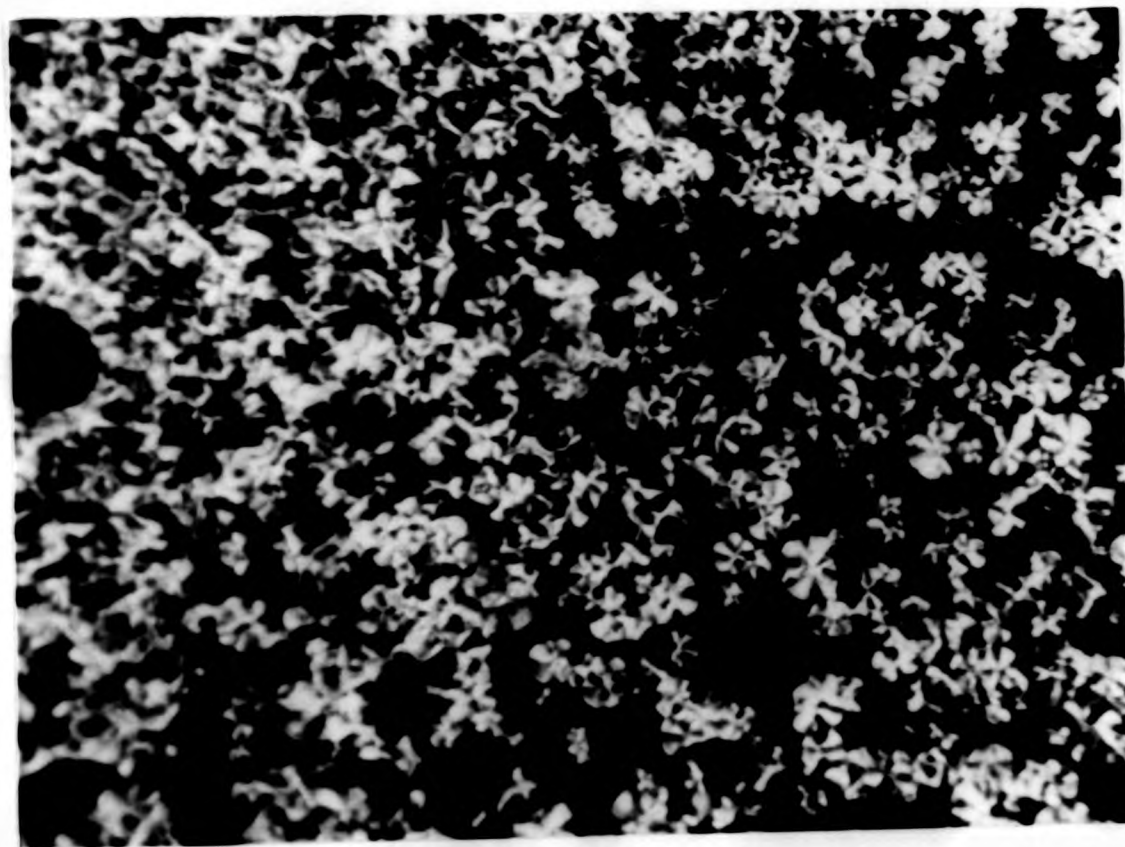


Plate 9-II The focal-conic smectic texture of copolymer
TA-II-MAA(75:25)

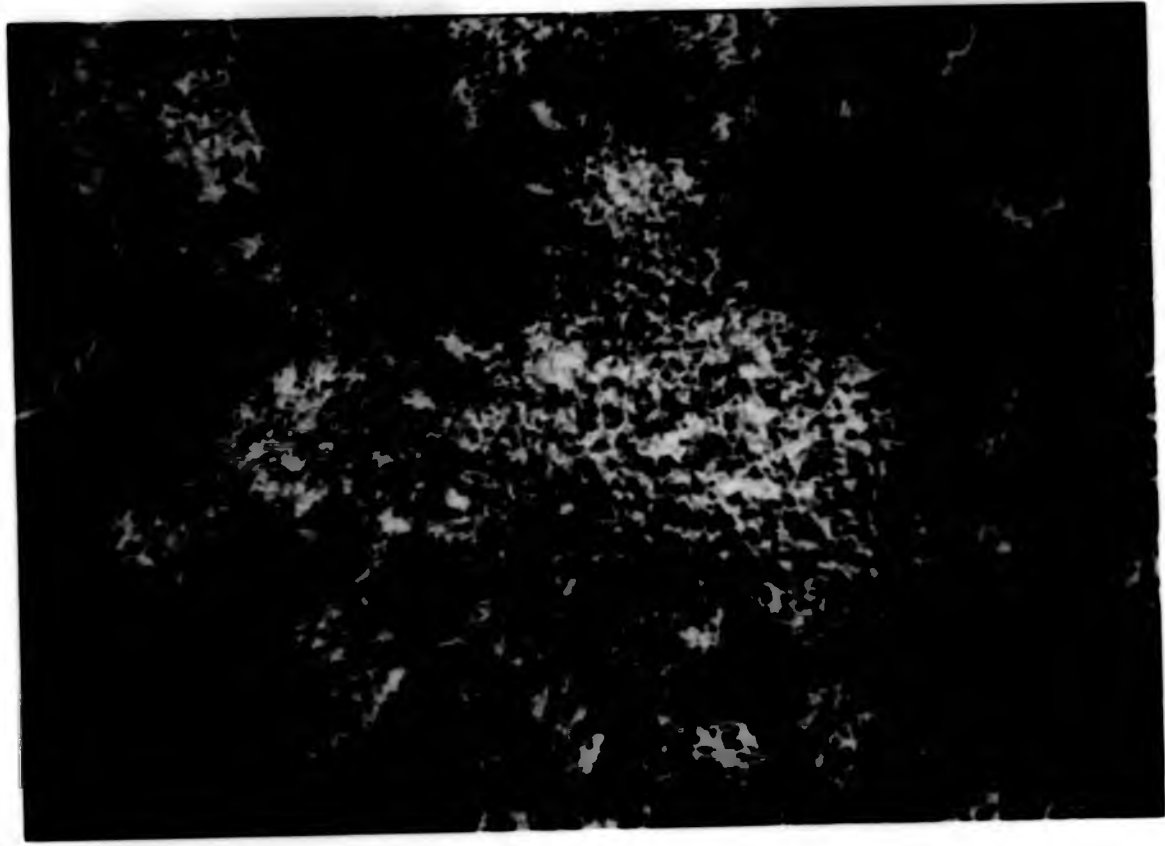


Plate 9-I The fan-like texture of polymer TA-II
with spherulite background

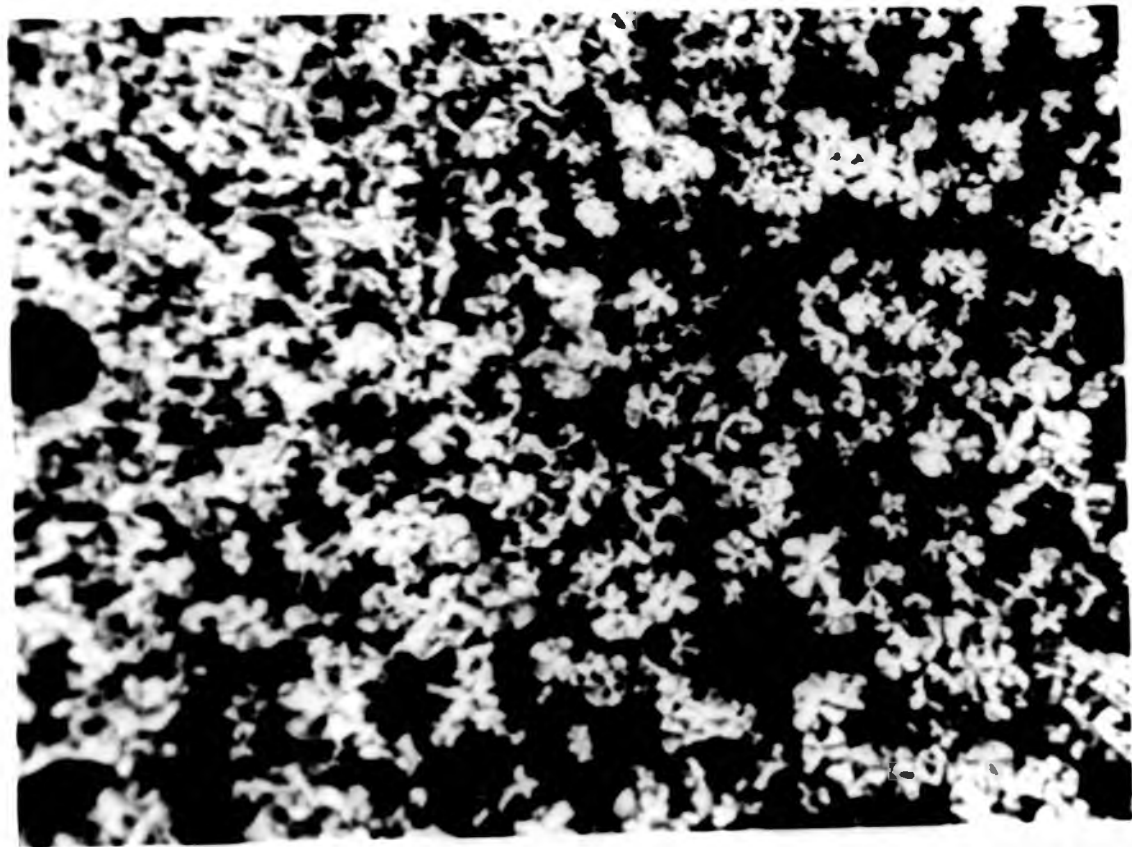
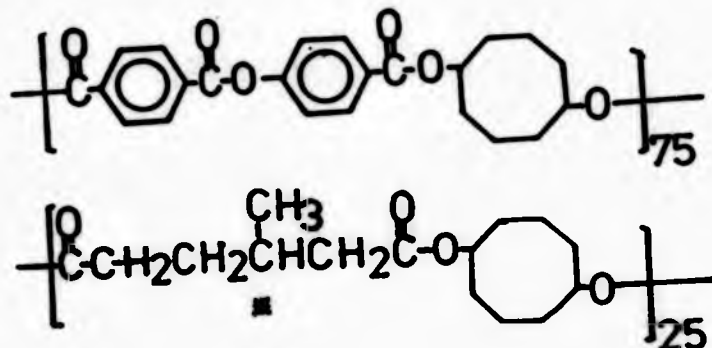


Plate 9-II The focal-conic smectic texture of copolymer
TA-II-MAA(75:25)

Copolymer TA-II-MAA(75:25), with the following structure, was prepared.



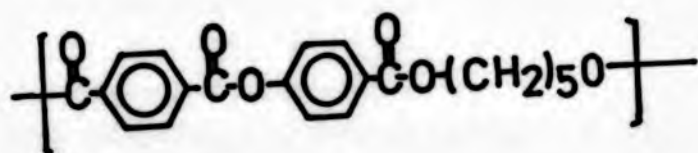
This copolymer contained 25% of (+)-3-methyl adipic acid(MAA). Figure 9-2 shows the DSC thermograms. The first heating scan(curve 1) displayed a large cold crystallisation exotherm at about 390K, and an extremely broad endotherm with two tiny kinks at 420K and 440K. The cold crystallisation exotherm disappeared in the second heating scan(curve 2), and an even broader endotherm extending from 483K to 460K was detected. The second order transition at 315K was assigned as T_g . Unless otherwise stated, the cooling rate was 20K/min. The same sample was then annealed at 415K for 1 hour, cooled and scanned. Three well resolved endotherms at 418K, 425K and 457K were obtained(curve 3).

Based on the transition temperatures of curve 3, the sample was carefully studied under the hot-stage microscope. When the isotropic melt was cooled to about 460K, weak stir-opal-scence was detected by pressing the cover slips. By quenching this homeotropic texture to 420K and maintaining it at this temperature for 2 hours, a focal conic texture resembling a smectic A phase in low molecular weight liquid crystals was observed(Plate 9-II). An identifiable texture for the homeotropic phase could not be obtained even by annealing the sample at 450K for 3 hours. If the transition at 425K is a

real smectic A phase, then the homeotropic texture can be only either a nematic phase or a twisted nematic phase (cholesteric). It is more likely to be the latter because of the presence of MAA. Hence, the mesomorphic sequence was assigned as:-

k 418K Sa 425K Ch 457K i.

A cyclooctane molecule is almost like two linear pentane molecules connected together. It is interesting to compare a polymer containing a cyclooctyl ring and its linear equivalent, in this case, 1,5-pentanediol. A polymer of the following structure was prepared:-



The DSC thermograms of this polymer are depicted in Figure 9-3. A very broad endotherm ranging from 350K to 410K was detected in the first heating scan (curve 1). By annealing the sample at 380K for 1 hour, two endotherms at 372K and 402K were obtained (curve 2). The glass transition was found at 322K. No liquid crystalline behaviour could be observed when studied by optical microscopy, instead, a leaf-like structure reminiscent of crystallites was developed after annealing at 370K (Plate 9-III).

Although the transition temperatures of polymer TA-II are only a few degrees higher than the above mentioned polymer, the contribution to the formation of a mesophase by the more rigid nature of the cyclooctyl unit is now clearly demonstrated.

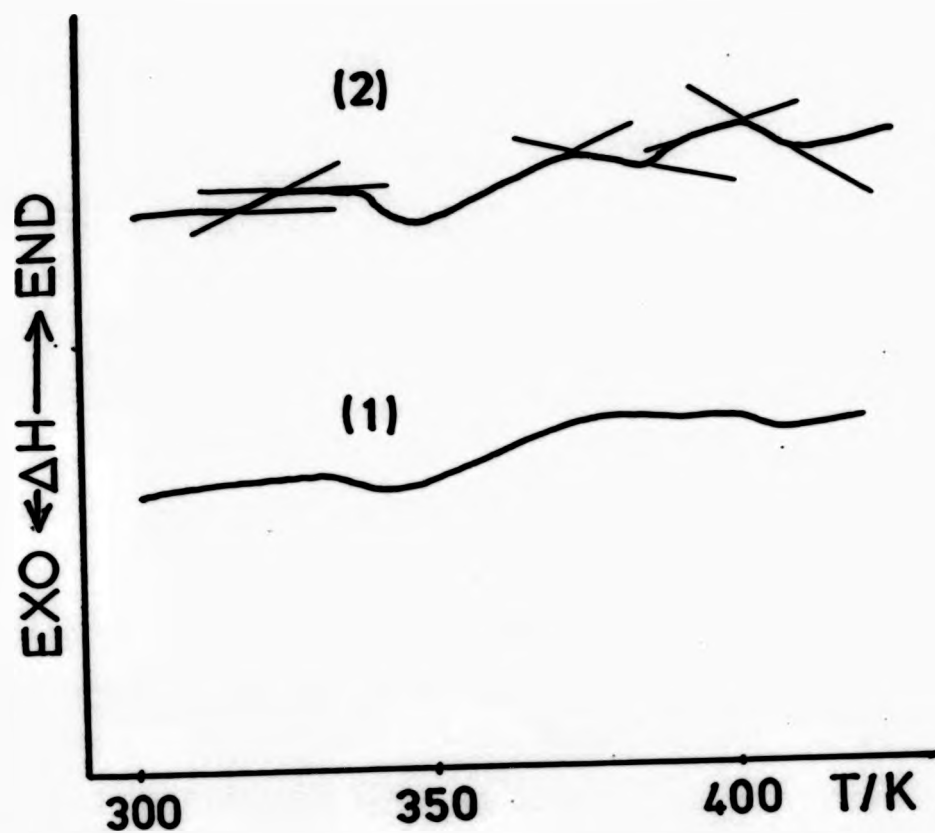


Fig. 9-3 DSC thermograms for polymer TA-II-PD
 (1) 1st heating scan
 (2) 2nd heating scan after annealing at 380K
 for one hour

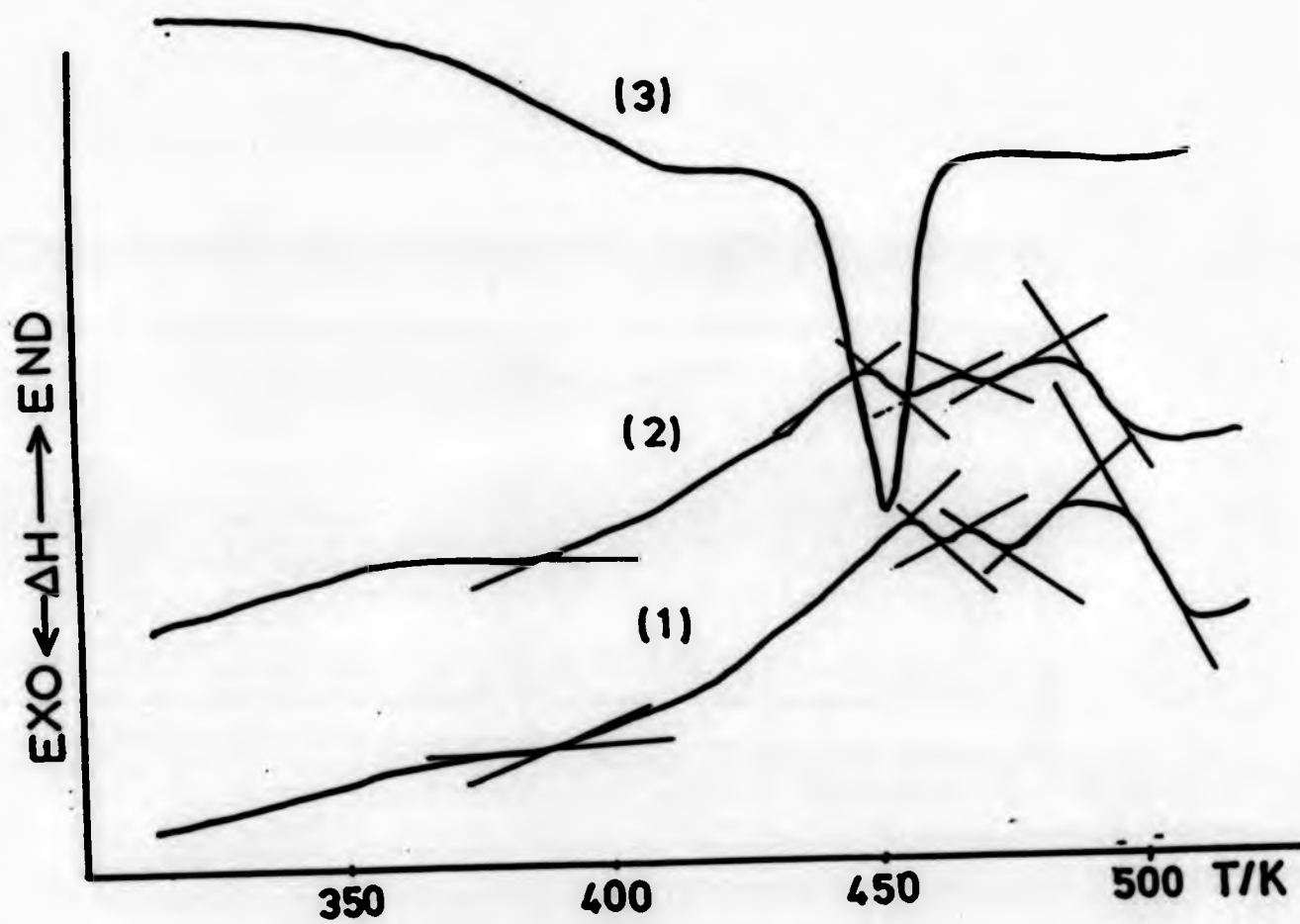


Fig. 9-4 DSC thermograms for polymer TA-I
 (1) 2nd heating scan
 (2) 1st heating scan
 (3) cooling scan



Plate 9-III The leaf-like crystallites structure of
polymer TA-II-PD



Plate 9-IV The blurred blue texture of polymer TA-I
at 483K

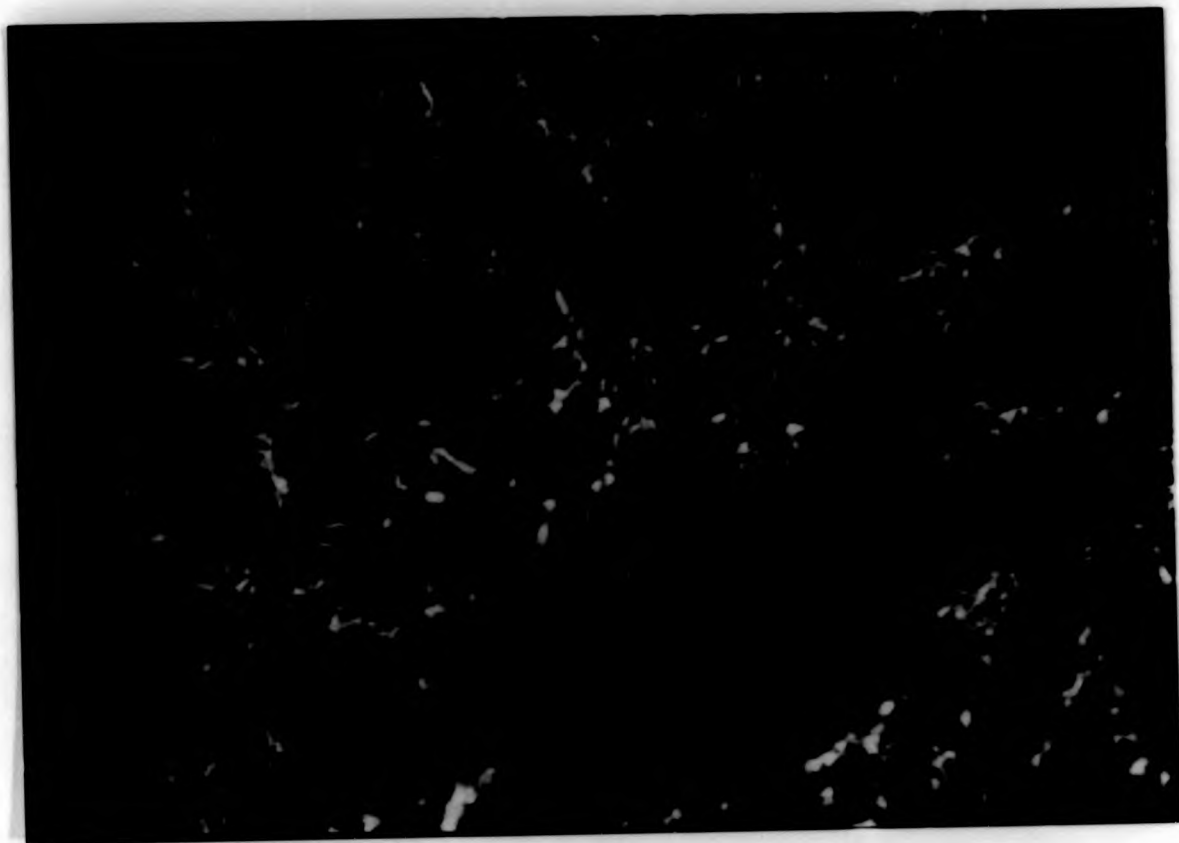


Plate 9-III The leaf-like crystallites structure of
polymer TA-II-PD



Plate 9-IV The blurred blue texture of polymer TA-I
at 483K



Plate 9-III The leaf-like crystallites structure of
polymer TA-II-PD



Plate 9-IV The blurred blue texture of polymer TA-I
at 483K

9.3 Polymer TA-I

When the eight membered ring was incorporated between two aromatic units even with very a long flexible spacer like decamethylene (Chapter Six), it still exhibited liquid crystalline behaviour. However, when the cyclooctyl unit in polymer TA-II was replaced by an equivalent linear unit (pentamethylene), a mesophase could not be observed anymore. So what is the actual role of this eight membered ring? Is it stiff enough to retain LC properties even with the shortest rigid unit eg. terephthalic acid, or does it merely function as a semiflexible spacer?

Poly-(p-phenylene terephthalate) melts well above 800K, it is interesting to see what will happen if one of the aromatic units is replaced by an eight membered ring.

The DSC thermograms of polymer TA-I are shown in Figure 9-4. The second heating scan (curve 1) indicated clearly three endotherms at 457K, 462K and 492K. A subsequent scan was fairly reproduceable (curve 2). An exotherm at about 451K was found in the cooling scan (curve 3). The glass transition was located at 383K which was also reflected by optical observation viz. the sample began to respond to shear.

Optical microscopic studies revealed that the sample cleared at 510K. By cooling the isotropic melt to 483K, a blurred blue texture began to develop (Plate 9-IV), and no obvious changes were observed even after annealing for 4 hours. Then, the sample was cooled slowly to ambient temperature, and a golden yellow colour texture resembling the broken focal-conic of a smectic C phase of low MW liquid crystals gradually started to appear (Plate 9-V). The blurred



Plate 9-V The broken focal-conic smectic texture of polymer TA-I at room temperature after annealing for 4 hours

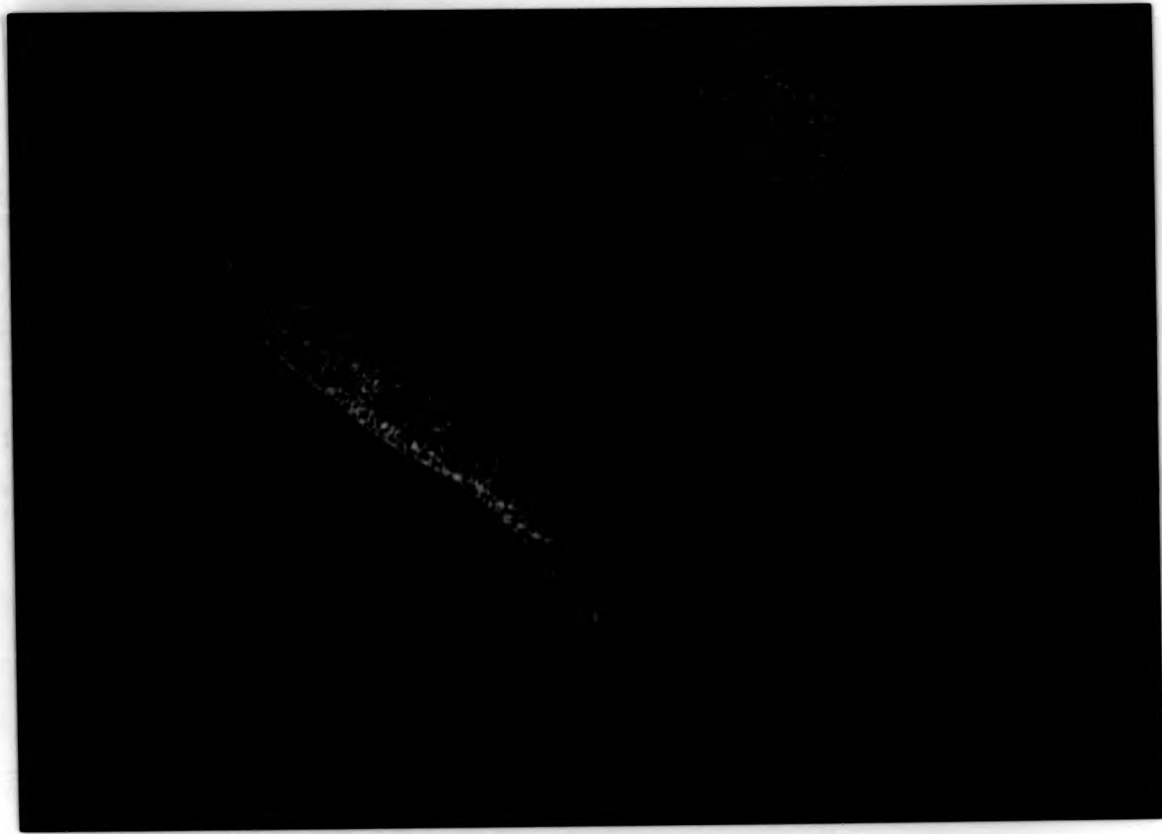


Plate 9-V The broken focal-conic smectic texture of
polymer TA-I at room temperature after annealing
for 4 hours

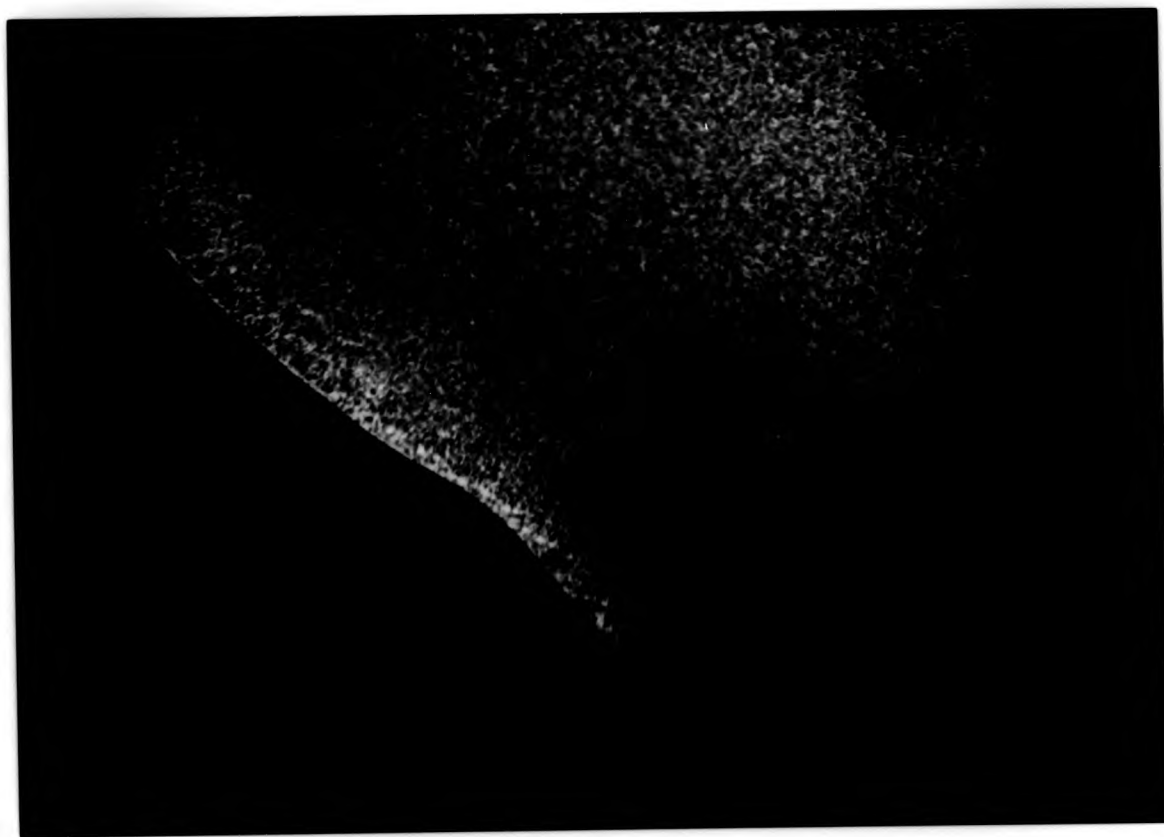


Plate 9-V The broken focal-conic smectic texture of
polymer TA-I at room temperature after annealing
for 4 hours

blue texture was optically isotropic, but very viscous. Certainly the data are inadequate to conclude the nature of the mesophases at this stage. In low molecular weight liquid crystals, the only optically isotropic mesophase is a smectic D phase but there are only a few examples of this phase<122>. Hence, for polymer TA-I, if one had to make a bold guess as to the mesomorphic sequence, one possible suggestion would be
k 457K Sc 462K Sd 492K i.

9.4 Comparison of Polymers of Different Mesogenic Length

A plot of mesogenic unit lengths against mesophase stability of polymers in which a common 'spacer' is present: the eight membered ring, is shown in Figure 9-5. The approximate length of the triad, diad and monad are 19A, 13A and 7A respectively. There is an enormous increase in mesophase stability(dT) when the rigid group is a triad ester. 'dT' of polymer TA-III (100K) is 70K higher than polymer TA-II. The dT of polymer TA-I is almost the same as polymer TA-II(30K) although in a much higher temperature region. The nature of the mesophases is also affected by the length of the rigid groups. Only polymer TA-III exhibited a nematic mesophase.

In general, one would expect the shorter the rigid group, the lower the transition temperatures. The abnormality witnessed in this series cannot be explained, whether it is a molecular weight effect, or due to the presence of chain end groups, will still need to be determined. It is well known in low MWLC compounds that the nature of the end groups is one of the determining factors for the formation of mesophase<17>.

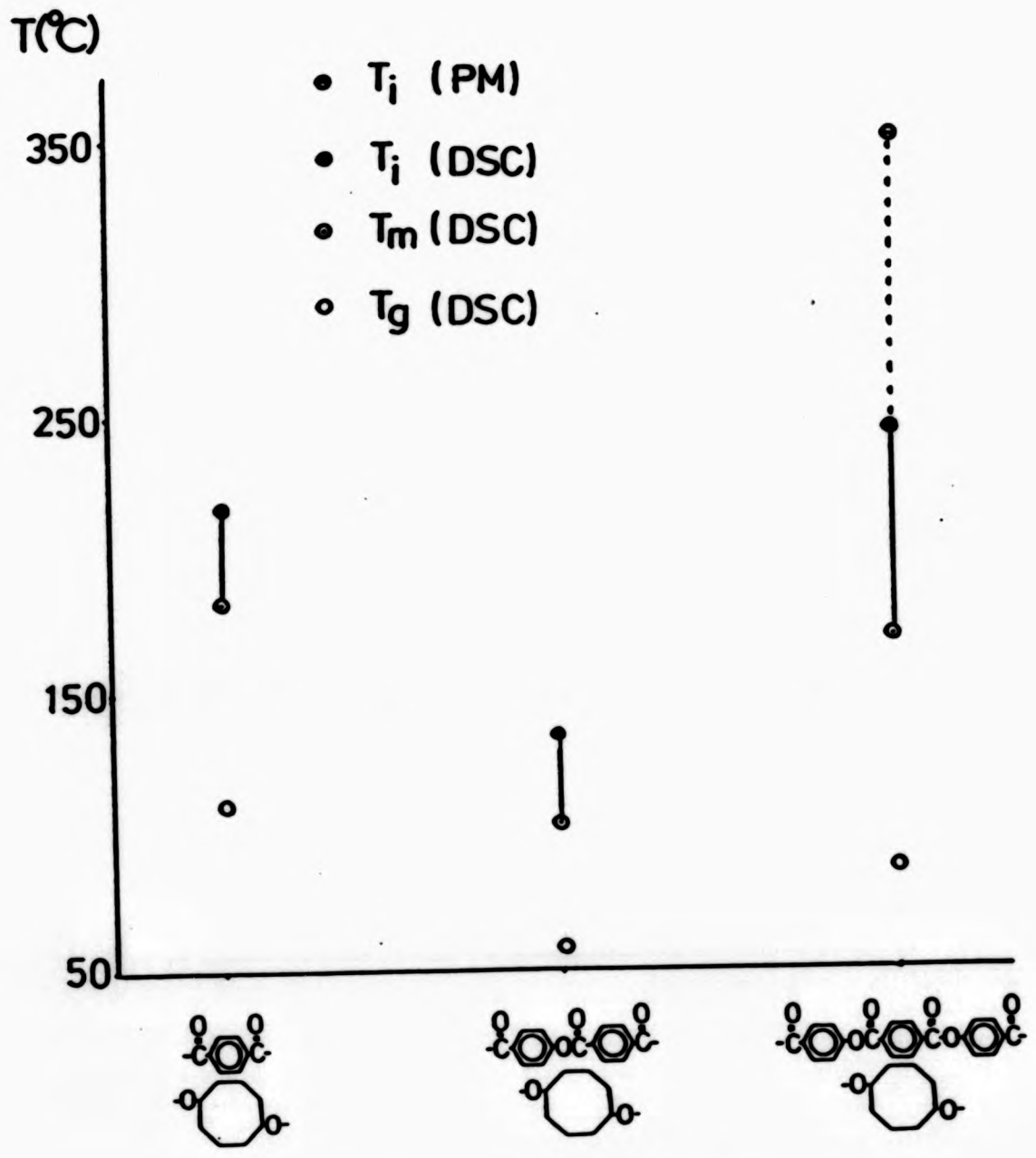
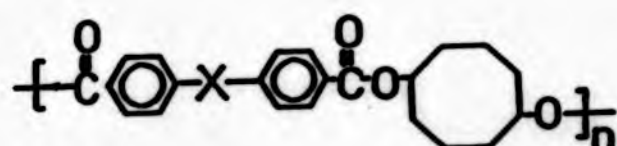


Fig. 9-5 Plots of mesophase range for polymer TA-I, polymer TA-II and polymer TA-III

CHAPTER TEN
EFFECT OF MESOGENS

The pioneering work on mainchain LC polymers began by incorporating bifunctional mesogenic monomers into the polymer backbone⁴⁷. The majority of these mesogens contained a short rigid link which connected two aromatic rings in the para positions. Their well characterised properties and their availability made them very easy to study. Azo, azoxy and trans-stilbene links are probably the most extensively investigated examples. However, these unsaturated linkages are very susceptible to heat and irradiation.

The schematic structure of the polymers under study is illustrated below



where X = N=N, N=NO and CH=CH.

These polymers were designated with the codes: AZO-CO, AZOXY-CO and STIL-CO, where CO stands for cis-1,5-cyclooctanediol.

10.1 Azo Link

A preliminary study using the hot-stage microscope revealed that this polymer began to decompose at about 550K. In order to obtain more reproducible results, the sample was only heated to 383K in the first heating scan and held at this temperature for 2 minutes to ensure there was no solvent residue. After cooling to room temperature at 20K/min, the sample was then scanned at a rate of 40K/min until decomposition started to occur. The decomposition temperature

was found at approximately 542K after several test runs. The cooling scan was obtained by setting the instrument to the auto-cooling mode at a rate of 40K/min in order to avoid excessive decomposition due to prolonged heating.

The DSC thermograms of polymer AZO-CO are depicted in Figure 10-1. According to curve 1, the glass transition temperature, melting temperature and the mesophase to isotropic temperature were at 478K, 509K and 540K (curve 2) respectively. Three exotherms were obtained from the cooling scan, the order of their appearance was 538K, 488K and 460K. The obscurity of the melting transition was attributed to the high cooling rate.

It is difficult to study the sample on the hot-stage because of its poor thermal stability. To overcome this obstacle, the hot-stage was preheated to 540K before the sample was loaded. The sample melted and cleared instantly. By switching off the thermostat and blowing nitrogen over the sample, the temperature was decreased rapidly to 513K when a nematic schlieren texture started to appear at the expense of the homeotropic background (Plate 10-I). On further cooling down to 490K, the sample was still very shearable (Plate 10-II), which was probably a result of thermal degradation leading to a lower molecular weight and thus a lower melting temperature as well. Hence, the mesomorphic order of polymer AZO-CO is:-

k 509K n 540K i

Iimura et al. <162> used the same mesogen to copolymerise with different alkanediols (n=6-12); they found these polymers did not show any liquid crystalline behaviour. However, when

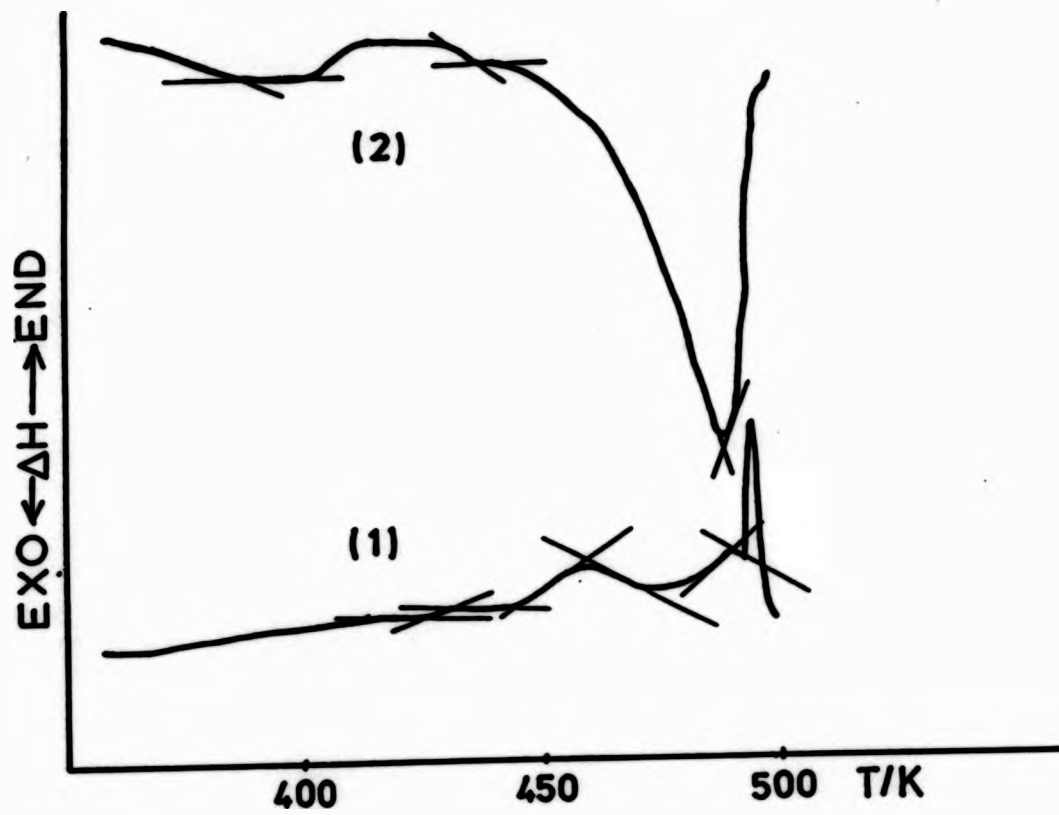


Fig. 10-1 DSC thermograms for polymer AZO-CO
 (1) heating scan
 (2) cooling scan

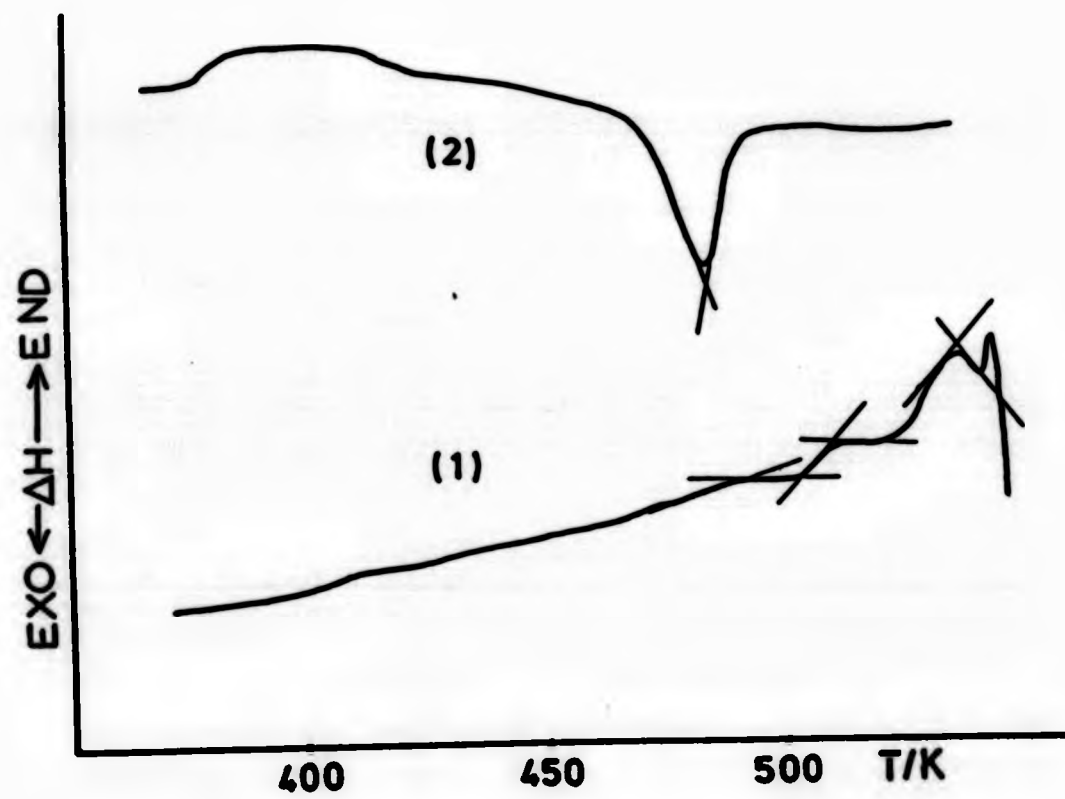


Fig. 10-2 DSC thermograms for polymer AZOXY-CO
 (1) heating scan
 (2) cooling scan

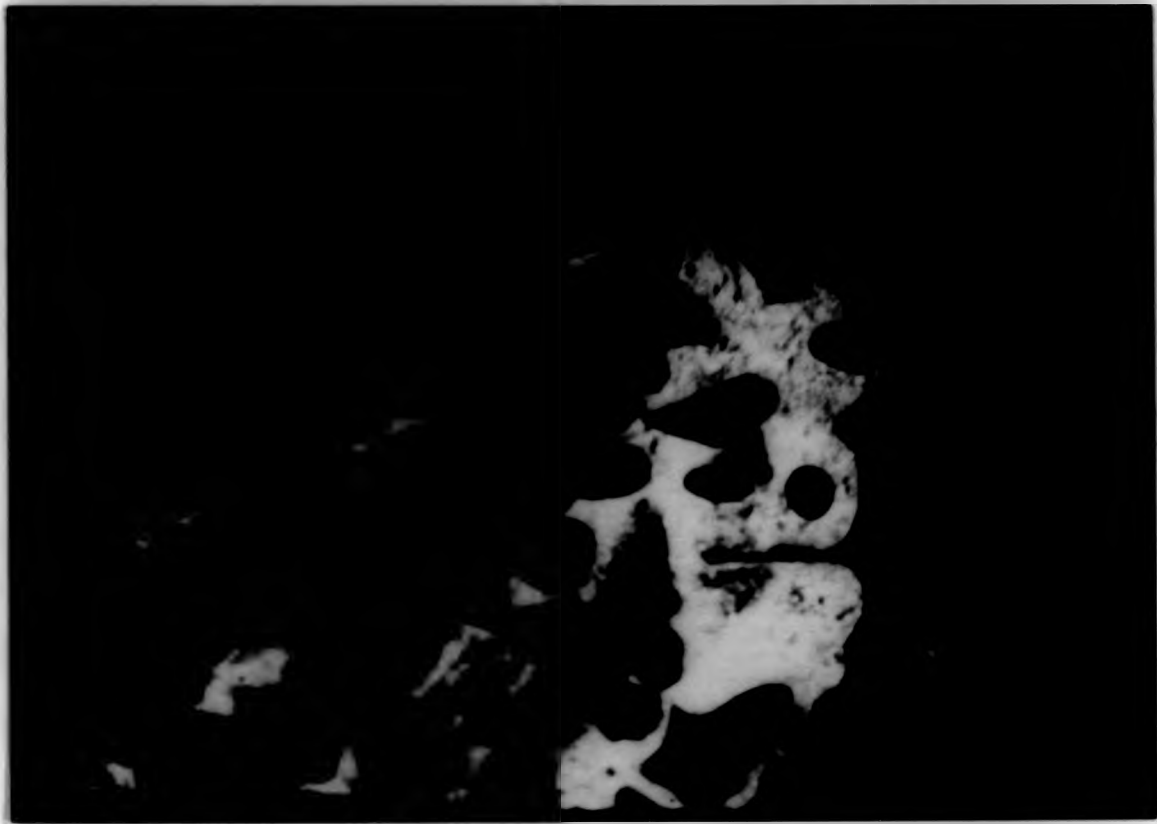


Plate 10-I The appearance of nematic schlieren texture from the homeotropic background of polymer AZO-CO



Plate 10-II Polymer AZO-CO at 490K when sheared with some degree of degradation



Plate 10-I The appearance of nematic schlieren texture from the homeotropic background of polymer AZO-CO



Plate 10-II Polymer AZO-CO at 490K when sheared with some degree of degradation



Plate 10-I The appearance of nematic schlieren texture from the homeotropic background of polymer AZO-CO



Plate 10-II Polymer AZO-CO at 490K when sheared with some degree of degradation

polymers of reverse ester linkage were synthesized, all of them displayed mesophase irrespective of the spacer length ($n=5-10$).

It seems that the eight membered ring has sufficient stiffness to retain liquid crystalline properties compared to the equivalent linear spacer.

10.2 Azoxy Link

Polymer AZOXY-CO was treated the same way as polymer AZO-CO. Figure 10-2 shows the DSC thermograms. The glass transition temperature, the melting temperature and the mesophase to isotropic transition temperature were assigned at 493K, 510K and 548K respectively (curve 1). The cooling scan displayed a huge exotherm at 493K (curve 2), which is believed to be the supercooled melting transition.

Optical observations revealed that the sample began to decompose rapidly at about 530K. As a result, the sample was loaded on a preheated hot-stage at 528K; the isotropic phase appeared spontaneously and the sample was quenched immediately to approximately 505K. A microphotograph was then taken at this temperature, Plate 10-III shows the threaded nematic texture. When the temperature decreased to 495K, the sample was sheared, and at the same time liquid nitrogen was poured over the top. Plate 10-IV shows the quenched nematic phase. The colour effect was due to different thicknesses, bear in mind, azoxy and azo groups are strong chromophores. Hence, the mesomorphic order of polymer AZOXY-CO should be:-

k 510K n 548K i

A series of poly(α, ω -alkanediol-*p, p'*-azoxybenzoate)s was



Plate 10-III The threaded nematic texture of polymer AZOXY-CO

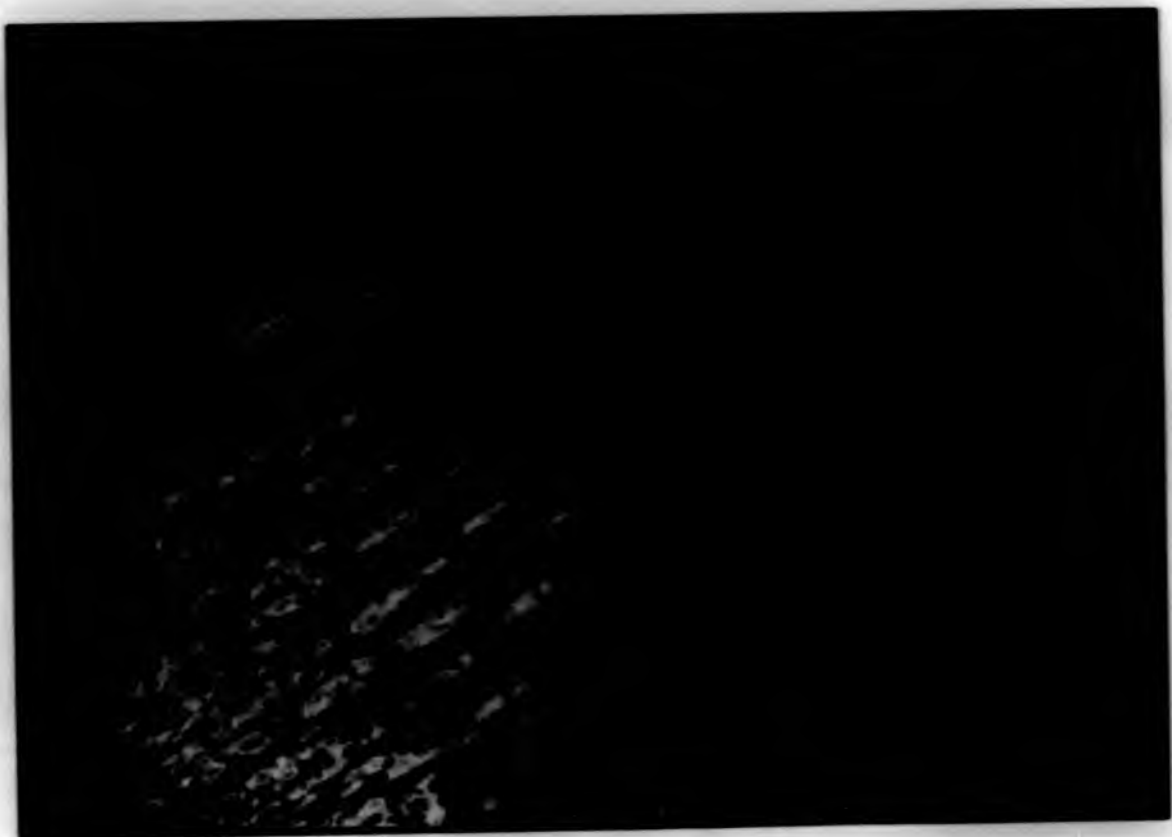


Plate 10-IV The quenched nematic phase of polymer AZOXY-CO

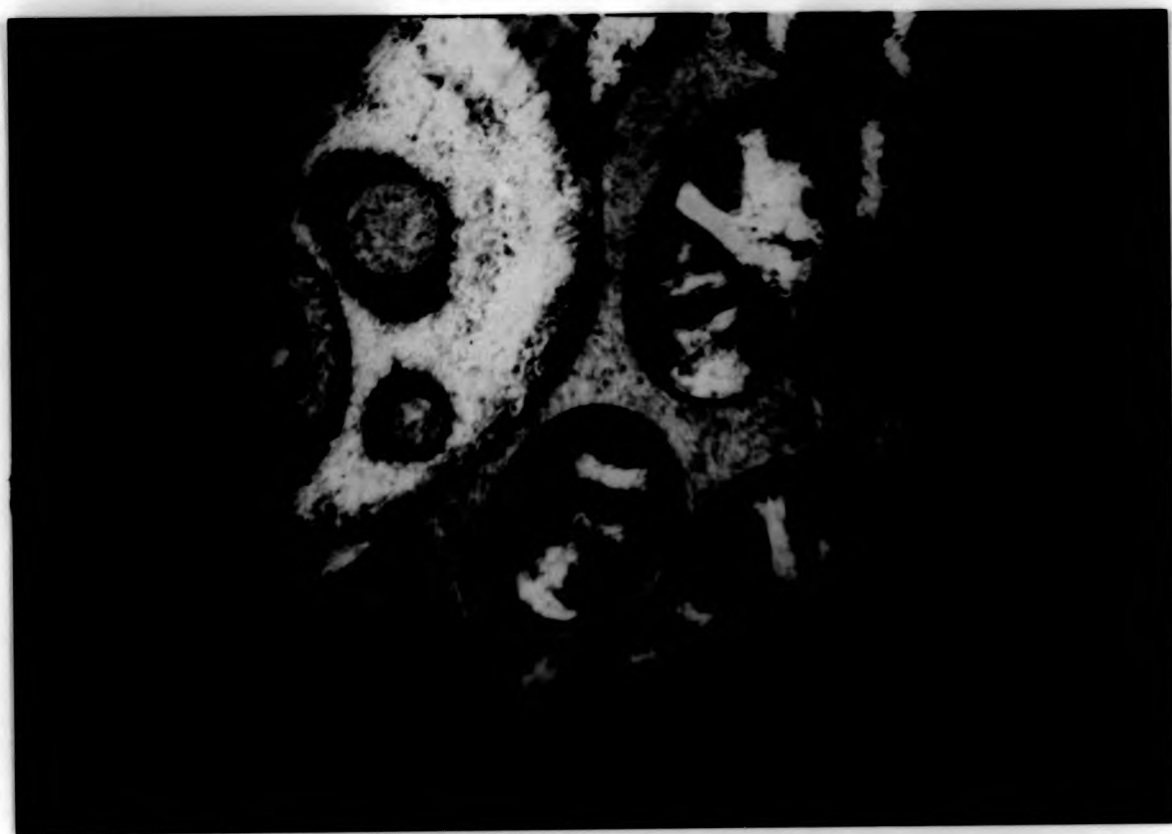


Plate 10-III The threaded nematic texture of polymer AZOXY-CO

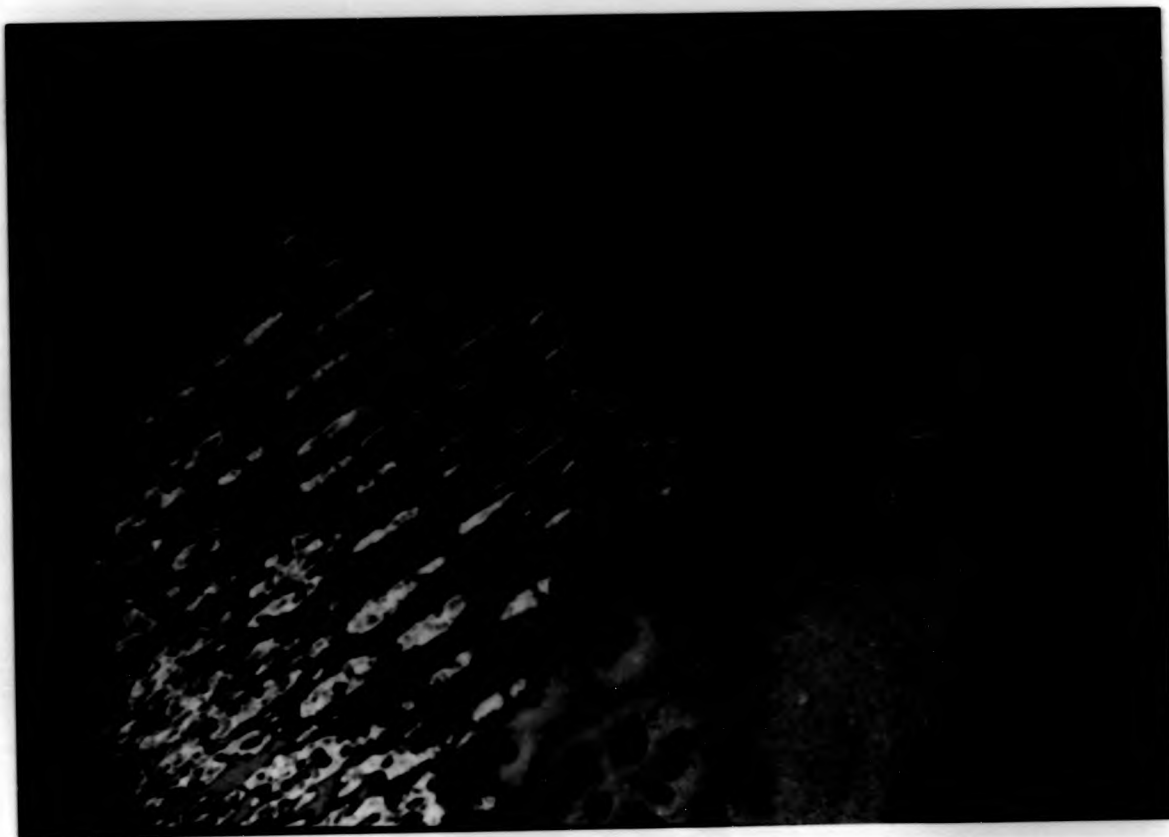


Plate 10-IV The quenched nematic phase of polymer AZOXY-CO



Plate 10-III The threaded nematic texture of polymer AZOXY-CO

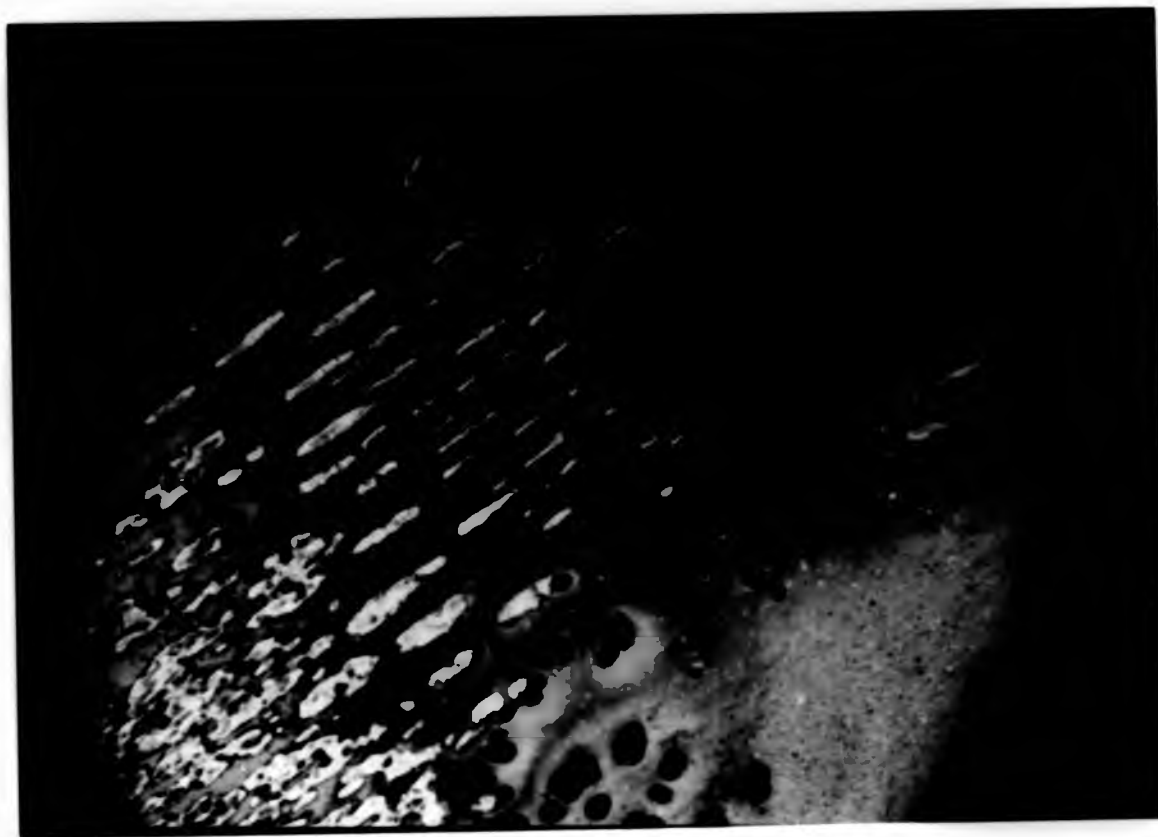


Plate 10-IV The quenched nematic phase of polymer AZOXY-CO

also prepared by Iimura et al.<162>. When the spacer was 1,5-pentanediol, the polymer exhibited a smectic phase of fan-like texture on cooling(monotropic). T_i and T_m of this polymer are at 508K and 460K respectively.

10.3 Trans-Stilbene Link

The DSC thermograms of polymer STIL-CO are depicted in Figure 10-3. Thermal treatment was similar to the previous samples despite the fact that this polymer is thermally more stable. Before the first scan, the sample was preheated to 500K at the rate of 80K/min, and quenched rapidly to room temperature. According to curve 1, the glass transition temperature and the melting temperature were assigned at 447K and 495K respectively, while the mesophase to isotropic transition was found at 563K accompanied by a small broad shoulder about 23K lower. The cooling scan(curve 2) revealed that the shoulder exerted a much larger supercooling effect compared with the other two. The sequence of appearance of these exotherms was 553K, 503K and 491K(curve 2).

Observation under the hot-stage polarizing microscope showed that when the sample was cooled from the isotropic state to 543K, the typical threaded texture of the nematic phase was obtained(Plate 10-V). On further cooling to 533K, a bead-like texture was observed(Plate 10-VI) which probably corresponds to the broad shoulder detected by DSC at 540K. Similar textures were also observed for Poly-(hexamethylene-p-biphenyl-4,4' carboxylate)<54> and some sidechain LC polymers<163>. This texture was generally recognised as a smectic A or C modification<54>. Therefore,

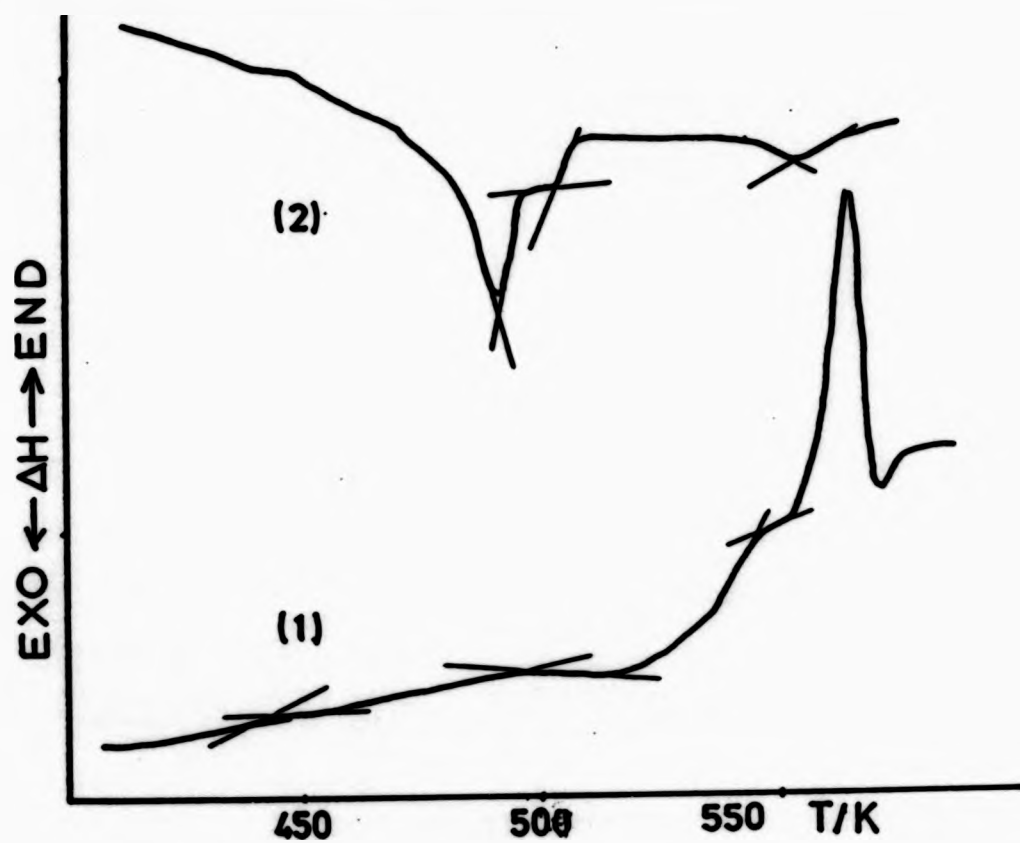


Fig. 10-3 DSC thermograms for polymer STIL-CO
(1) heating scan
(2) cooling scan



Plate 10-V The threaded nematic texture of polymer STIL-CO

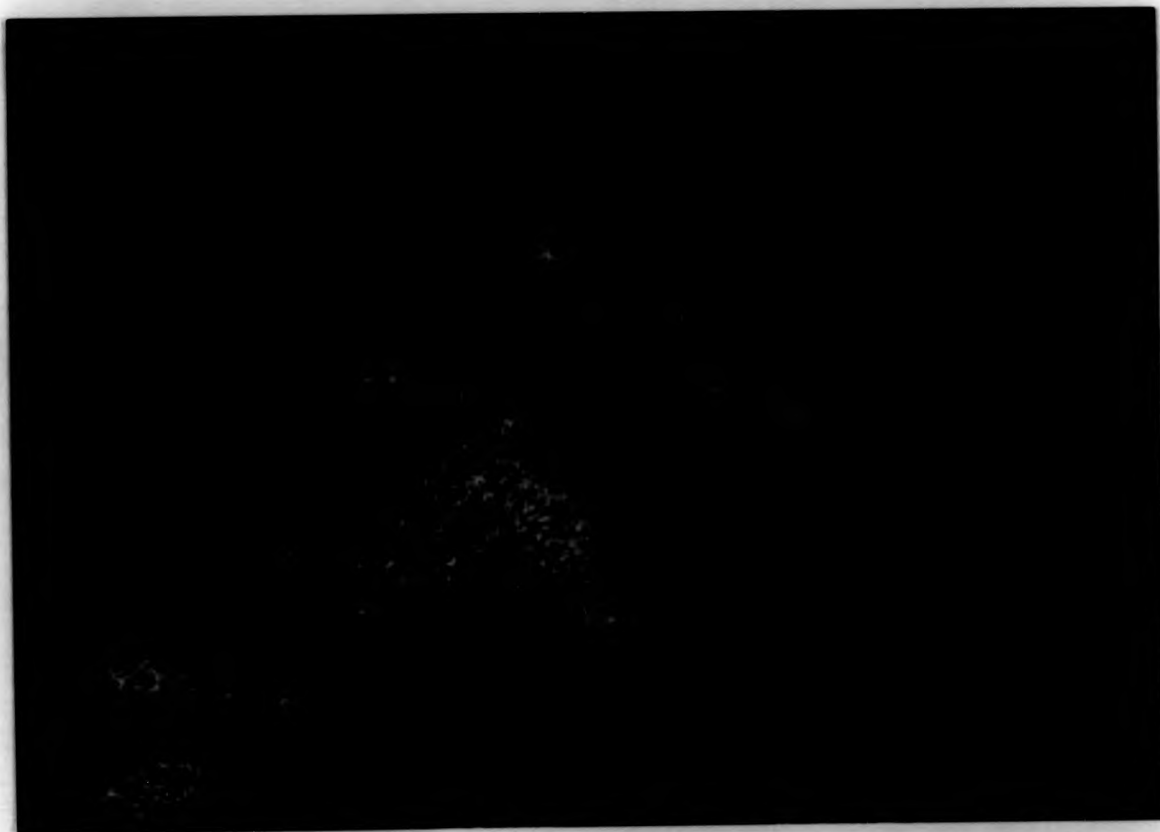


Plate 10-VI The bead-like smectic texture of polymer STIL-CO



Plate 10-V The threaded nematic texture of polymer STIL-CO



Plate 10-VI The bead-like smectic texture of polymer STIL-CO



Plate 10-V The threaded nematic texture of polymer STIL-CO



Plate 10-VI The bead-like smectic texture of polymer STIL-CO

the mesomorphic order is tentatively assigned as:-

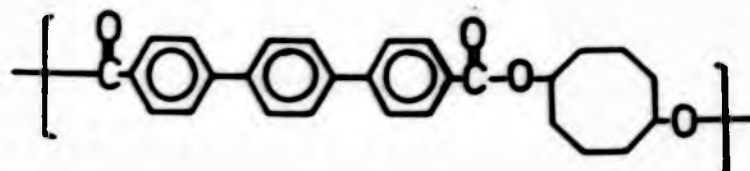
k 495K Sa 540K n 563K i

A polymer with an equivalent linear spacer (-CH₅-) was studied by Meurisse et al. <54>, they concluded that this polymer is liquid crystalline with T_m=458K and T_i=521K but no particular morphological feature was identified.

10.4 Rigid Groups Based on Rings Other than p-Phenylene

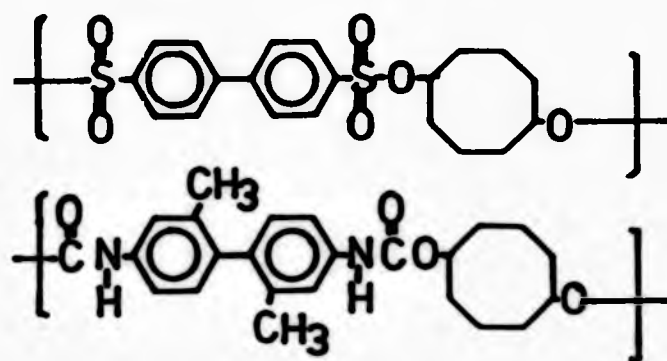
The terphenyl unit is a very rigid, extended mesogenic structure because of the direct linkage between phenylene rings. Meurisse et al. <54> prepared a series of polymers from the p,p'-carboxy terminated terphenyl, and these generally formed smectic mesophases if either an alkylene or a polyoxyethylene spacer was used.

A polymer of the following structure was synthesized:-



This polymer was insoluble in any solvents, and began to decompose at about 680K probably because of the less stable alicyclic unit.

Rigid monomers based on biphenyl like
 4,4'-biphenyl-disulphonyl chloride and
 3,3'-dimethyl-4,4'-biphenyl diisocyanate were also used to
 prepare polymers of the following structures:-



However, both polymers were totally intractable and decomposed at high temperature, thus liquid crystalline behaviour cannot be induced by solvents.

10.5 Comparison of Polymers Containing Different Mesogens

The proportion of cis/trans isomers in the system is not known, although the literature synthetic methods which were followed claimed to give exclusive trans isomer. All the forthcoming discussions have based on the assumption that the rigid linkages are in the trans-state.

Figure 10-4 shows the mesomorphic temperature ranges versus different kinds of mesogens. Accordingly, the order of thermal stabilities is:-



The azo and azoxy polymers which have mesogenic units of the same length as the stilbene unit(13.5A) possess higher melting temperatures. The azoxy polymer(dT=38K) has a wider range of mesophase stability than the azo polymer(dT=31K).

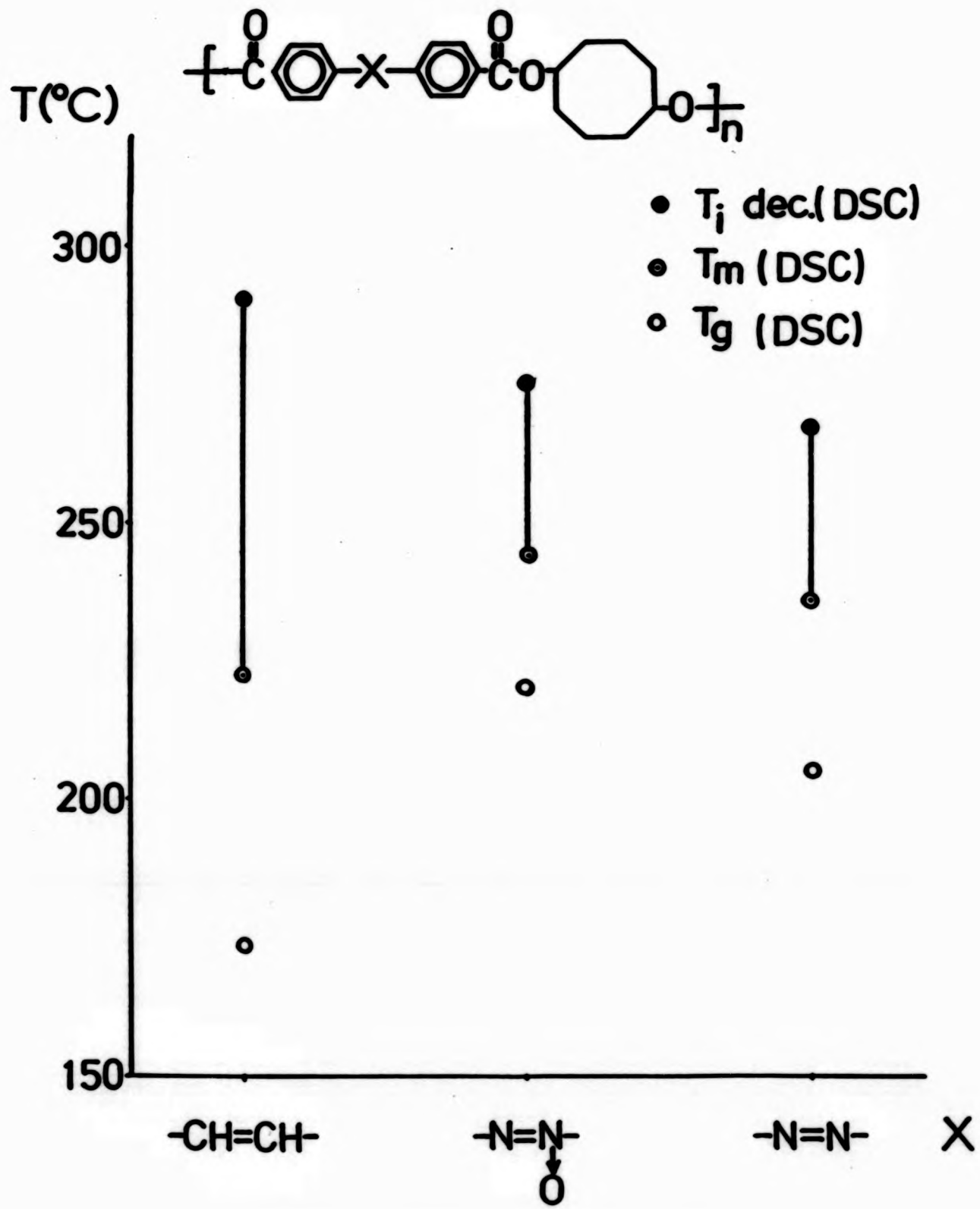


Fig. 10-4 Plots of mesophase range for polymer AZO-CO
 polymer AZOXY-CO and polymer STIL-CO

When the polarities are compared in terms of dipole moment, the almost zero value of azo benzene is very much lower than azoxy benzene(1.57u) <164>. It is probably this difference in the polarities which accounts for the narrower mesophase stability of the azo polymer. The azo group is apparently a less satisfactory rigid link compared with the azoxy group. A semi-rigid spacer like the eight membered ring enhanced the formation of mesophase in both azo and azoxy polymers. Alternatively when the spacer is a pentamethylene unit, only the strongly polarized azoxy polymer exhibits liquid crystalline behaviour. The much broader mesophase stability of polymer STIL-CO(dT=68K) remains unexplained.

These polymers have one thing in common, ie they all exhibit a nematic mesophase, compared with polymer TA-II; which consists of a diad mesogenic unit with approximately the same length(13A), and which shows only a smectic A phase. Although polymer STIL-CO is suspected to have a smectic to nematic transition, no further evidence can be provided at this stage.

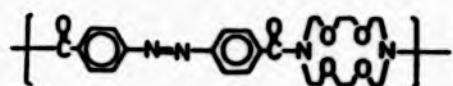
CHAPTER ELEVEN

EFFECT OF RING SIZE

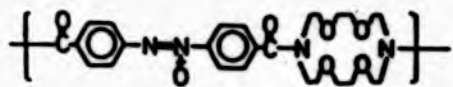
It is now becoming clear that an eight membered ring can be employed either as a spacer as was demonstrated in Chapter Nine or as part of a mesogen as was shown in Chapter Six. Hence the size of the cyclic unit must be a determining factor in the formation of liquid crystalline structure. Results show that the flexibility of the cyclic units is not a linear relation to the size of the ring(see Part Two of this thesis). As the number of atoms in the ring increases above a certain value(say $n=12$?) the cyclic unit can then only act as a spacer.

In this chapter, a large heterocyclic compound viz diaza-18-crown-6-ether(AZA18C) was used as a flexible monomeric unit to copolymerise with well known mesogenic monomers. The properties of these polymers were studied and compared with the corresponding cyclooctyl series. It is well known that crown ethers can chelate with cations, the possibility of tailoring the properties of polymers(eg LC polymers) will be very intriguing.

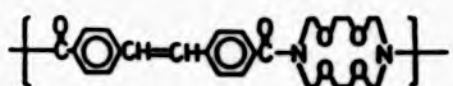
Polymers of the following structures were prepared (only the mesogenic units are shown), and designated according to the composition of the polymer.



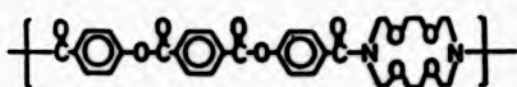
Polymer AZO-AZA18C



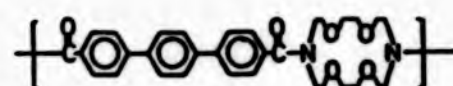
Polymer AZOXY-AZA18C



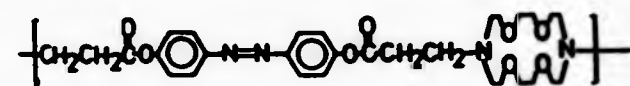
Polymer STIL-AZA18C



Polymer TA-AZA18CHB



Polymer TER-AZA18C



Polymer APDA-AZA18C

11.1 Polymer AZO-AZA18C

The DSC thermograms of polymer AZO-AZA18C are shown in Figure 11-1. For the undoped sample, T_g at 355K and T_m at 490K were obtained (curve 1). Optical studies revealed that for the undoped sample, very weak stir-opalescence was detected at about 350K (Plate 11-I). This texture could only be observed when the virgin sample was heated.

A doped sample was prepared according to the following workup. The sample was first dried in a vacuum oven overnight at 340K and then weighed. The number of cavities (diaz-18-crown-6-ether) was estimated (the weight of the sample divided by the molecular weight of the repeating unit). The sample was then dissolved in about 5ml of chloroform. To this solution was added equivalent amounts of K^+ ion (KSCN in methanol) needed to complex with the crowns. This mixture was allowed to stand at room temperature for four hours. The solvent was then evaporated and the sample dried in a vacuum

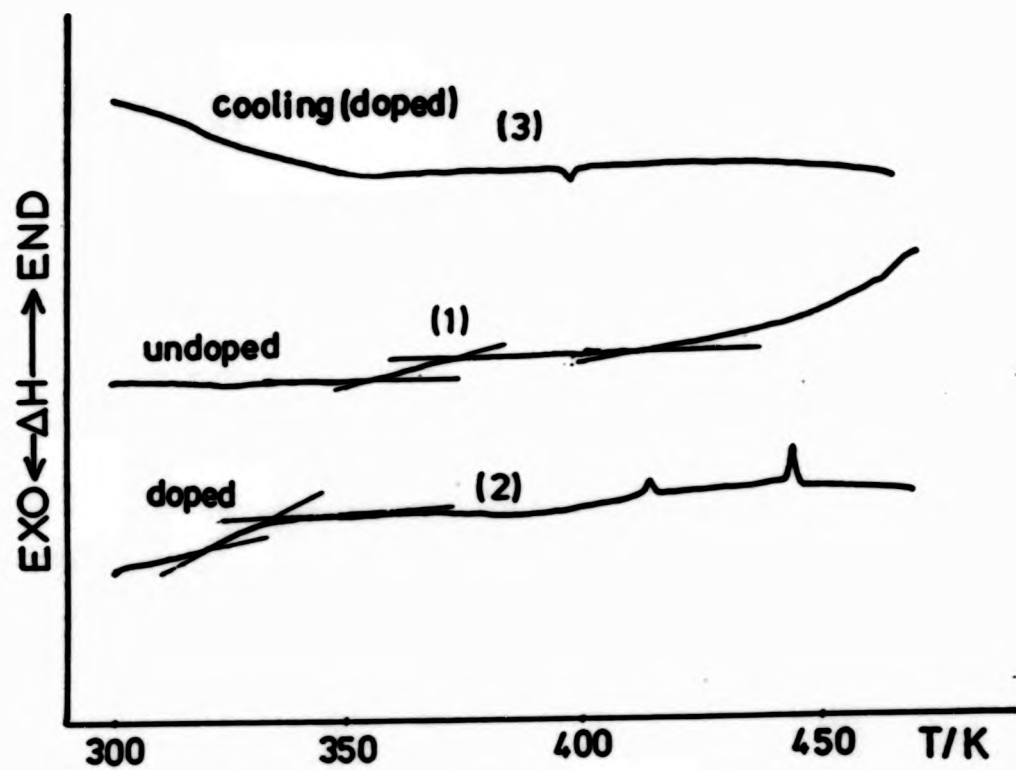


Fig. 11-1 DSC thermograms for polymer AZO-AZA18C
 (1) heating scan for undoped sample
 (2) heating scan for doped sample
 (3) cooling scan for doped sample

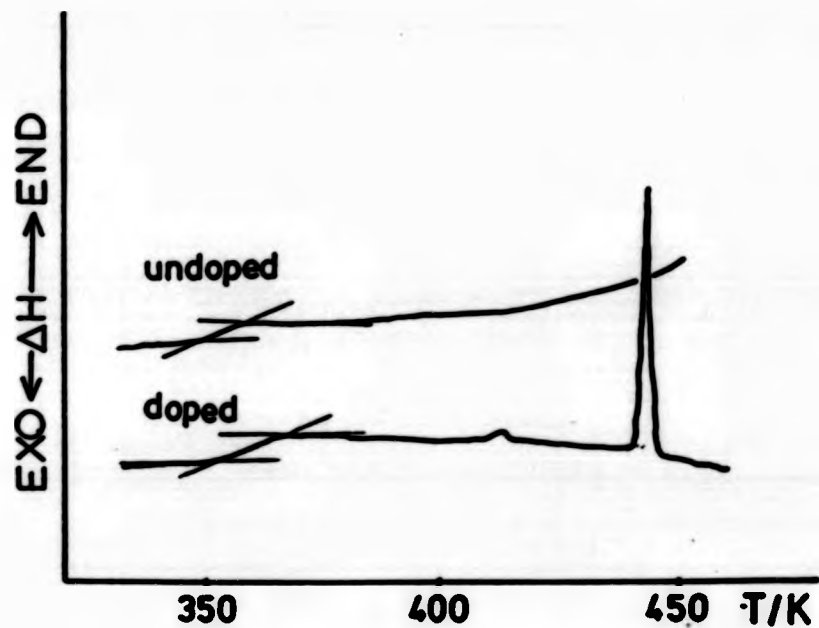


Fig. 11-2 DSC thermograms for polymer AZOXY-CO,
 heating



Plate 11-I Microphotograph shows weak stir-opalescence of polymer AZO-AZA18C at 350K



Plate 11-II Microphotograph shows weak stir-opalescence of polymer AZOXY-AZA18C at 356K



Plate 11-I Microphotograph shows weak stir-opalescence of polymer AZO-AZA18C at 350K



Plate 11-II Microphotograph shows weak stir-opalescence of polymer AZOXY-AZA18C at 356K

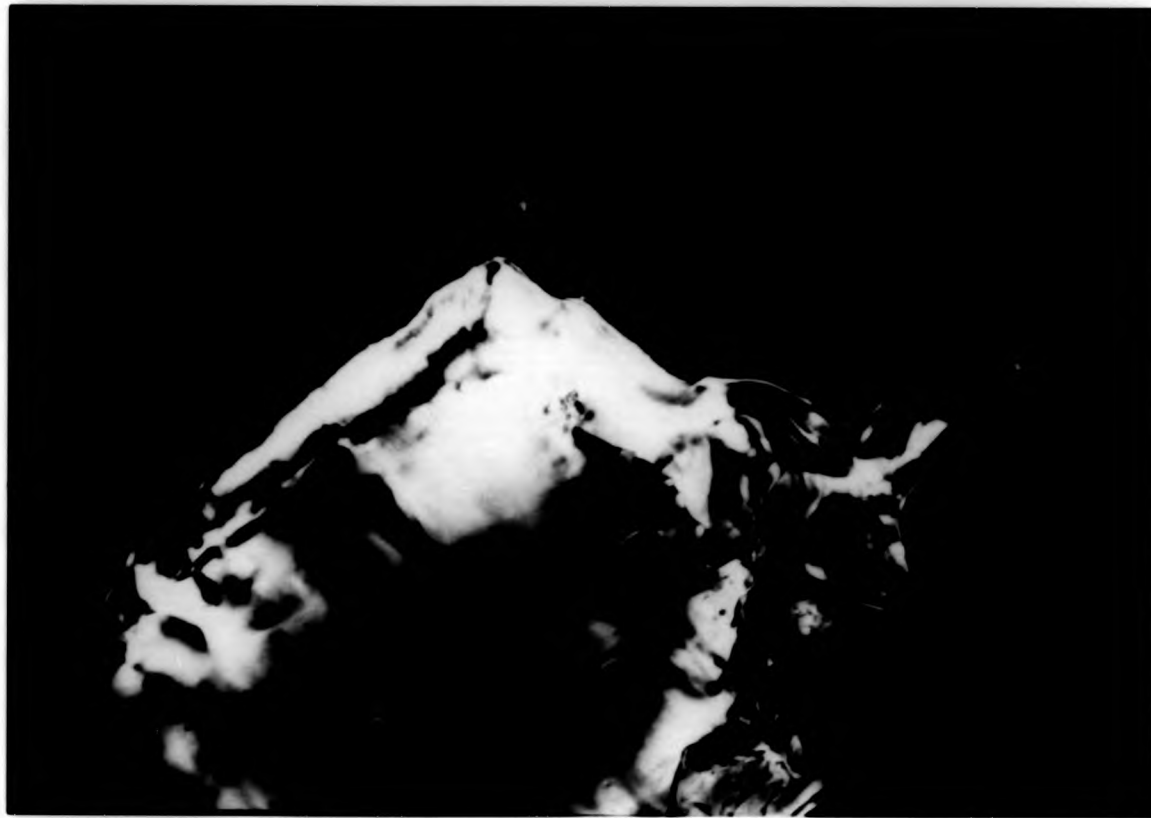


Plate 11-I Microphotograph shows weak stir-opalescence of polymer AZO-AZA18C at 350K



Plate 11-II Microphotograph shows weak stir-opalescence of polymer AZOXY-AZA18C at 356K

oven at room temperature for 48 hours. DSC measurements were carried out immediately after the sample was removed from the oven. Curve 2 (Figure 11-1), depicts the heating scan of the doped sample. A glass transition was clearly shown at 319K together with two other transitions at 414K and 444K. An exotherm at 397K was detected when the sample was cooled (curve 3). When studied under the hot-stage polarising microscope, the sample softened at about 318K and tiny crystallites were observed from this temperature onward till 446K. These crystallites reappeared when the temperature fell below 446K. No obvious birefringence can be observed.

It is interesting that T_g of the doped sample is 36K lower than the undoped sample. This result was not expected as one might think that the presence of cations will stiffen the polymer chains and hence increase T_g . The nature of the transitions at 414K and 444K was uncertain. If the one at 414K is the melting point, it is almost 76K lower compared with the undoped sample. If the polymer and the salt is a homogenous mixture, it should give only one melting point, hence, the transition at 444K is very confusing. The melting point of potassium thiocyanate is 446K, so the transition at 444K is possibly due to the melting of the potassium thiocyanate. As revealed by optical microscope, the crystallites disappeared gradually from 318K onward instead of suddenly vanishing at 446K, this should not happen if the polymer did not complex with the potassium ions. The possible explanation of this strange phenomenon is that only part of the potassium ions complexed with the polymer, the excess potassium ions act as plasticizer, hence, the lowering of both T_g and ' T_m '.

11.2 Polymer AZOXY-AZA18C

The DSC thermograms of polymer AZOXY-AZA18C are depicted in Figure 11-2. The T_g of the undoped sample was at 349K, while for the doped sample, T_g was 355K with two other transitions at 413K and 444K.

There is a slight increase in T_g in the presence of potassium ions. The endotherm at 414K at this stage is quite certain to be the melting point of KSCN, whether the transition at 413K is the real melting point of the doped polymer or actually due to impurities, cannot be answered at this stage.

Plate 11-II shows the texture of the undoped sample at 356K under the crossed polarisers. Again, stir-opalescence can only be observed for the first heating of virgin sample. Crystallites similar to polymer AZO-AZA18C were also observed.

11.3 Polymer STIL-AZA18C

The DSC thermograms of polymer STIL-AZA18C are displayed in Figure 11-3. The T_g of undoped and doped samples were found at 386K and 390K respectively. Two extra exotherms at 413K and 444K were again detected.

Very weak stir-opalescence was observed at 387K (Plate 11-III) for the undoped sample.

11.4 Polymer TA-AZA18CHB

The DSC thermograms of polymer TA-AZA18CHB are shown in Figure 11-4. The T_g of undoped and doped samples were detected at 317K and 352K respectively. No other transitions were

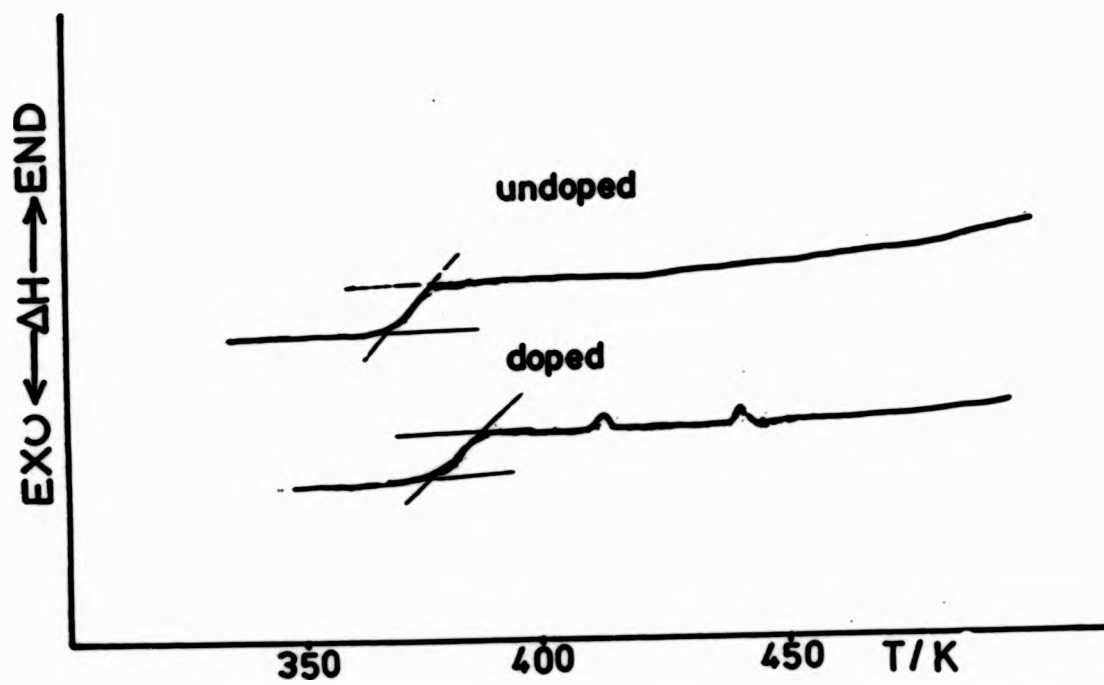


Fig. 11-3 DSC thermograms for polymer STIL-AZA18C, heating

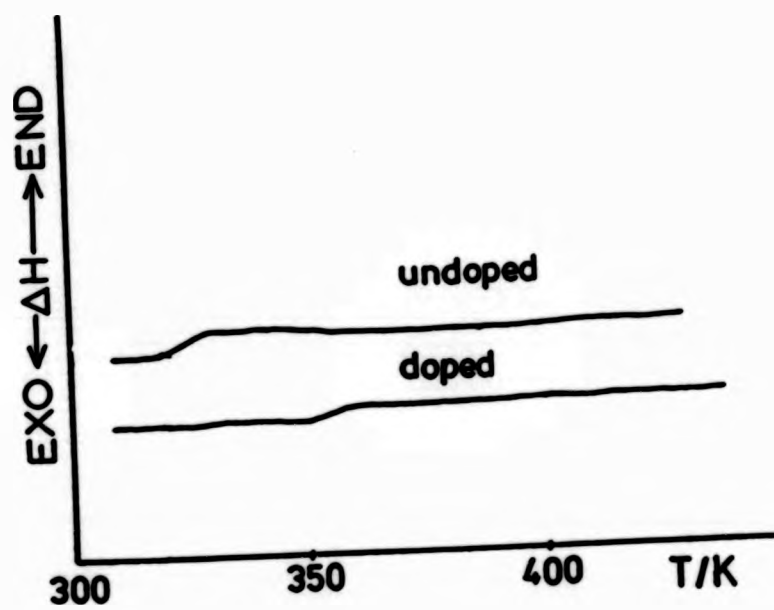


Fig. 11-4 DSC thermograms for polymer TA-AZA18CHB, heating

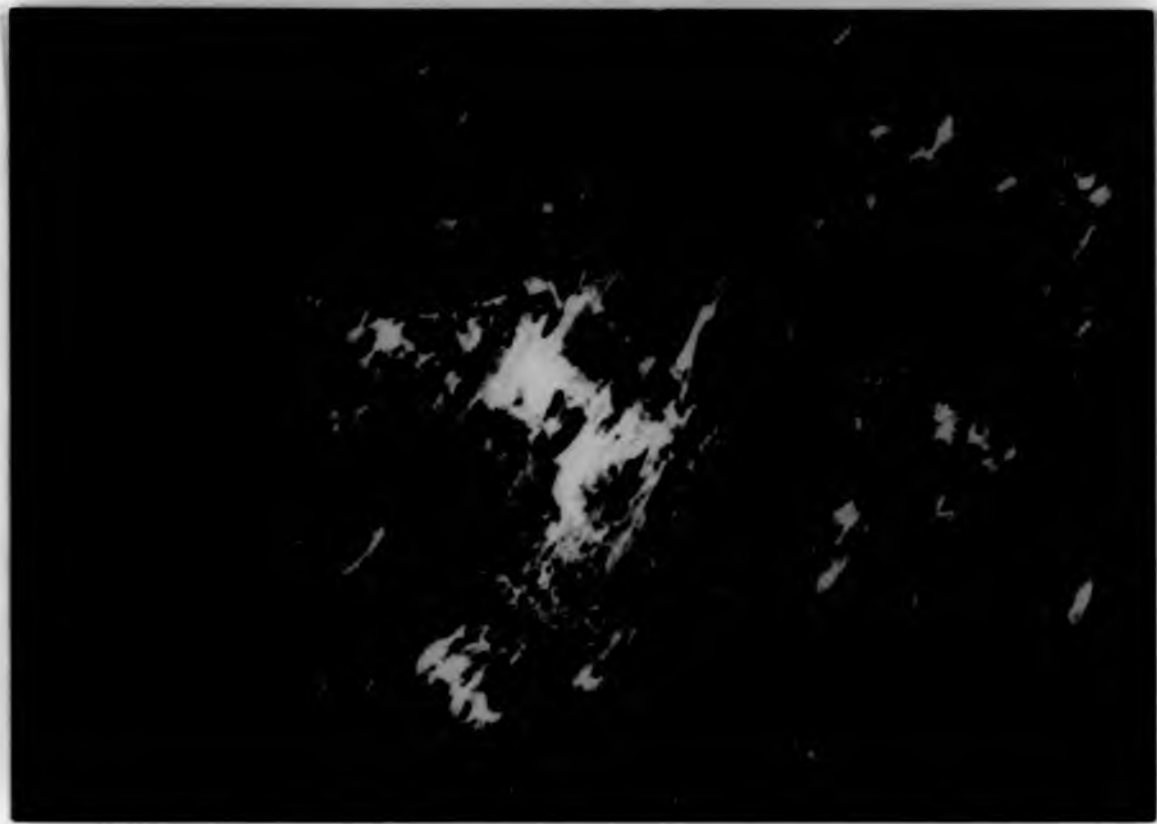


Plate 11-III Microphotograph shows weak stir-opalescence of
polymer STIL-AZA18C at 387K



Plate 11-IV Microphotograph shows weak stir-opalescence of
polymer TA-AZA18CHB at 320K

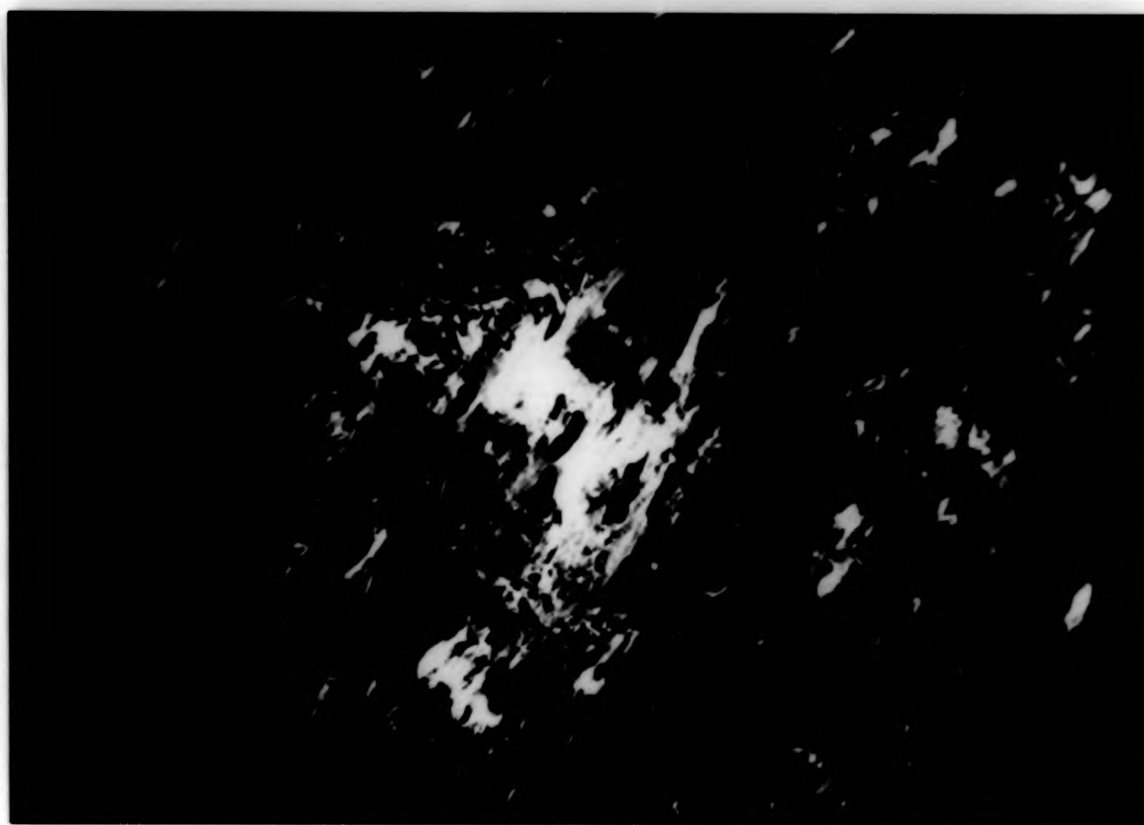


Plate 11-III Microphotograph shows weak stir-opalescence of polymer STIL-AZA18C at 387K

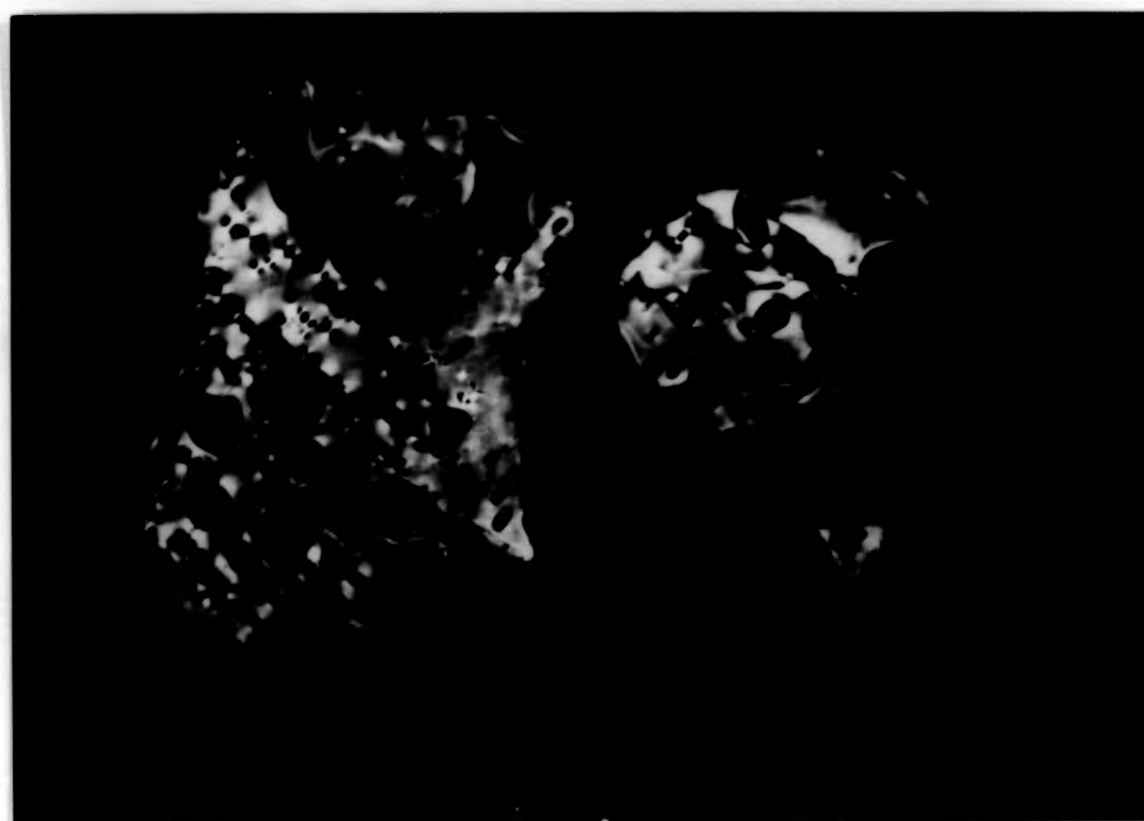


Plate 11-IV Microphotograph shows weak stir-opalescence of polymer TA-AZA18CHB at 320K

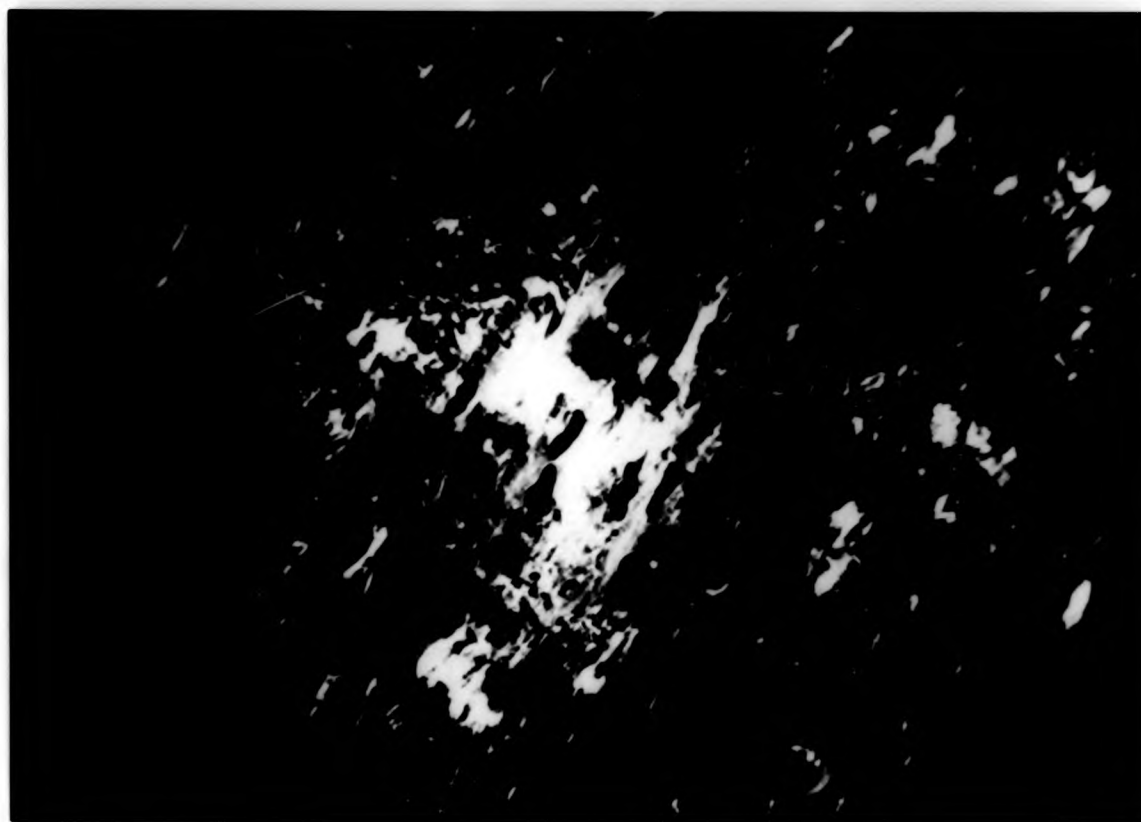


Plate 11-III Microphotograph shows weak stir-opalescence of polymer STIL-AZA18C at 387K

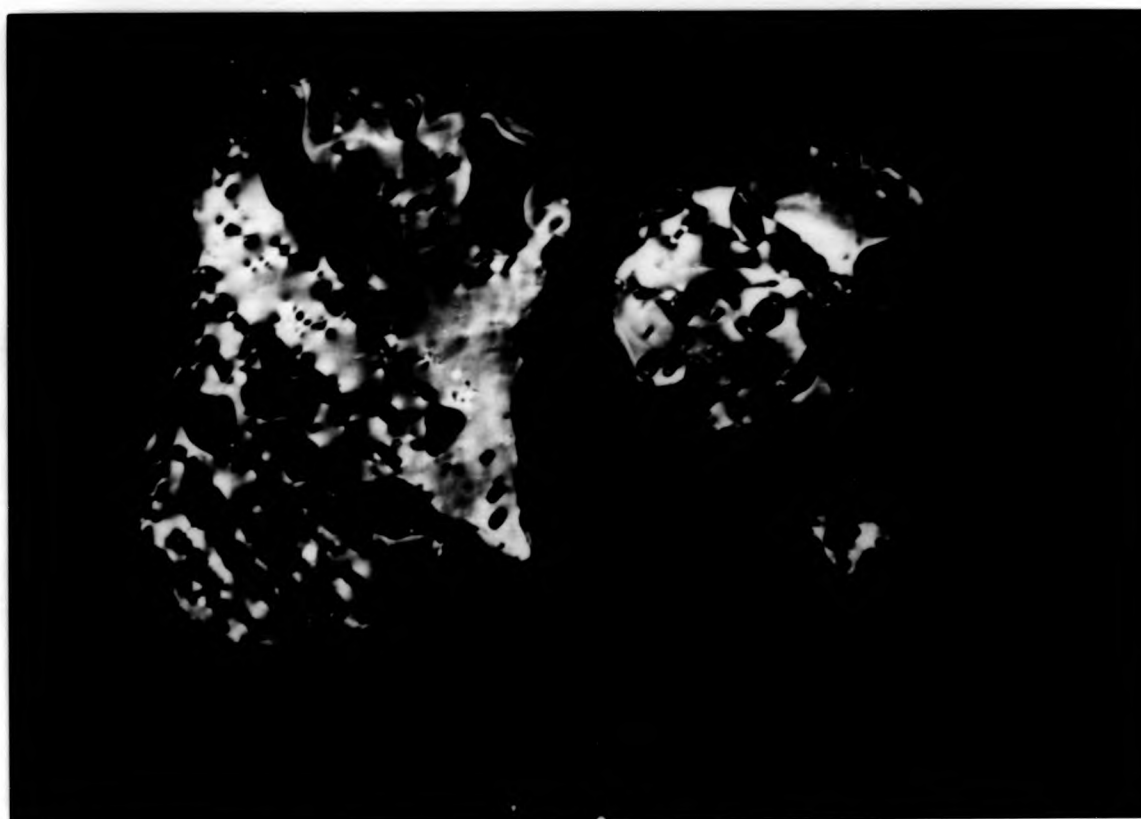


Plate 11-IV Microphotograph shows weak stir-opalescence of polymer TA-AZA18CHB at 320K

detected with the doped sample. A texture reminiscent of LC compounds was observed at 320K(Plate 11-IV).

11.5 Polymer TER-AZA18C

Up to this stage, it seems that the aza-18-crown-6-ether moiety is such a good flexible unit that it is not only able to lower the transition temperatures substantially but also impairs the liquid crystalline properties. Bear in mind, all the mesogenic monomers used in these studies exhibited LC behaviour with the eight membered ring. One would like to find out the effect of this eighteen membered ring spacer with very strong mesogens like the terphenyl unit.

Figure 11-5 depicts the DSC thermograms of polymer TER-AZA18C. The transitions at 510K and 538K were assigned as T_m and T_i respectively from the first heating scan(curve 1), while T_g was found at 407K according to the second heating scan(curve 2). Optical studies revealed that this polymer exhibits a highly homeotropic texture, and there was strong cohesion between the polymer and the glass cover slips which made shearing extremely difficult. Plate 11-V displays the texture observed at 543K by squeezing one cover slip over the other. The strong cohesion between the polymer and the glass surface may be attributed to the polar oxygen atoms in the aza-crown-ether. The mesophase of this polymer cannot be identified although it looks very similar to those observed in polymer AZO-AZA18C and polymer AZOXY-AZA18C. If this is a true LC polymer, then it is a unique thermotropic polyamide as far as the existing literature is concerned.

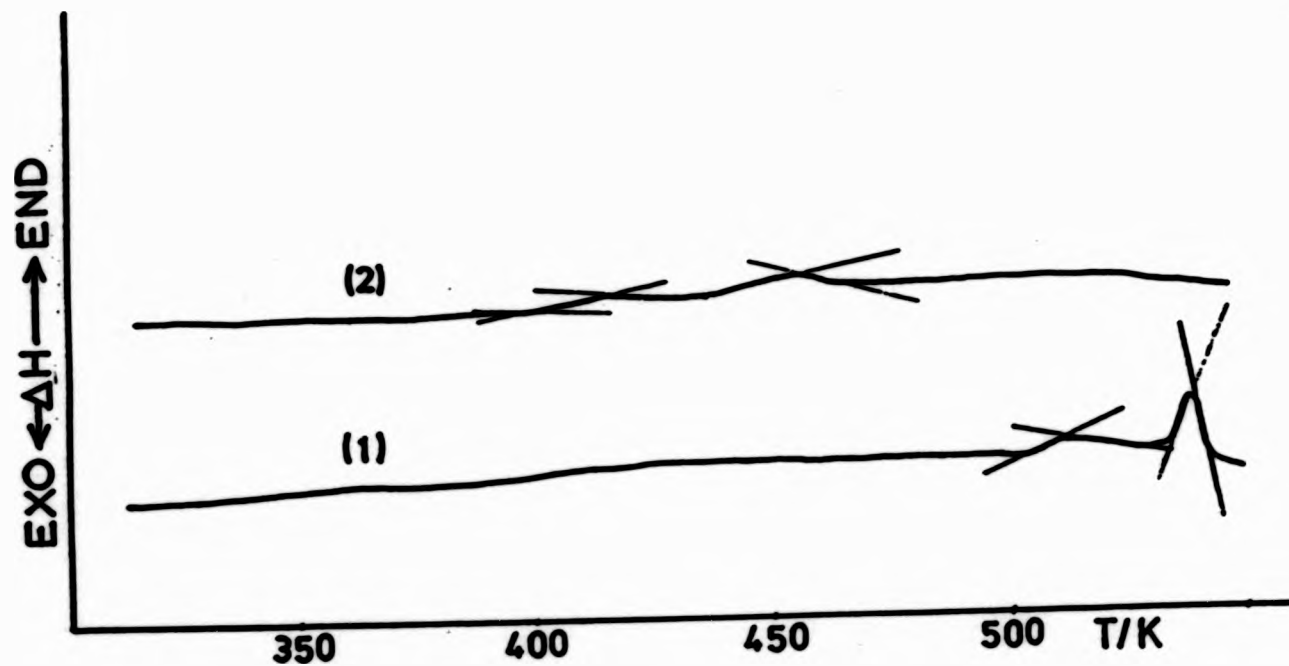


Fig. 11-5 DSC thermograms for polymer TER-AZA18C
 (1) 1st heating scan
 (2) 2nd heating scan

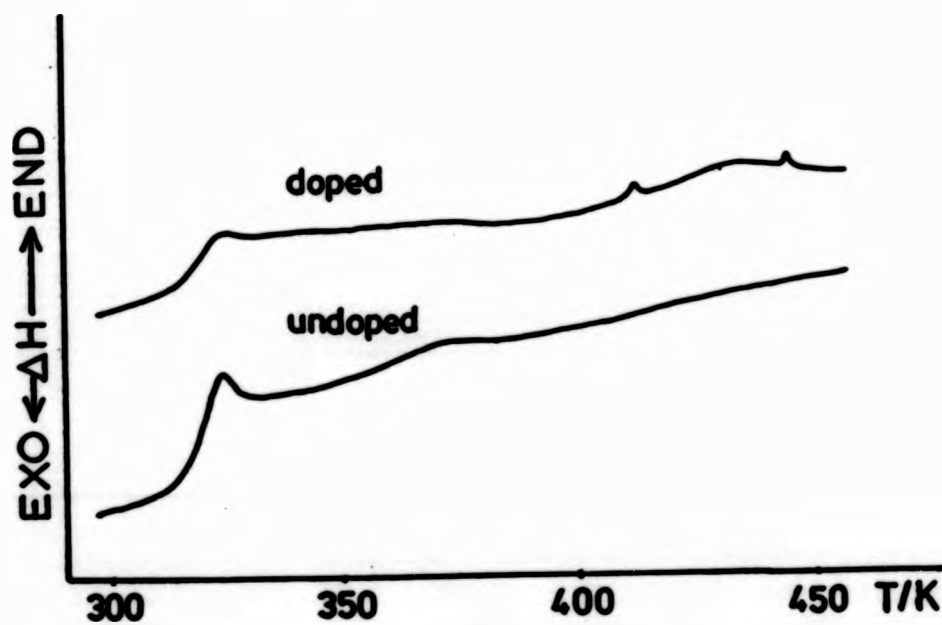


Fig. 11-6 DSC thermograms for polymer APDA-AZA18C,
 heating



Plate 11-V The texture observed when polymer TER-AZA18C
was squeezed between two cover slips at 543K



Plate 11-V The texture observed when polymer TER-AZA18C
was squeezed between two cover slips at 543K

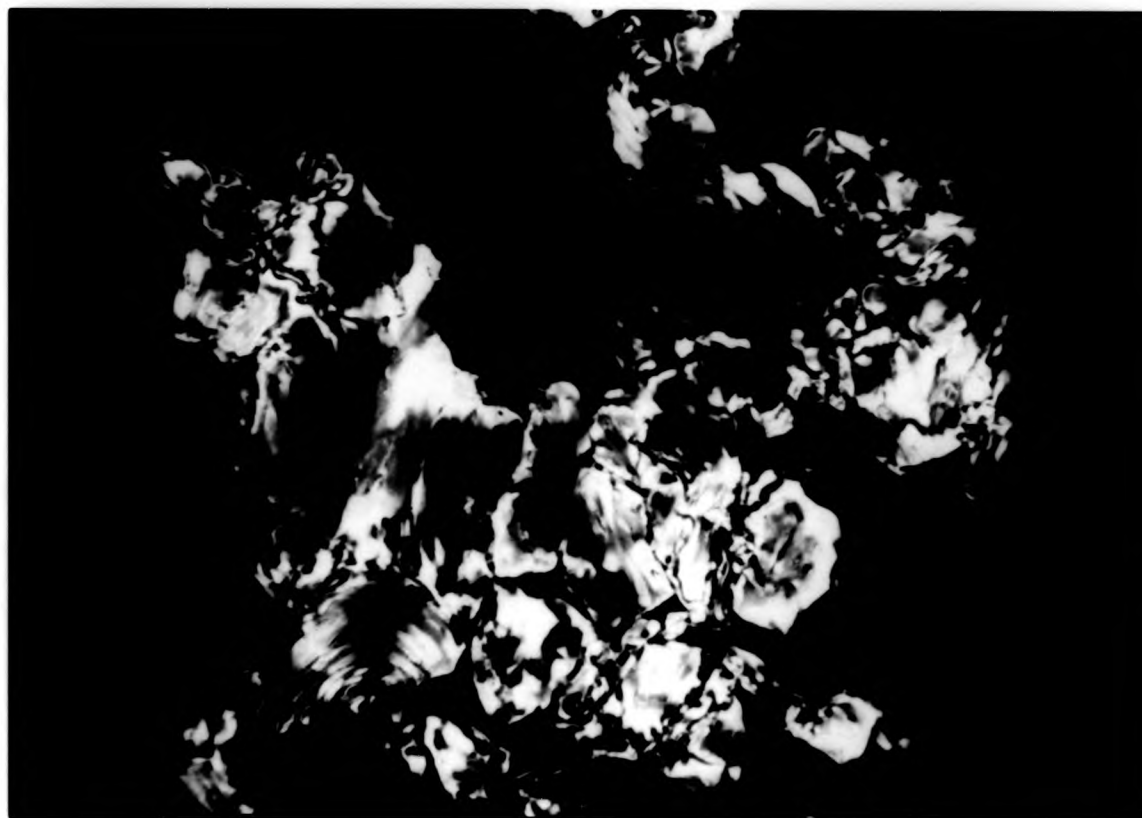


Plate 11-V The texture observed when polymer TER-AZA18C
was squeezed between two cover slips at 543K

11.6 Polymer APDA-AZA18C

Chiellini and coworkers^[165,166] prepared several series of poly(β -aminoester)s containing different mesogenic groups. The diamines employed included piperazine, 2-methylpiperazine and N,N'-Dimethylethylenediamine. Both nematic and smectic mesophases were reported.

Polymer APDA-AZA18C was synthesised based on the above hypothesis. However, the result was most disappointing in that the liquid crystalline behaviour of the monomer(APDA) was entirely destroyed.

Figure 11-6 shows the DSC thermograms. The T_{gs} of the doped and undoped samples were found at 316K and 315K respectively. Two endotherms were observed in the other doped polymers at 413K and 444K.

CHAPTER TWELVE

CONCLUSION

The feasibility of incorporating an eight membered ring into the backbone of polymers which possess liquid crystalline properties has been demonstrated in the preceding chapters. The following conclusion can now be drawn:-

(1) Effect of spacers

Aliphatic acids $\langle \text{HO-CO-(CH}_2\text{)}_n\text{-CO-OH} \rangle$ with values of n from 3 to 10 were copolymerised with monomer COHB. Dependent on the spacer length, polymers can exhibit different liquid crystal textures. Polymers with $n=3, 4$ and 10 were identified as smectic while the rest are all nematic. The odd-even effect was also observed in this series. The LC transitions of these polymers ranged from 343K to 413K, this could possibly be the only family of thermotropic LC polyesters possessing such a low transition temperature range.

(2) Effect of substituents

For industrially useful polymers, the ideal LC transition range is between 473K to 623K, hence, rigid units are used preferentially instead of flexible linear spacers. Substituents of different polarity and bulkiness attached to terephthalic acid were employed. Results show that the bromo and nitro substituted polymers exhibited LC transitions between 453K to 493K. These polymers are fibre forming based on preliminary studies.

(3) Effect of copolymerisation

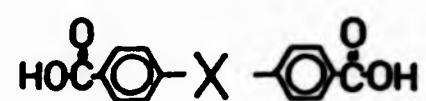
An optically active monomer was used for two reasons:-

(i) the LC transition can be lowered because of the copolymerisation effect and (ii) to obtain cholesteric texture (the texture which provides colours). It has been found that it is possible to freeze the cholesteric texture into the

glassy state. Results show that self-coloured polymers can be made without using any pigments or dyestuffs. In the light of decorative coating materials, this might be an interesting aspect.

(4) Effect of mesogens

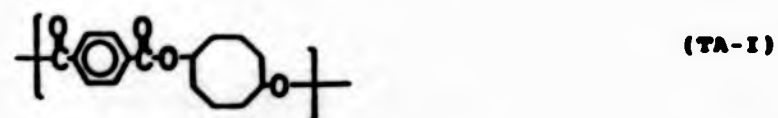
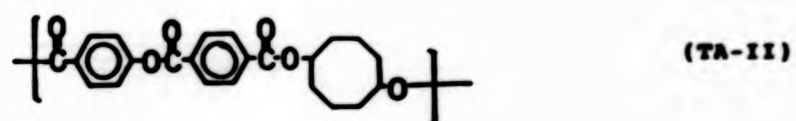
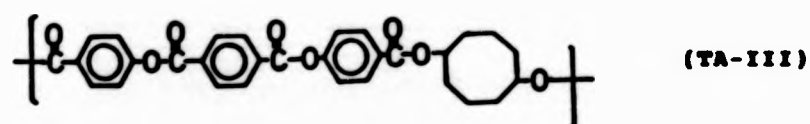
A lot of LC polymer research began with mesogenic monomers, it has been shown that not every mesogenic monomer (eg HO-CO-Ar-X-Ar-CO-OH) forms an LC polymer when linear spacers are used. As a result, several mesogens were synthesized, they are of the following structures:-



where X= N=N, N=NO, CH=CH and Ar. With the eight membered ring, they all exhibit LC properties with mesomorphic transitions ranging from 473K to 623K. All polymers are nematic.

(5) Effect of mesogenic unit length

Polymers possess LC properties because of the rigid units, the shortest employed so far is the biphenyl unit. Rigid blocks based on aromatic ester of the following structures were prepared:



Depending on the mesogenic unit length, not only different LC transition ranges but also different textures were obtained. The polymer incorporating the triad ester exhibited a nematic phase while the diad and terephthalic acid gave smectic modifications.

(6) Effect of ring size

The 8 membered ring was replaced by an 18 membered ring (diaz-18-crown-6-ether) to see if it was possible to tailor the LC properties by making use of the cation complexing ability of the crown ether. Preliminary results show that crown ether unit may be too flexible and indeed destroy the LC behaviour if a weak mesogen is used.

FUTURE WORK

The feasibility of incorporating an eight membered ring into the backbone of polymers which possess liquid crystalline properties has already been demonstrated. The task of the preliminary studies was to concentrate on synthesis and characterisation of LC mesophases. However, much more work still needs to be done in this area.

Although, in the text, most of the mesophases had been identified, X-ray diffraction remains of prime importance in determining the microstructures. Also, the molecular weight and the number of end groups play a decisive role. The ultimate use of mainchain thermotropic LC polymers is to produce high modulus fibres, hence, one should also look at the mechanical properties and the feasibility of melt spinning.

The quenching of cholesteric polymers into the glassy state

is very intriguing, published work is still very limited and deals mainly with synthesis. The relation between pitch length and the composition of copolymers is worth studying. Only one kind of spacer was employed in this study, the utilisation of other spacers like oxyethylenes, siloxanes, ether terminated aliphatics and/or large cyclalkyl rings should not however be overlooked.

As has already been demonstrated with the eight membered ring, it is possible to lower the LC transition to room temperature. Therefore, the ionic conductivity of LC polymers with oxyethylene spacers in the mesomorphic transition could be of tremendous interest.

The strength of mainchain LC polymers is only uniaxial, if one can crosslink these polymers, the advantages of inducing three dimensional stability are immense.

Finally, if one considers the eight membered ring with appropriate rigid units as a mesogen, then future research work should also cover sidechain LC polymers.

REFERENCES

1. F.Reinitzer, Monatshefte 9,421(1888).
2. E.A.Poe, 'The Narrative of A.Gordon Pym of Nantucket' p706 (Doubleday & Co. Inc., Garden City, N.Y., 1966).
3. O.Lehmann, Z.Phys.Chem. Leipzig 4,462(1889).
4. F.Reinitzer, Ann. Physik 27,213(1908).
5. L.Gattermann and A.Ritschke, Ber. 23,1738(1890).
6. L.Gattermann, Liebigs Ann.Chem. 347,347(1906).
7. L.Gattermann, Liebigs Ann,Chem. 357,313(1908).
8. D.Vorlander and H.Hauswaldt, Abh. d. Kaiserl. Leop. Carol. Dtsch. Akad. d. Naturf. 90,107(1909).
9. R.Schenck, Habilitationsschrift, Marburg, (1897).
10. G.Friedel, Ann.Physique 18,273(1922).
11. S.Chandrasekhar, B.K.Sadashiva and K.A.Suresh, Pramana 9: 471(1977).
12. S.Chandrasekhar, Philos.Trans.R.Soc. London A:309,93(1983).
13. N.H.Tinh, C.Destrade and G.Gasparoux, Phys.Lett. 72A,251(1979).
14. C.Destrade, N.H.Tinh, G.Gasparoux, J.Malthele and A.M.Levelut, Mol.Cryst.Liq.Cryst. 71,111(1981).
15. D.Vorlander, Chemische Kristallographic der Flussigkeiten, (Akad. Verlag-gas: Leipzig) p90, (1924).
16. C.Wiegand and E.Merkel, Z. Naturforsch 3B,313(1948).
17. G.W.Gray, 'Molecular Structure and the properties of Liquid Crystals' p314 (Acad.Press London, 1962)
18. D.Vorlander, Z.Physik.Chem. 105,211(1923).

19. J.A.Castellano, 'Liquid Crystals: The Fourth State of Matter' Ch.12, p439 Ed. by F.D.Saeva (Marcel Dekker, N.Y., 1979).
20. F.C.Bawden and N.W.Pirie, Proc.R.Soc. London SerB, 123,274,(1937).
21. D.G.H.Ballard (Courtaulds Ltd), British Patent 864,962(1958); U.S.Patent 3,121,766(1961).
22. A.Elliott and E.J.Ambrase, Faraday Diss. Chem.Soc. 9,246(1950).
23. C.Robinson, Trans. Faraday Soc. 52,571(1956).
24. C.Robinson and J.C.Ward, Nature (London) 180,1183(1957).
25. C.Robinson, J.C.Ward and R.B.Beevers, Faraday Diss. Chem.Soc. 25,29(1958).
26. C.Robinson, Tetrahedron 13,219(1961).
27. C.Robinson, Mol.Cryst. 1,467(1966).
28. A.Blumstein and E.C.Hsu in 'Liquid Crystalline Order in Polymers' Ch.3, p105, Ed.by A.Blumstein (Acad.Press, N.Y.,1978).
29. Wm.J.Toth, Ph.D Thesis (Princeton University 1971).
30. H.Finklemann and G.Rehage, Adv.Poly.Sci. 60,99(1984).
31. H.Ringsdorf and H.W.Schmidt, Makro.Chem. 185,1327(1984).
32. G.R.Meredith, J.Van Dusan and D.J.Williams, Macromolecules 15,1385(1982).
33. R.Buschl, T.Folda and H.Ringsdorf, Adv.Polym.Sci. 64,1(1985).
34. H.Schupp, B.Hupter, R.A.Van Wagener, J.D.Andracle and H.Ringsdorf, Colloid Polym.Sci. 260,262(1982).

35. W.Kreuder and H.Ringsdorf, Makro.Chem.Rapid Commun. 4,807(1983).
36. A.Skoulios, Adv.Liq.Cryst. 1,169(1975).
37. Y.Matsushita, K.Yamada, H.Hattori, T.Fujimoto, Y.Swada, M.Nagasawa and C.Matsui, Macromolecules 16,19(1983).
38. E.T.Samulski, Physics Today 35,40(1982).
39. E.T.Samulski, 'Liquid Crystalline Order in Polymers' Ch.5,p167 Ed. by A.Blumstein(Acad.Press., N.Y., 1978).
40. J.Hermans Jr., J.Colloid.Sci. 17,638(1962).
41. I.Goodman, J.E.McIntype and J.W.Stimpson(I.C.I. Ltd), British Patent 989,552(1962).
42. S.L.Kwolek(Du Pont), British Patent 1,198,081(1966).
43. S.L.Kwolek(Du Pont), British Patent 1,283,064(1968).
44. M.G.Dobb and J.E.McIntype, Adv.Polym.Sci 60,63(1984).
45. XYDAR (Dartco Mfg.Co.), Mod. Plastics 61,14(1984).
46. G.W.Gray and P.A.Winsor 'Liquid Crystals and Plastic Crystals' Vol 1,
(Ellis Horwood Chichester England, 1974).
47. A.Roviello and A.Sirigu, J.Polym.Sci. Poly.Lett.Ed. 13,455(1975).
48. D.Demus and R.Richter, 'Texture of Liquid Crystals' Springer Verlag Chemie. Weinheim(1978).
49. H.Kelker and R.Hatz 'Handbook of Liquid Crystals', Verlag Chemie Weinheim 1980.
50. G.R.Luckhurst and G.W.Gray, 'The Molecular Physics of Liquid Crystals' (Acad.Press., N.Y., 1979).
51. N.H.Hartshorne, 'The Microscopy of Liquid Crystals' Microscopic Publication Ltd. London, 1974.

52. C.Noel, F.Laupretre, C.Friedrich, B.Fayolle and L.Bosio, *Polymer* 25,808(1984).
53. C.Noel and J.Billard, *Mol.Cryst.Liq.Cryst.* 41,269(1978).
54. P.Meurisse, C.Noel, L.Monnerie and B.Fayolle, *British Polymer J.* 13,55(1981).
55. L.Strzelecki and D.Van Luyen, *Eur.Poly.J.* 16,299(1980).
56. L.Strzelecki and L.Liebert, *Eur.Poly.J.* 17,1271(1981).
57. S.Antoun, R.W.Lenz and J.I.Jin, *J.Polym.Sci. Poly.Chem.Ed.* 19,1901(1981).
58. A.Blumstein, S.Vilasagar, S.Ponrathnam, B.Clough and R.B.Blumstein, *J.Polym.Sci. Poly.Phys.Ed.* 20,877(1982).
59. B.Millaud, A.Thierry, C.Strazielle and A.Skoulios, *Mol.Cryst.Liq.Cryst.* 49,299(1979).
60. B.Fayolle, C.Noel and J.Billard, *J.de Physique* C3:40,485(1979).
61. B.W.Jo, J.I.Jin and R.W.Lenz, *Eur.Polym.J.* 18,233(1982).
62. C.Noel, J.Billard, L.Bosio, C.Friedrich, F.Laupretre and C.Strazielle, *Polymer* 25,263(1984).
63. W.R.Krigbaum, A.Ciferri, J.Asrar, H.Toriumi and J.Preston, *Mol.Cryst.Liq.Cryst.* 76,79(1981).
64. C.Viney and A.H.Windle, *J.Mater.Sci.* 17,2661(1982).
65. M.R.Mackley, F.Pinaud and G.Siekman, *Polymer* 22,437(1981).
66. H.Sackmann and D.Demus, *Mol.Cryst.Liq.Cryst.* 21,239(1973).

67. H.Sackmann and D.Demus, *Fortschr.Chem.Forsch.*
12,349(1969).
68. G.Galli, E.Chiellini, C.K.Ober and R.W.Lenz,
Makro.Chem. 183,2693(1982).
69. L.Bosio, C.Friedrich, Flaupretre, C.Noel and J.Virlel
Preprint, *Macro. IUPAC(Amhert)* 804(1982).
70. H.Finkleman in 'Polymer Liquid Crystals' Ed.
A.Cifferri, W.R.Krigbaum and R.B.Meyer
(*Acad.Press.*, N.Y., 1982)
71. R.W.Lenz and J.I.Jin, *Macromolecules* 14,1405(1981).
72. R.V.Talroze, S.G.Kostromin, V.P.Shibaev and N.A.Plate
Makro.Chem.Rapid Commun. 2,305(1981).
73. D.Coats and G.W.Gray, *Microscopy* 24,117(1976).
74. D.Demus, *Krist.Tech.* 10,933(1975).
75. D.Van Luyen, L.Liebert and L.Strzelecki, *Eur.Polym.J.*
16,307(1980).
76. H.Finkleman, J.Koldehoff and H.Ringsdorf,
(a) *Angew.Chem.* 90,992(1978)
(b) *Angew.Chem.* 17,935(1978).
77. H.Finkleman and G.Rehage, *Makro.Chem.Rapid Commun.*
1,733(1980).
78. J.Grebowicz and B.Wunderlich, *J.Polym.Sci.*
Poly.Phys.Ed. 21,141(1983).
79. J.Grebowicz and B.Wunderlich, *Mol.Cryst.Liq.Cryst.*
76,287(1981).
80. A.C.Griffin and S.J.Havens, *J.Polym.Sci. Poly.Phy.Ed.*
19,951(1981).
81. A.Blumstein and O.Thomas, *Macromolecules*
15,1264(1982).

82. J.I.Jin, S.Antoun, C.Ober and R.W.Lenz, *British Polymer Journal* 12,132(1980).
83. L.V.Azaroff, *Mol.Cryst.Liq.Cryst.* 60,73(1980).
84. A.DeVries, *Mol.Cryst.Liq.Cryst.* 10,31(1970).
85. A.C.Griffin and S.J.Havens, *J.Polym.Sci. Poly.Lett.Ed.* 18,259(1980).
86. E.S.Watson, M.J.O'Neill, J.Justin and N.Brenner, *Anal.Chem.* 36,1233(1964).
87. M.J.O'Neill, *Anal.Chem.* 36,1238(1964).
88. W.H.Wendlaut, 'Handbook of Commerical Scientific Instruements' Vol 2, (Dekker, N.Y., 1974).
89. Perkin-Elmer DSC-2, Instruction Mannel, (Perkin-Elmer Coporation Norwalk Conn. USA).
90. H.E.Bigelow, *Org.Synth. Coll.* Vol 3, p103(1963).
91. H.E.Bigelow, *Org.Synth. Coll.* Vol 2, p57(1962).
92. W.G.Toland, J.B Wilkes and F.J. Brutschy, *J.A.C.S.* 75,2263(1953).
93. T.W.Campell, *J.A.C.S.* 82,4126(1960).
94. N.J.Leonard and J.W. Curry, *J.Org.Chem.* 17,1071(1952).
95. M.Laus, *Makro.Chem.Rapid Commun.* 4,682(1983).
96. H.W.Hasslin, *Makro.Chem.* 181,301(1980).
97. H.Zahn, *Makro.Chem.* 29,70(1959).
98. C.Ober, R.W.Lenz, G.Galli and E.Chiellini, *Macromolecules* 16,1034(1983).
99. C.Ober and R.W.Lenz, *Polymer Journal* 14,9(1982).
100. P.G.deGennes, *C.R.Acad.Sci. Paris Ser.B*:281,101(1975).
101. R.W.Lenz, J.I.Jin, K.Feichtinger, *Polymer* 24,327(1983).
102. S.Fakirov, E.W.Fischer, R.Hoffmann and G.F.Schmidt *Polymer* 18,1121(1977).

103. A.C.Griffin and S.J.Havens, *J.Polym.Sci. Poly.Phys.Ed.* 19,951(1981).
104. D.Braun, U.Schulke, *Makro.Chem.* 187,1145(1986).
105. H. Arnold, H.Sackmann, *Z.Phys.Chem.(Leipzig)* 213,145(1960).
106. L.Richter, D.Demus and H.Sackmann, *J.Phys. Paris* 37:C-3,41(1976).
107. J.Watanabe and W.R.Krigbaum, *Macromolecules* 17,2288(1984).
108. J.I.Jin, E.J.Choi and K.Y.Lee, *Polymer Journal* 18,99(1986).
109. W.R.Krigbaum, J.Watanabe and T.Ishikawa, *Macromolecules* 16,1271(1983).
110. A.H.Al-Dujaili, A.D.Jenkins and D.R.W.Walton, *J.Polym.Sci. Poly.Chem.Ed* 22,3129(1984).
111. R.C.Roberts, *Polymer* 10,117(1969).
112. T.D.Shaffer and V.Percec, *J.Polym.Sci. Poly.Chem.Ed.* 24,451(1986).
113. T.D.Shaffer and V.Percec, *Poly.Bull.* 14,367(1985).
114. V.P.Shibaev and N.A.Plate, *Adv.Poly.Sci. Vol 60/61* (Springer Verlag Berlin, 1984). Ed. by M.Gordon.
115. Y.Ozcayir and A.Blumstein, *J.Polym.Sci. Poly.Chem.Ed.* 24,1217(1986).
116. G.W.Gray and P.A.Winsor 'Liquid Crystals and Plastic Crystals' Vol 2, (Ellis Horwood Chichester England, 1974).
117. J.Asrar, H.Toriumi, J. Watanabe, W.R.Krigbaum and A.Ciferri, *J.Polym.Sci. Poly.Phys.Ed.* 21,1119(1983).
118. F.C.Frank, *Faraday Diss. Chem.Soc.* 25,19(1958).

119. O.Lehmann, Ann Physik 2,649(1900).
120. C.W.Oseen, Trans. Faraday Soc. 29,883(1933).
121. J.Nehring and A.Saupe, J.Chem.Soc. Faraday Trans-2 68,1,(1972).
122. G.W.Gray and J.W.G.Goodby, 'Smectic Liquid Crystals' (Leonard Hill, London, 1984).
123. B.Millaud, A.Thierry and A.Skoulios, J. de Physique 39,1109(1978).
124. A.Ciferri, W.R.Krigbaum and R.Meyer Ed. 'Polymer Liquid Crystals' (acad.Press, N.Y.,1982).
125. H.J.Lader and W.R.Krigbaum, J.Polym.Sci. Poly.Phy.Ed. 17,1661(1979).
126. A.Roviello and A.Sirigu, Makro.Chem. 183,895(1982).
127. L.Strzelecki and L.Liebert, Eur.Poly.J. 16,303(1980).
128. C.K.Ober, J.I.Jin and R.W.Lenz, Advances in Polymer Sci. Vol 59, p103 (Verlag Berlin, 1984) ed. by M.Gordon and N.A.Plate.
129. P.J.Flory, Faraday Diss. Chem.Soc. 68,14(1979).
130. W.H. de Jen, J. Van der Veen and W.J.P.Govsens, Solid State Commun. 12,405(1973).
131. H.Stenschke, Solid State Commun. 10,653(1972).
132. G.W.Gray and K.J.Harrison, Faraday Symp. Chem.Soc. 5,54(1971).
133. G.W.Gray and A.Mosely, J.Chem.Soc. Perkin Trans. 2,97(1976).
134. G.W.Gray, J.Phys Paris 36,337(1975).
135. W.R.Young, I.Haller and A.Aviram, Mol.Cryst.Liq.Cryst. 13,357(1971).
136. G.Ronca and D.Y.Yoon, J.Chem.Phys. 76,3295(1982).

137. B.Wunderlich 'Macromolecular Physics' Vol 3, p77
(Acad.Press., N.Y., 1980).
138. M.J.S.Dewar and A.C.Griffin J.A.C.S. 97:23,6662(1975).
139. F.W.Billmeyer 'Textbook of Polymer Science' p154
2nd edition, Wiley-Interscience, N.Y., 1962.
140. D.Marzotko and D.Demus, Pramana Suppl. 1,189(1975).
141. K.Iimura, N.Koide, R.Ohta and M.Takeda, Makro.Chem.
182,2563(1981).
142. P.Meares 'Polymers: Structure and Bulk Properties' Bulter
and Tanner Ltd. London, 1967.
143. W.R.Young, I.Haller and D.C.,Green, J.Org.Chem.
37,3707(1972).
144. J.P.Van Meter, B.H.Klanderman, Mol.Cryst.Liq.Cryst.
22,285(1973).
145. J.C.Dubois and A.Beguin, Mol.Cryst.Liq.Cryst.
47,193(1978).
146. R.W.Lenz, J.Polym.Sci. Poly.Symp. 72,1(1985).
147. J.R.Schaeffgen (Du Pont) British Patent
1,507,207(priority 10 May 1974, USA).
148. Q.F.Zhou and R.W.Lenz, J.Polym.Sci. Poly.Chem.Ed.
21,3313(1983).
149. A.Furukawa and R.W.Lenz, Macro.Chem. Macro.Symp.
2,3(1986).
150. A.Bondi, J.Phy.Chem. 68,441(1964).
151. R.C.Weast Ed. 'Handbook of Chemistry and Physics',
48th Edn. (The Chemical Rubber Co., 1967)
152. V.P.Shibaev, H.Frinklemann, A.V.Kharitanov, N.Portugall,
N.A.Plata and H.Ringsdorf, Vysokmol.Soedin.
A23,919(1982).

153. J.Lematre, S.Dayan and P.Sixou, *Mol.Cryst.Liq.Cryst.* 84,267(1982).
154. P.Sixou, J.LeMatre, A.Ten Bosch, J.M.Gilli and S.Dayan *Mol.Cryst.Liq.Cryst.* 91,277(1983).
155. S.N.Bhadani and D.G.Gray, *Mol.Cryst.Liq.Cryst.* 99,29(1983).
156. I.Uematsu and Y.Uematsu, 'Polypeptide Liquid Crystals' in *Adv.Poly.Sci.* Vol 59, Ed. by M.Gordon (Springer Verlag Berlin, 1984).
157. S.Vilasagar and A.Blumstein, *Mol.Cryst.Liq.Cryst.* 16,307(1980).
158. K.Iimura, N.Koide, Y.Tsutsumi and M.Nakatami, *Reports on Progress in Polymer Physics in Japan* Vol XXV,297(1982).
159. W.R.Krigbaum, T.Ishikawa, J.Watanabe, H.Toriumi and K.Kubota, *J.Polym.Sci. Poly.Phy.Ed.* 21,1851(1983).
160. J.I.Jin, H.Park and R.W.Lenz 'Synthesis and properties of new cholesteric main chain polyesters' presented at 'IX International Conference on Liquid Crystals' Bangalore, India Dec.6-10(1982).
161. E.Chiellini and G.Galli, *Faraday Diss. Chem.Soc.* 79,241(1985).
162. K.Iimura, K.Koide and R.Ohta, *Reports on Progress in Polymer Physics in Japan* Vol. XXIV, 231(1981).
163. H.W.Hunter, Private Communication Stirling University Chem.Dept. 1986.
164. A.L.McClellan, 'Tables of Experimental Dipole Moments' W.H.Freeman and Company, London, 1963.
165. G.Galli, M.Laus, A.S.Angeloni, P.Ferruti, and E.Chiellini, *Makro.Chem.Rapid Commun.* 4,681(1983).

166. A.S. Angeloni, M. Laus, C. Castellari, G. Galli, P. Ferruti
and E. Chiellini, Makro.Chem. 186, 977 (1985).

PART TWO

MECHANICAL PROPERTIES OF POLYMERS CONTAINING CYCLOALKYL AND

AZA-CROWN-ETHER RINGS IN THE BACKBONE

'He in a new confusion of his understanding;

I in a new understanding of my confusion'

Robert Graves.

CHAPTER ONE

MECHANICAL PROPERTIES OF POLYMERS

1.1 Introduction

The mechanical properties of high polymers, ie their response to various types of external stress, result from both their unique macromolecular nature and their particular chemical and physical structure.

In polymers, as in low molecular weight organic glasses and crystals, the possibility of rotation about a single chemical bond exists. Depending on the temperature and the composition, there may be considerable molecular flexibility even in the solid state as a result of micro-Brownian motion of the various segmental units. At the same time, their high molecular weight causes polymers to have unusually high viscosity compared to organic liquids, in the temperature range above their major softening or melting temperature. Partly as a result of a broad molecular weight distribution and partly as a result of the many different forms of motion that can occur, the transition zone separating the rigid solid state from the viscous liquid state tends to be broad. Furthermore, if the average molecular weight is sufficiently high, the polymers, even though not chemically cross-linked, will convert, upon passing through the so called glass transition, to a flexible rubbery elastic solid rather than to a viscous liquid.

A feature of polymeric materials is that their mechanical behaviour is markedly affected by temperature. For amorphous polymers, upon passing through the softening region, the modulus falls from a value of the order of 10^9 Nm^{-2} in the glassy state to about 10^6 Nm^{-2} in the rubbery state⁽¹⁾. The amount of modulus reduction in the vicinity of

the glass transition is greatly reduced in crystalline polymers as compared with amorphous polymers and will depend upon the degree of crystallinity of the sample.

The manner in which stress-strain parameters, such as the tensile, shear, or bulk modulus, vary with temperature and with time is essential fundamental information that must be known or determined before intelligent use and application of a polymeric material is possible. It is desirable, therefore, to make experimental measurements of moduli over the widest possible temperature and frequency ranges for polymers of known composition and structure. This, however, is difficult to do experimentally and hence empirical procedures have been devised, especially for amorphous polymers, by use of some form of a time-temperature equivalence principle. Whether obtained under transient or dynamic conditions, data on mechanical stress-strain parameters, together with the data from the use of other physical tools, such as NMR^{<2>} and dielectric studies^{<3>}, provide a basis for determination of relaxation or retardation spectra, and for interpretation of relaxation mechanisms in terms of specific compositional and structural features.

1.2 Mechanical Properties

1.2.1 Description of Mechanical Properties

Mechanical behaviour has two significant aspects: strength and stiffness. In this work only the latter will be dealt with. The physical quantity that characterizes stiffness is the modulus.

For deformation in shear, the shear modulus, G , is given by:

$$G = R / T \quad (1)$$

where R is the shear stress (force per unit area), and T the angle of deformation (for small deformation).

For deformation in tension, the modulus is called Young's modulus, E , given by:

$$E = Q / Z \quad (2)$$

where Q is the stress (force per unit area), and Z is the relative increase in length, (dl/l) .

For compression, the modulus is called the bulk modulus, K , given by:

$$K = P / (-dV/V) \quad (3)$$

where P is the pressure, acting on all sides of the object, and $(-dV/V)$ is the relative decrease in volume.

For isotropic materials, these moduli are related by:

$$E = 2G (1+u) \quad \text{and} \quad (4)$$

$$E = 3K (1-2u) \quad (5)$$

where u is Poisson's ratio, which is a measure of the lateral contraction resulting from tension.

The proportionality between deformation and stress, expressed in equations (1) to (3), only holds for small deformations (eg, 0.1% for hard materials), so that only in this range of deformations is the modulus defined unambiguously.

1.2.2 Linear Viscoelastic Solids

Polymeric materials exhibit mechanical properties which come somewhere between a solid and a liquid and hence they are termed VISCOELASTIC. If the stress-strain relations are a

function of time but not of strain magnitude, such a material is then said to exhibit linear viscoelasticity.

Linear viscoelastic behaviour can be described in terms of simple combinations of spring elements, representing elastic response, in which Hooke's law is obeyed, and dashpot elements, representing viscous response in which Newton's law is obeyed. A linear element and a viscous element in series are said to constitute a Maxwell solid, while a linear element and a viscous element in parallel are said to constitute a Kelvin or a Voigt solid⁽⁴⁾. Each of these models predicts some aspects of observed polymers behaviour, but they also lead to some predictions not in accord with the response of actual polymeric materials.

The response of polymers to stress is a combination of an elastic response due to rapid local readjustments of bond angles and distances and a viscous, or time dependent response due to configurational changes, and it is necessary to find material parameters that can be used to describe this complex behaviour. Fortunately, many polymers, at least at small strains, appear to behave as linear viscoelastic materials. Such materials are said to obey the Boltzmann superposition principle and the response of the system to the external stimulus is a result of its entire past stress and strain history⁽⁴⁾.

1.2.3 Step Function Experiments⁽⁴⁾

The most characteristic features of viscoelastic materials are that they exhibit a time dependent strain response to a constant stress (creep) and a time dependent stress response

to a constant strain (relaxation).

Creep

The standard method of studying creep is simply to subject a specimen to a constant load, usually in axial tension, and then monitor the resulting deformation as a function of time by means of a cathetometer or by electrical methods.

Relaxation

It is possible to use the same experimental device for creep studies, in this case, the stress is measured as a function of time for a given constant strain. This is usually done by means of some type of servomechanism which continuously readjusts the applied stress so as to maintain the deformation constant.

1.2.4 Dynamic Experiments<3,4>

In addition to creep and stress relaxation experiments, another type of measurement is quite common. Here the stress or strain, instead of being a step function, is an oscillatory function with an angular frequency ω .

If the polymer is treated as a classical damped harmonic oscillator, both the elastic modulus and the damping characteristics can be obtained. Elastic materials convert mechanical work into potential energy which is recoverable; for example an ideal spring, if deformed by a stress, stores the energy and uses it to recover its original shape after removal of the stress. No energy is converted into heat during the cycle and so no damping is experienced.

Liquids on the other hand flow if subjected to a stress; they do not store the energy but dissipate it almost entirely

as heat and thus possess high damping characteristics. Viscoelastic polymers exhibit both elastic and damping behaviour. Hence if a sinusoidal stress is applied to a linear viscoelastic material, the resulting stress will also be sinusoidal, but will be out of phase when there is energy dissipation or damping in the polymer.

The dynamic modulus is expressed as a complex quantity, eg:

$$G = G' + iG'' \quad (6)$$

where G' is the in phase or storage modulus and G'' the out of phase or loss modulus.

The damping or the energy loss per cycle can be measured from the 'loss tangent', $\tan \delta$. This is a measure of internal friction and is related to the complex shear moduli by

$$\tan \delta(G) = G'' / G' \quad (7)$$

The damping in shear is not necessarily equal to the damping in tension. If we express Poisson's ratio u as a complex quantity, $u = u' - iu''$, from the relationship between complex quantities (eq. 4), the following equations are obtained

$$E'' = 2G''(1+u') - 2G'u'' \text{ and}$$

$$E' = 2G'(1+u') + 2G'u''$$

For hard solids, G''/G' is generally less than 0.1, and also u''/u' can only attain a maximum value of 0.1 whereas for isotropic plastics u' ranges from 0.3 to 0.45⁽⁵⁾. Thus:

$$G''u'' \ll G'(1+u') \text{ and}$$

$$E''/E' = G''/G' - u''/(1+u') \text{ or}$$

$$\tan \delta(E) = \tan \delta(G) - u''/(1+u') \quad (8)$$

Since for the isotropic hard solids the maximum value of $u''/(1+u')$ is of the order of 1/100, the difference between damping in shear $\langle \tan \delta(G) \rangle$ and damping in extension $\langle \tan$

$d(E) >$ is negligible, and it is then merely referred to as damping, $\tan \delta$.

The concept of deformability is sometimes more convenient than that of stiffness(modulus) of which it is the inverse. The pertinent quantity is called the compliance (J); it is the inverse of modulus, eg, the complex shear compliance, $J = J' - iJ''$ is related to the complex shear modulus by $J = 1/G$

1.3 Transitions and Relaxations in Amorphous Polymers

1.3.1 The Glass Transition

The classical method for experimental determination of the glass transition temperature(T_g) is dilatometry. Dilatometric methods are simple in principle but complex in practice. The displacement method is perhaps most commonly used.

In addition to dilatometry, calorimetry has been extensively employed, a discontinuity in heat capacity being observed at T_g .

The glass transition in amorphous polymers is accompanied by profound changes in their viscoelastic response. Thus the stress relaxation modulus commonly decreases by about three orders of magnitude in the vicinity of the T_g determined by calorimetry or dilatometry, and the creep compliance increases by about three orders of magnitude. In addition, under dynamic experimental conditions, the storage moduli and compliances behave in a similar manner to the corresponding static quantities. The loss moduli and compliances, on the other hand, exhibit maxima in the glass transition region, as does $\tan \delta$.

Many other profound physical changes occur at T_g in addition to the aforementioned, for example: refractive index $\langle 6 \rangle$, dielectric loss $\langle 3 \rangle$, line width of NMR $\langle 2 \rangle$ etc. It is important to notice that each experimental method will yield a different value for T_g and that even the same method will yield different results depending on the time scale.

Theoretical treatments of glass transition are based on the free volume theory and the thermodynamic theory $\langle 1,3,4 \rangle$.

1.3.2 Secondary Relaxations

Most polymers have one or more damping peaks in addition to the peak associated with the main glass transition. However, most of the damping peaks are due to the amorphous phase and occur at temperatures below T_g . They are called secondary transitions or loss peaks ($\tan \delta$) and usually labelled from the higher to the lower temperatures with the successive letter of the Greek alphabet: β, γ, δ , and so on. $\tan \delta$ is preferably plotted on a logarithmic scale (Figure 1-1), because the small loss peaks are more prominent and their slopes are straighter than they are in a linear plot. Moreover, this way of plotting is in better agreement with the relative accuracy of the damping measurement itself.

Nearly all tough ductile glassy polymers and those with high impact strength have prominent secondary transitions $\langle 7,8,9 \rangle$. Examples include polycarbonates, cellulose polymers, polysulfones, nylons, epoxy resins, polyethylene terephthalate, and polyvinyl chloride.

Only certain types of secondary transitions increase ductility and impact strength even if the transition is well

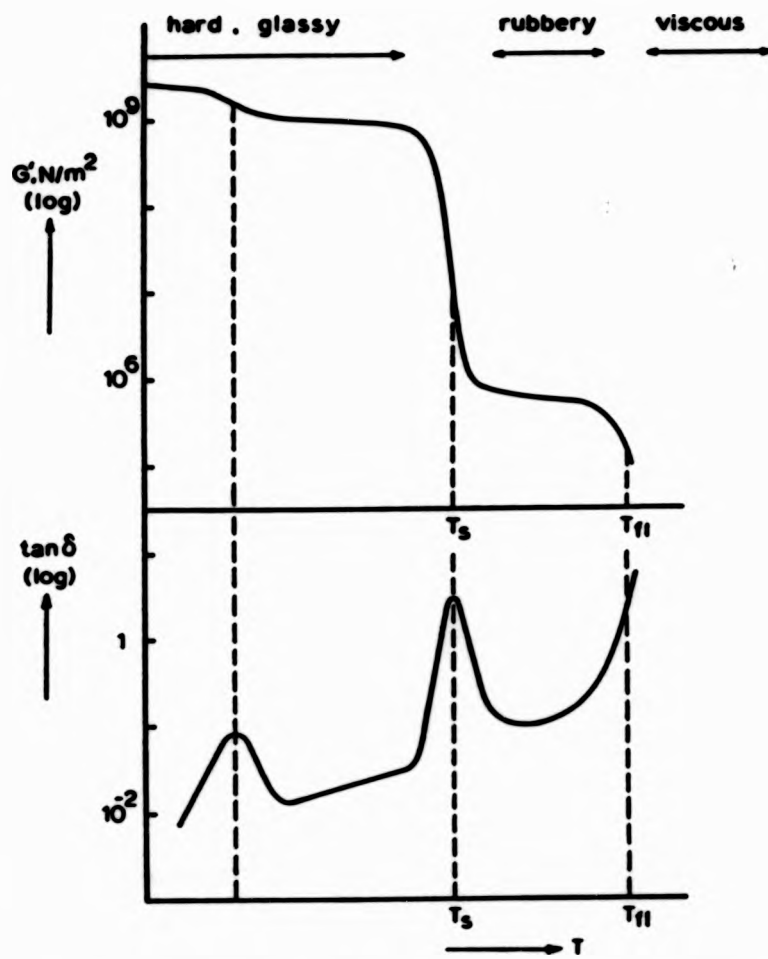


Fig. 1-1 Modulus G' and damping $\tan \delta$ as functions of temperature T for an amorphous polymer (schematic).
 T_s - softening temperature,
 T_{fl} - flow temperature.

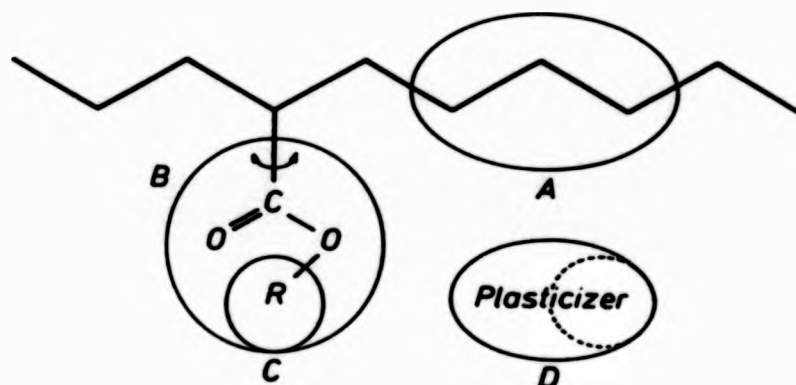


Fig. 1-2 The various kinds of groups whose movements give rise to secondary mechanical loss peaks.

below the test temperature<10,11>. Secondary transitions due to sidechains are less important than backbone motions in increasing ductility and impact strength. However, some secondary transitions due to backbone motions also are ineffective in producing ductility<12>.

The exact type of molecular motions responsible for secondary transitions is known in only a few cases, but most of them can be associated with one or more of the following general classifications(Figure 1-2)<13>:

Type A

Backbone chain motions of short segments or groups.

Type B

Side group motions such as rotations, librations, torsional oscillations, and wagging motions.

Type C

Backbone or sidechain motions made possible by defects in packing or configurations in the glassy or crystalline states.

Type D

Association or phase separation of impurities or diluents.

CHAPTER TWO
INSTRUMENTATION

2.1 Torsional Braid Analysis(TBA)

2.1.1 Introduction

TBA is a temperature programmable dynamic mechanical instrument originally developed by Gillham<14,15> from the conventional torsional pendulum. This instrument permits investigation of materials which cannot support their own weight by using a supporting substrate: a multifilament glass braid. A specimen is prepared by impregnating the substrate with a solution of the material, followed by thermal removal of the solvent, hence, less than 100mg of sample per experiment suffices. Absolute mechanical data(eg modulus) cannot be obtained by TBA technique because of the lack of knowledge of the specimen dimensions. Also the composite's stiffness changes with temperature and causes frequency deviations. Nevertheless, TBA is a useful technique in the way it provides information about secondary transitions particularly at low temperatures.

A torsional braid analyser model 100-B1, manufactured by Chemical Instruments of New York was used in the present study(Figure 2-1). The nominal frequency of measurement is approximately 1 Hz, and it is possible to operate over the temperature range 83-773K.

2.1.2 Sample Preparation

To a polymer solution(10-15 % wt/vol), was added a thoroughly cleaned braid(conventional glass cleaning method) which was left in for one hour. The braid was then dried by suspending it below an infrared lamp under a slight tension of about 35g. Depending on the volatility of the solvents being

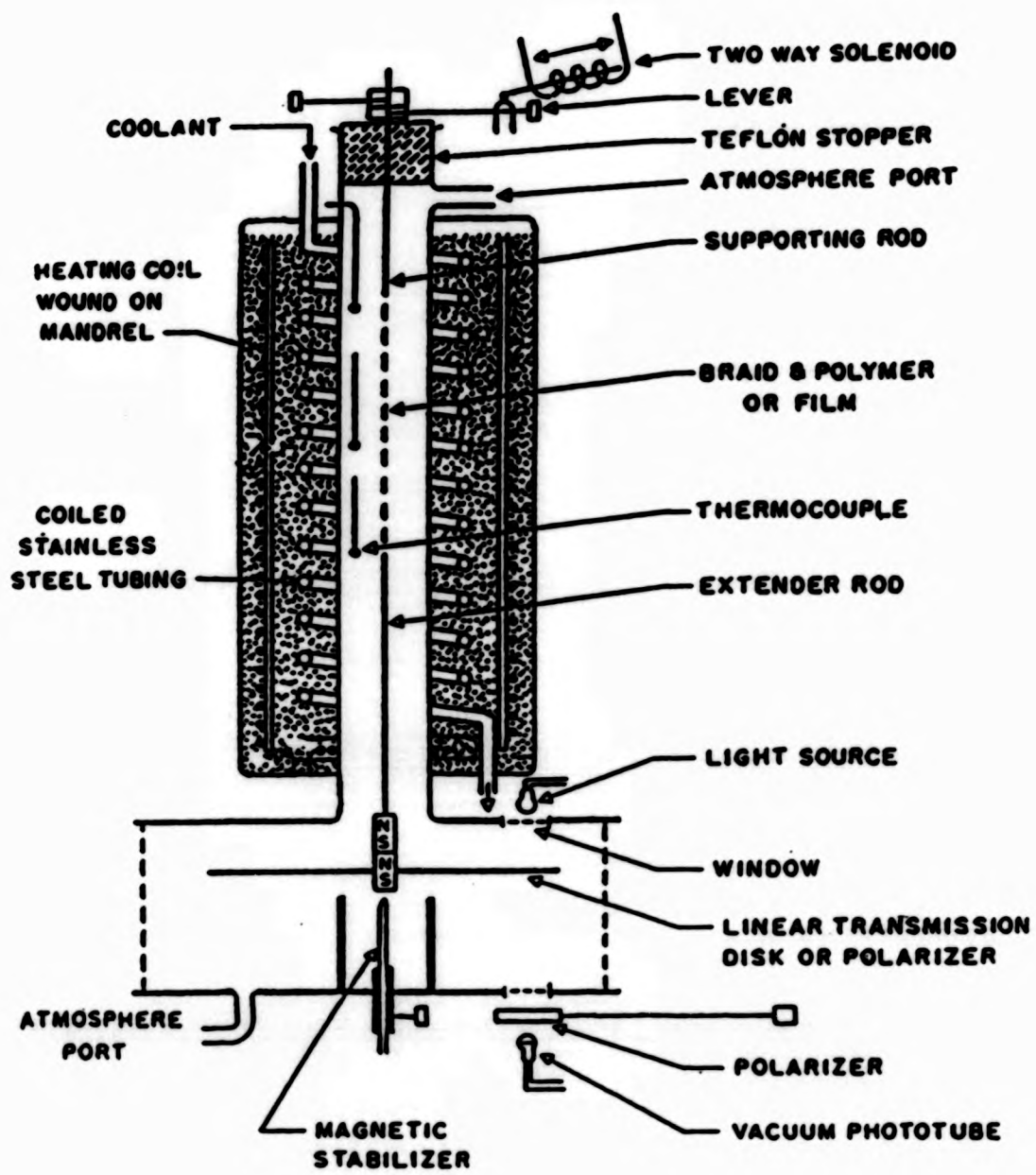


Fig. 2-1 Torsional pendulum and torsional braid apparatus of Gillham (schematic).

used, samples were either dried in a vacuum oven or inside the TBA chamber under a nitrogen purge above their glass transition temperatures (T_g based on DSC).

The treated braid was suspended in the sample chamber which was continually flushed by a nitrogen stream (about 20 cm³/min). Cooling was effected by circulation of nitrogen gas first through a cooling coil immersed in liquid nitrogen and then through the tubes surrounding the sample chamber. The sample was thermally equilibrated at the lowest temperature of the scan for at least 15 minutes before commencing measurements. The temperature was then allowed to rise slowly by gradually reducing the flow rate of the cooling gas to zero and allowing the apparatus to warm up itself. A programmed heater was used to control the temperature scan from 273K upwards. The average rate of heating was ca 2K/min.

Torsional oscillations were initiated every 2.5 minutes throughout the scan except in the vicinity of the glass transition, then the oscillations were manipulated manually in order to collect more points on the TBA spectrum. A typical set of damped oscillations is shown in Figure 2-2.

2.1.3 Theory and Interpretation of Results

Two parameters, the real part of the complex shear modulus and the logarithmic decrement, can be calculated from the damped waves of a homogeneous rod undergoing free torsional oscillations⁽¹⁶⁾. The real part of the complex shear modulus, G' , is directly proportional to the energy stored in deforming the sample and is given approximately by:-

$$G' = 2LI/(\pi \cdot r^4) \cdot \omega^2(4\pi^2 + d^2)$$

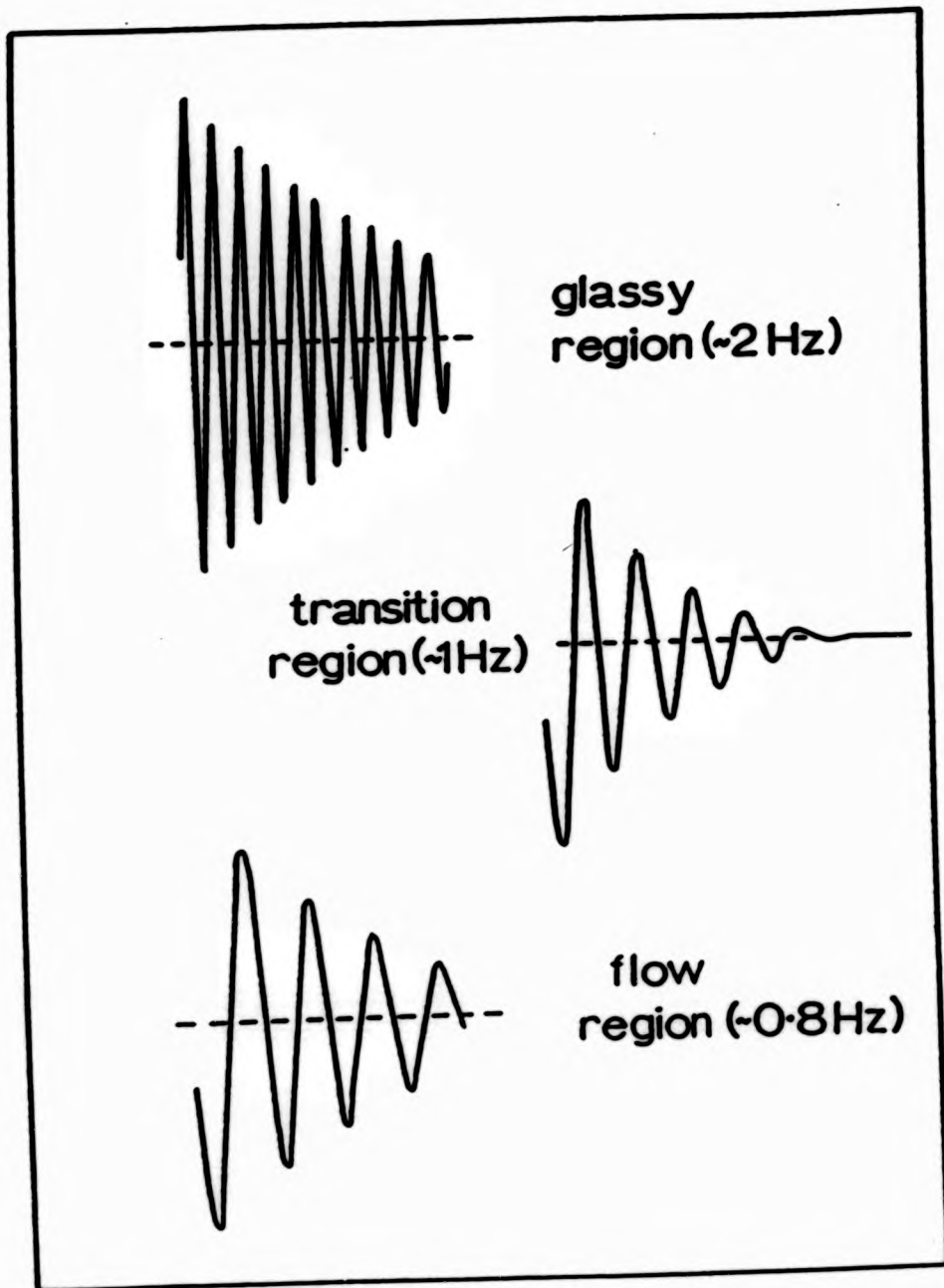


Fig. 2-2 Selected TBA oscillations.

In this expression, w is the frequency, d is the logarithmic decrement (l.d.), I is the moment of inertia of the oscillating system, r is the radius, and L is the length of the specimen. The logarithmic decrement is obtained from successive amplitudes $\langle A(n), A(n+1) \rangle$ of the decaying wave

$$d = \log(e) \langle A(n) / A(n+1) \rangle$$

and is related to the imaginary part G'' and the real part of the complex shear modulus by the approximate relation

$$d = \pi \cdot G'' / G'$$

Storage and loss of energy on cyclic deformation are characterized by (the real part of the shear) modulus and the logarithmic decrement respectively, which are plotted as function of temperature.

In torsional braid analysis the relative rigidity parameter, $1/p^2$, where p is the period of oscillation, is used as a measure of the modulus and is simply w^2 . This expression implicitly assumes that the contributions of dimensional changes, and changes in the damping characteristics, to the value of the relative rigidity are dominated by changes in the modulus of the polymer. A typical TBA spectrum is shown in Figure 2-3.

2.2 Osmometry

The molecular weights of polymers can be determined either chemically or physically. One of the physical methods most commonly used is to measure the colligative properties.

The relations between the colligative properties and molecular weight for infinitely dilute solutions rest upon the fact that the activity of the solute in solution becomes equal

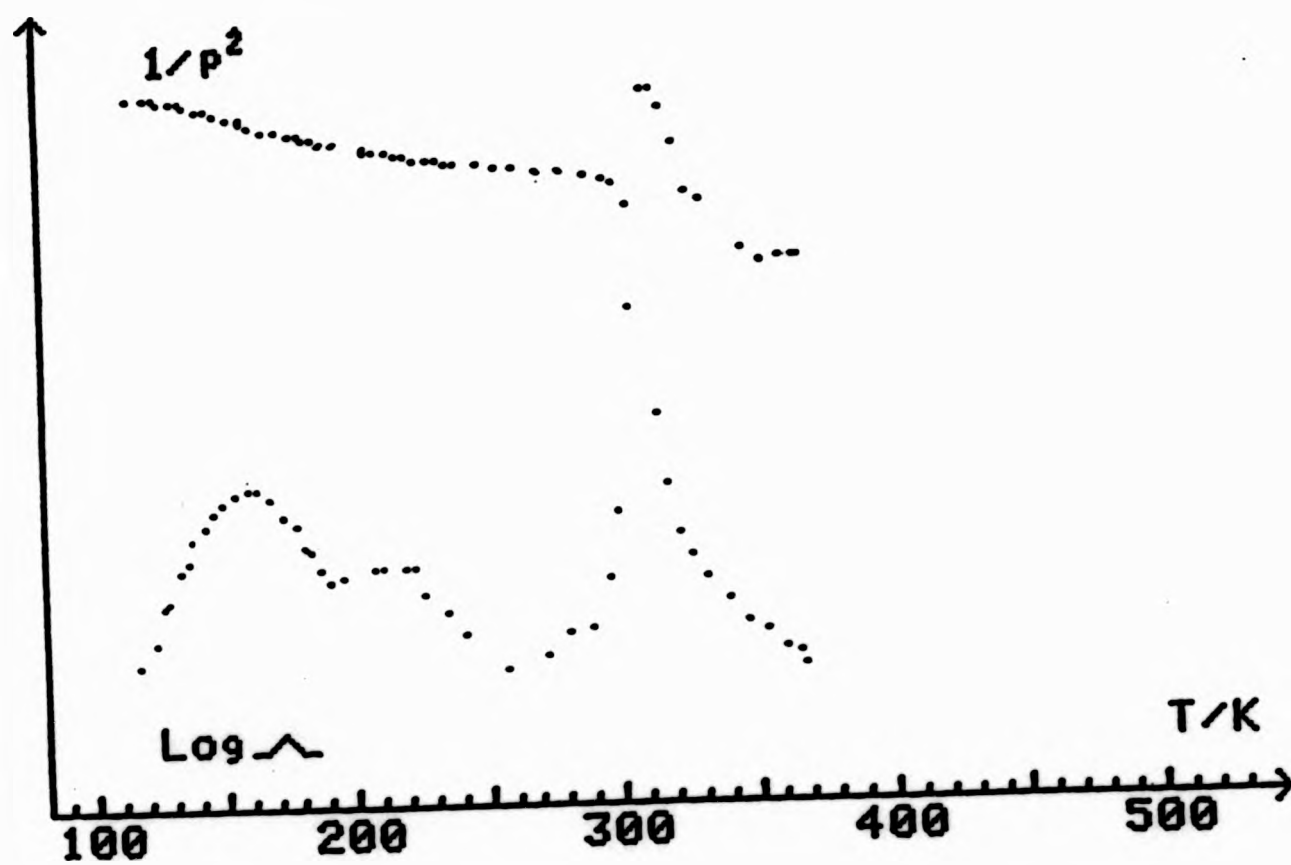


Fig. 2-3 A TBA spectrum shows the plots of logarithmic decrement and relative rigidity($1/p^2$).

to its mole fraction as the solute concentration becomes sufficiently small. The colligative property methods are based on boiling point elevation, freezing point depression, vapour pressure lowering and the osmotic pressure.

A colligative method effectively counts the number of molecules present and provides a number average molecular weight (M_n) defined by

$$M_n = \frac{\sum N_i M_i}{\sum N_i}$$

where N_i is the number of molecules of species i of molecular weight M_i .

The osmotic method has been more widely used than other colligative techniques for polymer systems.

2.2.1 Membrane Osmometer

The working equation for MW determination by osmotic pressure measurement is derived from the thermodynamic theory of polymer solution.

$$(\pi/c)_{c \rightarrow 0} = RT/M_n$$

where R is the gas constant, T is the temperature in Kelvins and $(\pi/c)_{c \rightarrow 0}$ is the limiting value at zero concentration (c). While a general expression for osmotic pressure at a finite concentration is

$$(\pi/c) = RT(1/M_n + A_2 c + A_3 c^2 + \dots)$$

where A_2 , A_3 are second and third virial coefficients respectively.

In general a straight line results whose intercept at $c=0$ is $1/M_n$ and whose slope is the second virial coefficient. In most cases, the term in c^2 may be neglected.

A Knauer membrane osmometer and detecting bridge were used

in this study. The basic features of this instrument are shown schematically in Figure 2-4.

All membranes (Sartorius, regenerated cellulose) were equilibrated in pure solvent at an appropriate temperature overnight before use. The pressure change between the upper sample cell and the lower solvent cell when polymer solution was added is detected by the diaphragm and registered on a chart recorder.

Membrane osmometry suffers from the diffusion of low molecular weight species through the membrane, hence, sample molecular weights of less than 15,000 g/mol are not recommended. In this situation, vapour pressure osmometry proves to be more satisfactory.

2.2.2 Vapour Pressure Osmometer (VPO)

It is clear that direct measurement of vapour pressure lowering in polymer solutions is unrewarding. It is possible, however, to utilise vapour pressure lowering indirectly through the technique of vapour phase osmometry, in which one measures a temperature difference relatable to vapour pressure lowering through the Clapeyron equation.

A Hewlett Packard model-302B Vapour Pressure Osmometer was employed in this work. A schematic diagram is shown in Figure 2-5.

The number average molecular weight of the sample can be calculated from the following equation:

$$M_n = K \langle V/c \rangle_c$$

where V is the output value of the Wheatstone bridge and c is the concentration. The factor K is a calibration constant. The

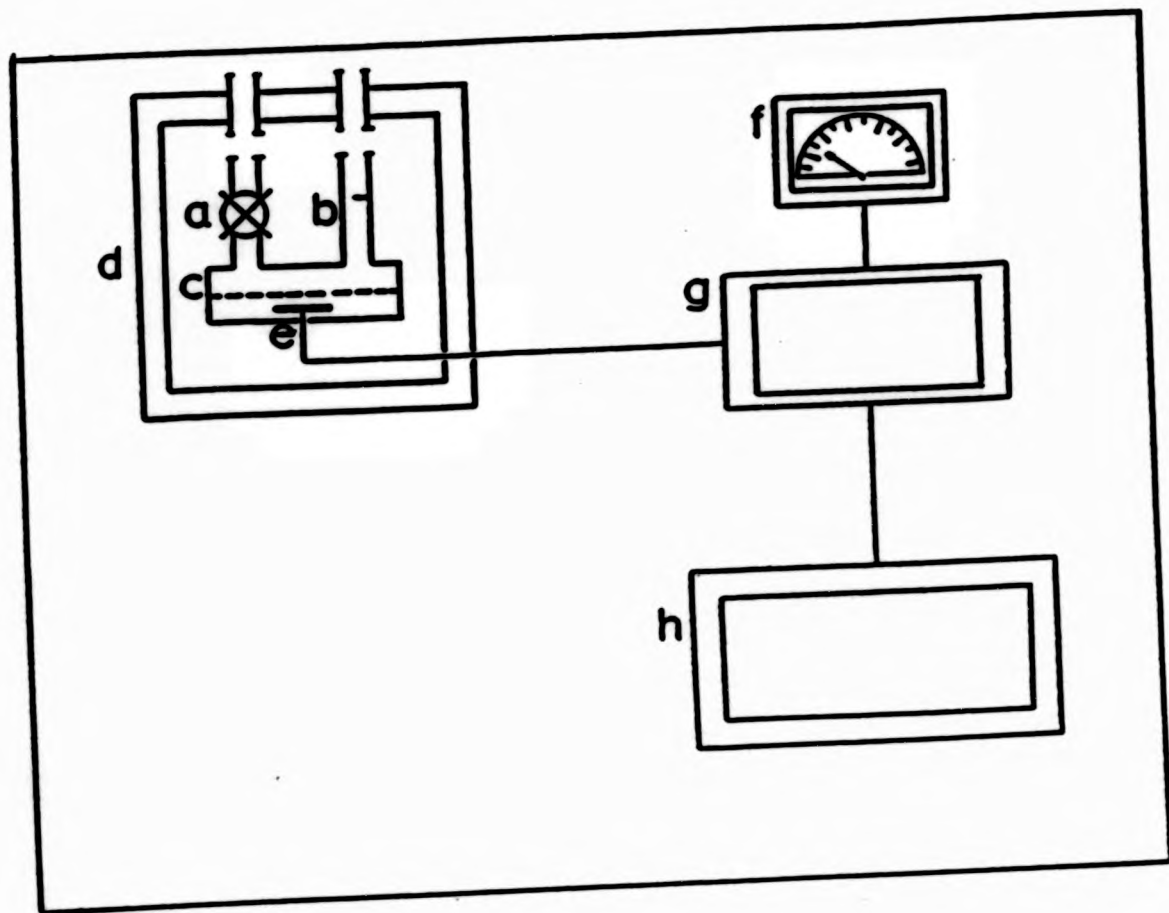


Fig. 2-4 Schematic diagram of membrane osmometer:

- (a) outlet valve
- (b) inlet valve
- (c) membrane
- (d) thermostatted chamber
- (e) pressure detecting membrane
- (f) osmotic pressure dial
- (g) Wheatstone bridge circuit
- (h) chart recorder.

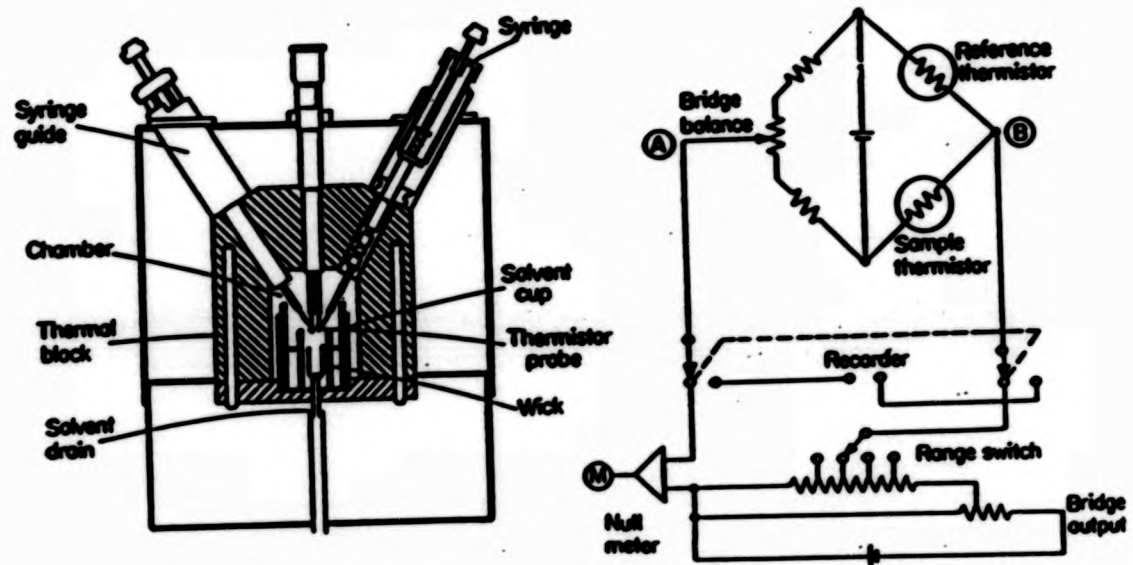


Fig. 2-5 Sample chamber and circuit diagram for a typical vapour phase osmometer.

instrument was calibrated with a concentration series of benzil (MW:210) solution, the output values (V) were plotted against concentrations (c), K was obtained by substituting the slope of the straight line into the above equation.

Effort was made to keep the drop size constant (spherical shape rather than pear shape). The temperature difference resulting from different rates of solvent evaporation from and condensation onto droplets of pure solvent and polymer solution maintained in an atmosphere of solvent vapour was registered by the thermistor and transformed into a proportional signal on the chart recorder. The time between each measurement was standardised at 30 minutes. The solution of the lowest concentrations was measured first in any series of concentration, followed by an increasing order.

Because of heat loss, the full temperature difference expected from theory is not attained.

2.3 Nuclear Magnetic Resonance (nmr)

¹H nmr spectra were recorded on a Hitachi Perkin-Elmer R24 (60 MHz) NMR spectrometer.

2.4 Mass Spectrometry

A JEOL Mass Spectrometer model JMS-D100 linked with a JEOL Gas Chromatograph (model JGC-10R) and data analysing computer was used.

2.5 Gas Liquid Chromatography

A Perkin-Elmer F11 equipped with a 3 meter 5% Carbowax column was used at a temperature of 150°C.

2.6 Elemental Analysis

Elemental analysis was carried out on a Model 1106 Carlo-Erba Analyser (Milan, Italy) under the standard conditions. C and H were determined directly, and O by difference.

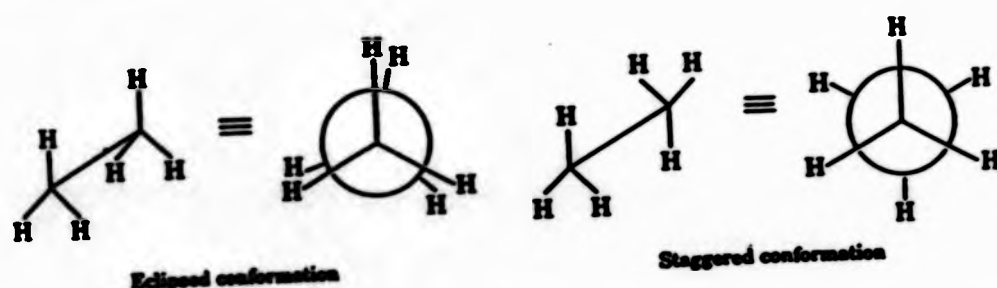
CHAPTER THREE

RING SYSTEMS

3.1 Introduction

In 1930, Weissberger and Sangewald⁽¹⁷⁾ suggested that rotation about single bonds was not free, their conclusion led to the speculations about the energy barrier to rotation about carbon-carbon single bonds. Depending upon the magnitude of the potential energy barrier (torsional strain), non-identical arrangements (CONFORMATIONS) of the atoms in a molecule can be obtained by rotation about one or more single bonds.

In acyclic compounds, for instance, ethane, there are two different rotational conformations: 'eclipsed' and 'staggered'; the staggered conformation is more stable than the eclipsed one, because the effects of interelectronic repulsions are minimized for this conformation (Figure 3-1).



The conformation theory developed for acyclic compounds, whereby certain conformers are preferred to others, can be applied to cyclic systems. Cyclic systems are usually classified according to the number of members in the ring, into four groups: (1) small rings, 3 and 4 membered; (2) common rings, 5, 6, and 7 membered; (3) medium rings, 8 to 11 membered; (4) larger rings, 12 membered and larger⁽¹⁸⁾.

3.2 Polymers Containing Ring Units

The thermal and mechanical properties of polymeric materials are closely related to the flexibility of the macromolecular chains. In a rubbery material, molecules can

dissipated energy of impact by segmental motions because rotational energy barriers in the mainchain are very small. Ring compounds such as cycloalkanes, cycloalkanones, lactones and crown ethers show more than one stable conformation or have metastable conformations, and it is possible for the molecule to pass from one conformation to another<19>. Accordingly, mobility of the rings in the chain backbone of a polymer may compensate for the effect of their bulk, which would stiffen the chain; and the rings can act as impact energy absorbers. It is worthwhile, therefore from the viewpoint of the design of mechanically interesting polymeric materials, to study polymers with rings in the backbone.

3.2.1 Polymers Containing Rings In The Sidechains

Some studies have been carried out on mechanical and dielectric relaxations arising from the internal movements of cyclalkyl groups in sidechains of various polymers such as: poly(cyclohexyl methacrylate) and poly(cyclohexyl acrylate)<20,21>, poly(vinyl hexahydrobenzoate) and poly(vinyl cyclohexyl ether)<21>, poly(vinyl cyclohexane)<21,22>, poly(cycloalkyl methacrylate) with ring sizes of 5 to 8<21,23>, poly(cyclododecyl methacrylate)<24>, poly(cyclododecyl acrylate)<24>, poly(3-cyclohexyl-1-propene)<24>, poly(4-cyclohexyl-1-butene)<22>, poly(vinyl cyclopentane)<22>, poly(3-cyclopentyl-1-propene)<22>, and poly(dicycloalkyl itaconates) with ring sizes of 7 to 12<25>.

Polymers with attached crown ethers have been reviewed<26,27,28>, however, there is no mention of any mechanical studies.

Heijboer demonstrated that if a secondary relaxation originates from the motion of sidechains alone, high impact strength cannot be expected. However, if the dynamic mechanical dispersion originates from the movements within the mainchain, attainment of high impact strength is very likely<5>.

3.2.2 Polymers Containing Saturated Rings In The Mainchains

3.2.2.1 Polymers Containing Cycloalkyl Units

Studies on polymers containing rings larger than cyclohexane are hardly found in the literature, probably due to the painstaking synthesis of difunctional monomers. Although, Kumanotani and coworkers have reported the synthesis and mechanical property studies of polymers containing large rings by using diallyl succinate and diesters of cycloalkyl-1,3-dipropionate<29,30,31>, all the rings were linked in non-symmetrical positions and those prepared from diallyl succinate were even cross-linked.

3.2.2.2 Polymers Containing Crown Ether Units

The early efforts to incorporate crown ethers into polymer backbones utilized the reaction of the dibenzo-crown-ethers with formaldehyde<32>. Subsequently, several others have prepared similar formaldehyde polymers from dibenzo-crown-ethers of different sizes<33,34>. The diamino derivatives of the dibenzo-crown-ethers readily reacts with the dichlorides and dianhydrides of diacids giving polyimides, polyamides, polyamidoimides, and polyetherimides<35,36>. Epoxide resins based on crown ethers have been obtained by

Japanese workers<37,38>. Polyethers and polyurethanes were synthesised by polycondensation starting from low molecular weight macrocyclic compounds with spiroxetane groups<39>.

Polymers containing diaza-crown-ethers were obtained and studied by Lehn and coworkers in 1975<40>. On the base of diaza-18-crown-6-ether, polyamides, polyurethanes and epoxide resins were synthesised.

It is because of the cation binding characteristics of crown ethers, that studies of polymers containing crown ethers in the backbone are restricted to this area. Mechanical properties studies are not found in the literature.

3.3 Synthetic Routes To Polymers Containing Rings In The

Mainchain

3.3.1 Step Growth Polymerisation

According to Carother<41>, if the reacting molecules are difunctional, linear, high molecular weight polymers are formed. In this way, structurally well defined polymers like polyesters, polyamides, polyurethanes etc., can be obtained if the stoichiometric balance is achieved.

3.3.2 Ring Opening Polymerisation

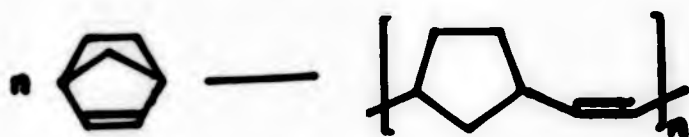
Cycloolefin monomers possessing unsaturation sites as constituents of the alicyclic rings, have the potential of undergoing polymerisation by two distinct mechanisms; the conventional addition polymerisation and the ring opening polymerisation, although, in most cases catalysts are required.

Ring opening polymerisations in general may be considered

as bond-reorganisation processes, whereby, for every bond which undergoes scission in the cyclic monomer, a new and similar bond is formed in the polymer. The conversions of cyclic ethers, lactones, or lactams to open chain polymers are well known methods in polymer synthesis^{<42>}.

The tendency of cyclic monomers to polymerise depends on two important factors; ring strain and entropy change during the reaction.

As early as 1954, Anderson and Merckling^{<43>} demonstrated that the use of Ziegler-Natta catalysts to polymerize bicyclo(2.2.1)hept-2-ene (Norborene) via ring opening polymerisation, resulted in a polymer containing a saturated five membered ring and a -C=C- group alternately (Eq. 3-1). Later on, Ofstead also polymerised bicyclo(2.2.2)oct-2-ene to give a six membered ring in the backbone^{<44>}.

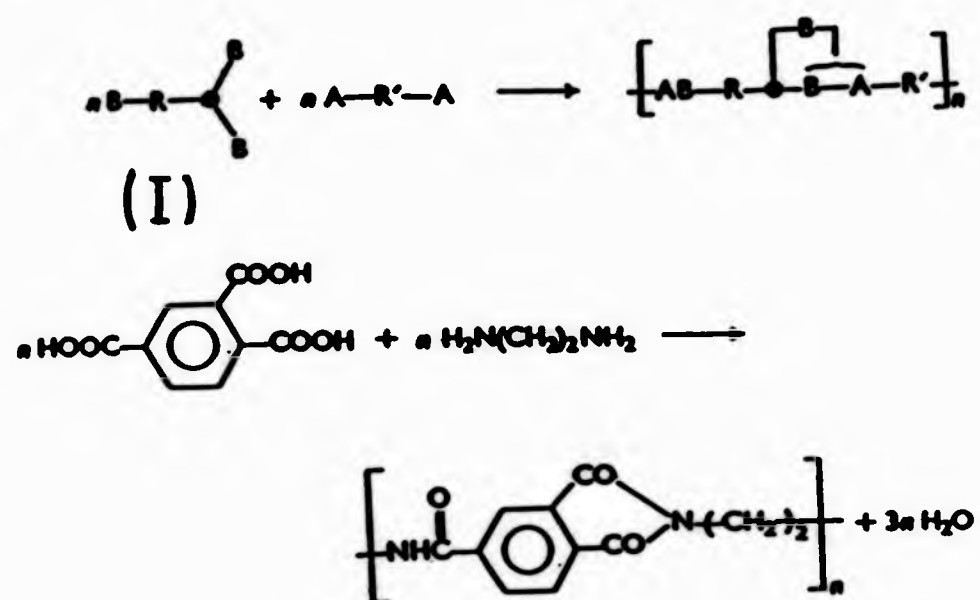


The structures of polymers obtained from ring opening polymerisation depends very much on the properties of the catalysts. There are no reports on polymers containing rings larger than cyclohexyl unit in the backbone by ring opening methods.

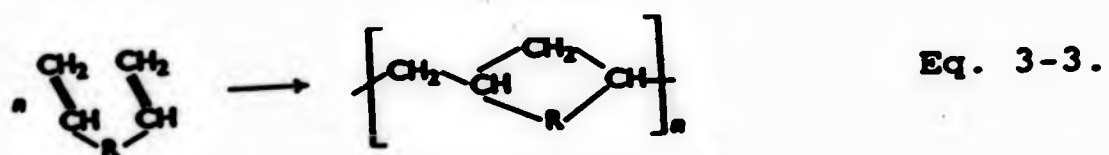
3.3.3 Ring Forming Polymerisation

A ring forming polymerisation produces polymer that contains a ring structure that is not present in any of the monomers. Ring-forming polymerisations that lead to linear polymers require that the monomers possess functionalities of

greater than two. At least one of the functions is necessary to form the ring. Equation 3-2 schematically depicts the polymerisation of a trifunctional monomer with a difunctional monomer to yield a linear product. This can occur because one B function in (I) reacts with the newly formed -BA- linkage. Its proximity to the -BA- linkage allows it to react in a different manner than the other B functions in (I).



Intra-intermolecular polymerisation in which a monomer with a functionality of four gives linear, soluble, high molecular weight polymer is shown schematically in Eq. 3-3.



Polymers prepared via ring forming polymerisation generally suffering from poorly defined structure because of the unpredictable degrees of cyclisation during propagation. The uses of polyfunctional monomers always leads to cross-linking. A comprehensive review of this topic can be found in Cotter and Matzner's book⁽⁴⁵⁾.

CHAPTER FOUR

EXPERIMENTAL

4.1 Synthesis of Medium and Large Rings

It has been recognised that the low yield of reactions designed for the synthesis of the small rings is due to the very unfavourable enthalpy change (bond angle strain), while for the common medium size rings although they have less favourable entropies of ring closure than the small rings, they have much more favourable enthalpies which allowed them to be prepared in good yield^{<46>}.

For large rings, as the ends required to react during the closure get further and further apart, the entropy of ring closure should become less and less favourable. Hence, synthesis of large rings becomes a very difficult task.

Preparation of difunctional large rings requires cyclisation of two linear difunctional monomers, and such reactions are best conducted under high dilution conditions so that the probability of cyclisation is higher than the probability of polymerisation. Frequently, the best one can do is to increase the probability of cyclisation to a competitive level, but not over that for polymer formation.

According to the literature, there are three possible ways to obtain large rings; (a) Blomquist's diketene reaction^{<47>}, (b) Ziegler's cyclisation of dinitrile^{<48>}, and (c) Dieckmann cyclisation of diester^{<49>}. In general, the diketene reaction is favoured for the synthesis of 14, and 16 membered rings, while for higher homologues there is not much difference between the Ziegler and Dieckmann reactions.

A high dilution apparatus was specially designed for the monomer's synthesis (Figure 4-1).

The Hershberg funnel is a modified self-pressurised

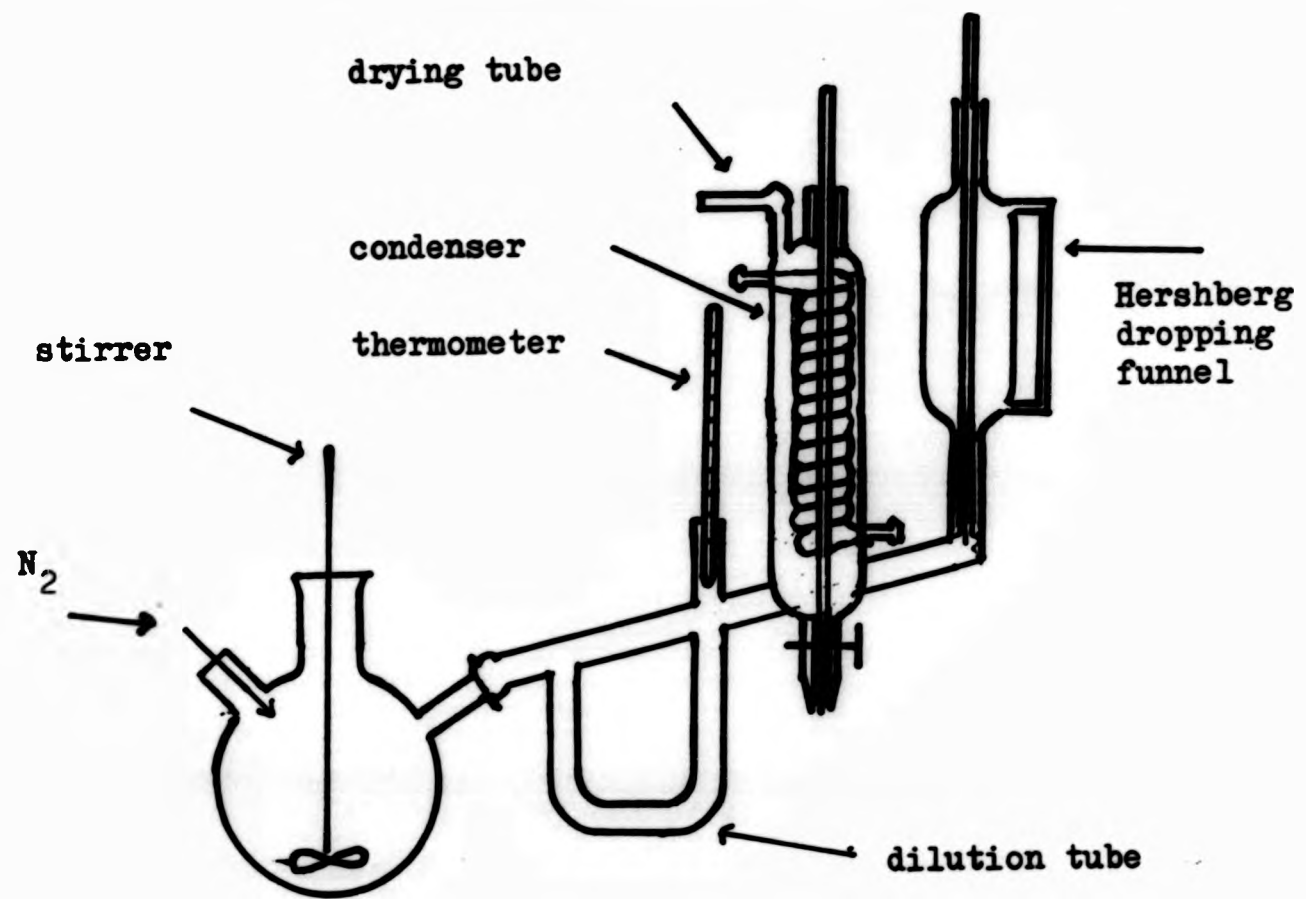


Fig. 4-1 High dilution apparatus

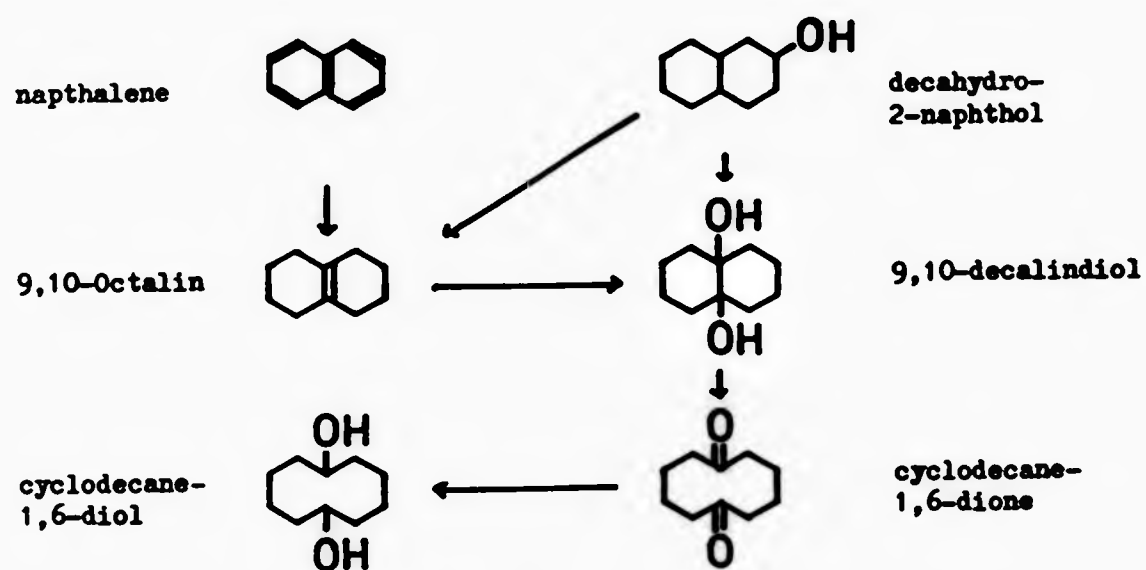
dropping funnel, it consists of a tungsten wire (0.5mm diameter) which can be moved up and down in a 0.55mm diameter bore. The Hershberg funnel was connected to a dilution tube (U shape). A modified condenser was employed in the Dieckmann reaction which is basically a Normag condenser incorporating a stop-cock so that the distillation rate can be controlled. All the reactions were carried out under a nitrogen atmosphere and a mechanical stirrer was fitted with a mercury seal.

Cyclisation reactions are very susceptible to moisture, all the solvents employed were rigorously dried before use, for example, benzene was refluxed over CaH_2 for 30 hours before distillation and then stored over sodium wire, triethylamine was dried over KOH for 2 days and stored over KOH immediately after distillation. The high dilution apparatus was dried at 400°C overnight and cooled with dry nitrogen blowing over just before each reaction.

4.1.1 Synthesis of 10 Membered Ring

(cyclodecane-1,6-diol) <50>

The diol was prepared from the corresponding diketone. According to literature, there are two routes by which the diketone can be made. The reactions involved are shown schematically below



Both methods have been tried, however conversion of naphthalene to octalin using Lithium and n-propylamine was very low.

(i) 9,10-Octalin

Decahydro-2-naphthol (42g) was dehydrated by a mixture of P2O5 (42g) and H3PO4 (89%:420ml). The temperature of the mixture was raised to 150C for ten minutes. Then, while this temperature was maintained, a slight vacuum was applied to the system and the Octalin was caused to distil with steam by the dropwise addition of water. The steam distillate containing the dehydrated material was treated with NaCl (25g) and the upper layer carefully separated and dried over activated molecular sieves overnight. This product was treated with

P2O5(14g) at 140C for three hours. The mixture was then cooled and ice was added to react with P2O5. The Octalin was taken up by ether. The ethereal solution was washed with water, dried over anhydrous Na2SO4 and the solvent evaporated. Distillation of the residue gave 24g of 9,10-Octalin(bp: 38-40C/0.06mmHg, yield:81%).

(ii) 9,10-Decalindiol

To a mixture of formic acid(90%:73ml) and H2O2(27%:27ml) the Octalin was added over a period of half an hour with thorough stirring. The temperature was kept at 45C during the addition and afterwards, first by cooling and later warming. After the addition, the mixture was warmed and stirred for another six hours and was left overnight. The product was diluted with water(160ml), then 50g NaCl was added and well mixed. An oily layer separated which soon solidified and it was left aside in the ice bath for several hours. The product was collected, washed once with water and pressed dry. The crude hydroformoxy derivative thus obtained was hydrolysed by adding it to an ice cold solution of NaOH(2M:14g) in water(26ml) with cooling(ice bath) and stirring. The mixture was then stirred at room temperature for half an hour and finally at 75-80C for another 20 minutes. The reaction mixture was next diluted with water(250ml)and after several hours the crystalline product filtered off, washed with water and roughly dried. The almost dry crystal was recrystallised from acetone(2.5 ml for every gram of diol). The white solid obtained was further purified by sublimation(mp:80-82C, yield:30%).

(iii) Cyclodecane-1,6-dione

Sodium dried benzene(42ml) was placed in a 250ml flask carrying a mechanical stirrer and a condenser. Benzene was well stirred and molten 9,10-decalindiol(7g) was added. In this way undissolved diol was left as a finely dispersed powder. Lead tetraacetate which was stored over glacial acetic acid was dried over KOH pellets in a desiccator before use, 22g of it was then introduced at room temperature and in 5 to 6 lots during one and half hours at suitable intervals. After the addition, the reaction mixture was stirred for another 3 hours and finally refluxed for 30 minutes then left at room temperature overnight. Excess lead tetraacetate was destroyed by adding some glycerol. The precipitated lead tetraacetate was washed with benzene(4x5ml). The combined filtrate and washings were washed with brine(4x10ml), and solvent was removed. The residue was recrystallised from dichloromethane. (mp:94-96C, yield:14%). M/e:168

$C_{10}H_{16}O_2$ (168.24) Calc. C=71.39 H=9.59

Found C=71.02 H=9.35

(iv) Cyclodecane-1,6-diol

$LiAlH_4$ (1.28g) was dissolved in 64ml anhydrous ether. Ethereal diketone solution(1g in 26ml ether) was added dropwise to the above mixture with vigorous stirring. The temperature was maintained at 28C for 30 minutes. Water was then added carefully until decomposition of excess $LiAlH_4$ was completed. The filtrate was dried over anhydrous Na_2SO_4 . The solvent was then stripped off and recrystallised from acetone(mp:126-128c, yield:64%).

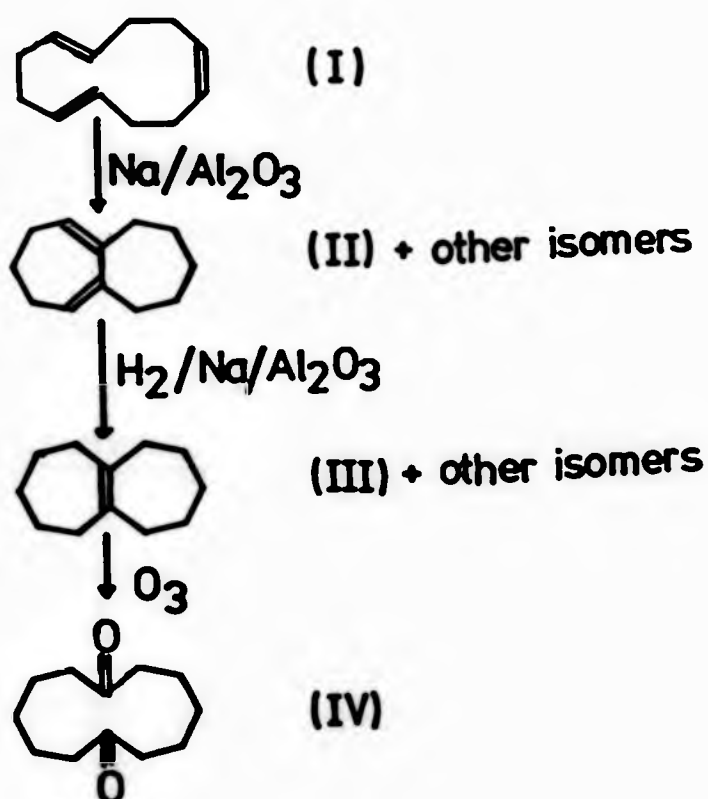
$C_{10}H_{20}O_2$ (172.27) Calc. C=69.72 H=11.70

Found C=69.84 H=11.22

4.1.2 Synthesis of 12 Membered Ring

(cyclododecane-1,7-diol) <52>

It has been shown that bicyclo(5.5.0)dodecadiene(II) can be formed by isomerisation of cyclododeca-1,5,9-triene(I) on 'high surface' sodium<51,52>. Partial hydrogenation of conjugated dienes can be performed on the same catalyst to give bicyclo(5.5.0)dodecene isomer(III). The 12 membered diketone(IV) can be obtained by ozonolysis of compound(III).



(i) Isomerisation Step

Neutral aluminium oxide(20g) was dried at 500C for 20 hours and transferred to a one litre round bottom flask under dry nitrogen. Freshly cut sodium(0.9g) was added and the stirred mixture heated slowly to 200C. The molten metal became dispersed on the alumina surface and assumed a dark blue colour.

After cooling, cis,trans,trans-cyclododeca-1,5,9-triene(20g)

dissolved in heptane(200ml) was added, and the mixture refluxed with stirring until the gas chromatogram showed that all the starting material had been consumed, and that five new main peaks had appeared. This required about 3 days.

(ii) Hydrogenation Step

The above mixture was filtered, and the solution was then added to a one litre flask containing freshly prepared sodium-aluminium oxide catalyst. To this mixture hydrogen gas was introduced, and stirring and refluxing was continued. After 7 days, the gas chromatogram showed a simplification into two main peaks. The catalyst was then filtered off and washed with heptane. The catalyst was immediately destroyed with methanol.

(iii) Ozonolysis Step

The catalyst free heptane solution(about 200ml) from the reduction was transferred to an ozonation vessel(a two necked flask), and a mixture of glacial acetic acid(100ml) and water(100ml) was added. After cooling to 0C, oxygen gas was bubbled in via a ozoniser (Ozoniser MKII, BOC Cryoproducts) for 24 hours.

The aqueous acetic acid layer was separated from the heptane layer, neutralised with sodium bicarbonate, and extracted three times with ether. The ether solution was dried with anhydrous CaCl₂ and evaporated. The viscous oily residue soon crystallised. The solid was filtered off and recrystallised twice from methanol to give 1.3g 1,7-cyclododecanedione(mp:133-135C). M/e:196

C ₁₂ H ₂₀ O ₂ (196.29)	Calc.	C=73.43	H=10.27
	Found	C=73.64	H=10.58

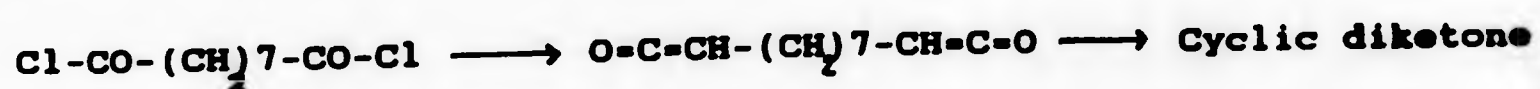
(iv) Reduction Step

The diketone(1.3g) obtained was mixed with 15ml of tetrahydrofuran(THF), and added to a suspension of LiAlH_4 (3g) in THF(15ml). The mixture was allowed to reflux overnight under a dry nitrogen atmosphere. Excess LiAlH_4 was destroyed by careful addition of water. After filtration, the residual white solid was washed with 100ml of THF. The combined THF solutions were then evaporated, and the solid left behind recrystallised from ethanol/water mixture to give 0.4g cyclododecane-1,7-diol(mp:170C).

$\text{C}_{12}\text{H}_{24}\text{O}_2$ (200.32) Calc. C=71.94 H=12.08
 Found C=71.53 H=12.26

4.1.3 Synthesis of 16 Membered Ring(cyclohexadecane-1,9-diol)<47>

Acid chloride of azelaic acid can be dehydrogenated by triethylamine to form the bifunctional ketene derivative. This ketene condensed linearly to give the ketene polymer, but under condition of high dilution, cyclic ketene can be obtained. Hydrolysis and decarboxylation of the cyclic ketene gives the diketone.



(i) Azelaoyl Chloride

Thionyl chloride(28g) was added to azelaic acid(20g), the mixture was heated at 60C for two hours and then at 65C with dry nitrogen blowing over until evolution of hydrogen chloride and sulphur dioxide ceased. Vacuum distillation at 166C/18mm

gave 25g of azelaoyl chloride.

(ii) Cyclisation Step

The high dilution technique was employed. Azelaoyl chloride(10g) in benzene(500ml) was transferred to the dropping funnel and added dropwise to a solution containing 1000ml benzene and 30ml triethylamine over 40 hours under reflux. Triethylamine hydrochloride salt and polymeric material was formed during reaction. After the addition, the reaction mixture was cooled to room temperature and filtered. The yellow solution was then washed with dilute HCl(5%) and water until the washings became neutral. The benzene solution was dried over anhydrous MgSO₄ and evaporated.

(iii) Hydrolysis and Decarboxylation

To the residual light yellow oil was added 20ml ethanol and, very slowly with cooling, a solution of 7.2g potassium hydroxide in 20ml ethanol. The solution was then allowed to stand at room temperature for ten hours and refluxed for another hour. A precipitate, presumably potassium carbonate, started to form shortly after the addition of alkali. The mixture was diluted with 50ml of water and extracted with ether. The ether extract was washed with water until neutral, dried over MgSO₄, and finally evaporated. The residual yellow oil was run over a neutral alumina column using benzene as eluant. After evaporation, the residue soon solidified and was purified by vacuum sublimation to give cyclohexadecane-1,9-dione which melts at 55C(yield 5%).

M/e:252

C₁₆H₂₈O₂(252.40) Calc. C=76.14 H=11.18

Found C=75.98 H=11.54

(iv) Reduction

The above diketone was reduced to cyclohexadecane-1,9-diol by using LiAlH_4 in THF. (mp:99C, yield:70%).

$\text{C}_{16}\text{H}_{32}\text{O}_2$ (256.43) Calc. C=74.94 H=12.58
 Found C=74.86 H=12.21

4.1.4 Synthesis of 18 Membered Ring

(cyclooctadecane-1,10-diol) <49>

The corresponding diketone can be prepared via Dieckmann cyclisation of diethyl ester of sebacic acid using potassium t-butoxide in xylene under high dilution conditions.

(i) Diethyl Sebacate

30g of sebacic acid, 60g of absolute alcohol, 40ml of toluene and 0.2g of concentrated H_2SO_4 were mixed in a 250ml flask attached to a short fractionation column with a downward condenser and heated in an oil bath at 150C. After the acid dissolved, an azeotropic mixture of ethanol, toluene and water began to distil at about 75C. The distillate was collected in a flask containing 50g of anhydrous K_2CO_3 . The filtrate was then returned to the reaction flask and the distillation process repeated. The crude diethyl ester was purified by vacuum distillation at 103C/0.07mm to give 35g diethyl sebacate.

(ii) Dieckmann Cyclisation

To a refluxing solution of 600ml xylene and 54g potassium t-butoxide was added 25.8g diethyl sebacate in 200ml xylene dropwise over a period of 24 hours. During this period, ethanol/xylene mixture was removed by distillation at approximately the same rate as the diester addition. The

reaction mixture was finally cooled to room temperature. Polymeric material was formed throughout the reaction.

The reaction mixture was then made acidic by adding glacial acetic acid in large excess. After filtering off the polymeric material, the solution was washed with water(200ml) three times, and was concentrated by reduced pressure evaporation. To the yellow residue was added a dilute solution of HCl(3M), hydrolysis and decarboxylation was effected by refluxing overnight. The reaction mixture was then extracted with ether, and the combined solution washed with 10% NaHCO₃ solution. After evaporation, the residue was run over an alumina column using ether as eluant. The almost white solid was then purified by vacuum sublimation to give 0.4g cyclooctadecane-1,10-dione(mp:89C). M/e:280

C ₁₈ H ₃₂ O ₂ (280.45)	Calc.	C=77.09	H=11.50
	Found	C=77.34	H=11.79

(iii) Reduction

Cyclooctadecane-1,10-dione was reduced to cyclooctadecane-1,10-diol by using LiAlH₄ in THF(mp:124C, yield:80%).

C ₁₈ H ₃₆ O ₂ (284.49)	Calc.	C=76.00	H=12.76
	Found	C=75.87	H=12.60

4.1.5 Synthesis of 22 membered ring

(cyclodoeicosane-1,12-diol)<49>

This monomer was also synthesised via Dieckmann cyclisation reaction described above. The physical properties and yield of these preparations are shown as following

(i) cyclodoeicosane-1,12-dione

mp:55C Yield:4% M/e:336

C₂₂H₄₀O₂(336.56) Calc. C=78.51 H=11.98

Found C=78.12 H=11.65

(ii) Cyclodoeicosane-1,12-diol

mp:115C Yield:68%

C₂₂H₄₄O₂(340.59) Calc. C=77.58 H=13.02

Found C=77.11 H=13.23

4.2 Synthesis of Diazacrown Ethers

Diazacrown ethers can be prepared either by using high dilution techniques or template synthesis. The former was employed in the following synthesis.

4.2.1 Synthesis of Diaza-12-crown-4-ether<53>

(1,7-dioxa-4,10-diazacyclododecane)

Diaza-12-crown-4-ether is usually prepared by cyclisation of 1,5-diamino-3-oxapentane and diglycolic acid dichloride followed by reduction of the diamide.

In spite of low yield due to formation of polymeric materials, difficulties were also encountered in the diamine synthesis.

4.2.1.1 1,5-Diamino-3-oxapentane

According to Lehn^{<54>} diamines can be obtained by Gabriel synthesis, this method was employed in the synthesis of diaza-24-crown-8-ether and will be mentioned later.

1,5-diamino-3-oxapentane here was prepared from the corresponding diazide by reduction. Three different kinds of reducing agents have been employed viz LiAlH_4 , the less common H_2S , and catalytic hydrogenation using Palladium.

(i) 3-Oxapentane Diazide



Sodium azide (23.01g) was added into a stirring solution of bis-(2-chloroethyl) ether (30g) in 50ml of anhydrous dimethyl sulphoxide (DMSO) and the temperature was kept at 90C for 4 hours. The mixture was then poured into 50g of ice and extracted with ether. The ether phase was thoroughly washed with water, dried over anhydrous Na_2SO_4 and evaporated. Vacuum distillation gave 31g 3-oxapentane diazide (bp:43C/0.01mm)

(ii) LiAlH_4 as Reducing Agent

LiAlH_4 was dissolved in 400ml of anhydrous tetrahydrofuran (THF), and to this solution was added 24g 3-oxapentane diazide in 80ml of THF. The mixture was refluxed for 18 hours under a nitrogen atmosphere. The residual LiAlH_4 was destroyed by adding water (20ml), NaOH (15%, 24ml) and water (15ml) respectively. The granular white solid obtained was extracted with THF in a Soxhlet extractor for 24 hours. The solvent was then stripped off and the residue was distilled at 24C/0.15mm (yield:3g). H nmr: (CDCl_3) 1.3(- NH_2 , s),

2.9(-CH-N-,t), 3.5(-CH2-,t)ppm

(iii) H₂S as Reducing Agent<54>

Hydrogen sulphide was bubbled through a boiling solution of 3-oxapentane diazide(25g) and triethylamine(1.65ml) in ethanol(33ml) for 24 hours. After cooling, concentrated HCl solution was added slowly and the precipitated sulphur was filtered off. NaOH(16g) was added to the filtrate with cooling and continuously extracted with chloroform for 24 hours. Vacuum distillation gave 0.5g product.

(iv) H₂/Pd as Reducing Agent

1.5g of Palladium on charcoal(5%) was added to a glass jar containing 20g 3-oxapentane and 60ml dry ethanol. Hydrogenation was effected using a low pressure hydrogenator (Parr Hydrogenator) under a pressure of 10N/m². Vacuum distillation gave 8.5g of product.

4.2.1.2 Diglycolic Acid Dichloride



To 13.4g of diglycolic acid covered with chloroform(150ml), 45g of phosphorous pentachloride was added at once. After standing for 10 minutes at room temperature, the mixture was heated slowly to reflux temperature over a period of 1 hour and was then left under reflux for 2 hours. The solvent was evaporated at room temperature under reduced pressure. Then, the phosphorous oxychloride formed during the reaction was taken off(24C/0.2mm). The remaining oil was distilled at 56-57C(0.2mm) and gave 13.4g of a colourless liquid.

0.5ml NaOH(15%) and 2ml of water. The mixture was filtered and the solvent evaporated. The residue was run over a neutral Al₂O₃ column using benzene as eluant. After concentration, recrystallisation from benzene/heptane gave 0.3g product (mp:83-84C). H nmr(CDCl₃): 2.4(-NH,s), 2.8(-CH₂-N-,t), 3.66(-CH₂-,t)ppm

4.2.2 Synthesis of Diaza-24-Crown-8-Ether<53>

(1,7,10,13,19,22-hexaoxa-4,16-diazacyclotetracosane)

Both Gabriel synthesis and reduction of the corresponding diazide have been tried to prepare the linear diamine. The preparations are described as follows.

4.2.2.1 1,11-Diamino-3,6,9-Trioxaundecane

(i) Gabriel Synthesis

(a) Tetraethylene Glycol Dibromide

150g of tetraethylene glycol and 50g of anhydrous pyridine were slowly added to 364g of phosphorous tribromide while agitating and cooling the mixture. After cooling to room temperature, the mixture was poured onto ice and extracted with ether. The combined extracts were washed with water and then dilute HCl(10%). After evaporation, the residual oil was distilled at 124C/0.4mm to give 54g of the titled compound. H nmr(CDCl₃): 3.7(-CH₂-,m)ppm

(b) Tetraethylene Glycol Diphthalimide

52g of diphthalimide was mixed with 16.13g of KOH in 162ml of absolute ethanol. The mixture was stirred for 24 hours, and 57g of potassium phthalimide was obtained after filtration. 47.57g of tetraethylene glycol dibromide was mixed with 220ml

of dimethylformamide and 57g of the potassium phthalimide obtained above, and the mixture was heated for 8 hours at 100C. After cooling, the mixture was poured into 1200ml of cold water. The precipitate was filtered, washed with water and then acetone, and dried under vacuum. Recrystallisation from ethanol gave 44.5g the titled compound(mp:109C). H nmr(CDCl₃): 3,6(-n-CH₂-,s), 3.8(-CH₂-CH₂-O-,m), 7.8(-Ar-,m)ppm
 (c) 1,11-Diamino-3,6,9-Trioxadecane

44.5g of the above compound was suspended in 175ml of ethanol and heated under reflux. 19.2g of hydrazine(64%, 30ml) was added and heating was continued for 3 hours. After cooling, 10M HCl was added until pH 1 was obtained and the mixture was heated under reflux for an additional hour. The residual mixture was filtered, and ethanol was removed from the filtrate. To the residual liquid was added 45ml of water and the solution was then saturated with KOH. The mixture was filtered to remove precipitated KCl, poured into a liquid-liquid extractor and extracted with benzene for 4 days. After concentration, the residual oil was distilled at 106/1.28mm to give 2g the titled compound. H nmr(CDCl₃):

1,3(-NH₂,s), 2.85(-CH₂-N-,t), 3.48 & 3.6(-CH₂-O-, t & s)ppm

(ii) Reduction of the Diazide

(a) 1,11-Diazide-3,6,9-Trioxaundecane

Sodium azide(13.65g) was added to a stirring solution of tetraethylene glycol dibromide(20g) in 100ml of anhydrous DMSO and kept at 90C for 4 hours. The mixture was then poured into 200ml cold water and extracted with ether. After concentration, the titled compound was distilled at 119C/0.15mm to give 7g of colourless oil.

(b) 1,11-Diamino-3,6,9-Trioxaundecane

Hydrogen gas was bubbled, through a solution containing 7g of diazide obtained above, 200ml ethanol and 1g of Palladium(5% on charcoal), at 50C for 24 hours using a low pressure hydrogenater. After concentration and distillation, 2.8g of the titled compound was obtained.

4.2.2.2 Tetraglycolyl Acid Chloride

(a) Tetraglycolyl Acid

100g of nitric acid(density:1.38) was heated to 45C and then 20g of tetraethylene glycol was added in small portions so as to keep the temperature at about 45C. After the addition was completed, the mixture was stirred at 45C for 1 hour and then at 80C for another hour. The solution was evaporated under reduced pressure at 80C for 4 hours, a viscous paste of brownish colour was obtained. 100ml to 120ml benzene was added and the last trace of water present was distilled off. The diacid was a viscous oil(yield:22g).

(b) Tetraglycolyl Acid Chloride

22g of the acid obtained above, 40g oxalyl chloride, 200ml anhydrous benzene and 5 drops of anhydrous pyridine were mixed and stirred for 6 hours. After filtration and concentration, 25g of slightly yellow viscous oil was obtained. The titled compound did not crystallise. H nmr(CDC13): 3.75(-CH2-O-,m), 4.52(-CO-CH2-,s)ppm

4.2.2.3 5,15-Dioxo-1,7,10,13,19,22--Hexaoxa-4,16-Diazacyclotetracosane

This reaction was carried out by employing high dilution

technique. A solution of 8g of 1,11-diamino-3,6,9-trioxa-undecane in 300ml anhydrous benzene and a solution of 5.4g tetraglycolyl chloride in 300ml benzene were added to 800ml benzene over a period of 20 hours with vigorous agitation and under a nitrogen atmosphere. On termination, the solution was filtered and solvent evaporated. The oily residue was run over a neutral Al₂O₃ using benzene as eluant. After evaporation of the solvent, the titled compound was produced as a viscous oil (yield: 0.5g). H nmr(CDCl₃): 3.6(-CH₂-O- & -CH₂-N-, m), 3.85(-CO-CH₂-O-, s)ppm

4.2.2.4 1,7,10,13,19,22-Hexaoxa-4,16-Diazacyclotetracosane

Reduction was carried out using 0.3g LiAlH₄ and 0.5g of the above compound in 20ml of THF at 70C for 20 hours. (yield:0.15g). H nmr(CDCl₃): 3.5-3.9(-CH₂-N- & -CH₂-O-, Broad peaks), 4.0-4.3(-CO-CH₂-O-, very broad peaks)ppm

4.3 Synthesis of Polymers

Polymers containing rings larger than eight carbon atoms are prepared following the methods described in Chapter 4, part one of this thesis. Polymerization condition in every case was 0.8 per cent stannous octoate based on the weight of the diol, chlorobenzene as solvent, at 100C for 24 hours. All the isocyanates employed were purified by vacuum sublimation before use.

CHAPTER FIVE

POLYMERS CONTAINING CYCLOALKANES AND

AZA-CROWN-ETHERS IN THE BACKBONE

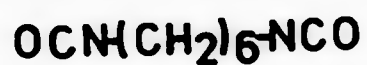
5.0 Introduction

It is now well established that secondary relaxations in amorphous or partially crystalline polymers can result from the rotations of side groups attached to the mainchain or from limited motions within the chain backbone. These are often detected by locating a loss process in a dynamic mechanical spectrum. To date the exact origins involved in these relaxations have been established in only a few systems<23>.

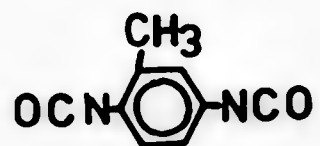
It has been demonstrated that relaxations of pendant cycloalkyl rings by ring inversions can occur below the glass transition temperature<25> and it is interesting to see how these 'rings' behave in the sub-glass transition temperature range when they are incorporated in the polymer backbone.

Polyurethanes and polyureas based on cycloalkanediols, aza-crown-ethers and diisocyanates were prepared. The diisocyanates commonly used are few in number, four different diisocyanates of the following structures were employed in the subsequent studies:

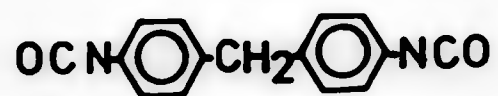
Hexamethylene diisocyanate (HDI)



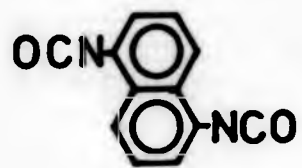
Tolylene-2,4-diisocyanate (TDI)



Diphenylmethane-4,4'-diisocyanate (MDI)



Naphthylene-1,5-diisocyanate (NDI)



All the saturated rings are designated according to the number of atoms in the ring.

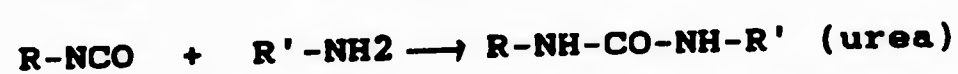
Hence, 'HDI-AZA18C' represents a polymer composed of aza-18-crown-6-ether(AZA18C) and hexamethylene diisocyanate(HDI). While the saturated cycloalkyl units are denoted by the number of atoms, for example, '8-TDI' means cyclooctyl unit(8) and tolylene 2,4-diisocyanate(TDI).

5.1 Polvurethanes and Polyureas

5.1.1 General Chemistry<55>

The common reactions of isocyanates can be grouped into two main types: (a) the reaction of isocyanates with compounds containing reactive hydrogens and (b) self addition to give a polyisocyanate.

The addition to compounds containing reactive hydrogen like amines and alcohols are the best known and the most useful in practice.



Hence, the addition of diisocyanates to diamines or diols yield high molecular weight substances. These reactions are the backbone of polyurethane chemistry. In addition, isocyanates undergo further reactions with the groups containing active hydrogen which are present in all the primary products of the reactions mentioned above. Thus isocyanates can react with urethane to give allophanate and with urea to give biuret.



Fortunately, the relative rates of these reactions are much less than that of the normal reaction unless the reactivity of the diol is low or the polymerisation temperature is higher than 150C.

5.1.2 Reactivity of Intermediates<55>

The reaction of an isocyanate with an alcohol is essentially a nucleophilic attack of the alcohol on the carbon

atom of the isocyanate group followed by a 1,3 shift of the hydrogen atom. Hence, aromatic isocyanates would be expected to be more reactive than aliphatic isocyanates. Substitution of electron withdrawing groups on the aromatic ring enhances the reactivity, while steric hindrance will have the opposite effect.

In a similar manner the reactivity of the alcohol increases as its nucleophilicity increases, hence primary alcohols react readily at room temperature, secondary alcohols usually react only about 0.3 times as fast, while tertiary alcohols react much more slowly, approximately 0.005 times as fast as the primary^{<55>}.

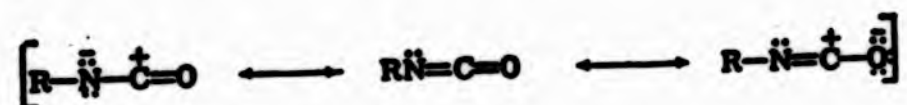
5.2 Effect of Catalysts and Solvents

According to Lyman^{<56>}, the ideal conditions necessary to obtain high molecular weight polyurethane without using catalysts are to use aprotic solvents like DMSO at a temperature less than 150C. As a starting point, the above conditions were followed using TDI as a linking unit. The material obtained was designated as polymer 8-TDI:1, its number average molecular weight was about 4000 which was measured by VPO, and its inherent viscosity in DMF at 50C was 0.097.

Apparently, the molecular weight was unsatisfactory although the solvent was vigorously dried and polymerisation was carried out under a dry nitrogen atmosphere to exclude moisture. This could possibly be due to the low reactivity of the secondary -OH group and the electron donating -CH₃ group attached. As a result, the use of catalysts were attempted in

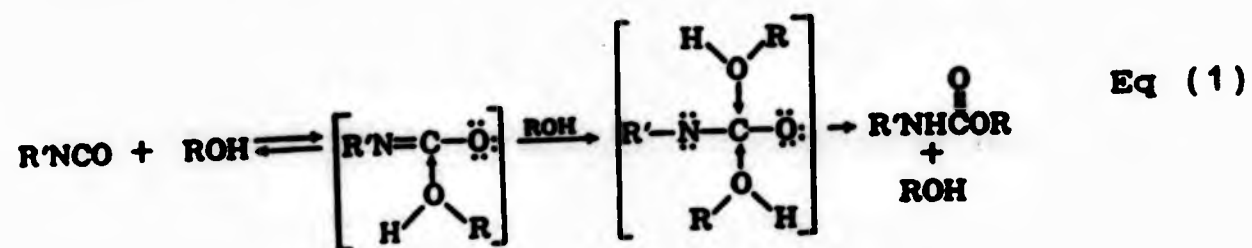
order to facilitate the building up of the molecular weight.

In chemical reactions, the isocyanates may react as might be expected in one or more of the following resonance forms:

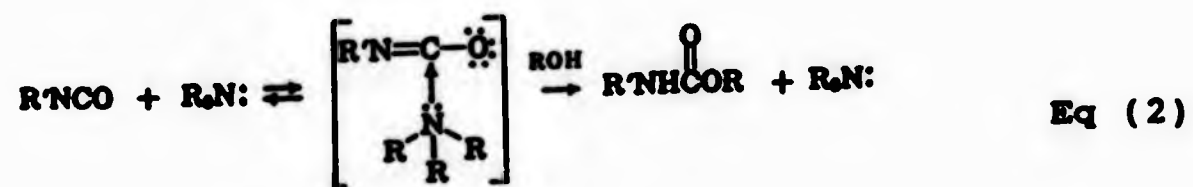


Such resonance structures obviously suggest the possibility of ionic reactions, with electron donors attacking the carbonyl carbon and electron acceptors attacking the oxygen or nitrogen. Hence, catalysis by Lewis acids and bases might be expected.

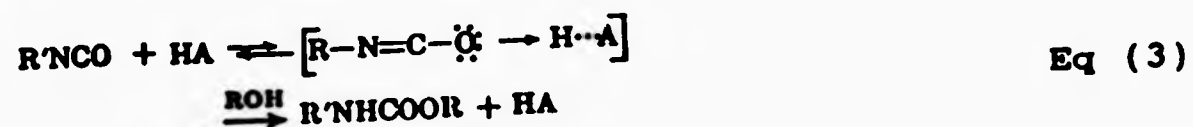
As proposed by Baker and coworkers^(57,58,59), the reaction sequence may be pictured as in equation (1)



A basic catalyst could participate similarly, as shown in equation (2)



In addition, one might expect an acid catalyst to participate as in equation (3).



Other electron accepting materials, eg metal compounds, could be expected to serve as Lewis acids and hence as catalysts.

From these examples it is apparent that a general scheme for the reactions of isocyanates with active hydrogen compounds may be as follows:



Table 5-1 shows the effects of catalysts and solvents on the inherent viscosities. The amount of catalyst used in each polymerisation was based on the weight of the diol. Two different kinds of catalysts were used, they are stannous octoate (Lewis acid) and triethylenediamine (Lewis base). There was a general increase in viscosity when catalysts were employed.

As was mentioned in the preceding paragraph, isocyanate-alcohol reactions can be catalysed by a Lewis base, for comparison purposes triethylamine was also used to verify its catalytic effect.

Polymer 8-TDI:2 which used triethylamine as catalyst shows only a slight increase in viscosity when compared with polymer 8-TDI:1. However, when triethylenediamine was employed, there was quite a significant increase in viscosity (polymer 8-TDI:3).

Table 5-1 Effect of solvent and catalyst to polymer 8-TDI

<u>Sample</u>	<u>Solvent</u> ^a	<u>Catalyst</u> ^b	<u>Viscosity</u> ^c (10 ⁻¹)	<u>M.W.</u>
8-TDI:1	DMSO	-	0.97	4,000
8-TDI:2	DMSO	TE(2.8%)	1.15	
8-TDI:3	DMSO	TD(2.8%)	1.44	
8-TDI:4	DMSO	TD(3.6%)	1.38	
8-TDI:5	DMSO	TD(4.0%)	1.32	
8-TDI:6	DMSO	SO(0.4%)	1.08	
8-TDI:7	DMSO	SO(2.0%)	1.57	
8-TDI:8	DMSO	SO(2.8%)	1.74	
8-TDI:9	CB	SO(0.16%)	1.12	
8-TDI:10	CB	SO(0.8%)	3.45	
8-TDI:11	CB	SO(1.6%)	2.26	
8-TDI:12	NB	SO(1.6%)	2.38	

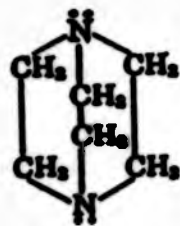
Table 5-2 Effect of solvent and catalyst to polymer 8-MDI

8-MDI:1	DMSO	SO(0.8%)	0.88	12,000
8-MDI:2	CB	SO(0.8%)	2.99	

Note:

- a) DMSO Dimethylsulphoxide
CB Chlorobenzene
NB Nitrobenzene
- b) TE Triethylamine
TD Triethylenediamine
SO Stannous Octoate
- c) Inherent viscosity in DMF at 50°C

Based on Baker's mechanism, Farkas and Flynn^(60,61) thought that the higher catalytic effect of triethylenediamine



is due to relief of steric hindrance so that the nitrogen atoms are more readily accessible to the reactants, while for triethylamine, the carbon-nitrogen bonds are capable of free rotation around the nitrogen atoms, this may sterically hinder the close approach of another molecule.

The amount of triethylenediamine used was also critical. The viscosity decreased with increased concentration of catalyst, this phenomenon was shown by polymers 8-TDI:3, 4, and 5. Triethylenediamine was purified by sublimation before use, this should eliminate the possibility of impurity, so the reduced viscosity may be due to the decomposition of the catalyst at high temperature which disturbed the stoichiometric balance.

Stannous octoate seems a better catalyst than triethylenediamine in this situation, and this was reflected in the higher viscosities of polymers 8-TDI:7 and 8.

However, the polymerisation using chlorobenzene suffered from early precipitation. The higher viscosity may be attributed to the narrower molecular weight distribution. The number average molecular weight of this polymer could not be obtained using a membrane osmometer because the membrane degenerated at 74°C which was the temperature recommended by the manufacturer when DMF is the solvent. Nitrobenzene was also tried (polymer 8-TDI:12), the result was similar to chlorobenzene.

From the above study we can conclude that stannous octoate is a better catalyst than triethylenediamine, while chlorobenzene is a better solvent than DMSO.

This conclusion was further verified by polymer 8-MDI. Table 5-2 shows the results. With the amount of catalyst kept constant, the viscosity of polymer using chlorobenzene as solvent was three times higher than that using DMSO ($M_n=12000$).

5.3 Polymers Containing Aza-crown-ethers

5.3.1 Polyamides

The TBA damping spectra of the aza-18-crown-6-ether polyamides series are shown as a function of linking unit in Figure 5-1, where $-\log(1/n)$ is plotted as a function of temperature for each sample. The spectra are displayed vertically to allow easier comparison.

The temperatures corresponding to the various damping maxima are recorded in Table 5-3 together with the T_g located by DSC.

In accordance with normal practice, the transitions in any polymer sample are identified by the Greek letter α , β , γ .

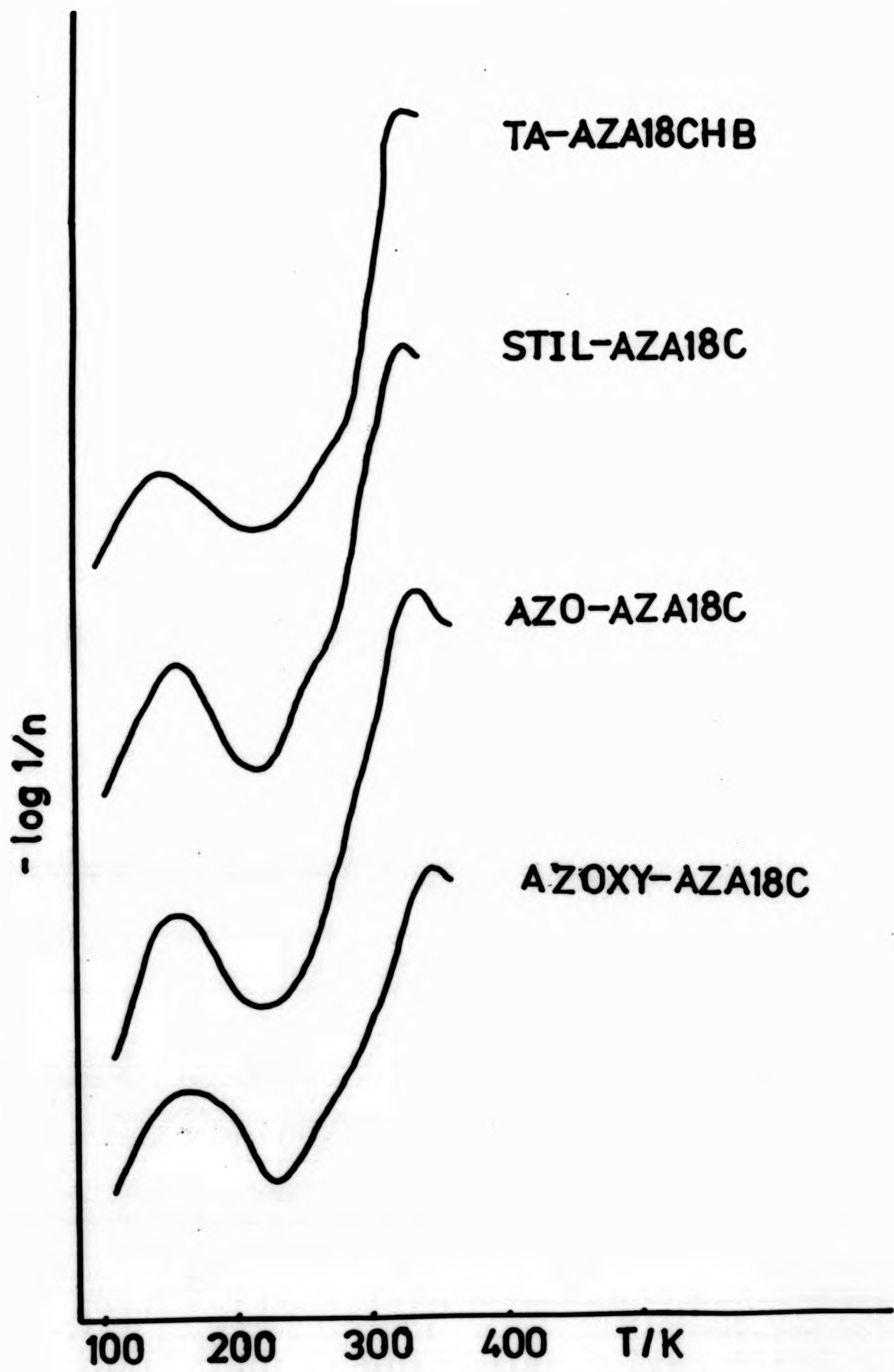


Fig. 5-1 Plots of the logarithmic decrement for polymer TA-AZA18CHB, polymer STIL-AZA18C, polymer AZO-AZA18C and polymer AZOXY-AZA18C.

Table 5-3 The damping maxima of AZA18C polyamides

<u>Sample</u>	<u>Damping maxima TBA(K)</u>				<u>Tg DSC(K)</u>
	<u>α</u>	<u>β</u>	<u>γ</u>	<u>δ</u>	
TA-AZA18CHB	320	140	-	-	317
STIL-AZA18C	320	156	-	-	386
AZO-AZA18C	332	156	-	-	355
AZOXY-AZA18C	344	164	-	-	349

Table 5-4 The damping maxima of AZA18C polyureas

<u>Sample</u>	<u>Damping maxima TBA(K)</u>				<u>Tg DSC(K)</u>	<u>Mol. Wt.</u>
	<u>α</u>	<u>β</u>	<u>γ</u>	<u>δ</u>		
NDI-AZA18C	428	288	216	164	413	
TDI-AZA18C	396	260	216	160	392	18,500
MDI-AZA18C	408	280	212	152	387	133,000
HDI-AZA18C	320	-	216	160	303	30,000

Table 5-5 The damping maxima of AZA12C polyureas

<u>Sample</u>	<u>Damping maxima TBA(K)</u>				<u>Tg DSC(K)</u>
	<u>α</u>	<u>β</u>	<u>γ</u>	<u>δ</u>	
TDI-AZA12C	450	200	-	-	470
MDI-AZA12C	440	200	-	-	455
HDI-AZA12C	328	208	136	-	315

etc., where the alpha transition is that occurring at the highest temperature, beta the next highest, and so on.

These polymers have been discussed in Chapter Eleven in the first part of this thesis. Unlike conventional polyamides, these polymers do not possess H-bonding atoms, as a consequence, their glass transitions are relatively low.

All these spectra have two features in common, the alpha transition in the temperature range 320-344K and a beta transition in the low temperature region between 140K and 164K.

The alpha relaxation is due to large scale conformational rearrangements of the chain backbone. These rearrangements involve cooperative thermal motions of individual chain segments. This relaxation can be identified easily in a dynamic spectrum as the modulus falls rapidly and the damping rises through a maximum value. The alpha relaxation is usually an indication of the glass transition.

Below the glass transition, the polymer molecules can be described as in a frozen state, molecular motions arising from the rigid linking units are either restricted or insignificant. The striking relaxation which happens in the temperature range 140-160K must be the result of intramolecular relaxation of the ring. It is believed that rings with more than 12 atoms are highly flexible, no cis-trans isomers can exist because of the nearly free rotation about C-C or the O-C bonds; it is assumed that large rings exist predominantly in the form of extended rectangles composed of zig-zag conformations⁽⁴⁶⁾.

5.3.2 Polyureas

5.3.2.1 Aza-18-crown-6-ether

Four different diisocyanates have been chosen as linking units, from the flexible HDI to the rigid NDI, the order of increasing rigidity is as follows:-



The TBA damping spectra for the aza-18-crown-6-ether series of polyureas are shown in Figure 5-2 as a function of different linking units. The temperatures corresponding to the various damping maxima are recorded in Table 5-4 together with the T_g located by DSC.

As would be expected, the alpha transitions are affected by the rigidity of the linking units; for example, the alpha transition of polymer HDI-AZA18C is almost 100K lower than polymer NDI-AZA18C. Although the molecular length of MDI is very close to those linking units used in the polyamide series, its alpha transition is nearly 80K higher than their average. This is apparently due to the urea linkage which is capable of H-bonding thereby increasing the stiffness of the backbone. It is also the presence of H-bonds which raises the alpha transition of polymer HDI-AZA18C close to the polyamides despite the more flexible nature of the hexamethylene unit.

In addition to the alpha transition, three distinct damping maxima can be seen in polymers MDI-AZA18C, TDI-AZA18C and NDI-AZA18C, while for polymer HDI-AZA18C only two are identifiable.

All four polymers have a relaxation peak in the temperature range 152-164K which is also seen in the polyamide series. This we can attribute to intramolecular conformational changes

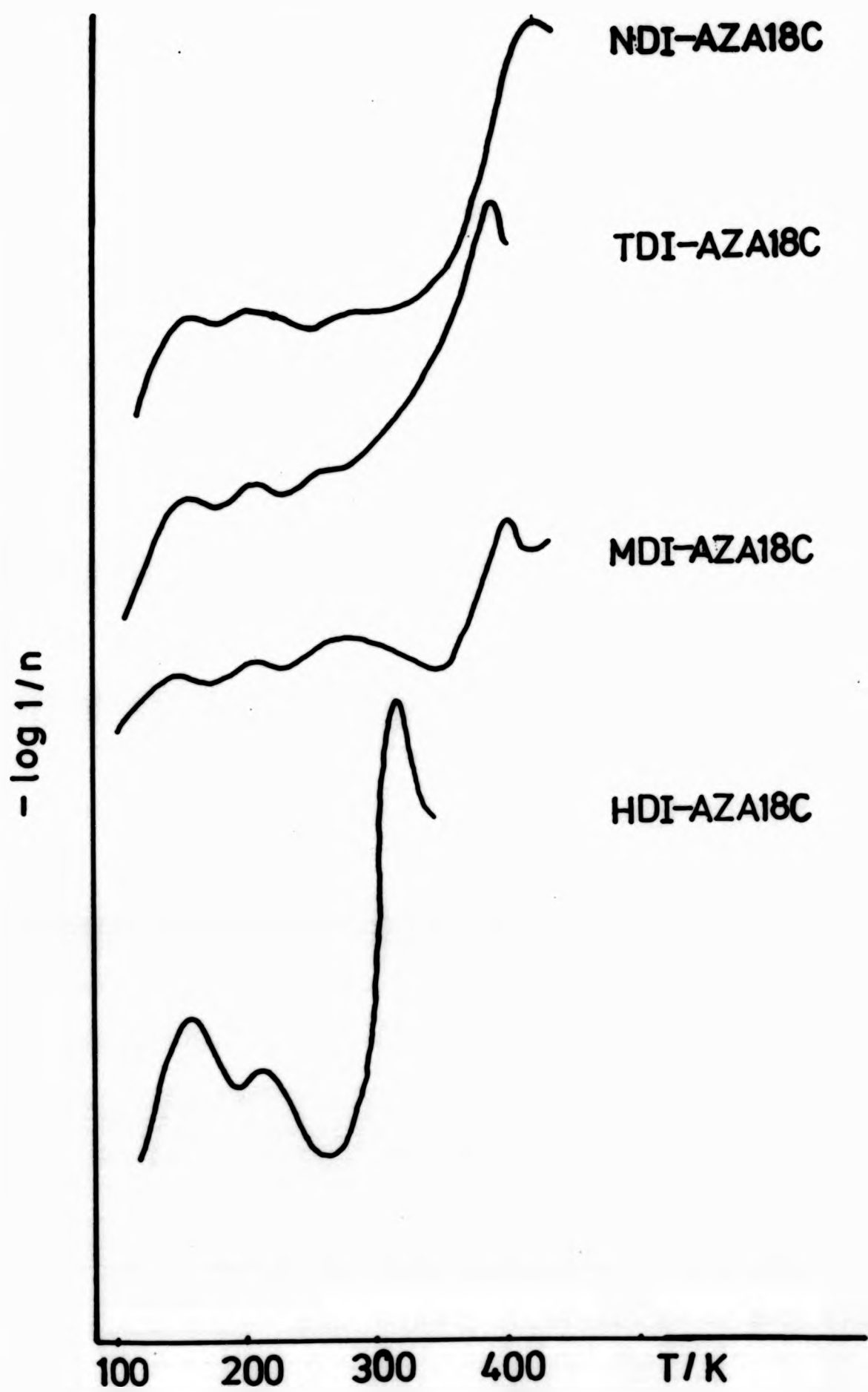


Fig. 5-2 Plots of logarithmic decrement for polymer NDI-AZA18C, polymer TDI-AZA18C, polymer MDI-AZA18C and polymer HDI-AZA18C.

of the ring which appear to be independent of the linking units and the linking groups. Although the intensity of the damping peaks obtained by TBA should not be treated as absolute, the difference in magnitude between polymer HDI-AZA18C and the rest could mean something has happened.

There is an intrinsic difference between HDI and the other linking units. HDI is considered as very flexible because of the methylene sequence. It is well known that a long methylene sequence ($n > 4$) in polymer can have restricted movement below the glass transition temperature, for examples: polyethylene, polyamides, polyesters and oxide polymers, this relaxation is usually observed at about 152K (1 Hz) ^{<3>}. A number of simple movements have been suggested for this restriction motion, these included the Reneker effect, the Pechhold 'kinkblock' movement, and crankshaft rotations.

The Reneker effect ^{<63>}

In the Reneker effect a 180° rotation moves a -CH₂- unit out of colinearity with a mainly trans backbone conformation, and this irregularity may then migrate along the chain by further bond rotation (Figure 5-3).

The Pechhold 'Kinkblock' movement ^{<64>}

The amorphous portion of the polymer is pictured in terms of a meander model with bends produced by gauche conformations disrupting sequences of trans bonds. Smaller 'kinks' or bends are also thought to form and aggregate into blocks of three or four (Figure 5-4).

Crankshaft rotation

The 'crankshaft' rotation was proposed by Schatzki ^{<65>} and Boyer ^{<66>}. These authors suggested that the trans/gauche

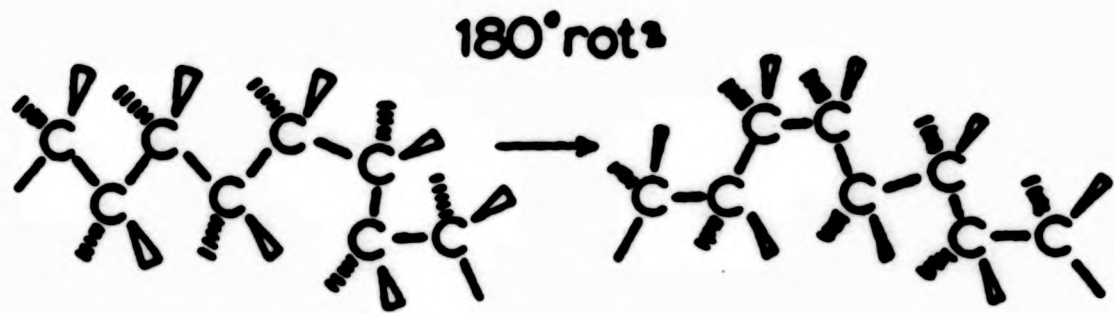


Fig. 5-3 Reneker defect

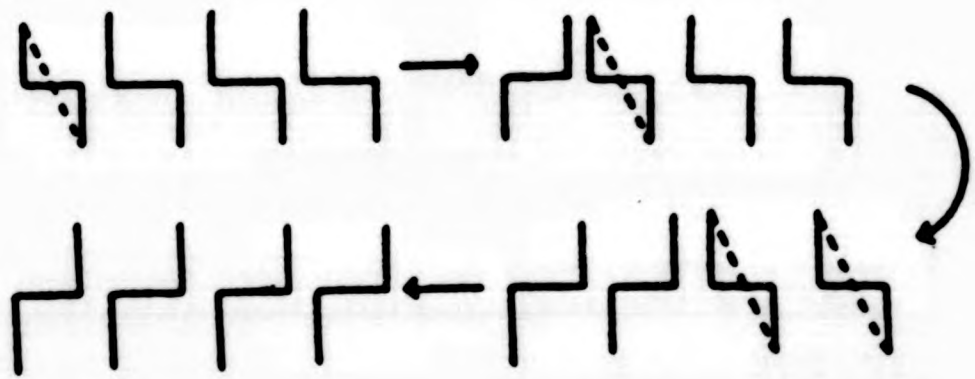


Fig. 5-4 Kink block ($tg^+t \rightarrow tg^-t$)

arrangements in the chain allow bonds to become colinear and a rotational movement about those bonds moves the intervening unit without disturbing the rest of the chain (Figure 5-5).

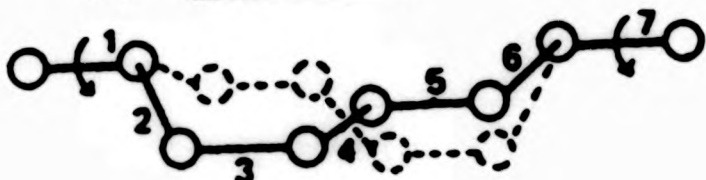
Based on strain energy calculations Boyd and Breitling⁽⁶⁷⁾ criticised the crankshaft mechanism as an unlikely process to occur in a glassy medium at temperatures where such motions were postulated such as the gamma transition in polyethylene. These authors considered a modified Boyer unit in which the stem bonds are parallel but not colinear. In this way, a crankshaft motion can be generated which actually moves along the chain rather than remaining fixed within four carbon atoms (Figure 5-6). They called this a 'flip-flop' mechanism.

As in all these crankshaft models, bond colinearity is required, and this may not always be a high probability structure.

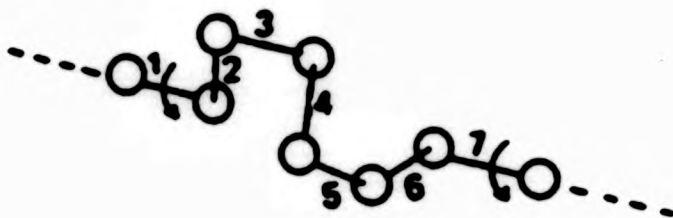
Cowie⁽⁶⁸⁾ proposed an alternative or complementary mechanism with the Boyd-Breitling flip-flop model which was called 'limited bond conformational rearrangement'. The Cowie approach considered the elementary process of the rearrangement in a linear sequence which entails migration of a gauche bond two positions along the chain without a sign change. Formally this is represented by a ttg- to g-tt sequence change and is illustrated in Figure 5-7. Virtually no geometric rearrangement need occur outside the three-bond unit concerned in the transformation, and the unit incorporates six methylene units in which the two stem bonds remain essentially anchored in the matrix. Hence, the large damping peak at 160K of polymer HDI-AZA18C might be a superimposition of two relaxations of different origins; the intramolecular

CRANKSHAFT MOTIONS

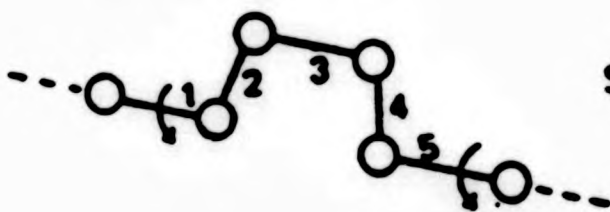
(a) Schatzki



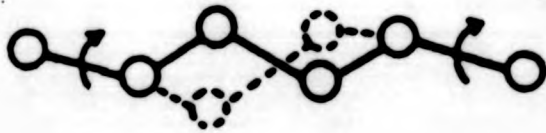
tg^+tg^-



(b) Boyer



strained



unstrained

$tg^-t \rightarrow tg^+t$

Fig. 5-5 Crankshaft motions
(a) Schatzki model
(b) Boyer model

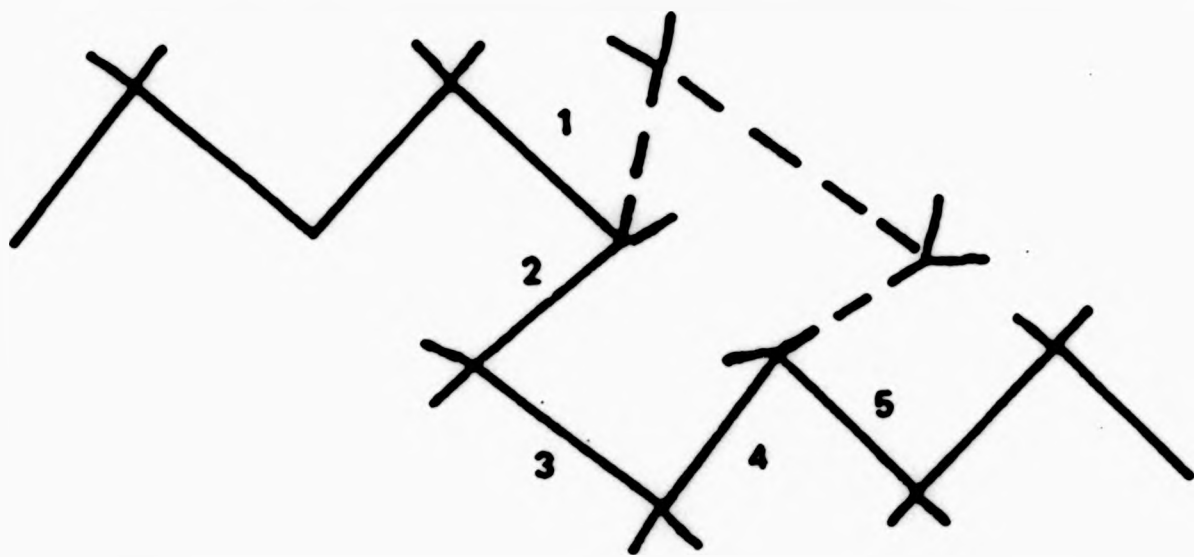


Fig. 5-6 Boyd-Breitling flip-flop motion

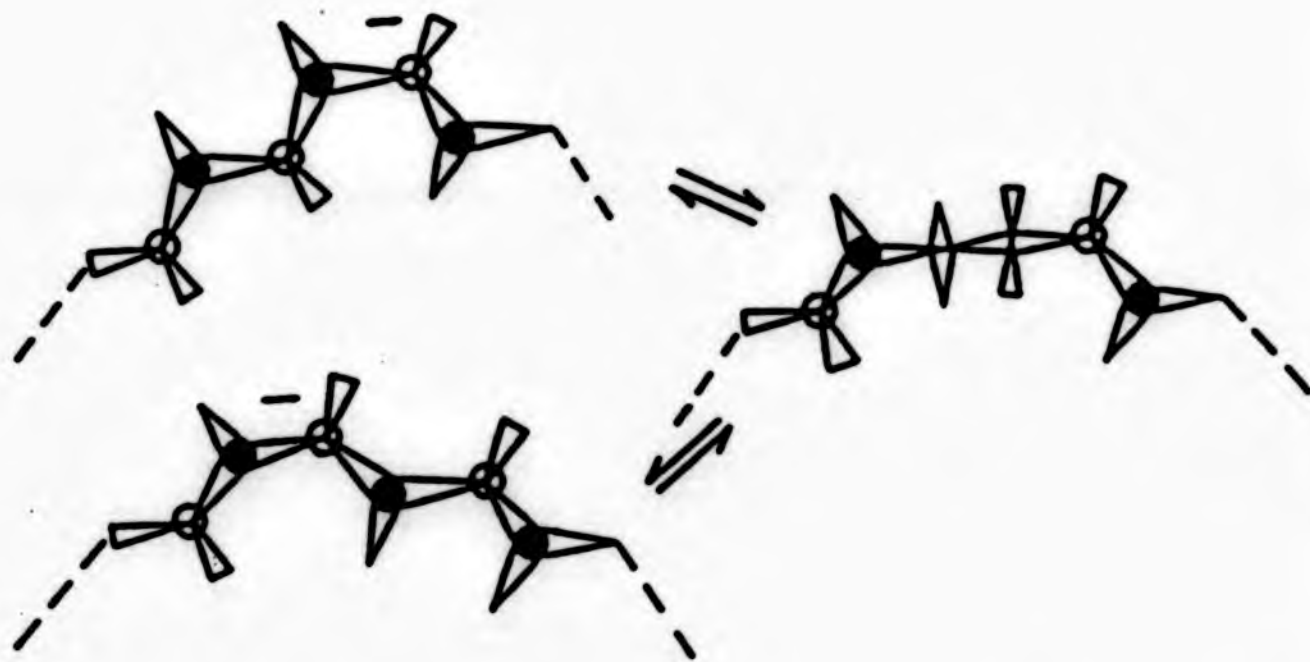


Fig. 5-7 Schematic representation of an elementary process involving migration of a gauche bond two positions without a sign change or significant disturbance of the adjacent segments.

conversion of the ring and the restricted relaxation of the linear methylene block. It could also reflect greater ease of intramolecular rearrangement in the ring attached to the more flexible units, ie more conformations available and so a more intense relaxation peak.

In addition to the damping peak due to the ring, the gamma transitions of polymers MDI-AZA18C, TDI-AZA18C, NDI-AZA18C, and HDI-AZA18c are located in the temperature range 212-216K. This damping peak is less prominent and is absent in the polyamide series. The origin of this relaxation is probably attributed to the rotation of the urea linkage: $-N-CO-NH-$.

The linking group of the polyureas under study is structurally very similar to the conventional amide group: $-R-CO-NH-$. An early interpretation of the damping peak for nylon 612 at 210K(1 Hz) was assigned by Woodward<69> to be the motions of the chain segments including amide groups which were not hydrogen bonded to the neighbouring chains. On the basis of dielectric studies, Curtis has proposed this relaxation process involves the motion of a water-polymer complex<70>. Although all the polymers were rigorously dried before use, this possibility cannot be ruled out.

Figure 5-2 also shows the presence of a beta transition in the temperature range 260-288K for those polyureas containing rigid units(MDI, TDI and NDI). The origin of this damping peak is uncertain, as it is in the proximity of the alpha transition, it is possibly due to segmental rearrangement of the mainchains in the disordered phase of the polymer. This phenomenon has also been found in polyethylene oxide<71>.

Crown ethers are renowned for being capable of complexing

with cations, one would think the intramolecular motion of the crown ether moieties should be restricted once a cation is harboured within the ring. Figure 5-8 shows the damping spectra of the doped and undoped polymer HDI-AZA18C. The dopant used was potassium thiocyanate. The doping procedure is analogous to those described in Chapter Eleven of the first part of this thesis.

Figure 5-8 clearly shows the collapse of the damping peak at 160K after doping while the beta transition at about 216K remains almost unchanged. The same phenomenon can also be seen in polymer MDI-AZA18C(Figure 5-9). As well as the disappearance of the peak at 152K, the beta transition at 280K is now also suppressed. Apparently segmental rearrangement of the mainchains are impeded due to the 'clamped' ring.

5.3.2.2 Aza-12-crown-4-ether

The dynamic mechanical spectra of aza-12-crown-4-ether polyurea series are shown in Figure 5-10. An appropriate solvent could not be found for polymer NDI-AZA18C, indeed, this polymer began to decompose at about 560K according to DSC. The damping maxima of only polymers HDI-AZA12C, MDI-AZA12C and TDI-AZA12C are listed in Table 5-5 along with the T_g obtained by DSC.

As was demonstrated in the aza-18-crown-6-ether series, the alpha transition depends on the nature of the linking units. This effect is more prominent in the present series of polymers, for example, the difference between polymers TDI-AZA12C and HDI-AZA12C is 122K, while for the AZA18C equivalents it is only 76K. This difference is indisputably

HDI-AZA18C

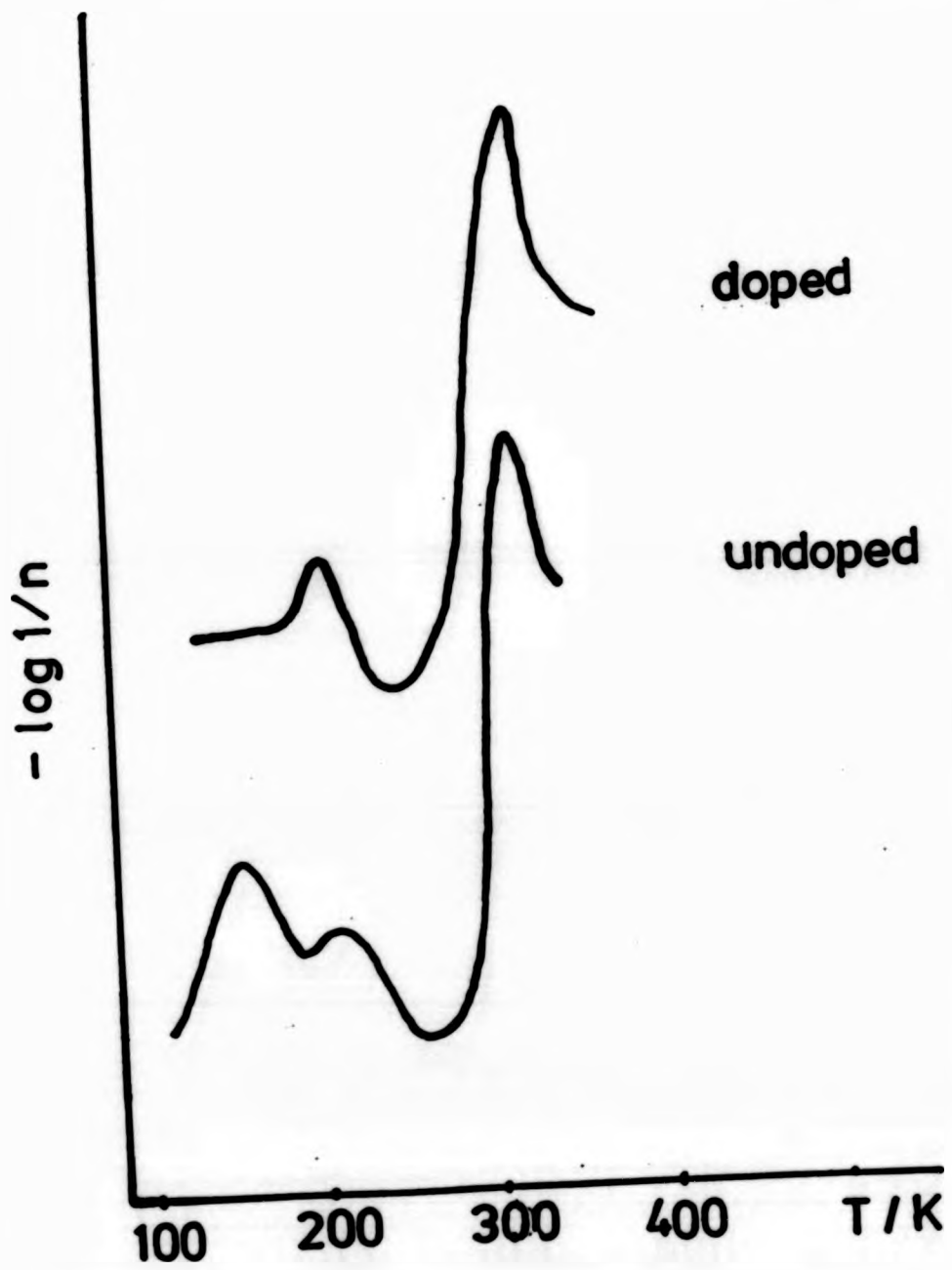


Fig. 5-8 Plots of logarithmic decrement for doped and undoped polymer HDI-AZA18C.

MDI-AZA18C

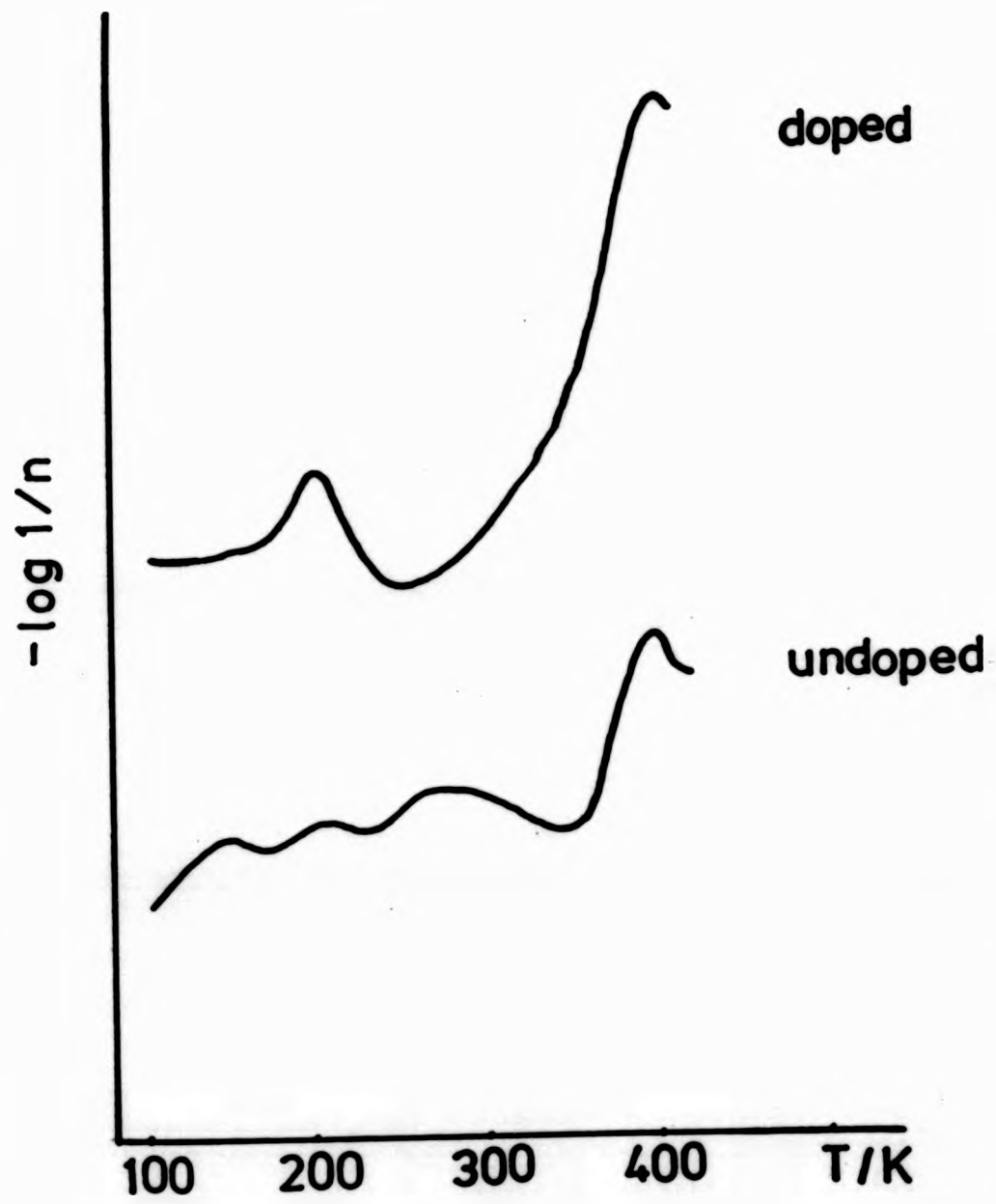


Fig. 5-9 Plots of logarithmic decrement for doped and undoped polymer MDI-AZA18C.

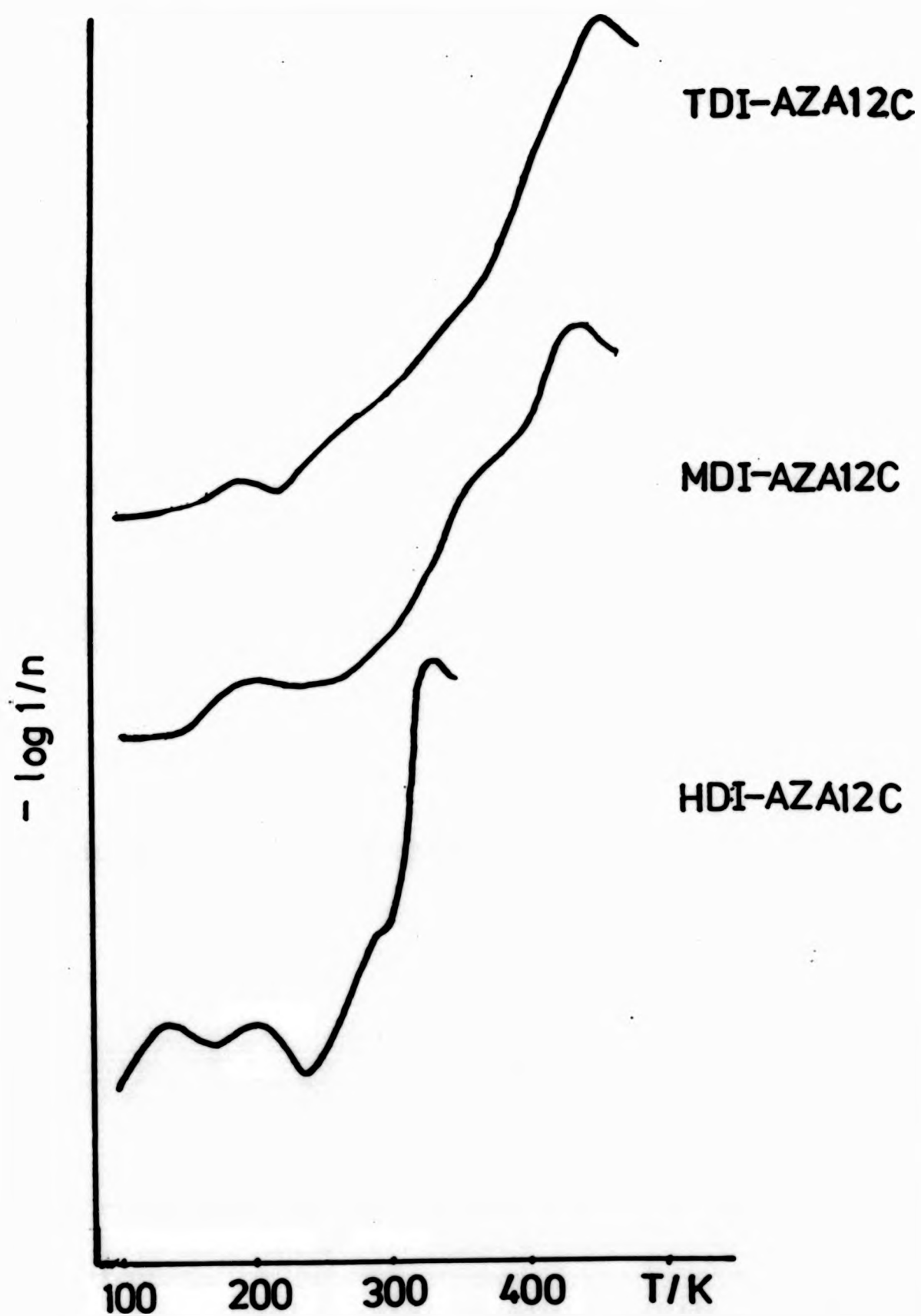


Fig. 5-10 Plots of logarithmic decrement for polymer TDI-AZA12C, polymer MDI-AZA12C and HDI-AZA12C.

due to the change in size of the rings.

With increasing temperature, more modes of vibration in the polymer chain become active, thus increasing the empty space or 'free volume' in the system. Amorphous polymers can be depicted as having more empty space because of the badly packed interlacing chains compared with crystalline or semi-crystalline polymers. One would expect the polymer with the larger 18 membered ring to occupy more space than the smaller 12 membered ring, which is in fact reflected by a lower alpha transition. In other words, the 12 membered ring has a higher rigidity.

There is only one major sub-glass transition damping peak which can be seen in polymers TDI-AZA12C and MDI-AZA12C at about 200K, while for polymer HDI-AZA12C two distinct damping maxima at 208K and 136K were observed.

Bearing in mind the aza-18-crown-6-ether series, in which the relaxation of the 18 membered ring was assigned to the 160K damping peak and with regard to the higher rigidity of the 12 membered ring, the beta transition for this polymer may arise from intramolecular motions of the 12 membered ring. The beta transition with an average value of 203K is about 40K higher than the corresponding event in the aza-18-crown-6-ether series.

The secondary transition related to the motion of the linking group like those observed in AZA18C series (at about 214K) is not found, possibly it is too close to the temperature region which the motion of the ring occurs, and could not be resolved by the TBA technique.

The gamma transition of polymer HDI-AZA12C at 136K is most

likely caused by the motion of the methylene sequence.

5.3.2.3 Aza-24-crown-8-ether

The dynamic spectrum of polymer MDI-AZA24C is shown in Figure 5-11. The alpha relaxation was found at 400K (DSC Tg=380K). Three damping peaks were also identified at 284K, 200K and 148K.

The damping peak at 200K is most probably due to the motion of the linking group as reported in the AZA18C series. The gamma relaxation at 284K is very close to polymer MDI-AZA18C(280K) and can be attributed to segmental rearrangement of the mainchain sequence. As one would expect the effect of ring size should become less critical as the ring gets bigger. The loss process at 148K is probably a result of the intramolecular conversions of the 24 membered ring.

No further polymers were synthesized because of difficulty in preparing the monomer.

5.3.3 Conclusion

For comparison purpose, Figure 5-12 depicts the damping spectra of polymers MDI-AZA12C, MDI-AZA18C and MDI-24C. The glass transition as a function of ring size is also shown in Figure 5-13.

Based on the above studies, the following conclusions can be drawn.

(1) The alpha relaxation process is dependent upon the nature of the linking units if the ring size remains constant. The more rigid the linking unit the higher the alpha transition,

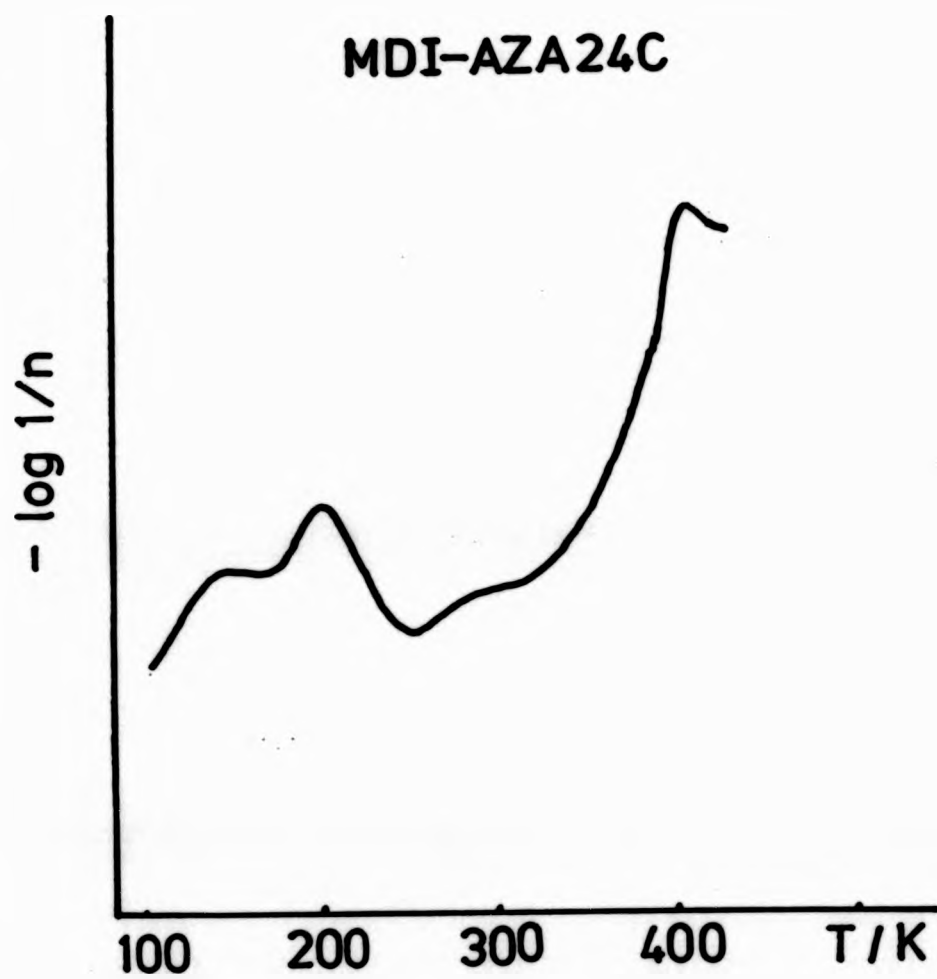


Fig. 5-11 Plots of logarithmic decrement for polymer MDI-AZA24C.

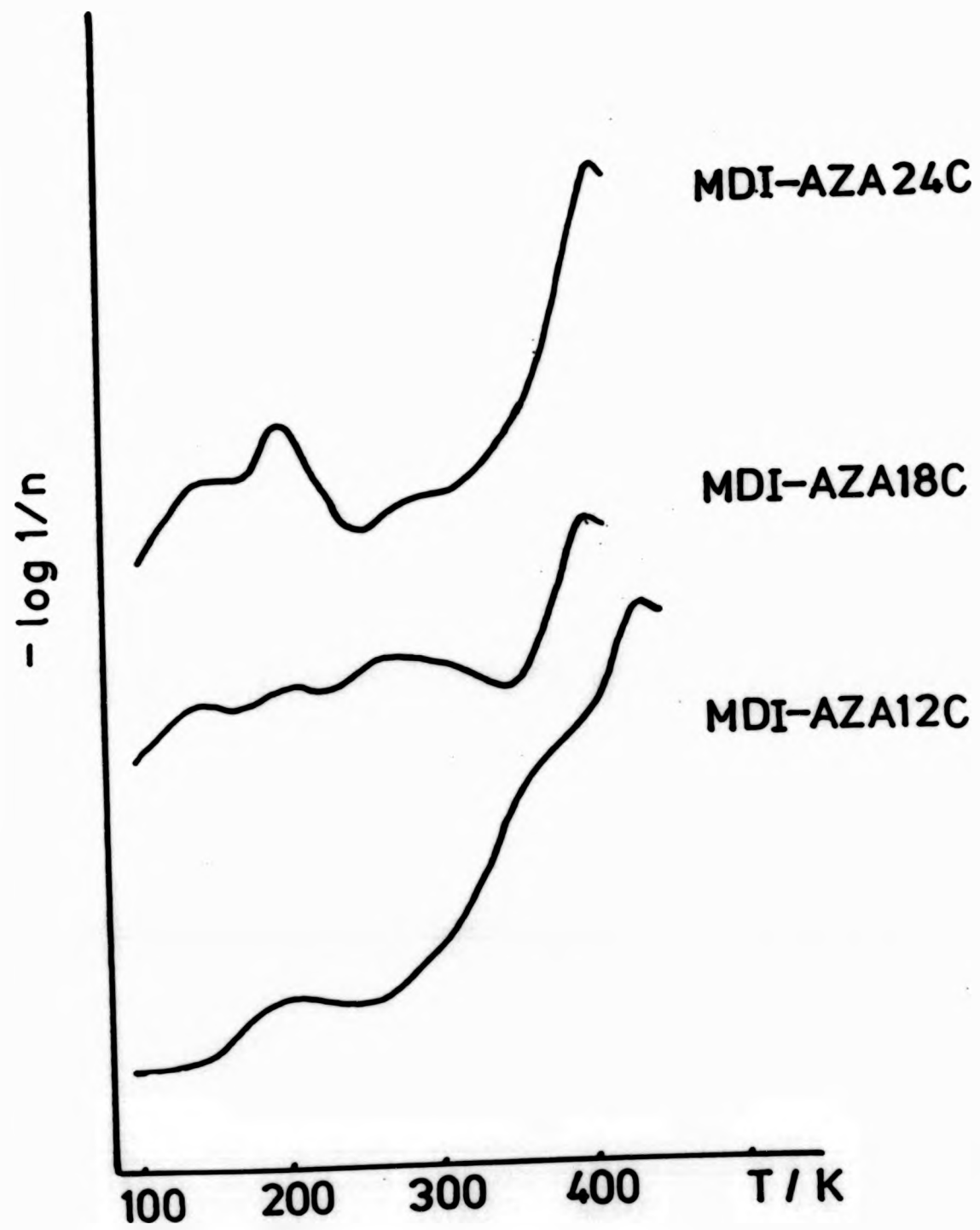


Fig. 5-12 Plots of logarithmic decrement for polymer MDI-AZA12C, polymer MDI-AZA18C and polymer MDI-AZA24C.

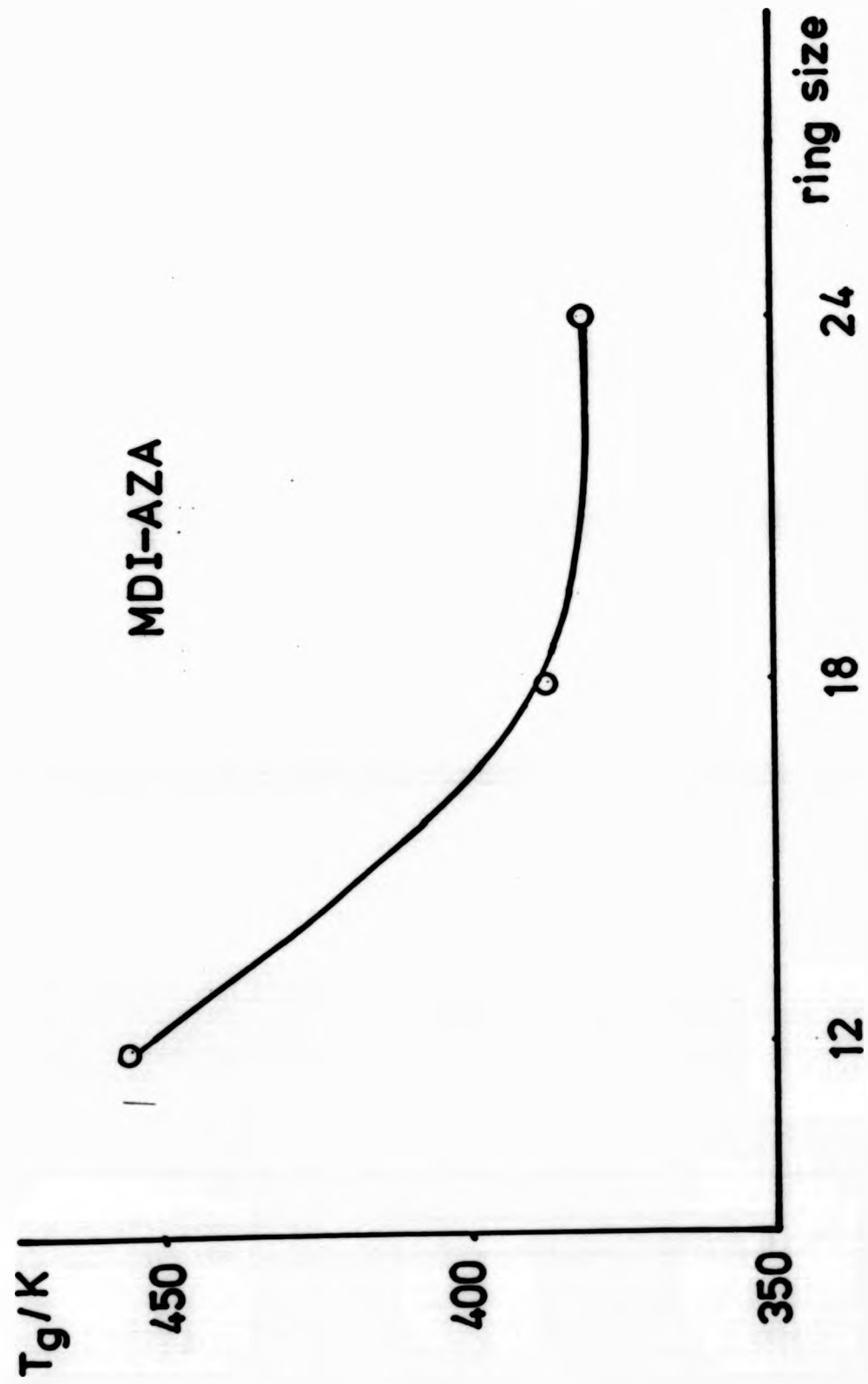


Fig. 5-13 Plot of glass transition temperature as a function of ring size of crown ethers.

- (2) The alpha relaxation which is thought due to large scale movement of the mainchain is dependent on the free volume in the polymer system; the 12 membered ring which will have least free volume has the alpha transition shifted to a higher temperature(360K),
- (3) The ring can be immobilised by incorporation of cation,
- (4) The intramolecular conformational changes of the 12, 18 and 24 membered ring occur at about 203K, 160K and 148K respectively and
- (5) The relaxations due to the motions of the linking groups vary little and consistently appear in the temperature range 200-212K.

5.4 Cycloalkanes

5.4.1 Cyclooctyl unit

5.4.1.1 Effect of Linking Units

The TBA damping spectra of polymers 8-MDI and TDI-8 are shown in Figure 6-14. The temperatures corresponding to the various damping maxima are recorded in Table 5-6 together with the DSC determined Tg.

Two distinct loss peaks were observed below the alpha transition in each polymer. The gamma transitions at 211K is most likely due to the relaxation of the 8 membered ring. Cowie and McEwen have studied the intermolecular motion of Poly(dicyclooctyl itaconate) and concluded that the pendant 8 membered ring relaxes at about 175K based on TBA technique<25>. These authors also measured the activation energy associated with the relaxation process and postulated three possible conformational changes in the cyclooctyl ring

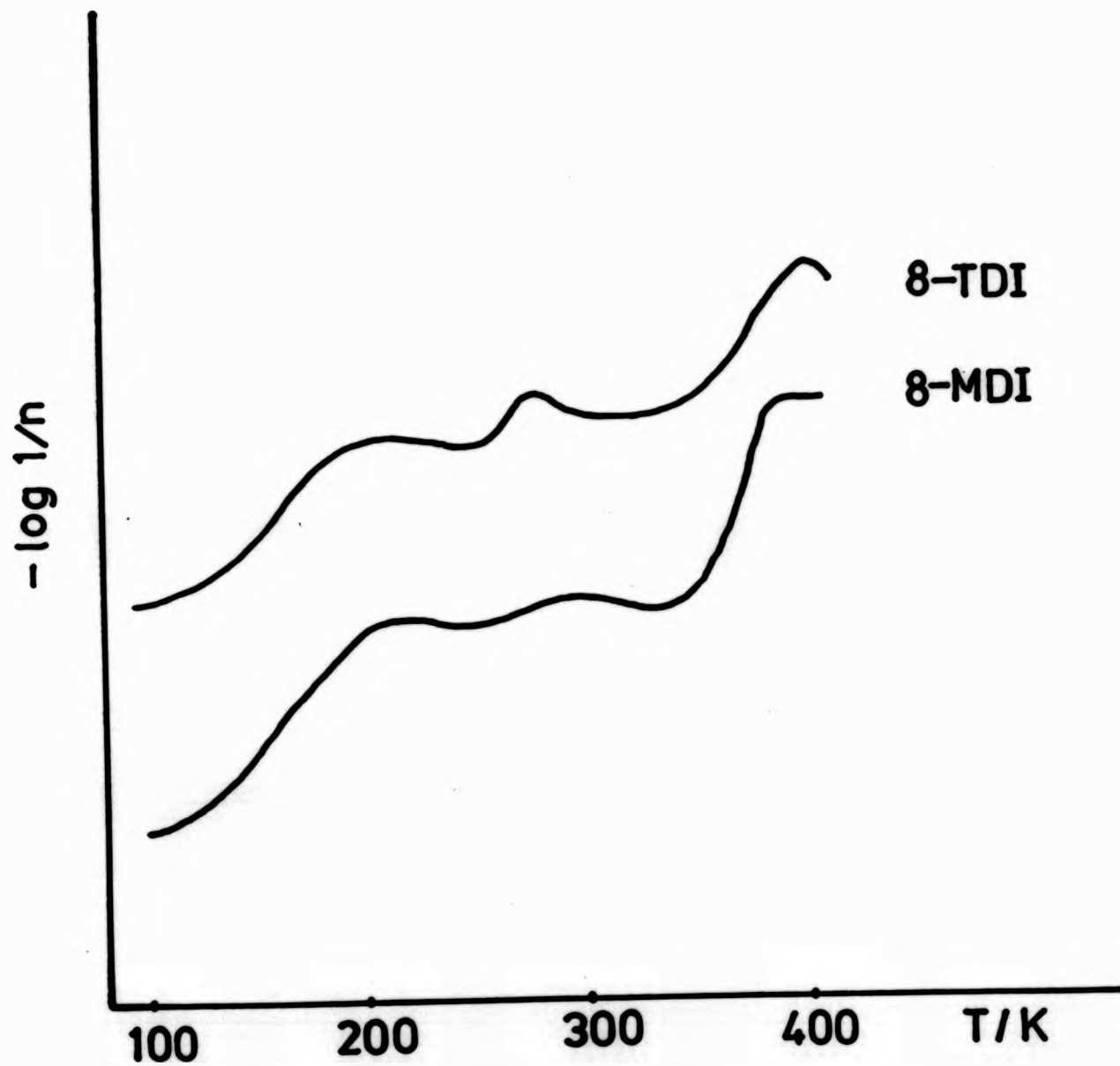


Fig. 5-14 Plots of logarithmic decrement for polymer 8-TDI and polymer 8-MDI.

Table 5-6 The damping maxima of polymers containing cyclooctyl unit

<u>Sample</u>	<u>Damping maxima TBA(K)</u>				<u>T_g DSC(K)</u>
	<u>α</u>	<u>β</u>	<u>γ</u>	<u>δ</u>	
8-MDI	391	277	211	-	359
8-TDI	386	276	211	-	398

Table 5-7 The damping maxima of copolymers Bu-8-TDI

<u>Sample</u>	<u>Damping maxima TBA(K)</u>				<u>T_g DSC(K)</u>
	<u>α</u>	<u>β</u>	<u>γ</u>	<u>δ</u>	
Bu-TDI	340	294	205	128	346
Bu-8-TDI(75:25)	385	271	205	126	358
Bu-8-TDI(50:50)	380	-	205	128	350
Bu-8-TDI(25:75)	385	285	205	-	356
8-TDI	391	277	211	-	359

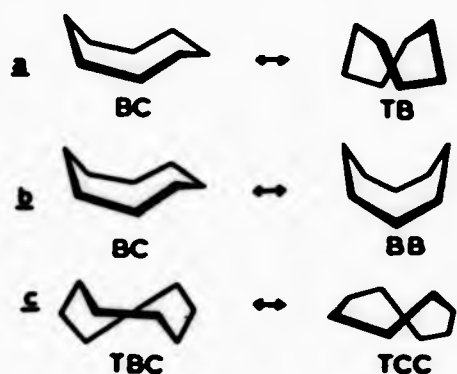
Table 5-8 The damping maxima of polymers containing cyclodecyl unit

<u>Sample</u>	<u>Damping maxima TBA(K)</u>				<u>T_g DSC(K)</u>
	<u>α</u>	<u>β</u>	<u>γ</u>	<u>δ</u>	
10-MDI	415	285	220	-	415
10-HDI	401	-	219	163	303

Table 5-9 Effect of ring size on glass transition temperatures

<u>Ring size</u>	<u>T_g DSC(K)</u>		
	<u>MDI</u>	<u>HDI</u>	<u>TDI</u>
8	359	303	398
10	415	363	420
12	420	-	-
16	408	382	-
18	376	369	-
22	366	348	-

viz (a) boat-chair to a twist-boat (b) boat-chair to boat-boat and (c) twist-boat-chair to twist-chair-chair. These mechanisms are illustrated as follows:



There is not enough information here to postulate the exact conformational changes due to the cyclooctyl ring. However one might expect the 'flipping' of the ring in the backbone should be more difficult than in the sidechain, hence it is not unreasonable to have a relaxation at a higher temperature.

The beta relaxation at about 276K is postulated to be due to segmental rearrangement of the polymer backbone as this event was also observed in the AZA18C series (average value=276K), see section 5.3.2.1.

5.4.1.2 Effect of Copolymerisation

A series of copolymers based on TDI, 1,4-butanediol and cis-1,5-cyclooctanediol were prepared. These copolymers are designated as Bu-8-TDI(75:25), Bu-8-TDI(50:50) and Bu-8-TDI(25:75) where 'Bu' means butanediol. The numbers in the bracket represent the feed ratio of butanediol and cis-1,5-cyclooctanediol respectively.

The damping spectra of these polymers are shown in Figure 5-15. The damping maxima are recorded in Table 5-7 along with

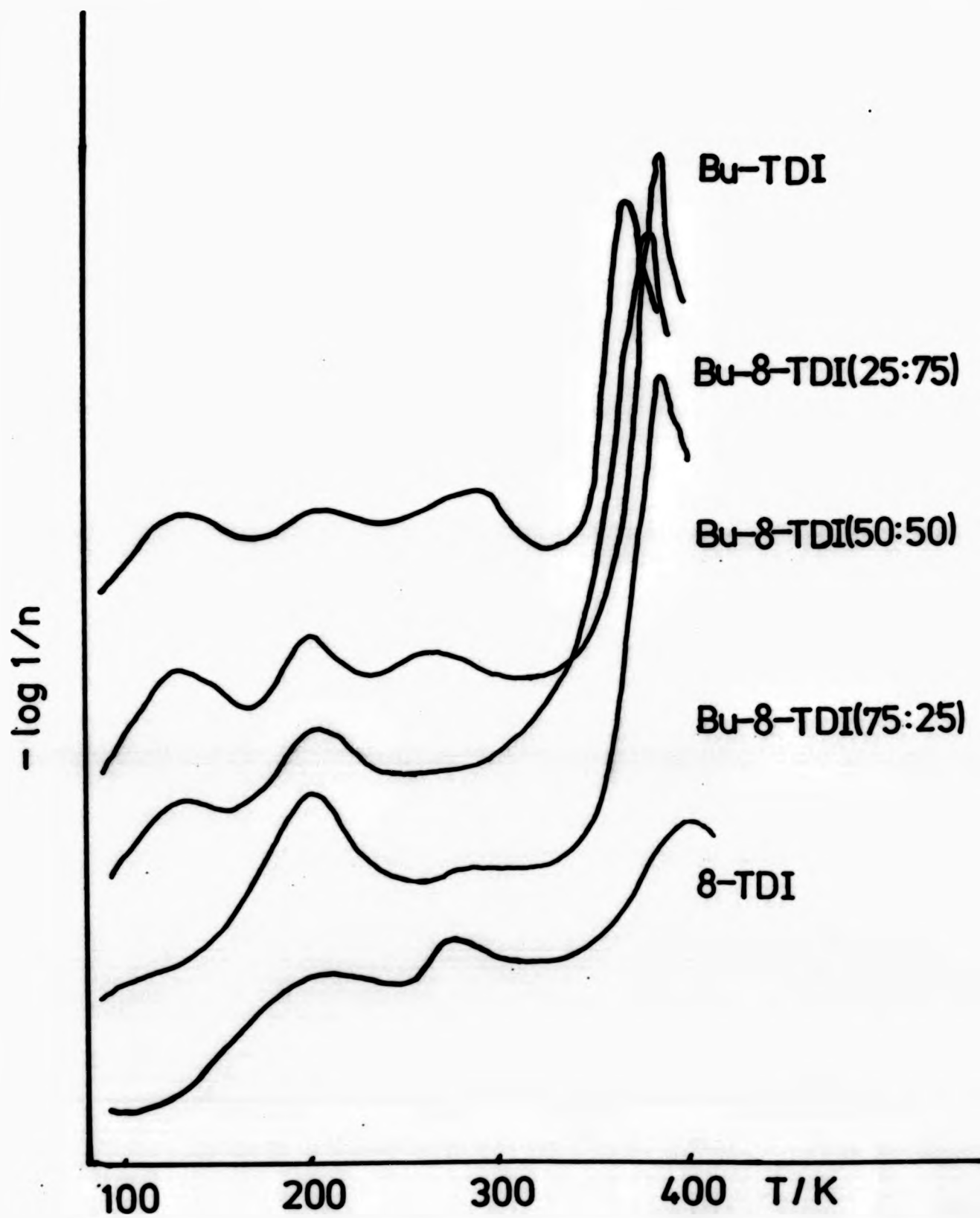


Fig. 5-15 Plots of logarithmic decrement for polymer Bu-TDI, polymer Bu-8-TDI(25:75), polymer Bu-8-TDI(50:50), polymer Bu-8-TDI(75:25) and polymer 8-TDI.

the glass transition temperature obtained by DSC.

Three damping peaks can be seen in the spectrum of polymer Bu-TDI at 294K, 205K and 128K. The origins of these loss peaks are thought to be segmental rearrangement of the backbone(294K), rotation of the linking group(205K) and restricted rotation of the methylene sequence(128K). These results are in good agreement with those obtained by Jacobs and Jenckel<72>.

The magnitude of the damping peak due to restricted rotation of the mainchain diminishes gradually as the composition of cyclooctyl ring increases and eventually disappears in the absence of butanediol.

As is pointed out in section 5.3.2.2 TBA is not sensitive enough to resolve damping peaks closed to one another, this is further demonstrated here. The gamma relaxations of the copolymers lie between 205K(polymer Bu-TDI) and 211K(polymer 8-TDI). The damping peak at 205K of polymer Bu-TDI is unambiguously due to the motion of the linking group, -NH-CO-O-, while for polymer 8-TDI, the broad damping peak at 211K must cover the motions of both the cyclooctyl ring and the linking group.

The beta transition temperature decreases gradually as the composition of the cyclooctyl ring increases.

5.4.2 Cyclodecyl Unit

The damping spectra of polymers 10-MDI and 10-HDI are shown in Figure 5-16, and the damping maxima are recorded in Table 5-8 along with the DSC determined Tg.

The profile of the spectrum of polymer 10-MDI is indeed

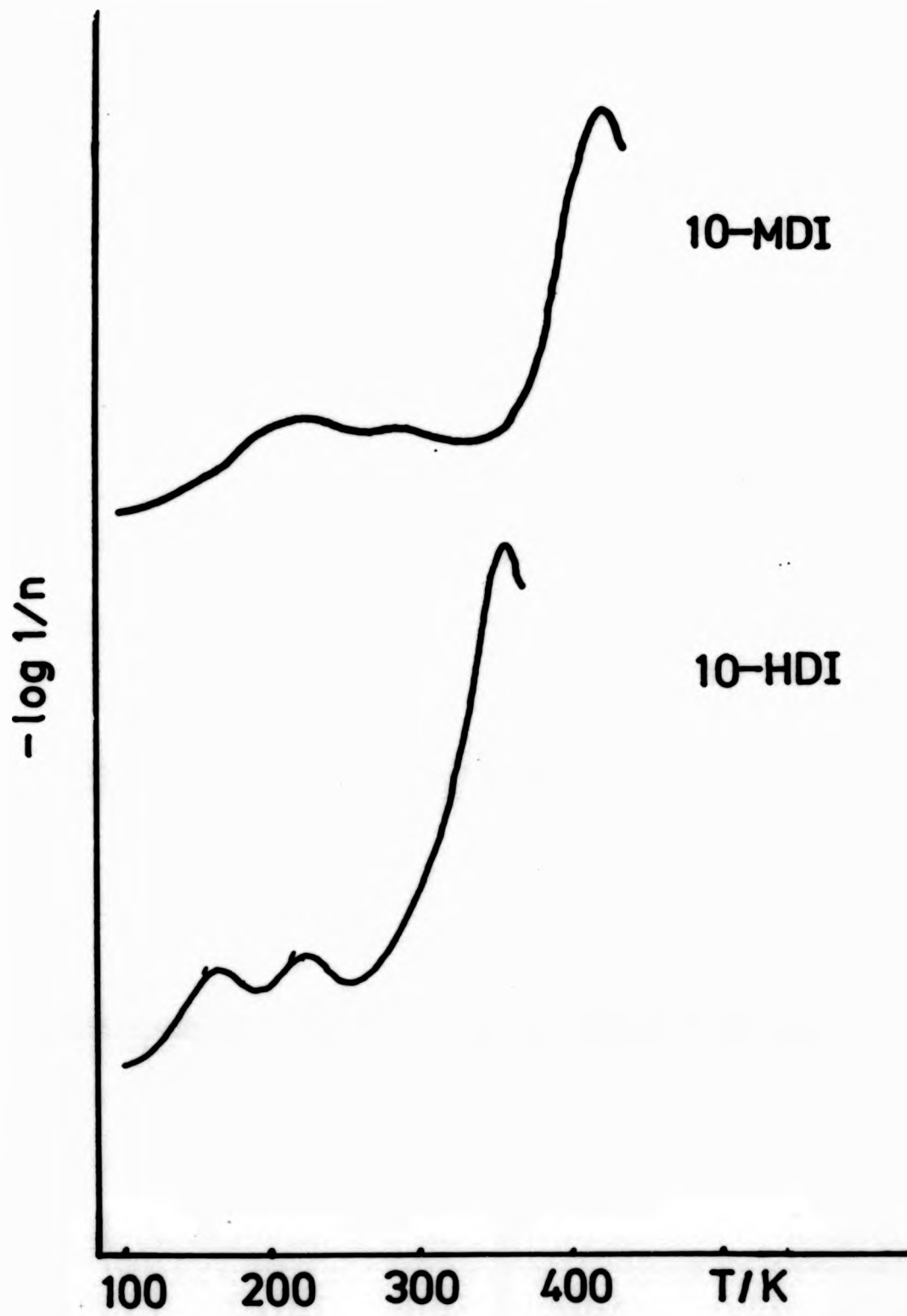


Fig. 5-16 Plots of logarithmic decrement for polymer 10-MDI and polymer 10-HDI.

very similar to that of polymer 8-MDI (see Figure 6-14). Two relaxations at 285K and 220K can be seen, they are about 8K higher than the corresponding events in polymer 8-MDI (211K and -277K). It is not unreasonable to assign the origins of these transitions based on that of polymer 8-MDI as these two polymers differ only in two carbon atoms in the ring. Hence, one would postulate the beta transition at 285K is due to limited segmental rearrangement of the mainchain while the gamma transition is the combined motions of the 10 membered ring and the urethane group. The higher transition temperatures of polymer 10-MDI reflects that the 10 membered ring has greater bulk than the 8 membered ring and will restrict rotation of the chain. Experimental facts for the conformation of cyclodecane have been obtained from X-ray analysis of the trans-1,6-diaminocyclodecane dihydrochloride by Dunitz et al. <73>. These authors found that the molecule had a very much reduced torsional strain compared with the ordinary crown, at the expense of a considerable amount of bond angle bending. Cyclodecane can be looked upon as having an idealized conformation which is part of a diamond lattice which is then distorted somewhat to allow more separation between the excessively close pairs of transannular hydrogens (Figure 5-17). This conformation is characterized by great rigidity.

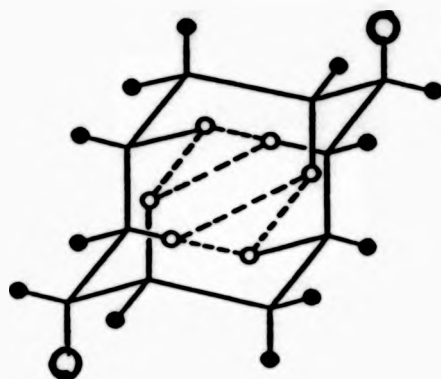


Figure 5-17

The beta transition (219K) of polymer 10-HDI is very close to the gamma transition of polymer 10-MDI. As has been demonstrated in the AZA18C, AZA12C and 8 membered series (see sections 5.3.2.1, 5.3.2.2 and 5.4.1.1), the intramolecular conformational change of the ring is basically independent of the linking units and the linking groups. Hence, one would postulate that the peak at 219K (polymer 10-HDI) is also due to the motions of the ring and the linking group while the gamma transition at 163K is due to restricted movement of the methylene sequence.

5.4.3 Polymers Containing Larger Rings

The synthesis of cycloalkyl diols proved to be a very difficult task, but despite the setback in obtaining sufficient monomers, finding an appropriate solvent for these polyurethanes is also another major problem. Most of these polymers cannot be hot pressed simply because degradation occurs at high temperature due to the nature of the urethane linkage. Nevertheless, two series of polymers were prepared just to have a rough idea about the effect of the ring size on the glass transition temperature.

Two different diisocyanates were employed viz MDI and HDI. In Figure 5-18, the glass transition temperatures are plotted as a function of the size of the rings. The glass transitions

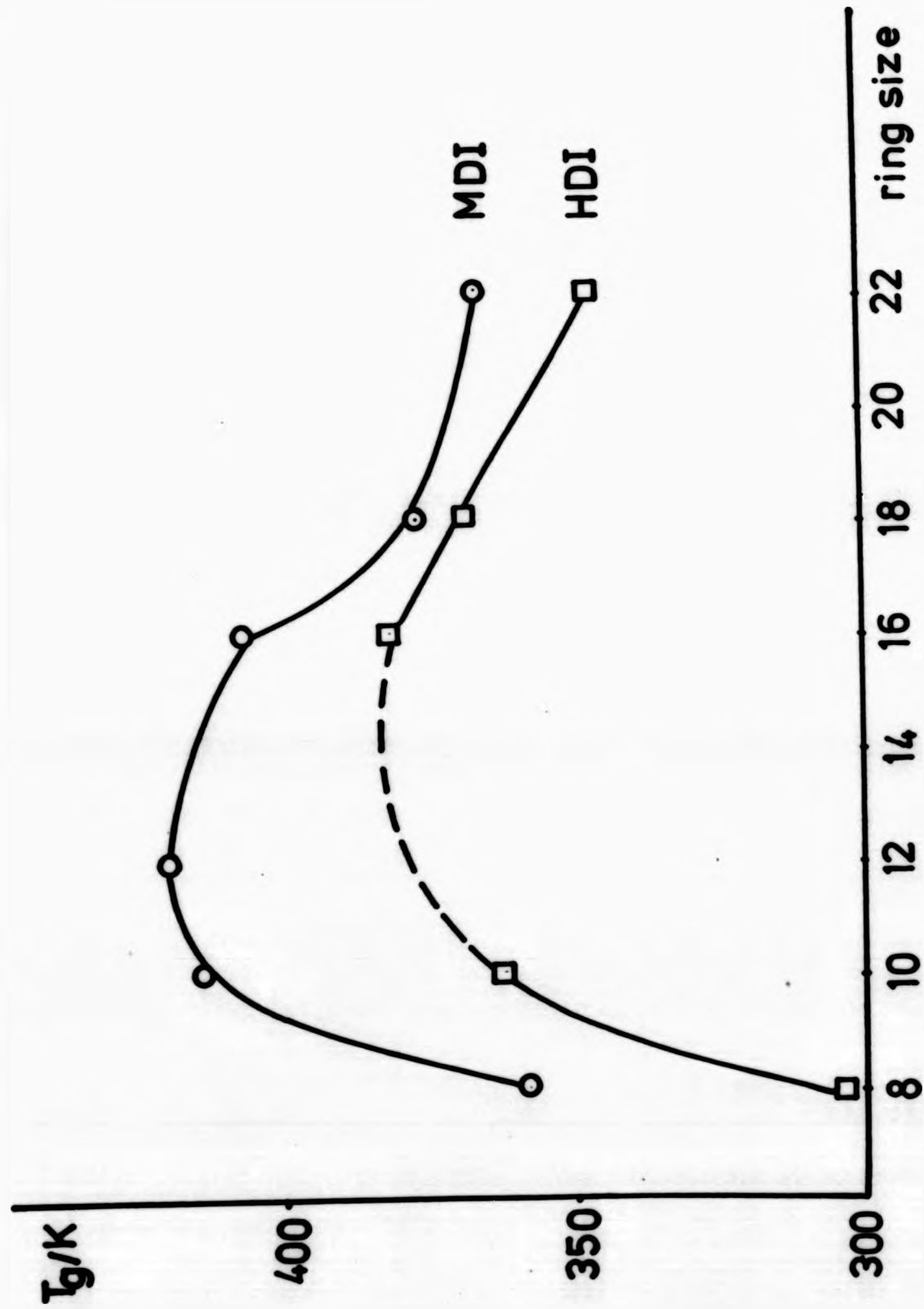


Fig. 5-18 Plot of glass transition temperatures as a function of ring size of cycloalkane.

were obtained by DSC and are shown in Table 5-9.

In the MDI series, it seems that the glass transition temperature increases from $n=8$ to a maximum ($n=12$) then decreases gradually and possibly levels off once n is greater than 22. Similar trends can be seen in the HDI series.

As was demonstrated in section 5.3, the MDI-AZA-C series (Figure 5-13) the glass transition temperature drops consistently from $n=12$ to $n=24$.

In addition, the effect of the linking units seems to diminish as the ring gets bigger. The difference in glass transitions between HDI and MDI polymers when $n > 16$ is only about 20K compared with the 8 and 10 membered ring (approx. 50K).

5.4.4 Conclusion

- (1) The above studies demonstrate that catalysts are required in polyurethane polymerisation using secondary alcohols like cycloalkyl diols. Among these catalysts, stannous octoate is more effective than triethylenediamine for increasing the molecular weight. The concentration of catalyst employed is also critical particularly in the case of triethylenediamine. Relatively high molecular weight polymers can be obtained when chlorobenzene is used as solvent in the polymerisation. Polyurethanes containing large rings are generally intractable even with strong solvents for example, sulphonic acid, phenol, trifluoroacetic acid etc.. Most of these polyurethanes decompose at high temperature and so cannot be hot pressed.
- (2) The relaxation of the 8 membered ring occurs at 211K.
- (3) The relaxation of the 10 membered ring occurs at 219K.

- (4) Polymers with a flexible linking unit like HDI exhibit restricted movement of the methylene sequence at about 160K, this phenomenon is also observed in the azacrown series.
- (5) Preliminary studies show that the glass transition temperature of the cycloalkyl polymer increases from $n=8$ to $n=12$ and then decreases gradually. This effect is more prominent when a semi-rigid linking unit like MDI is used.

REFERENCES

1. A.V.Tobolsky, 'Properties and Structure of Polymers', Interscience N.Y. 1960
2. D.E.O'Reilly and J.H.Anderson, 'Physics and Chemistry of the Organic Solid State' D.Fox Ed. Vol2, p121-341, Interscience N.Y. 1965
3. N.G.McCrum, B.E.Read and G.William, 'Anelastic and Dielectric Effects in Polymeric Solids' John Wiley & Sons Ltd. 1967
4. J.D.Ferry, 'Viscoelastic Properties of Polymers' John Wiley N.Y. 1970
5. J.Heijboer, Doctoral Thesis, Leiden, 1972
6. R.H.Wiley and G.M.Brauer, J.Poly.Sci., 3,647(1948)
7. L.E.Nielsen, 'Mechanical Properties of Polymers' Van.Nostrand Reinhold N.Y. 1962
8. R.F.Boyer, Polymer Eng.Sci., 8,161(1968)
9. L.Bohn, Kunststoffe, 53,826(1963)
10. J.Bussink and J.Heijboer, 'Physics of Non-crystalline Solids', J.A.Prins Ed. Interscience N.Y. 1965 p388
11. R.N.Johnson, A.G.Farnham, R.A.Clendinning, W.F.Hale and C.N.Merriam, J.Poly.Sci., A1,2375(1967)
12. J.Heijboer, J.Poly.Sci., Part C: 16,3755(1968)
13. J.Heijboer, 'Molecular Basis of Transitions and Relaxations', D.J.Meier Ed. Gordon and Breach Science Publishers 1978 p75
14. A.F.Lewis and J.K.Gillham, J.Appl.Poly.Sci., 6,422(1962)
15. J.K.Gillham and A.F.Lewis, Nature, 195,1199(1962)

16. A.F.Lewis and J.K.Gillham, *J.Appl.Poly.Sci.*,
7,685(1963)
17. A.Weissberger and R.Sangewald, *Z.Physik.Chem.*,
B9,133(1930)
18. V.M.Potapov, 'Stereochemistry' MIP publisher Moscow,
English Edition 1976
19. F.A.L.Anet and R.Anet, 'Dynamic Nuclear Magnetic
Resonance Spectroscopy', L.M.Jackman and F.A.Cotton
Eds. Academic press N.Y. 1975, Chap. 14
20. J.Heijboer, *Kolloid Z.Z. Polym.*, 171,7(1960)
21. V.Frosini, P.Magagnini, E.Butta and M.Baccaredda,
Kolloid Z.Z. Polym., 213,115(1976)
22. C.G.Seefried Jr. and J.V.Koleske, *J.Poly.Sci.*
Poly.Phys., 14,663(1976)
23. J.Heijboer, 'Proceeding of the International Conference
on Physics of Non-crystalline Solid' North Holland,
Amsterdam, p231(1965) and *Ann N.Y. Acad.Sci.*,
279,104(1976)
24. H.Daimon, PhD Thesis, Tokyo University(1975)
25. J.M.G.Cowie and I.J.McEwen, *Macromolecules*,
14,1374(1981)
26. J.S.Bradshaw and P.E.Scott, *Tetrahedron*, 36,461(1980)
27. L.J.Mathias, *J.Macromol.Sci-Chem*, A15,853(1981)
28. V.A.Barabanor and S.C.Davydova, *Polmer Sci. USSR*,
24,1007(1982)
29. S.Isaoka, M.Mori, A.Mori and J.Kumanotani, *J.Poly.Sci.*,
PartA 8,3009(1970)
30. N.Matsumoto, H.Daimon and J.Kumanotani, *J.Poly.Sci.*
Poly.Chem.Ed., 18,1665(1980)

31. N.Matsumoto and J.Kumanotani, J.Poly.Sci. Poly.Phys.Ed., 19,689(1981)
32. J.Pedersen, U.S.Pat. 3,687,978(1972)
33. E.Blasius, K.P.Janzen, W.Adrian, G.Klautke, R.Lorscheider, P.G.Maurer, V.G.Nguyen, T.Nguyen Tien, G.Scholten and J.Stockerer, Z.Anal.Chem., 284,337(1977)
34. E.Blaissus, K.P.Janzen and W.Neumann, Mikrochimia Acta, 279(1977)
35. L.W.Frost, U.S.Pat 3,956,136(1976)
36. M.S.Volkova, T.M.Kiseleva and M.M.Koton, Vysokomol.Soyed., B19,743(1977)
37. H.Okamura, S.Aoyama and M.Hiraoka, Jap.Pat. No 52-109600(1978)
38. H.Okamura, I.Kato, M.Hiraoka and K.Toriumi, Ger.Offen 89: 122632r(1978)
39. C.G.Krespan, U.S.Pat. 3,952,015(1977)
40. S.Bormann, J.Brossas, E.Franta, P.L.Gramain, M.Lirch and J.Lehn, Tetrahedron, 31,2791(1975)
41. W.H.Carothers, J.A.C.S., 51,2548(1929)
42. R.W.Lenz, 'Organic Chemistry of Synthetic High Polymers', Interscience N.Y. (1967)
43. A.W.Anderson and N.G.Merckling, U.S.Pat. 2,721,189(1955)
44. N.Calderon, J.Macromol.Sci., C7,105(1972): Ref.25
45. R.J.Cotter and M.Matzner, 'Ring Forming Polymerisations', Academic Press N.Y (1969)
46. E.L.Eliel, N.L.Allinger, S.J.Angyal and G.A.Morrison, 'Conformational Analysis', Interscience 1965 Chap.4

47. A.T.Blomquist, J.Prager and J.Wolinsky, J.A.C.S., 77,1804(1955)
48. K.Ziegler and R.Aurnhammer, Ann., 513,43(1934)
49. N.J.Leonard and C.W.Schimelpfenig Jr., J.A.C.S., 23,1708(1958)
50. A.K.Koli, J.Indian Chem.Soc., LI,1012(1974)
51. A.J.Hubert, J.Chem.Soc., Part C, 2149(1967)
52. T.Alvik and J.Dale, Acta.Chem.Scand.Short Comm., 25,1153(1971)
53. J.M.Lehn, U.S.Pat. 3,888,877(1975)
54. S.Kulstad and L.A.Malmsten, Acta.Chem.Scand., B,469(1979)
55. J.H.Saunders and K.C.Frisch, 'Polyurethanes: Chemistry and Technology' Vol I & II, Wiley-Interscience N.Y. 1964
56. D.J.Lyman, Rev. Macromol.Chem., 1,191(1966)
57. J.W.Baker, M.M.Davies and J.Gaunt, J.Chem.Soc., p24 (1949)
58. J.W.Baker and J.B.Holdsworth, J.Chem.Soc., p713 (1947)
59. J.W.Baker and J.Gaunt, J.Chem.Soc., p9,19 & 27 (1949)
60. A.Farkas, G.A.Mills, W.E.Erner and J.B.Maerker, Ind.Eng.Chem., 51,1299(1959)
61. A.Farkas and K.G.Flynn, J.A.C.S., 82,642(1960)
62. J.W.Britain and P.G.Gemeinhardt, J.Appl.Poly.Sci., 4,207(1960)
63. D.H.Reneker, J.Poly.Sci., 57,539(1962)
64. W.Pechhold and S.Blazenbrey, Angew.Makromol.Chem., 22,3(1972)
65. T.F.Schatzki, J.Poly.Sci., 57,496(1962)

66. R.F.Boyer, Rubber Chem. Technol., 36,1303(1963)
67. R.H.Boyd and S.M.Breitling, Macromolecules,
7,855(1974)
68. J.M.G.Cowie, J.Macromol.Sci.Phys., 4,569(1980)
69. A.E.Woodward, J.A.Sauer, C.W.Deeley and D.E.Kline,
J.Colloid Sci., 12,363(1957)
70. A.J.Curtis, J.Res.Nat.Bur.Std., 65A,185(1961)
71. Y.Ishida, M.Matsuo and M.Takayanagi,
J.Poly.Sci. Part B, 3,321(1965)
72. H.Jacobs and E.Jenckel, Macromol.Chem., 43,132(1961)
73. J.D.Dunitz and H.M.M.Shearer, Helv.Chem.Acta.,
43,18(1961)